Spray drying of fruit juice with vegetable fibre as a carrier

A thesis presented in fulfilment of the requirements
of the degree of
Doctor of Philosophy
in Chemical and Process Engineering
at the University of Canterbury

Kloyjai Cheuyglintase

January 2009

Department of Chemical and Process Engineering
University of Canterbury
Christchurch, New Zealand

Abstract

The production of free flowing powder by spray drying of sugar-acid rich foods requires an appropriate carrier. High molecular weight materials such as maltodextrins are commercially used as a drying aid because of their high glass transition temperature (T_g). Alternatively, fibre-rich by-products from fruit and vegetable juice processing might provide high molecular weight elements that are suitable as a drying support. This study aimed to understand the variables affecting the spray-dried product of fruit juice so that non-sticky fibre-based juice powder could be obtained.

Freeze dried carrot fibre was centrifically-milled to 50-100 µm sizes. Three sugar determination methods; enzymatic, enzyme membrane and HPLC with RID, were compared. The freeze drying performance of fructose, fructose + carrot fibre and fructose + carrot fibre + malic acid had the glass transition temperatures measured by differential scanning calorimetry (DSC) at 0.1 °C min^{-1}. The results from the freeze drying were used as a key for the possibility of spray dried apple juice + carrot fibre. Similar methods were used to study freeze dried fructose + maltodextrin (DE max 9.8) and fructose + maltodextrin + malic acid. Dried sucrose, glucose and fructose were used to study glass transition temperature of melted amorphous sugars and mixtures by the visual experiment and DSC at 0.1°C min^{-1} of heating and cooling scans. The Gordon-Taylor equation was used to predict the T_g of anhydrous two-sugar mixtures from experimental and literature data. The Coachman and Karaze equation was used to predict T_g of three-sugar mixtures and compared to the experimental data. Spray dried powders of fructose + carrot fibre of 30, 40, 50, 60 and 70% w/w and apple juice concentrate + carrot fibre of 30, 40, 50, 60, 70% w/w at 165/75°C inlet/outlet temperature in a laboratory scale drier were compared to that of fructose + maltodextrin (DE max 9.8) and apple juice concentrate + maltodextrin of 50, 60 and 70% w/w (dry basis). Dielectric analysis in the range 200 Hz - 1 MHz between 10-105 °C were applied to find the onset T_g (based on DSC results) from freeze dried mixtures of 14, 21, and 28% w/w (dry basis) carrot fibre+ fructose.

The enzymatic method was found to be the most accurate method for sugar determination of fruit juice but the HPLC method was the most practical one. The results of T_g values of sugars and mixtures melted showed that the T_g values from heating and cooling scans of

fructose, glucose and sucrose were in good agreement with literature. Fructose acted as a plasticizer; an increase in the fructose fraction decreased the T_g of sugar mixtures. Sucrose increased the T_g of the mixtures while the T_g of the three-sugar mixtures was less variable when there was a moderate to high proportion of glucose. The visual T_g values of sugars and mixtures were 7-28 °C higher than the onset DSC heating and cooling T_g values. This result suggested that more than one method should be used to study the glass transition of substances. The Gordon-Taylor equation did not fit well the T_g values of the dry sugars and their mixtures from this experiment. The variations might have been due to the degradation of sugar samples on the melting process. The Coachman and Karaze equation gave a good prediction of the three-sugar mixtures from this experiment.

The carrot fibre was found to be crystalline. Carrot fibre increased the T_g of freeze dried fructose and decreased stickiness of fructose. Increasing malic acid fraction decreased T_g of the mixtures. Freeze dried fructose + maltodextrin showed higher hygroscopicity than freeze dried fructose + carrot fibre. It was not possible to determine T_g of fructose + maltodextrin + malic acid due to the swelling and hygroscopicity of the freeze dried samples. T_g values of freeze dried fructose + carrot fibre and fructose + maltodextrin were found to high enough to allow spray drying of these mixtures.

The minimum fraction of carrot fibre to facilitate spray drying of fructose and apple juice concentrate was found to be 30%. Mixtures with maltodextrin at a fraction lower than 50% could not be successfully spray dried. When spray drying fructose + carrot fibre, apple juice + carrot fibre, fructose + maltodextrin and apple juice + maltodextrin at the appropriate ratios most of the powder stuck to the drier walls. The powder swept from the wall was free flowing with moisture content of approximately 2-4%. The T_g values of these powder indicated the wall build-up might be avoided in larger scale drying. T_g values of spray dried powder from the mixtures with fibre and maltodextrin were found to be not very different. The yield from mixtures with carrot fibre was three times higher than those of mixtures with maltodextrin. This cast doubts that T_g alone could be a good indicator for the stickiness of spray dried material. The microscope images and DSC scans of spray dried powders of fructose + carrot fibre and apple juice + carrot fibre showed crystalline material. The particle of spray dried fructose + maltodextrin and apple juice + maltodextrin were mostly amorphous. The crystals are more physically and chemically stable than the amorphous form. Thus carrot fibre is a good additive in spray

drying of fruit juice. Dielectric analysis at low frequency was able to possible detect T_g of single and double components. For food polymer with many components it was found that T_g value was not consistently dependent on frequency.

In conclusion, carrot fibre was a more effective carrier for spray drying than maltodextrin when compared on a mass basis and spray drying condition. Since edible fibre is an essential element needed by the human body, spray drying of fruit juice using fibre as a carrier showed the great potential of fibre in the application of fruit juice spray drying. In the case of clear juice, after reconstitution, the fibre can be easily separated from the juice as there seemed to be no chemical binding between the juice and the fibre during the spray drying process.

Acknowledgements

The author would like to thank the Royal Thai Government for the full financial support. Thank you Dr Ken Morison, for his patient supervision and fully support for all necessary requirements both in the research and personal matters.

Thanks to Dr Peter Kilmartin from the University of Auckland for providing the dielectric cell to use in the DEA experiments. Thank you Dr Diang for sharing her experience in DSC thermogram analysis of foods. Thank you Dr Mieng Lim from NZ Food Standard, for sharing her experiences on DSC and freeze drying experiments. Thanks to Dr. Shusheng Pang and Jingge Lee for always being good friends, warm welcome and support in general. Special thanks to Dr John Abrahamson, for always offering suggestions and comments on the experiments, including the work offered as a lab demonstrator which gave very useful experiences in the spray drier and plate heat exchanger. Many thanks for permanent patient support in DSC experiments and DSC information to Dr Thomas Hughes. Thank you all friends who share their time, experiences, knowledge, and social life at Chemical and Process Engineering Department during the year 2003-2008. Thank you, Dr Tony Paterson from Massey University for his voluntary suggestions about the transition on DSC thermograms and the particle analysis. Thank you Dr Jan Wikaira (Chemistry Department) and Kerry Swanson (Geology Department) University of Canterbury, for the polarizing microscope and the microscope images. Thank you all the technicians, secretary and assistant secretary at Chemical and Process Engineering Department. Special thanks to Jo for editing the thesis. Thanks to Helen, Rick and Jenny for their encouraging and personal support.

Deep thanks to my husband, Dr Sripan Cheuyglintase for his patience while I was away and for mental support. Thank you my daughter, Sasikunya who was very great in her responsibility and helping take care of her brother during the time that she was in Christchurch. Thank you, Nikki, Ward, and all Thai friends and the Thai temple in Christchurch including all the monks who help taking care of my son and general assistance. Finally, thank you Kesajee Sooksangeeam, my sister who helped take care of my children from time to time during my study.

Table of Content

Chapter 1 Introduction

1.1 Introduction

Fruit and vegetable juices are beverages with a high nutritional content of vitamins and minerals. They are generally considered to contain antioxidants for human health. The best way to consume fruit and vegetable juice is to drink the fresh juice immediately obtained from simple squeezing. To some extent this might not be convenient in the daily life of most people. In addition, fruit and vegetable are seasonal products. During the season the production is often in excess. Storage is needed in order to have the juice last longer or to last for the rest of the year. Commercially, fruit juices are generally available as two types of product, pasteurized fresh juice and juice reconstituted from concentrate. Concentration can reduce the storage volumes and facilitates the preservation for a longer shelf life. A better preservation of fruit juice might be in a powdered form. Juice in a powdered form has packaging, storage and transportation advantages. It is convenient for instant use in liquid preparations and in various application including seasoning blends, confectionary, pharmaceuticals, beverage mixes, weaning foods and health products.

Juice powder can be produced by many methods, such as vacuum, freeze, drum, air and spray drying. The techniques to dry fruit juice are very specific for each drying method. Unfortunately, the sugar and acid content of fruit juice makes the drying process very complicated. The drying complication is related to physio-chemical changes during drying of the juice. A drying aid is a necessary part of the fruit juice drying.

Spray drying is a technique widely used in many industries, as an effective method to obtain various dried products (Masters, 2004). However, applications of spray drying of fruit and vegetable juice are very limited. Jayaraman and Das Gupta (2007) discussed spray drying of fruit juices, pulps and pastes with additives. Fruit juices that have been spray dried include tomatoes, bananas and, to a limited extent, citrus fruit, peaches and apricots.

The high sugar content, consisting primarily of the reducing sugars, glucose and fructose, and also acidity in fruit juice presents a problem (Bhandari et al., 1993). At low moisture levels the products are very hygroscopic, readily picking up moisture from the air to become sticky and difficult to handle (Kudra, 2003; Jayaraman & Das Gupta, 2007). Fruit

juice powders must be protected from the atmosphere during and after drying (Bates et al., 2001).

Stickiness is a problem of the dried juices. Even with little remaining moisture in the powder at high temperatures (greater than ~ 70ºC), the product will be in a glassy syrupy state and will stick to machinery, vastly complicating materials handling. Maltodextrins or other low dextrose equivalent (DE) corn syrups can reduce the stickiness of the powder, but then the reconstituted juice is not pure (Bates et al., 2001; Kudra, 2003).

Phase and state transitions, including glass transition, have an important role in the control of spray drying processes and the products obtained. The transitions are important in understanding the stability of dehydrated spray dried products. The glass transition of amorphous substances in food affects the development of the particle properties during spray drying and subsequent agglomeration processes. The particle temperature and water content during dehydration are required in order to understand and reduce undesired stickiness and caking of particles at different stages of the drying process and during powder handling. Moreover, such understanding is essential in controlling stability of spray dried products and to avoid deterioration resulting from crystallisation or chemical and enzymatic reactions (Roos, 2002; Bhandari & Howes, 1999).

Differential scanning calorimetry (DSC) is widely used to find the glass transition temperature of materials (Foster et al., 2005; Roos 1995; Takiyama et al., 2002). DSC detects the typical change of specific heat at T_g.

Researchers have found the dielectric properties of food are not only closely correlated with water content and temperature but also with the physical change in a material. They are related to the physical state and are significantly affected by phase transitions, such as melting of ice and the glass transition. Dielectric measurements can sensitively measure changes in the state of amorphous food materials (Laaksonen & Roos, 2000, 2001).

In practice, some fruit juice powder can be spray dried when a sufficiently high concentration of natural fibres remain in the juice. The edible fibre components are mostly parts of cell walls of plants. The use of fibres, obtained from fruit or vegetable

processing, as carriers to produce free flowing powder in spray drying offers a great potential to avoid foreign substances and further utilisation of the waste materials. The use of fibre as a carrier in spray drying could also be applied to other food products to be a natural alternative to the carriers used presently (Edward & Langrish, 2004).

The fibre of fruit and vegetable is composed of structural polysaccharides. It consists of pectin, hemicellulose, cellulose, lignin and other components. A study of dietary fibre in carrot pomace found a high content of cellulose and lignin (Nawirska & Kwansniewska, 2005). Researchers have found that the glass transition temperature of the fibre component was as high as maltodextrin at low dextrose equivalent value (Georget et al., 1999; Salmen et al., 1984). This information shows the high potential of carrot fibre as a drying aid.

1.2 Objectives

The main aim of this study was to understand the variables affecting the properties of the product obtained by spray drying fruit juice, so that a non-sticky fibre-based juice powder could be produced. It was hypothesised that carrot fibre can be used as an effective carrier for the production of fruit juice powder by spray drying.

The important factors affecting spray drying of fruit juice are the sugar and acid contents in the juice. Thus this study included the determination of sugar in fruit juice by an enzymatic method, an automated enzyme membrane method, and an HPLC method. The glass transition temperature of the main sugars in fruit juice including fructose, glucose and sucrose, and their mixtures were investigated by differential scanning calorimetry (DSC). Maltodextrin (a commercial additive) was used instead of carrot fibre to compare performance. The freeze drying and spray drying performance, and glass transition temperature of fructose + carrot fibre and fructose + maltodextrin were investigated. Dielectric analysis was performed for the mixture of fructose + carrot fibre. The effect of acid on the glass transition temperature of mixtures was tested by using malic acid in mixtures of fructose + carrot fibre. Apple juice concentrate was used to study the spray drying performance and glass transition temperature of mixtures with maltodextrin and carrot fibre. The microstructure of the spray dried powders was investigated.

Chapter 2 Literature review

2.1. Chemical composition of materials

2.1.1 Chemical composition of fruit juice

The major components of fruit juices are carbohydrates, acids, nitrogen compounds, polyphenols (a large group of chemical compounds that include pigments, flavour compounds and tannin), mineral and vitamins (Camerlingo *et al.*, 2007; Wosiacki *et al.*, 2007). The carbohydrate and acid components together with moisture in fruit juice are very important to its physical changes during processing and storage. The true chemical content information of fruit juice provides an opportunity to optimize the quality and production during processing.

The composition of fruit juice depends on the variety, weather, soil, season, growing conditions, maturity and post harvest handling of the fruit. Some details about these factors affecting the chemical composition of apples and carrots are including later in this section.

The dissolved solid content of most natural fruit juices lies between 6 - 15% by weight (Azoubel *et al.*, 2005; Ramos & Ibarz; 1998; Gunko *et al.*, 2006; Vaillant *et al.*, 2001; Cassano *et al.*, 2003; Camerlingo *et al.*, 2007). The maturity of fruit affects the amount of total soluble solids in fruit juice differently. A study in physicochemical properties of Josapine pineapple found that the total soluble solids was higher at the early ripening stage and decreased toward the end of ripening period (Shamsudin *et al.*, 2007). On the other hand, the total soluble content of pomegranate steadily increases during the fruit development period (Gozlekci & Kaynak, undated). The dissolved solids are largely mixtures of two monosaccharides, fructose and glucose, and a disaccharide, sucrose (Ramos & Ibarz, 1998; Chinici *et al.*, 2005, Dolinsky *et al.*, 2000). Maltose, xylose, and less common sugars are also found in fruit juice. Citric and malic acid are the main acids in juices (Chinici *et al.*, 2005; Gunko *et al.*, 2006). A number of other acids can be found in selected plant foods. For example, grapes have considerable tartaric acid. Oxalic acid and benzoic acid are found in a number of fruits (Chinici *et al.*, 2005).

Chemical components of apples

Berüter (1985) stated that during the development of apple fruit, the major sugar that accumulates in the fruit is fructose with a smaller amount of sucrose. The fructose and sucrose are formed in the flesh of the apple fruit from sorbitol, the main C-translocate (translocation of carbon molecule in sorbital into fructose and sucrose) between leaf and fruit. After CO_2- photosynthesis in leaves, sucrose was also found to be translocated into the fruit. Both the sorbitol and sucrose are converted to other sugars such as glucose within the fruit. Klages *et al.* (2001) found that the crop load affected leaf photosynthesis and leaf carbohydrate with more carbon transported to individual fruit under low crop loads of Braeburn apple in New Zealand.

In the fruit flesh of the apple the conversion of sorbital to fructose is catalysed by NAD-dependent sorbital dehydrogenase. The formation of glucose is dependent on the O_2 consuming sorbital oxidase, and the oxidation of sorbital-6-phosphate to glucose-6-phosphate is catalysed by an NADP-dependent sorbital-6-phosphase dehydrogenase (Berüter, 1985).

Berüter (1985) studied the variation of sugars in the flesh of the growing apple after full bloom and the pattern of change in concentrations of sorbital, glucose, fructose and sucrose. It was found that there was a high level of sorbital about two weeks after full bloom but the level declined rapidly. The sorbital content remained low from that period until harvest. The fructose and sucrose accumulated steadily during fruit growth whereas the amount of glucose present in the apple fruit decreased after about seven weeks after full bloom. The reduction of glucose was found to be accompanied by starch accumulation which reached a peak after about 12-13 weeks after full bloom. When the content of starch dwindled, the level of glucose tended to rise again. This is due to the respiration of the apple fruits during ripening.

Berüter (2004) stated that the major organic acid in apple is malic acid. It was found that the malic acid accumulates in the young apple fruit up to 100 µmol g^{-1} fresh weight, and decreased again during growth and ripening. Berüter (2004) gave graphs of the carbohydrate and malate content during fruit growth of low acid and high acid apples in Switzerland (Figure 2.1). This shows the similar amount of glucose and sucrose in a low acid apple in some stage after full bloom, the dominance of fructose, the pattern of

increase and decrease in starch, the decline of sorbital, and the variation of malate during apple growth.

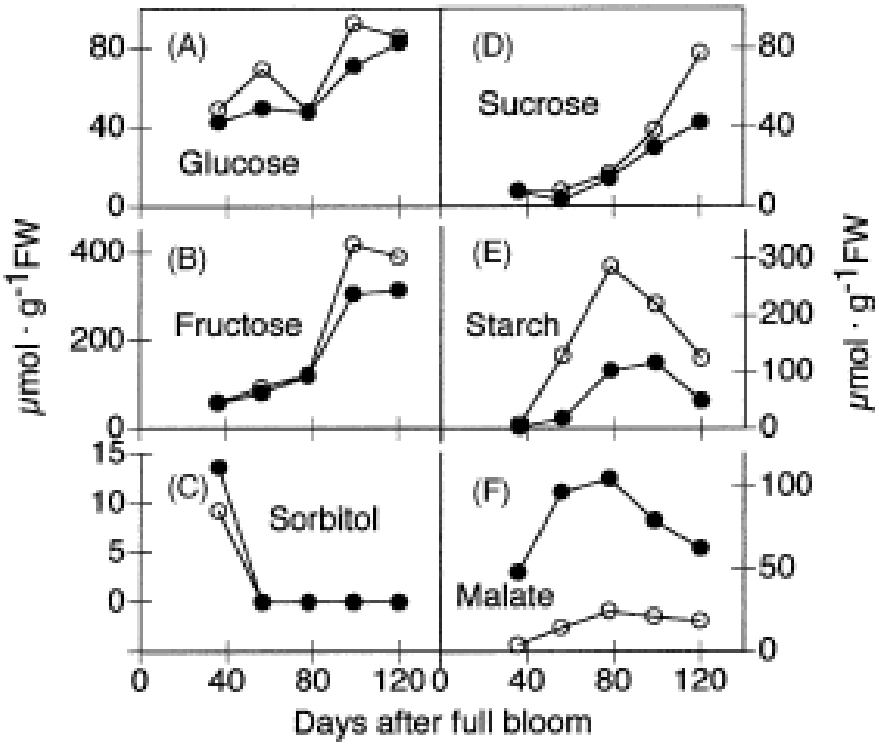

Figure 2.1 Carbohydrate and malate content of a low acid apple (open symbol) and a high acid apple (close symbol) over the course of fruit development (Berüter, 2004).

Camerlingo *et al.* (2007) reported the approximate composition of raw apple juice obtained after pressing apples (detail in Table 2.1). Average values of the component of clarified apple juice by Youn *et al.* (2004) and of the sugars and other components of seven cider apple varieties by Campo *et al.* (2006) are also shown in Table 2.1. From Table 2.1, it is seen that the fructose is the dominant component of apple juice. The glucose and sucrose content in apple juice are similar. The analysis method might also affect the reported composition of the juice.

Table 2.1 Approximate composition of apple juice components ([a] Camerlingo *et al.*, 2007; [b]Youn *et al.*, 2004; [c] Campo *et al.*, 2006)

Compound	Concentration (%)[a]	Concentration (%)[b]	Concentration (%)[c]
Water	86-90	-	-
Sugars	10-12	-	-
Fructose	4.6-7.0	6.24-7.91	5.17
Glucose	2.0	2.54-3.52	1.48
Sucrose	2.7	1.72-2.02	1.80
Malic acid	0.3-0.7	0.35-0.60	0.89
Oxalic acid	-	0.05-0.13	-
Citric acid	-	0.06-0.13	0.024
Pectin	0.1-0.5	-	-
Starch	0.05-0.5	-	-
Polyphenols	0.1	-	-
Proteins	0.06	-	-
Vitamins (ascorbic acid)	0.05 (gL^{-1})	0.09-1.34(gL^{-1})	-
Ashes	0.2	-	-

[a] analysis method for sugars not given

[b] sugar content determined by HPLC method

[c] sugar content determined by enzymatic method

Harvesting of apples depends on many factors such as the size of the fruit, colour, acidity, favour and storability. The record of harvesting date from previous years is a good index of the harvesting date of apples. The variation of temperature within one month after full bloom was used to predict the harvesting date. In the United States of America, the average time after full bloom to harvest of Gala and Fuji apples is 110-120 days and 170-185 days, respectively (Hui, 2006). A study in the variation of firmness, soluble solids, titratable acidity and starch index of apple fruit on different days after full bloom of the flower found that the total soluble solids and starch index (the gradual change of starch to sugar, lower value, higher amount of starch presenting in the fruit) increased during development. Details are shown in Table 2.2 (Fellman *et al.*, 2002).

Table 2.2 Variation in quality and chemical composition of apple at different day after full bloom of flower (DAFB) (Fellman *et al.,* 2002)

DAFB	Firmness(N)	Soluble solids (%)	Titratable acidity (%)	Starch Index(1-5)*
119	88.9	9.9	0.5223	1.6
142	84.8	11.3	0.4918	2.0
151	81.7	12.4	0.4539	2.9
163	76.4	13.3	0.4698	3.9

*starch index is the gradual change of starch to sugars; a higher value indicates that a higher amount of starch has changed to sugars.

Compo *et al.* (2006) determined the sugar content of seven varieties of cider apples, over five weeks before harvesting time by an enzymatic method. The study found a range of 6-9% total sugars. During the five weeks of study the amount of sugars increased to reach maximum values and then decreased. A study of the sugar composition of clarified apple juice by sugar oxidation in alkali (Somogyi method) by Wosiacki *et al.* (2007) confirmed that the fructose component was dominant, however the average value of sucrose was higher than glucose. The fructose, glucose and sucrose content of the juice samples were 6.63, 1.87 and 3.07 g/100 mL respectively. The effect of growing region on sugar composition of clarified apple juice from three different areas in Brazil found variations in fructose, glucose and sucrose content.

By using an HPLC with a refractive index detector Brause and Raterman (1982) found that the sugar content of over 15 different apple varieties were in the range of 5.6-8.1% fructose, 1.7-4.1 % glucose and 0.7-2.7% sucrose.

Sugar content of carrot

Sugar content of carrot varies considerably among the varieties and was influenced by environment, harvesting time and storage condition. Sucrose, glucose, fructose, and maltose were considered to be the common sugars of carrots. Alabran and Mabrouk (1973) reported that in fresh carrots, total sugar content ranges from 3.46-10.74%. Otsuka and Take (1969) found 0.379% glucose, 2.08% maltose, and 2.41% sucrose in fresh carrots grown in Japan. Alabran and Mabrouk (1973) used gas liquid chromatography method to detect free sugars in fresh carrot and reported that there were 3.39% sucrose, 3.34% glucose and 1.05% fructose in fresh carrot.

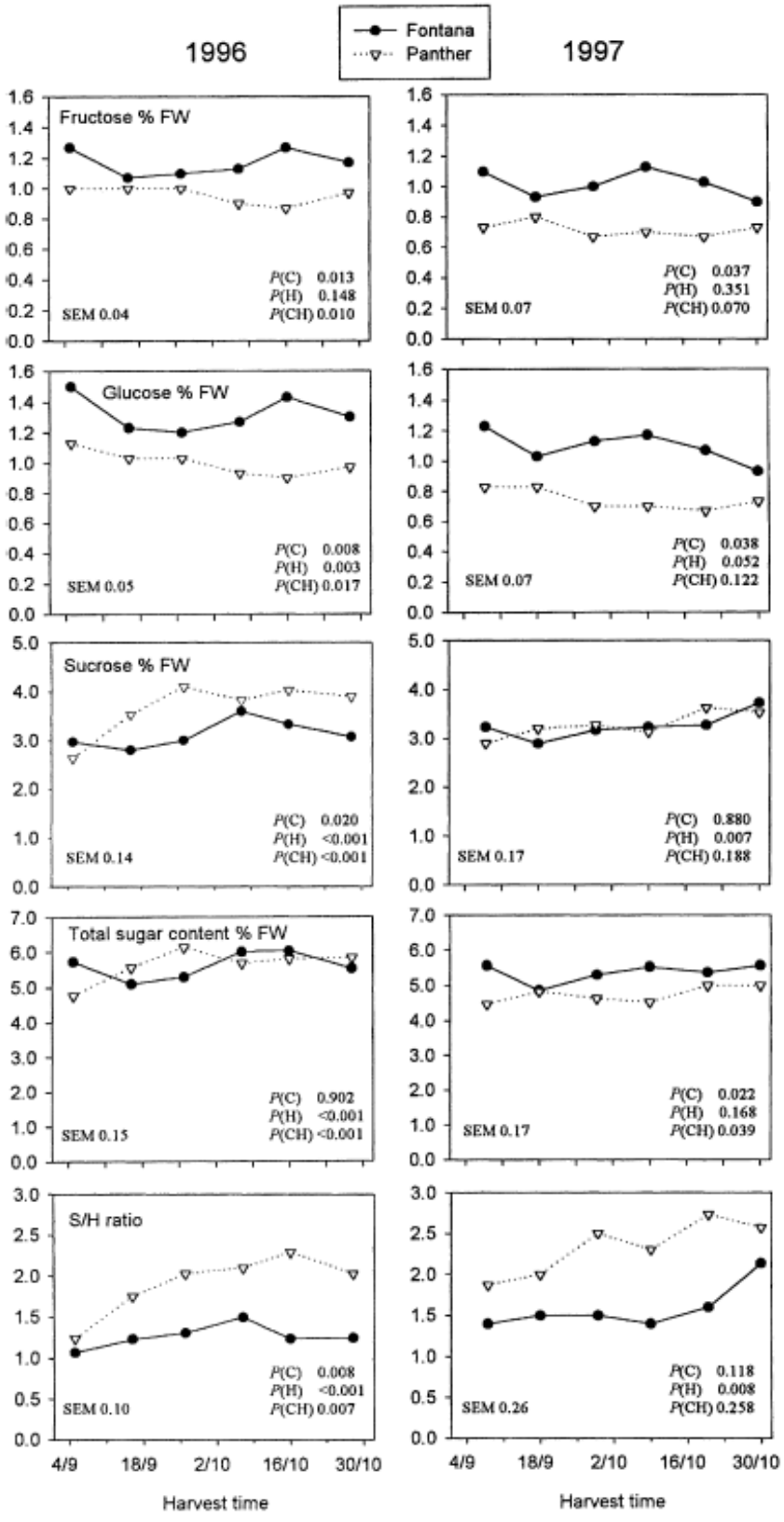

Figure 2.2 Content of soluble sugars and the sucrose to hexose ratio at different harvest date and year of Fontana and Panther carrots. Probability values are given for the effects of cultivar (C), harvest time (H) and for their interaction (CH) (Suojala, 2000).

Suojala (2000) studied the changes in soluble sugar content of two carrot varieties at harvest and storage during the years 1995-1997 by a gas liquid chromatography method. The results showed that the total sugar and sucrose content at the beginning of the harvest period were higher during the coldest year than the warmest year. The amount of sugars in the Fontana variety carrot seemed higher than that of the Panther variety carrot. Figure 2.2 shows the sugar content of both varieties in the years 1996 and 1997. Fontana carrots contained more fructose and glucose than the Panther carrots, while the sucrose was higher in Panther carrot than in Fontana carrots. But in year 1997, the amount of sucrose in both varieties was about the same for all the harvesting time. The variation of all sugars had found in both varieties in both years.

The storage time affected the amount of sugars in carrot with either an increase then a decrease as found in fructose and glucose of Fontana carrots in year 1995, or a decrease then followed by an increase as found in fructose and glucose of Fontana in year 1996. The detail of changes in sugars of carrot during storage, are shown in Figure 2.3. The variation of all sugars with dates of harvesting and storage time was found from both varieties.

2.1.2 Chemical component of fruit and vegetable fibre

The main component of fruit and vegetable fibre is the cell wall. The primary cell wall mainly consists of two phases; a microfibrillar phase and a matrix phase (Ishii & Shimizu, 2001). These are complex composites of polysaccharides, proteins, phenolics and lignin. The polysaccharide consists of three broad categories cellulose, hemicellulose and lignin.

Cellulose

Cellulose is the major polymer found in all plant cell walls. It is composed of bundles of crystalline cellulose microfibres embedded in an amorphous matrix of hemicellulose and pectin (Bartolomé & Rupérez, 1995; Yildiz & Gümü•kaya 2007). The cellulose is in the form of rods or microfibrils spiralled together in the wall of plant cell. Chemically cellulose consist of long, linear chains of glucose residues covalently linked by • (1-4) glucosidic bonds with a degree of polymerization (DP) of between 2000 and 6000 in primary cell walls to more than 10000 in secondary walls. The long linear chains of pure glucose are termed glucans. A single cellulose fibre of 3.5-4 nm diameter contains 30-40

glucan chains held together by a very large number of hydrogen bonds. Its glucan chains interact closely through hydrogen bonding, excluding water to produce areas of crystallinity which is insoluble in water and resistant to reagents (Albersheim *et al.*, 1997).

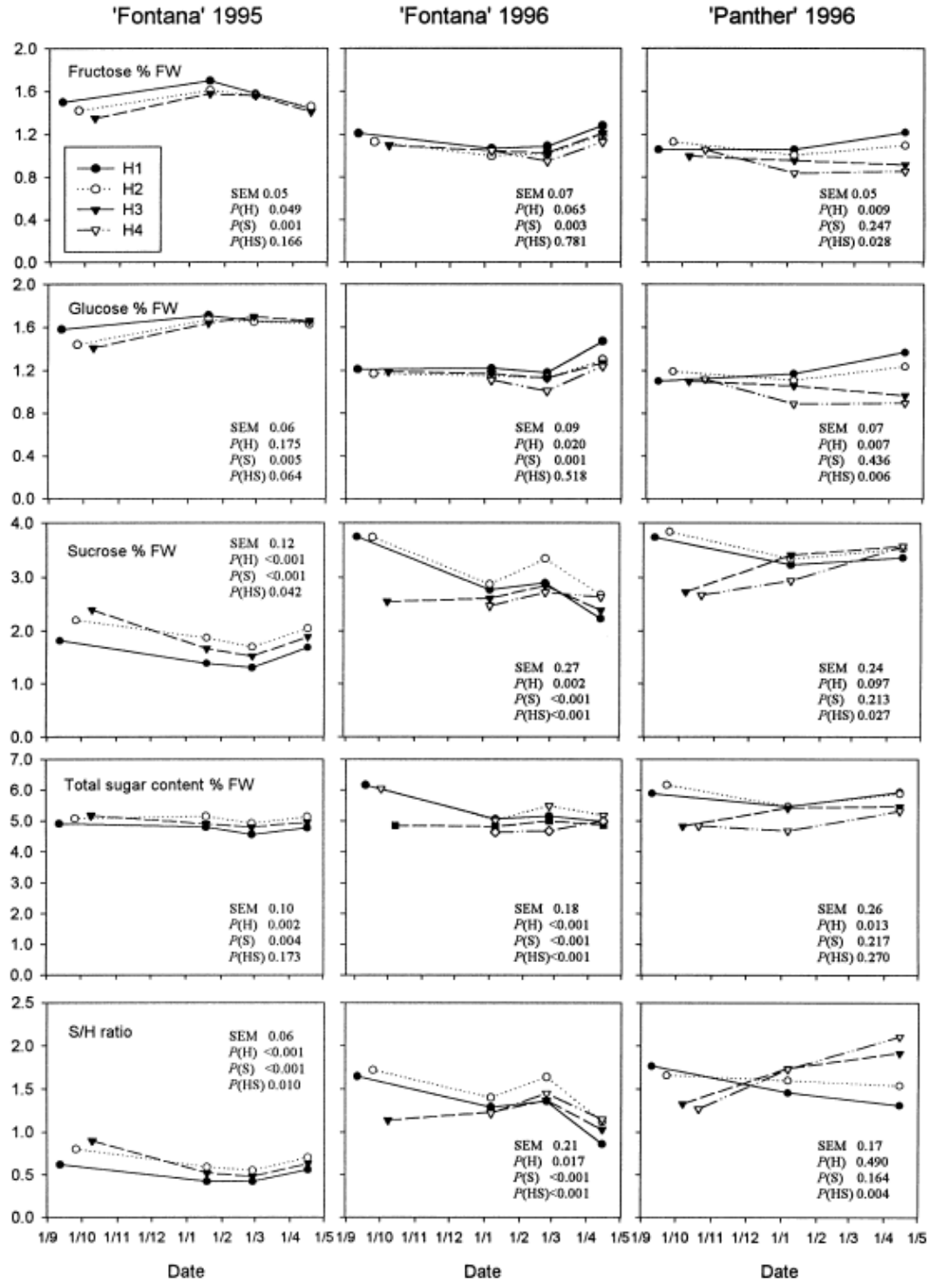

Figure 2.3 Changes in sugar composition of carrots during storage in year 1995-1996. First points refer to the values at harvest. Probability values are given for the effects of harvest time (H), storage time (S) and their interaction (HS) (Suojala, 2000).

The naturally-occurring crystalline structure is known as Cellulose I. Several other forms (II, III, and IV) can be produced as a result of thermal or mechanical treatments. Cellulose II is the most stable thermodynamically. Cellulose is the single most abundant polysaccharide component of vegetable. A study of dietary fibre found that there was 51.6% of cellulose in carrot pomace (Nawirska & Kwansniewska, 2005).

There are, however, relatively weak segments of the microfibril with weaker internal bonding. These are called amorphous regions or dislocations.

The crystalline region is isolated to produce microcrystalline cellulose. Microcrystalline cellulose has been widely used as an additive in pharmaceutical and food products because of its high binding capacity, good flowability, thickening, compactibility, and compressibility (Shileout *et al.*, 2002; Bhimte & Tayade, 2007).

Processing of fibre with temperature and humidity has been found to have some effect on cellulose. A study of the heat treatment of the cell wall component of wood by Yildiz and Gümü•kaya (2007) found that the degree of cellulose crystallinity increases to a certain temperature which might be as high as 200 °C. Moderate increases in crystallinity of cellulose were also found with exposure to humid atmospheres. The suspension of cellulose in water and subsequent drying resulted in variable increases in relative crystallinity of cotton linters (Weimer *et al.*, 1995). The hygroscopicity and structure of cellulose crystals were also found to change with temperature. Yildiz and Gümü•kaya, (2007) found that when the crystallinity of cellulose was modified by high temperature, the hygroscopicity of wood fibre was decreased due to the degradation of hemicellulose at high temperature. The monoclinic structure ratio of cellulose in wood samples was found to decrease while the triclinic structure ratio was increased with thermal modification. Figure 2.4 shows a typical microdiffraction pattern of *Cladophora* (a branching, green filamentous alga) microcrystalline cellulose with the monoclinic and triclinic structures (Imai *et al.*, 1997).

The physical modification of cellulosic materials was found to increase the potential of cellulose to react with other chemical compounds. Caulfield and Moore (1974) found that the ball milling of fibre not only reduces particle size, but severely disrupts the crystalline order of the cellulose in addition to increasing the amorphous character. The size

reduction increased the availability of surface of both amorphous and crystalline cellulose. The reduction of crystallinity as well as particle size was known to increase the accessibility and susceptibility of cellulose to reagents. It was found that the accessibility of the crystalline component was greater than that of the amorphous component of the cellulose. During acid hydrolysis recrystallization of cellulose was found to take place.

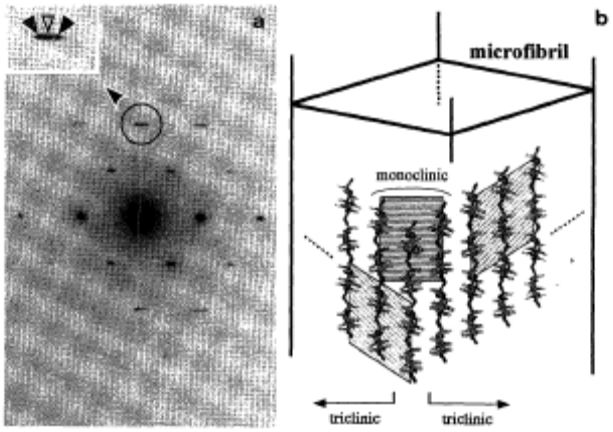

Figure 2.4 Diffraction diagrams of cellulose (a) and proposed model (b) as seen in the diagonal direction of its cross section. a: A typical micro diffraction pattern of *Cladophora* cellulose. The central spot is located precisely on the meridian (open arrowhead) which derives from monoclinic structure. The other two spots (solid arrowheads) are from triclinic structure. b: Proposed model showing lateral distribution of two structures, triclinic and monoclinic: monoclinicity may always appear between two triclinic structure having different slope of ab planes (Imai *et al.*, 1997).

The sugar content in cellulose of various fruits and vegetable studied by Voragen *et al.* (1983) are shown in Table 2.3. The main sugar found in the cellulose fraction of all fruits and vegetables presented is glucose. There are trace amounts of arabinose, xylose and galacturonan in the cellulose of some fruits and vegetables. Carrot cellulose only has very small amount of xylose and uronic acid.

Pectic polysaccharides

Schols and Voragen (1994) stated that pectic polysaccharides consist of polysaccharides rich in galacturonic acid (GalA) and often contain significant amount of rhamnose (Rha), arabinose (Ara), and galactose (Gal). They are thought to be present throughout all

primary cell walls and probably form a gel matrix interspersing the cellulose-hemicellulose network.

Table 2.3 Sugar composition in mol-% of cellulose fraction (Voragen *et al.*, 1983)

Materials	Rha/Fuc	Ara	Xylose	Manose	Galacturonan	Glucose	Uronic acid
Raspberries	-	1.5	6.8	-	-	82.2	8.5
Strawberries	-	1.1	1.1	-	1.4	91.3	5
Cherries	-	4.2	1.1	-	1.8	93.1	1.5
Papaya	-	-	-	-	3	96.6	1.6
Pineapple	-	7.6	14.9	-	-	72.4	2.8
Mango	-	-	2.3	-	-	94.3	3.4
Apple	-	7.6	1.7	3.5	-	78.3	8.8
Pear	-	1.4	10.6	-	-	83.2	4.8
Carrots	-	-	2.2	-	-	95.1	2.7
Cucumber	-	3.6	1.2	1.9	5.7	82.3	5.3
Onions	-	0.9	-	-	8.5	88.8	1.8

The three major pectic polysaccharides currently defined are: homogalacturonan (HG), rhamnogalacturonan-I, and rhamnogalacturonan-II. Fruit and vegetables are particularly rich in pectin polysaccharides (Giovane *et al.*, 2004). In addition to HG and RG-I, primary cell walls often contain neutral-sugar-rich molecules. The sugars in pectin from beet pulp are arabinose, rhamnose, galactose, and glucose from 10-17% depending on the extraction procedure (Phatax *et al.*, 1988). Stevens and Selvendran (1984) found that the cortex of ripe apples contain around 40% of pectic polysaccharides. Nawirska and Kwansniewska (2005) found 3.88% pectin in carrot pomace. The sugar content in pectin of various fruits and vegetable studied by Voragen *et al.* (1983) are shown in Table 2.4. The pectin of apple, pineapple, pear and cherries are dominant in arabinose. Carrot pectin has small amount of arabinose and galactutonan. All fruits and vegetables pectin are dominant in the amount of uronic acid except pineapple.

Hemicelluloses

Hemicelluloses are also found in all plant fibres. They can differ greatly in different cell types, and in different species. Hemicelluloses are polysaccharides bonded together in relatively short, branching chains. They are usually solubilized only by treatments that disrupt the hydrogen bonds which link them strongly to cellulose microfibrils such as

increasing strengths of alkali. Hemicelluloses have very hydrophilic sites to which water can readily bond. Fruit fibres were found to have moisture sorption properties similar to hemicelluloses (Chiou & Langrish, 2007).

Table 2.4 Sugar composition in mole % of pectin fraction (Voragen *et al.*, 1983)

Materials	Rha/Fuc	Ara	Xylose	Manose	Gaclaturonan	Glucose	Uronic acid
Raspberry	1.6	3.4	2.6	5.5	3.5	4.9	78.5
Strawberries	2.3	9.5	1.5	-	8.4	6.9	71.4
Cherries	2.3	20.6	1.4	2.1	5.9	1.5	66.3
Papaya	3	4.5	4.5	1	6.7	1	79.3
Pineapple	0.7	29.8	36.5	0.6	9.7	4.2	18.4
Mango	1	15.5	1.8	0.6	4.4	2.7	74
Apple	1.4	23.3	2	0.4	4.1	1.3	67.5
Pear	1.8	21.5	2.5	0.8	3.2	11	59.2
Carrots	1	7.9	-	-	11.8	2	77.4
Cucumber	0.6	5.8	2.2	-	11	1.8	78.7
Onions	0.6	3.8	2.3	0.6	40	4.4	48.3

The prominent hemicelluloses in primary walls of edible vegetables and fruits of dicotyledonous plants including apple, are the xyloglucans (Stevens & Selvendran, 1984). They consist of a backbone of (1-4)-linked •-glucose (as in cellulose) to which side chains of (1-6) linked •-xylose residues may be attached. A proportion of the xylose residues have other sugars attached including (1-2)-linked •-galactose and disaccharides of frucose and galactose. The other components of hemicellulose are the xylans. The main sugars in the hemicellulose of pineapple and sugar beet pulp were found to be xylose, arabinose, galactose and glucose (Bartolomé & Rupérez, 1995; Sun & Hughes, 1998). Nawirska and Kwansniewska (2005) found 12.3% of hemicelluloses in carrot pomace. The sugar content in hemicellulose of various fruits and vegetable studied by Voragen *et al.* (1983) are shown in Table 2.5. Xylose is dominant in all hemicelluloses of fruits presented. Hemicellulose of vegetables including carrot has fewer amounts of the sugars presented in this table. However, carrot hemicellulose seems to have a moderate amount of galacturonan, glucose and uronic acid.

Lignin

Lignin consists of three monolignol monomers, methoxylated to various degrees: *p*-coumary alcohol, conniferyl alcohol, and sinapyl alcohol. These are incorporated into lignin in the form of the phenylpropanoids *p*-hydroxyphenyl (H), guaiacyl (G), and syringal (S) respectively. Lignins can account for as much as 20-30% of the dry weight of plant tissue (Jackman & Stanley, 1995). Nawirska and Kwansniewska (2005) found 32.2% of lignin in carrot pomace.

Table 2.5 Sugar composition in mol-% of hemicellulose fraction (Voragen *et al.*, 1983)

Materials	Rha/Fuc	Ara	Xylose	Manose	Galacturonan	Glucose	Uronic acid
Raspberry	2.6	7.3	36.6	6.9	8	25.2	13.7
Strawberries	1.8	4	20.1	9.8	12.9	44.1	7.4
Cherries	5.1	10.8	16.2	12	16.9	28.9	10.1
Papaya	5.9	2.3	49.2	3.4	7.1	20.9	11.3
Pineapple	0.8	23.5	54.4	0.3	5.7	10.3	4.9
Mango	1.3	6.8	44.9	21	1.1	17.8	7.2
Apple	3.8	33.7	21.1	0.6	9.2	20.6	11
Pear	3.7	5.8	52.1	3.4	6.1	21.5	7.4
Carrots	3.3	14.3	4.7	3.9	25.2	26.3	22.3
Cucumber	2.3	5	20	9.3	15.4	36.8	11.3
Onions	1.6	3.5	6.1	2.9	48.4	27	10.5

2.2 Phase and state transition of food polymer

A change in physical state which affects physical properties of materials is a phase transition. The three basic physical states of pure substances are solid, liquid and gaseous states (Roos, 1995). Solid in a crystalline form often melts when it is heated. An amorphous (non-crystalline) solid shows a transition when it softens as the temperature is raised (Sperling, 2006; Williams, 1971). A transition of physical state is caused by a change in temperature or pressure and can be observed by a change in heat capacity, viscosity or texture (Roos, 1995; Sperling, 2006). Water is a substance that can be in those three basic physical states perfectly. Since it is the main component in foods, the change in physical state of water seems to have a lot of effects on the phase change of foods. The mixture components of foods generally have their transition over a range of

temperatures below or above the transition point of the pure principle component (Roos, 1995; Bhandari *et al.*, 1997).

Crystalline polymers will have some amorphous portion (Seymour, 1971; Newey & Weaver, 1990; McCrum *et al.*, 1991). The same sample of a polymer can have both a glass transition and a melting temperature. But only the amorphous portion undergoes the glass transition, and the crystalline portion undergoes melting only. The polymer chains that melt are not the chains that undergo the glass transition (Seymour, 1971; Williams, 1971; Cahn *et al.*, 2005).

The combination of temperature, moisture content and time influences state changes of substances (Roos, 1995; Franks & Murase, 1992). Nucleation and crystallisation in aqueous solutions might occur in normal cooling processes. With rapid cooling, the solute might become a water soluble amorphous solid (Franks & Murase, 1992). Since the main components of foods are mixtures of carbohydrate, protein, minerals and fat, the physical states of foods are extremely sensitive to water content (Roos, 1995).

2.2.1 Melting of crystalline polymers and sugars

The melting of crystalline polymers occurs and continues until complete melting at a constant temperature (the melting point), even though heat is still added to the polymers. Melting requires the latent heat of melting and none of the heat goes into raising the temperature. Once the polymer has melted, the temperature begins to rise again, but now it rises at a slower rate. The molten polymer has a higher heat capacity than the solid crystalline polymer (Cahn *et al.*, 2005). Any change brought about by addition or removal of heat, such as melting, freezing, boiling or condensation, which has a latent heat involved, is called a first order transition (Roos, 1995; Cahn *et al.*, 2005).

Sugars in crystalline form melt over a temperature range, rather than at a well-defined single temperature. The phenomenon is subject to a strong hysteresis effects (Cahn *et al.*, 2005). A study in the melting behaviour of D-sucrose, D-glucose and D-fructose by Hurtta *et al.* (2004) found that sugars did not have sharp melting temperatures. The melting endotherms (detail about the melting endotherm of sugar from DSC scans is in Section 4.6.12) of sugars are sensitive to water, impurities and crystallinity. Some sugars may caramelize and become brown concomitantly with the melting process and they may

also decompose before melting. Hurtta *et al.* (2004) reported melting temperature range of D-sucrose is 160-192 °C with general values of 185-190 °C. The melting range of D-glucose is 146-165 °C and that of D-fructose is 102-130 °C. Table 2.6 shows various melting temperature of D-sucrose, D-glucose and D-fructose from many references reported by Hurtta *et al.* (2004). The melting temperatures may differ between sugar anomers. •- and • anomers of the same sugar are in equilibrium in water, but in the crystalline state one anomer dominates.

Table 2.6 Literature values of melting temperatures of D-sucrose, D-glucose and D-fructose (Hurtta *et al.*, 2004)

References	Melting temperature (°C)		
	D-Sucrose	D-Glucose	D-Fructose
Shallenberger & Birch (1975)	160-186	146(•)	102-104
		148-150(•)	
Broido *et al.* (1966)		146	
Roos (1993)	(173) 190	(143) 158	(108) 127
Raemy & Schweizer (1983)	(160) 185	(135) 150	(80) 115
Slade & Levine (1988)	192	158	124
Ramos-Sanchez *et al.* (1988)	180	156	121
Wungtanagorn & Schmidt (2001)		(158) 146	(114)132
Fan & Angell (1995)			105
Saleki-Gerhardt & Zografi (1994)	188		
Orsi (1973)		165	120
Gloria & Sievert (2001)	188		
Vanhal & Blond (1999)	190		
Lide (1993-1994)	185-186	146(•)	103-105
		150(•)	
Hurtta, *et al.* (2004)	179.7±0.2	148.6±0.3	103.8±0.4
	186.8±0.5	146.4±3.4	103.2±0.2

2.2.2 Crystallization of sugar

Walstra (2003) stated that a crystal consists of a material in a solid state in which the building entities, molecules, atoms or ions, are closely packed so that the free energy of the material is at minimum. Crystals are often found in foods and during food processing

and include ice, sugars, salts, and triacylglycerols (Roos, 1995; Walstra, 2003). It is a complex process often with three steps: nucleation (formation of nuclei), propagation (crystal growth) and maturation (crystal perfection) (Roos, 1995). Fuisz *et al.* (1993) stated that the growth of crystals involves simultaneous transfer of heat and mass in a multi-phase, multi-component system. In addition, fluid and particle mechanics and thermodynamic instability further complicate the conditions involved. Supersaturation of sugar induces crystallization. Nucleation of sugar crystals during supersaturation is relatively uncontrollable. Consequently, the size and shape of the resulting crystals are unpredictable. Roos (1995) referred to Flory (1953) to explain that crystallization takes place in polymers that have a sufficiently ordered chain structure.. Nucleation and crystallization of polymers occur slowly in comparison with low molecular weight compounds. The slow crystallization is due to the restrictions of molecular motions that are required for molecular arrangements to form the crystalline structure.

One of the methods for producing microcrystalline sugar was by concentration of a solute in the presence of seed crystals added thereto followed by further removal of solvent. This method produces sugar crystals having an average size in the range of 325 – 425 microns (Dmitrovsky *et al.*, 1976).

A process for the crystallization of sugar which requires heat intensive concentrating and heating for nucleation was suggested by Chen *et al.* (1982). The crystallization of sugar syrups was by concentration of the material to a solids content of 95-98% by heating to a temperature of about 107 °C - 150 °C. The resulting concentrated syrup was maintained at a temperature not less than 116 °C to prevent premature crystallization, and then a premix was added. The premix consisting of an active ingredient such as a volatile flavour, an enzyme, an acidic substance such as ascorbic acid, a fruit juice concentrate, or a high invert sugar substance. The combination was subjected to impact heating until a crystallized sugar product with the active ingredient is formed with moisture content less than 2.5%.

A process for the crystallization of sugar resulting from the transformation of an amorphous shearform sugar mass (a bi-dimensionally stabilized sugar crystalline frame) to a new crystalline sugar was invented by Fuisz, *et al.* (1993). The transformation was presented by forming a bi-dimensionally stabilized sugar crystalline frame from an outer

portion of the amorphous shearform mass followed by conversion of the remaining portion of the mass to a substantially crystalline structure which retains the cross-sectional dimension of the sugar crystalline frame. The amorphous shearform masses were produced in the shape of elongated needles or rods. Each rod had an outer portion which forms the surface of the rod and a remaining portion which was the amorphous mass within the body. Therefore, the process and product consisted of a crystalline frame first formed from the outer portion and a completely crystalline structure built thereon by conversion of the remaining portion of the amorphous mass to crystalline form. The stability of the bi-dimension was achieved by initially establishing the crystalline frame and ensuring that the conditions were controlled to maintain the frame during conversion. This was done by contacting shearform amorphous sugar with water in a substantially non-aqueous gaseous environment at a rate and in an amount which crystallizes amorphous sugar on the outer portion of the mass. Afterward, conversion was accomplished by continued controlled contact of the shearform amorphous mass with water at a rate and in an amount which maintains the shell and permits the remaining portion of the mass to crystallize.

2.2.3 Amorphous glassy state

An amorphous substance is a substance at a non-equilibrium and non-crystalline state. When saturation conditions prevail and a solute remains non-crystalline the supersaturated solution is amorphous (Fenema, 1996). An amorphous solid is generally called a glass if it exhibits a glass transition and is characterized by a viscosity of greater than 10^{12} Pa s (Fenema, 1996, Cahn *et al.*, 2005; Sperling, 2006, Allen, 1993; Roos, 1995). A substance existing as an amorphous solid is said to be in a glassy state (Cahn *et al.*, 2005).

An amorphous material can be produced by a rapid cooling of solution or removal of solvent water (Chiou & Langrish, 2007). Freeze drying and spray drying are common methods to produce powder in an amorphous form. Amorphous materials produced by different methods have different physical properties, such as particle surface area, size and structure which make their thermal transitions differ (Haque & Roos, 2006). In the amorphous state of spray dried materials, the mixture of low molecular weight sugars present in fruit and vegetable juices could be made as either a completely amorphous

product or there could be some microcrystalline regions dispersed in the amorphous mass (Senoussi *et al.*, 1995).

2.2.4 Glass transition

Definition and mechanism of glass transition

The glass transition is a transition that occurs specifically in amorphous materials. The glass transition temperature (T_g) is the temperature at which a supersaturated solution (amorphous liquid) converts to a glass (with falling temperature) or vice versa (Fenema, 1996; Roos, 1995; Williams, 1971; Sperling, 2006). The glass transition relates to the phenomena observed when a supercooled, malleable liquid or "rubbery" (like rubber in appearance such as elasticity, toughness) material is changed into a disordered solid glass upon cooling below T_g, or when this solid form is changed upon heating into a liquid.

The glass transition is a second-order phase transition (Williams, 1971; Roos, 1995; Fennema, 1996; Sperling, 2006). The thermodynamic quantities of enthalpy, entropy and volume of the two phases are the same at the transition temperature. There is no latent heat of the phase change, but there is a discontinuity in the heat capacity, Gibbs energy, specific volume, modulus, refractive index, density, thermal conductivity, and electrical properties (Lievonen & Roos, 2003; Roos, 1995; Newey & Weaver, 1991; Sperling 2006). Figure 2.5 shows the change in volume (a) and modulus (b) during glass transition.

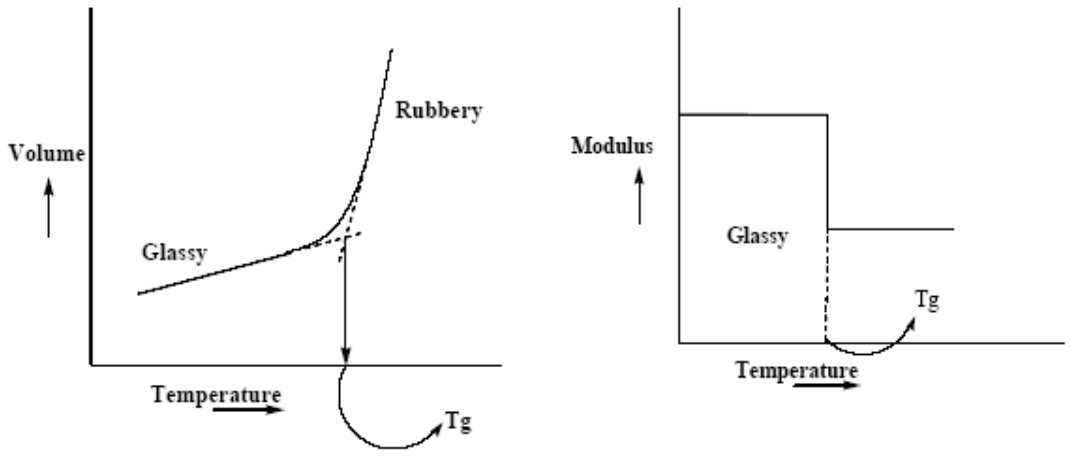

(a) **(b)**

Figure 2.5 Change in physical properties of substance at T_g (Otles & Otles, 2005).

When a material is cooled through its transition, the large amplitude cooperative movements within the material above T_g stop (Allen, 1993; Sperling, 2006; Cahn *et al.*, 2005). The cooling rate must be great enough so that no significant quantity of crystals can form. The critical rate depends on the kinetics of nucleation and growth. Any liquid will form a glass if it is cooled rapidly enough (Cahn *et al.*, 2005, Sperling, 2006). The glass transition occurs over a temperature range, the width of which is controlled by the heterogeneity of the system. The greater the heterogeneity the wider the transition ranges (Allen, 1993).

The glass transition is a kinetic process; the temperature at which the system vitrifies (forms a glass) depends on the cooling rate, the higher the cooling rate, the higher the glass transition temperature (Allen, 1993; Cahn *et al.*, 2005; Williams, 1971). Walstra (2003) stated that the value of T_g depends somewhat on the temperature history and is always below the melting temperature, often by 100 K or more.

For the partially crystalline polymers, the dependence of viscoelastic properties on temperature can be as shown in Figure 2.6. The viscoelastic behaviour with temperature can appear at five regions as glass, leathery, rubbery plateau, elastic or rubbery flow and liquid flow (Slade & Levine, 1991).

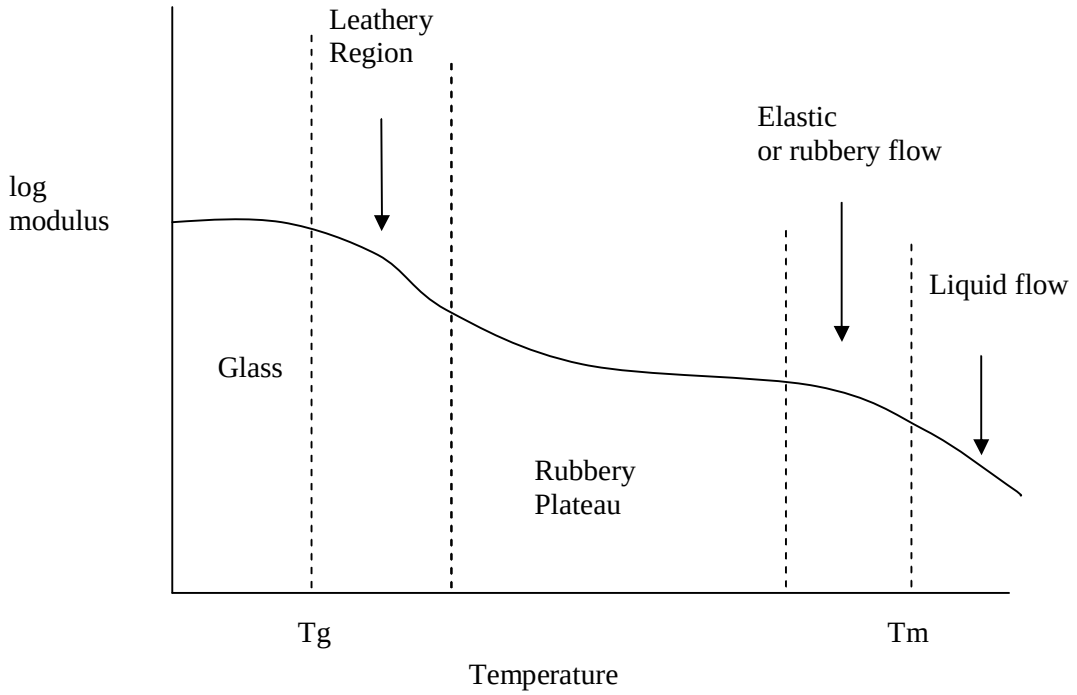

Figure 2.6 A curve of the modulus as a function of temperature, illustrating the five regions of viscoelastic behaviour characteristic of synthetic partially crystalline polymers (Slade & Levine, 1991).

Basic theories of glass transition

There are three basic theories involved in the occurrence of glass transition i.e., free volume theory, kinetic theory and the thermodynamic theory (Sperling, 2006; Roos, 1995). The free volume theory assumes that molecular motion depends on the presence of holes, vacancies or voids that allow molecular movement. The holes between molecules provide the free volume that is needed for molecular arrangement. This theory is based on the change in volume expansion coefficient that occurs at the glass transition (Roos, 1995, Sperling, 2006). Below T_g the local conformational arrangement of the polymer segments are probably independent of both molecular weight and temperature (Sperling, 2006). The free volume theory can be used to relate viscoelastic motion to temperature and time and to explain thermal expansion at temperatures below and above T_g (Roos, 1995).

The kinetic theory of T_g considers the time-dependent characteristics of the T_g and the time-dependent molecular relaxations that take place over the T_g range (Williams, 1971). The kinetic theory assumes that matter may have holes within a molar volume, or it may exist in a no-hole situation with molar excess energy. Removal of holes decreases

volume. In the glassy state the number of holes and their spatial positions become frozen and the molecules cannot move to holes (Sperling, 2006). The change in the number of holes that go through the glass transition yields the change in heat capacity. The most important characteristic of kinetic or relaxation phenomena is that the value of T_g measured depends on the experimental time scale and method of measurements. Values of the T_g reported for any particular polymer may vary over a 10 to 15 °C range (Williams, 1971).

The thermodynamic theory assumes that T_g attains a true equilibrium at an infinite long experiment. The true T_g may be observed at a temperature about 50 °C lower than that observed with common times of experiments (Sperling, 2006). The thermodynamic theory of T_g requires that a glassy phase with an entropy that is negligibly higher than that of the crystalline phase can be formed (Roos, 1995).

The concept in molecular structure has two kinds of factor that affect the temperature of the glass transition in polymers. These two factors are the strength of bonding between the long molecules and their ability to "wriggle" once a section has become free. There are few, if any, instances where changes of molecular structure unequivocally affect one of these factors without affecting the other (Newey & Weaver, 1991).

T_g and state diagrams

Information about glass transition temperatures can be shown by state diagrams, which describe the effect of composition on stability, and present temperature and moisture effects on viscosity, structure, and crystallization. State diagrams may also show the formation of the amorphous state and describe various temperature-moisture and time-dependent phenomena (Slade & Levine, 1993; Roos, 1995; Sablani *et al.*, 2004).

Figure 2.7 shows a state diagram of a carbohydrate during the formation of an amorphous state. The materials may exist as rubbers or glasses at a concentration higher than the solubility limit. In the rubbery state solutes may become sticky, collapse or crystallize depending on temperature, time and moisture content. In the glassy state below T_g amorphous materials are assumed to be stable. Materials with solute concentrations lower than that in the maximally freeze-concentrated solution (C_g') show ice formation below the equilibrium melting temperature (T_m) but maximum ice

formation is achieved only below the melting point of ice in contact with the maximally freeze-concentrated solute (T_m') but above the T_g of the maximally freeze-concentrated solution (T_g') (Roos & Karel, 1993).

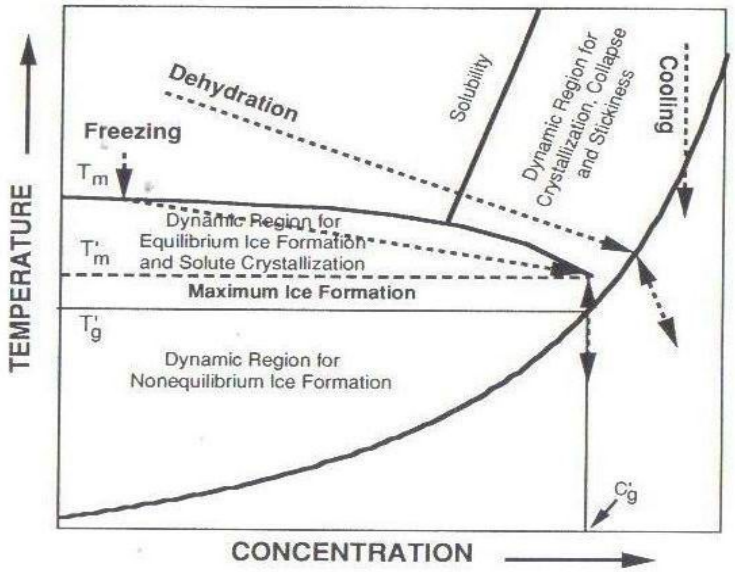

Figure 2.7 Schematic state diagram showing processes which result in formation of an amorphous state in carbohydrates (Roos & Karel, 1993).

Influence of T_g on freeze drying

Freeze drying is a low temperature process that produces product with high quality nutrition, aroma and taste. The processes included in freeze drying are freezing of a liquid product followed by sublimation of water. Evaporation of moisture from product during freeze drying produces a porous final product. Since the moisture removal does not pass through a liquid phase, the structure of the product remains natural which the solid network should be able to hold the porous structure (Bhandari & Howes, 1999).

The freeze drying process involves three stages: the freezing stage, the primary drying stage and the secondary drying stage.

In practice, materials display one of two different types of freezing behaviour: (a) the liquid phase suddenly solidifies (eutectic formation) at a temperature that depends on the nature of solids in the sample, or (b) the liquid phase does not solidify (glass formation), but rather it just becomes more and more viscous until it finally takes the form of a very stiff, highly viscous liquid. In this case there is no eutectic temperature, but a minimum

freezing temperature (Liapis & Bruttini, 2007). This temperature is the glass transition temperature of the materials suggested by many researchers (To & Flink, 1978; Bhandari & Howes, 1999).

A summary of the freeze drying process explained by Liapis and Bruttini (2007) is as follows. In the freezing stage, the material to be freeze dried is cooled down to a temperature at which all the material is in a frozen state. This temperature is below the solidification temperature of materials. If it is a solution with an equilibrium phase diagram that presents a eutectic point, the freezing temperature has to be set below the eutectic point. The eutectic point of fructose is -9 °C at 0.48 mass fraction of fructose in water (Walstra, 2003). If the material has no eutectic temperature, the freezing temperature will be the possible minimum temperature. According to Roos (1995) the term eutectic refers to crystallization of both solvent and solute, which, in biological materials may occur at freezing temperatures. Binary solutions of food components such as salts and sugars in water often form eutectic solutions. This can happen as both the solute and water crystallize at some temperature below the initial freezing temperature of water in the solution. Apparently, below the eutectic temperature both the solvent and solute exist in the crystalline state. The eutectic behaviour of organic compounds such as sugars is more complicated and their supersaturated solutions often solidify into the glassy state before eutectic crystallization occurs. In sugar mixtures the eutectic behaviour and also crystallization behaviour are affected by the component compounds.

In the primary freeze drying stage, the frozen solvent is removed by sublimation; this requires that the pressure of the freeze drier at which the product is dried is less than or near the equilibrium vapour pressure of the frozen solvent. If the frozen pure water (ice) is processed, then sublimation of pure water at or near 0 °C and at an absolute pressure of 4.58 mmHg (0.611 kPa) could occur. Since the water usually exists in a combined state of food material, the material must be cooled below 0 °C to keep the water in the frozen state. During this stage the temperature of the frozen layer is most often at -10 °C or lower at absolute pressures of about 2 mmHg (0.267 kPa) or less. As the solvent (ice) sublimes the sublimation interface (plane of sublimation), which started at the outside surface (Figure 2.8), recedes and a porous shell of dried material remains. The latent heat of sublimation (2840 kJ/kg ice) can be conducted through the layer of dried material and

through the frozen layer as shown in Figure 2.8. The vaporized water vapour is transported through the porous layer of dried material.

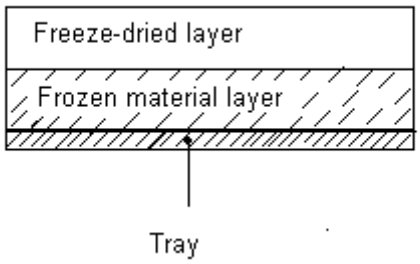

Figure 2.8 Diagram of material on a tray during freeze drying (Liapis & Bruttini, 2007).

The maximum temperature at which the frozen layer remains frozen also depends on the freezing behaviour of material. If the material has a eutectic form, the temperature should not exceed the lowest eutectic, to prevent melting in the frozen layer. The melting at the sublimation surface or any melting that would occur in the frozen layer can cause gross material faults such as puffing, shrinking, and structural topologies filled with liquid solution. When melting has occurred at some point in the frozen layer, the solvent at that point cannot be removed by sublimation. Therefore, there is process failure in the drying of the frozen material because the frozen solvent (water) can no longer be removed from the frozen layer by sublimation alone, and there has also been, at the least, loss in structural stability.

If the material has a glass form and if the minimum freezing temperature exceeds the glass transition temperature then the phenomenon of collapse can occur (To & Flink, 1978; Bhandari & Howes, 1999). The glass transition temperature depends on the water content of material to be freeze-dried (Walstra, 2003).

The shape of the pores, the pore size distribution, and pore connectivity of the porous network of the dried layer formed by the sublimation of the frozen water during the primary drying stage depends on the ice crystals that formed during the freezing stage. This dependence is of extreme importance because the parameters that characterize the mass and heat transfer rates in the dried layer are influenced significantly by the porous structure.

In many cases, at the end of the freezing stage, 65-90% of the initial water is in the frozen state and the remaining (10-35%) of the initial water is in the sorbed (non-frozen) state.

The secondary drying stage involves the removal of water that did not freeze (sorbed or bound water). The desorbed water vapour is transported through the pores of the material that is dried. The bound moisture present is due to physical adsorption, mechanical adsorption and water of crystallization. Its effect on the drying rate and overall drying time is very significant. The bound water is removed by heating the product under vacuum. But the amount of heat that can be supplied to the product cannot be increased freely because there are certain constraints that have to be satisfied during the secondary drying stage. The constraints have to do with the moisture content and the temperature of the product; these two variables influence the structural stability as well as the product stability during and after drying. The product temperatures at this stage are usually between 10-35 °C for heat sensitive product and 50 °C or more for less heat sensitive products.

Jayaraman and Das Gupta (2007) discussed that the aspect that determined the structure of fruit juice during freeze drying is the phenomenon of collapse. Freezing of foods causes aqueous solutions to separate into two phases: ice crystals and concentrated aqueous solution. The properties of this concentrated aqueous solution depend on composition, concentration and temperature. If during drying the temperature is very low, the mobility in the extremely viscous concentrated phase is so low that no structural changes occur during drying. But if the temperature is above a critical level (known as the collapse temperature), mobility of the concentrated solution phase may be so high that flow and loss of original structure occurs. This is known as the phenomenon of collapse.

Effect of crystallinity on T_g

Semicrystalline polymers also exhibit a glass transition, though only in the amorphous portions of the polymers. The molecular-motion restricting crystallites often increases T_g.. Sperling (2006) discussed that sometimes the glass transition of highly crystalline polymers appeared to be masked. The T_g of many semicrystalline polymers might appear as double glass transitions (Boyer, 1973). The lower T_g (T_g (L)), relates to the portion that

is completely amorphous or relatively free from restraints caused by the presence of crystalline material. The upper T_g (T_g (U)), arise from the semicrystalline part under restraint by crystallites and varies with crystallinity and morphology. The lower transition correlates with the molecular mobility and should be used in all correlation with chemical structure (Boyer, 1973). A numbers of researchers have found double T_g in semicrystalline polymers (Ivin, 1977).

2.2.5 Prediction of glass transition temperature

The Gordon-Taylor equation is a very well-known equation that is used to predict the glass transition temperature of binary mixtures of water and a single solute (Roos, 1995; Champion *et al.*, 1997).

$$T_g = \frac{w_1 T_{g1} + k w_2 T_{g2}}{w_1 + k w_2} \qquad (2.1)$$

where the value of k is obtained by the fit of the equation to the experimental T_g values for different concentrations of mixtures. w_1 is the mass fraction of the solute, T_{g1} is glass transition temperature of anhydrous solute, and w_2 and T_{g2} are corresponding values for pure water. T_{g2} is often taken as -135 °C. From theory $k = \Delta c_{p2}/\Delta c_{p1,}$ where Δc_p are values of the change of specific heat capacity of the components at T_g. Exact Δc_p values are difficult to obtain experimentally and various values have been reported for amorphous materials (Roos, 1995a). Roos and Karel (1991) experimentally determined T_g values at various water contents to calculate k values for sugars. Roos (1993) reported that the k value of various sugars could be related to their anhydrous T_g value. A linear relationship between k and T_g was used to derive k values for various carbohydrates (Roos, 1993). Figure 2.9 shows k values from equation 2.1 of sugars as a function of the anhydrous T_g.

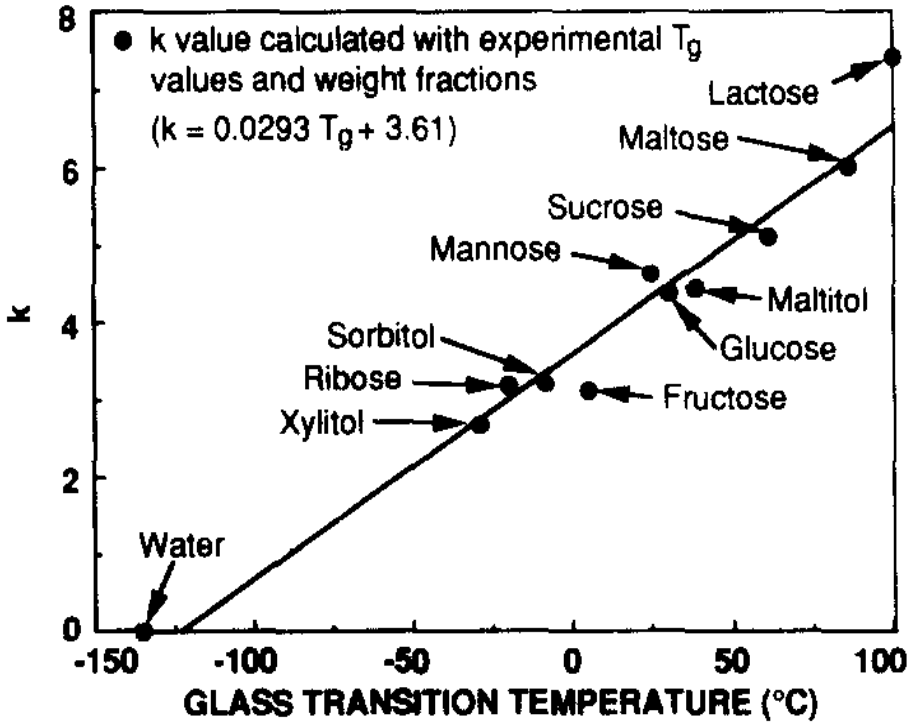

Figure 2.9 *k* value from equation 2.1 of sugars as a function of the anhydrous T_g. The regression equation obtained allows prediction of the constant *k* in equation 2.1 based on the anhydrous T_g value (Roos, 1993).

The Couchman and Karasz equation has been used for two or more components and when a carrier was used in spray drying (Bhandari *et al.*, 1999; Roos, 1995).

$$T_g = \frac{x_1 T_{g1} + (\Delta c_{p1} / \Delta c_{p2}) x_2 T_{g2}}{x_1 + (\Delta c_{p1} / \Delta c_{p2}) x_2} \qquad (2.2)$$

where x_1, T_{g1}, • c_{p1} and x_2, T_{g2}, • c_{p2} are the mole fraction, glass transition temperature and change in heat capacity at the glass transition of the components 1 and 2 respectively.

Linear relationship relates to binary mixture of dry homologous oligosaccharides

A linear relationship for binary mixtures of dry homologous oligosaccharides is given in equation 2.3. This model has been applied to maltotriose/glucose and maltohexaose/glucose mixtures (Avaltroni *et al.*, 2004).

$$T_g = x_1 T_{g1} + x_2 T_{g2} \qquad (2.3)$$

where x is the mass fraction.

Prediction of T_g of a multicomponent system

For an n-component system, Bhandari and Howes (1999) suggested that equation 2.2 can be expanded as;

$$T_{gm} = \frac{\sum_{i=1}^{n} w_i \Delta c_{pi} T_{gi}}{\sum_{i=1}^{n} w_i c_{pi}} \qquad (2.4)$$

where T_{gm} is the glass transition of the mixture w_i is the mole fraction of component i, Δc_{pi} is the change in heat capacity of component i between glassy and rubbery states and T_{gi} is the glass transition temperature of component i.

2.2.6 Crystallization in food powders

Jouppila and Roos (1994) found that within certain conditions amorphous powders transformed to crystals which have a lower energy state (Jouppila & Roos, 1994). The transition is time-dependent and occurs when water content or temperature exceeds a critical value (Haque & Roos, 2006). Temperatures above T_g allow molecular mobility and the rearrangement of molecules to the crystalline state. Crystallization in the solid glassy state below T_g is kinetically inhibited (Levine & Slade, 1986). The rate of crystallisation of amorphous materials is highest somewhere between T_g and the melting temperatures. The crystallisation rate of lactose powder has been found to increase with increasing temperature difference between storage temperature and T_g (Haque & Roos, 2004).

Researchers have found that water induces crystallization in amorphous foods (Burnett *et al.*, 2004; Chiou & Langrish, 2007). The study in time-dependent crystallization of amorphous food related materials found that the rate of crystallization of glucose and sucrose from the amorphous state was dependent on moisture content (Roos, 1995). In amorphous foods, crystallization may occur concurrently with other changes in the physical structure. Both the rate of structural transformations and crystallization increase as the viscosity decreases with increasing T-T_g (Roos, 1995).

Usually the T_g values of stable food powders are well above ambient temperature. However, most food materials show substantial absorption of water at high relative humidity, which facilitates crystallization as the T_g is then depressed below the ambient temperature (Roos, 1995; Haque & Roos, 2004; 2005; 2006). Crystallization releases absorbed water that, in closed containers, further plasticizes the remaining amorphous portion of the material (reducing T_g). As a result, T-T_g increases, which causes an increasing rate of crystallization with increasing crystallinity. Materials which have moisture transfer with the environment, such as during determination of adsorption isotherms, show loss of water in proportion to crystallinity. Thus, the moisture content in the amorphous part remains fairly constant, and crystallization proceeds at a rate defined by a constant T-T_g (Roos & Karel, 1992).

Crystallization causes the greatest changes to the physical properties of food polymers. It may considerably affect food stability, and it may cause impaired rehydration properties of food powders. It also affects textural properties, for example crystallization of starch in bakery products results in staling. Lactose crystallization in milk powders leads to increased free fat and flavour deterioration, and it may also promote non-enzymatic browning. Amorphous sugars are often used to entrap flavour compounds, which become protected from oxidation and release, probably because of slow diffusion in the glassy state. The crystalline materials are not able to entrap other compounds, which become completely released after crystallization. As a result, volatiles are lost and lipids become exposed to oxygen (Roos, 1995). On the other hand, crystalline materials are not sticky. Chiou and Langrish (2007) suggested that the problems of stickiness in spray drying of foods might be reduced by increasing the crystalline fraction of spray dried powders.

A study of crystallization of the amorphous component in spray dried powders found that the higher molecular weight component with higher T_g took longer to crystallize (Chiou & Langrish, 2007). Crystallization of low molecular weight materials can also be delayed by incorporation of high molecular weight substances or other sugars (Roos, 1995).

2.2.7 Stickiness and sticky point temperature (T_{st})

Stickiness is the inclination of powder to adhere to a contact surface including cohesion of particles and adhesion of powder to the chamber wall, roof, cyclone and collection ducts (Barbosa-Canovas & Juliano, 2005). It is associated with the presence of high concentrations of mono- and disaccharide sugars, including acids component of fruit juice (Bhandari *et al.*, 1997; Adhikari *et al.*, 2001; Barbosa-Canovas & Juliano, 2005). The cohesion and adhesion of materials depend on the chemical composition, moisture content, contacting surface properties and operating conditions. Roos (1995) indicated that the main cause of stickiness is plasticization of particle surfaces which allows a sufficient decrease of surface viscosity for adhesion. In amorphous powders, adhesion and cohesion occur when the particle surface has a critical viscosity between 10^7 and 10^{12} Pa.s (Downton *et al.*, 1982; Sperling, 2005, Boonyai *et al.*, 2004, Allen, 1993). This critical viscosity occurs at temperatures 10-20 °C above T_g and varies with the moisture content of the powders (Roos & Karel, 1991). The magnitude of the adhesion force depends on the contact area and the strength of the bridge material (Barbosa-Canovas & Juliano, 2005).

Interaction of water with solids is the main cause of stickiness and caking in low moisture food powders (Barbosa-Canovas & Juliano, 2005). Water plasticization in foods reduces viscosity and improves the molecular mobility of the system which allows liquid and solid bridges formation and caking (Peleg, 1993). (Detail about water plasticization in foods is in Section 2.2.10).

The amorphous and glass transition state of different sugars, such as sucrose, maltose, glucose and fructose, influence drying performance and T_g of the juice powders (Bhandari *et al.*, 1997; Barbosa-Canovas & Juliano, 2005; Goula, *et al.*, 2008). The mechanism of sticking and caking of amorphous sugars is through the phase change of the amorphous sugars from a glass to a rubber at temperatures above T_g (Roos & Karel, 1993; Roos, 2002; Foster *et al.*, 2006). T_g has been used as the most fundamental indicator of the sticky behaviour of any sugar and acid-rich foods (Slade *et al.*, 1993; Roos & Karel, 1991).

The sticky point temperature is the temperature at which dry food powder transforms to a viscous state. If a free-flowing solid at certain moisture content is heated beyond a

certain temperature, its flow properties change abruptly. The temperature when the particles begin to stick to each other is the sticky point temperature (Lockemann, 1999; Rahman, 1995; Adhikari *et al.*, 2003). The sticky point temperature indicates appearance of a powdery material when it moves from a non-sticky particulate form to a sticky lumpy material. It will not provide a true picture of the temperature and moisture at which the surface of a drop is most sticky, because the drying is not a reversible process (Adhikari *et al.*, 2003). Jaya and Das (2007) stated that the sticky point temperature is the value at which a powdery material will start caking. The stickiness of dried powders normally develops when the transition from glassy to rubbery takes place. As a result, stickiness and adhesion phenomena of foods should not occur below T_g (Barbosa-Canovas & Juliano, 2005). In addition, if the glass transition temperature of the powder is increased, the sticky point temperature will also increase.

Foster *et al.* (2005) showed that the rate of change in powder cohesiveness with time increases as the T-T_g increases. For amorphous sucrose at low T-T_g values (T-T_g • 10 °C), the change in cohesiveness with time was slow and only a small change can be seen which did not result in a noticeably sticky or lumpy powder. The T-T_g values of 16-22 °C gave much higher changes in cohesiveness with time. Foster *et al.* (2005) found the T-T_g values for instantaneous sticking of materials as shown in Table 2.7.

Table 2.7 T-T_g values for the instantaneous sticking of materials (Foster *et al.*, 2005)

Sugar	T-T_g (°C)
Lactose	25.0
Sucrose	23.0
Maltose	19.0, 25.3, 29.0
Glucose + Lactose	35.0, 37.4
Galactose + Lactose	30.8
Fructose + Lactose	41.3

Paterson *et al.* (2006) showed the relationship of the glass transition of lactose and the stickiness of dairy powder that temperature above T_g of lactose at around 37.5 °C at various relative humidity was a critical temperature where the dairy powder surface became sticky. This relationship is shown in Figure 2.10.

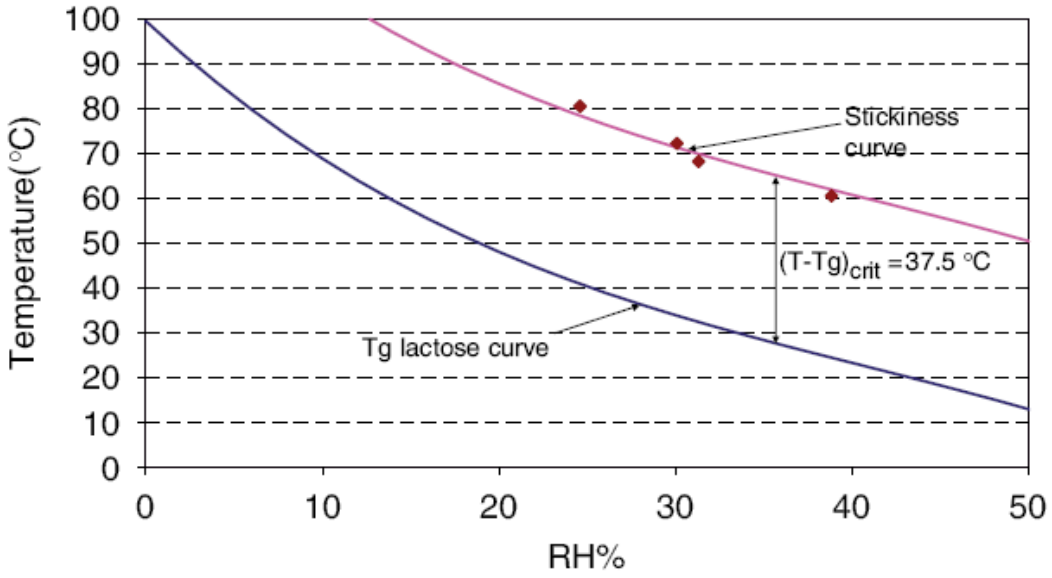

Figure 2.10 The stickiness curve of the whole milk powder shows the $(T\text{-}T_g)_{critical}$ above the T_g line of lactose at various RH (Paterson *et al.*, 2006).

The sticky point temperature of orange juice powder using maltodextrin, liquid glucose and methylcellulose as carriers was found to be at around 44 °C at 2% moisture (Chegini *et al.*, 2008). The sticky-point temperature of tomato powder increased when moisture content decreased (Van Arsdel, 1973). Figure 2.11 shows the relationship of moisture content, glass transition temperature and sticky point temperature of vacuum dried mango, pineapple and tomato with added maltodextrin and tricalcium phosphate (Jaya & Das, 2007). In that study, the ratios of maltodextrin (DE 38): fruit pulps were at 0.093:1, 0.065:1 and 0.033:1 respectively. The tricalcium phosphate at 0.015:1 was used for anti-caking in the three types of vacuum-dried powder. The difference between glass transition temperature and sticky point temperature however were found from 2.5 to 15.5 °C depended on the nature of raw materials and amount of maltodextrin. The difference of these two temperatures was also found to vary with moisture contents. For pineapple powder, the glass transition and sticky point temperature appeared to be very close to each other (minimum difference of around 2.5 °C).

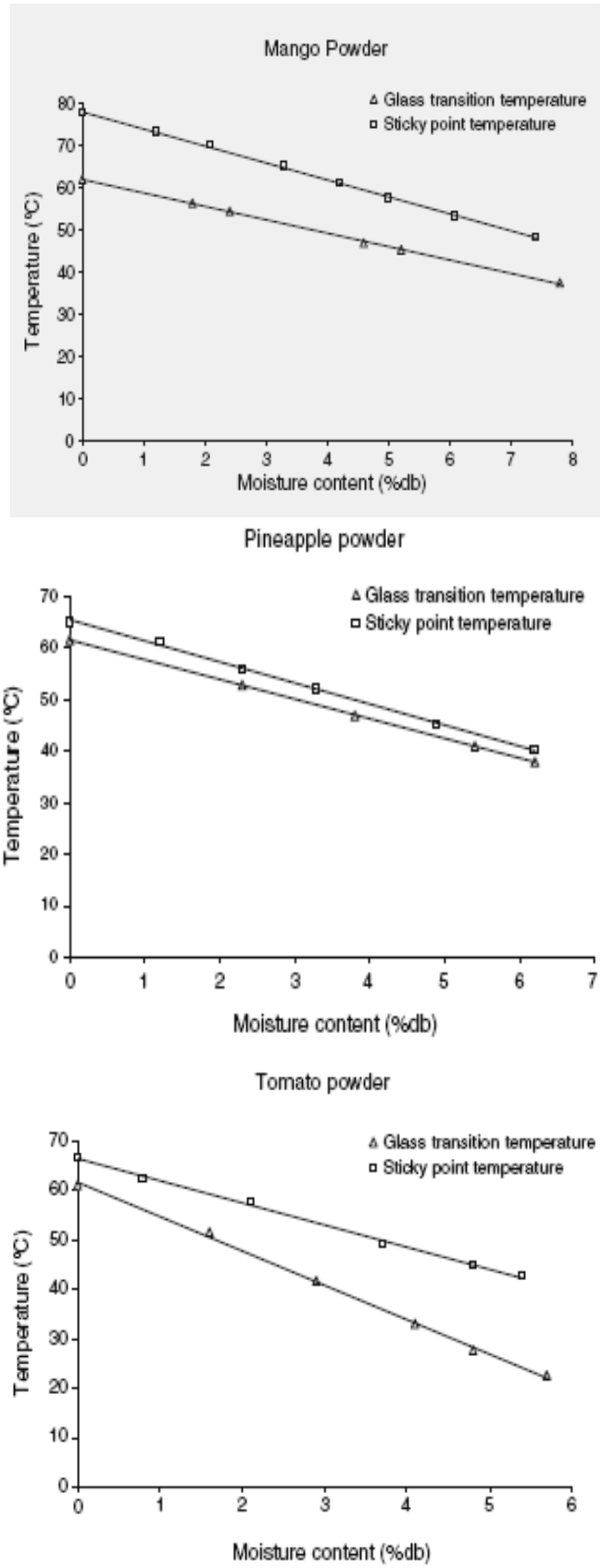

Figure 2.11 The relationship of moisture content, glass transition temperature and sticky point temperature of vacuum dried mango, pineapple and tomato with added maltodextrin and tricalcium phosphate (Jaya & Das, 2007).

2.2.8 Sugars and acids in fruit juice associated to stickiness

Powder stickiness is more specifically associated with the presence of high concentrations of sugar and acids in the product. The physical properties of individual sugars and acids in fruit juice influence differently the powder properties such as hygroscopicity, solubility, melting point and T_g. Stickiness may be due to the overall influence of all properties of sugars and acids during spray drying. The sugars and acids in fruit juice include fructose, dextrose, sucrose, lactose, maltose, glucose, maltrins, citric acid and malic acid. There is a range of possible compositions, but the physical properties may often be due to a principle component (Roos, 1995). The sugars and acids with higher T_g and melting point temperature are easier to dry (Bhandari *et al.,* 1997).

Among the various sugars in fruit juice, fructose is the most difficult sugar to successfully spray dry (Bhandari *et al.,* 1997). Fructose always exists as a very viscous and deformable plastic and seems never to attain a perfect solid state during normal spray drying conditions. Pure fructose solutions remained completely sticky even though their moisture approaches zero (Adhikari *et al.,* 2003). Increasing fructose content in mixtures decreases T_g and increase stickiness of the mixtures (Roos, 1995).

2.2.9 Plant fibre components and T_g.

A study of the T_g of carrot cell wall components at low moisture (0-20% wb) found the T_g reduced with increasing water content as expected. The T_g of cell wall component was less affected by water at high levels (Geoget *et al.,* 1998).

Georget *et al.* (1999) studied the thermal transitions of freeze-dried carrot and its cell wall component and found that the DSC re-scan showed that water is directed to the sugar-rich phase resulting in a reduction of T_g, similar to the T_g of sucrose. The T_g of the cell wall-rich phase was greater than that of the sugar-rich phase. This value shifted to a higher temperature both with decreasing moisture content and as amorphous polysaccharides were progressively removed to leave a cellulose-rich residue (Georget *et al.,* 1999). Table 2.8 shows cell wall components of carrot fibre and their T_g values from various researchers. It is expected that the T_g of carrot fibre obtained in the current research will be related to the values given Table 2.8 together with the composition discussed in Section 2.1.2.

Table 2.8 T_g of cell wall component in carrot fibre (Georget *et al.*, 1999; Salmen *et al.*, 1984)

Materials	T_g (°C)
Overall cell wall material	65-67
Cell wall without ionic cross-linked pectins	58-60
Cell wall without esterified pectins	94
Cellulose	103(220[a])
Lignin	200(205[a])
Hemicellulose	200(220[a])

[a] from Salmen *et al.* (1984)

Specific characteristics of T_g of lignin and hemicelluloses at different moisture contents had been reported by Slade and Levine (1991) (see Section 2.2.10).

Aguilera *et al.* (1998) used several extraction methods to isolate cell wall component from apple tissue to find the glass transition temperature of the fibre by DSC. The DSC scans at 10 °C min^{-1}, showed that there were no transitions in the thermograms below 200 °C.

2.2.10 T_g of anhydrous sugars and some food components

The T_g values of various anhydrous mono-, di-, and oligosaccharides have been determined experimentally (Roos, 1995). T_g values for common carbohydrates are given in Table 2.9 with respective Δc_p values, melting points (T_m) and the T_m/T_g ratio. The T_m/T_g values are useful in the characterization of the physical properties of single amorphous components. Sugars with high T_m/T_g values tend to crystallize rapidly (Roos, 1995). The most important single factor affecting T_g values of anhydrous food homopolymers, such as glucose polymers (maltodextrins), is molecular weight (see Table 2.10) (Bhandari & Howes, 1999). Researchers observed that the T_g of homopolymers was related to their molecular weight (M) decreasing linearly with increasing values of $1/M$. Similarly, the T_g of maltodextrins has been shown to decrease with increasing $1/M$ (Roos, 1995; Bhandari & Howes, 1999).

Table 2.9 T_g, change of specific heat at T_g (• c_p), melting temperature (T_m) and the ratio of T_m/T_g for anhydrous pentoses, hexoses and disaccharides (Roos, 1993)

Compound	T_g(°C)	(• c_p) (J/g°C)	T_m (°C)	T_m/T_g [a]
Pentose				
Arabinose	-2	0.66	150/(160)	1.56(1.60)
Ribose	-20	0.67	70(86)	1.36(1.42)
Xylose	6	0.66	143(157)	1.49(1.54)
Hexose				
Fructose	5	0.75	108(127)	1.37(1.44)
Fucose	26	-	133(145)	1.36(1.40)
Galactose	30	0.50	163(170)	1.44(1.46)
Glucose	31	0.63	143(158)	1.37(1.42)
Manose	25	0.72	120(134)	1.32(1.37)
Disaccharide				
Lactose	101	-	-(214)	-(1.30)
Maltose	87	0.61	--	--
Sucrose	62	0.60	173(190)	1.33(1.38)

[a] Onset temperature for the transitions; the values in parenthesis refer to the peak temperature values of the melting endotherms; the ratios of T_m/T_g based on Kelvin unit.

Many polymers and most carbohydrates have the T_m/T_g ratios between 1.3 and 1.5 based on the onset values of the transitions obtained using a DSC (Table 2.9) which the melting temperature is about 100 °C above T_g (Slade & Levine, 1991).

Table 2.10 Glass transition temperature of various food materials.

Food materials	T_g (°C)
Citric acid[a]	6
Tartaric acid[a]	18
Malic acid[a]	-21
Lactic acid[a]	-60
Maltodextrins DE 36 MW 550[b]	100
Maltodextrins DE 25 MW 720[b]	121
Maltodextrins DE 20 MW 900[b]	141
Maltodextrins DE 10 MW 1800[b]	160
Maltodextrins DE 5 MW 3600[b]	188
Starch[c]	243
Water[c]	-135

[a] Bhandari *et al*., 1993 [b] Roos and Karel, 1991(b); [c] Roos, 1995

The T_g values of anhydrous high molecular weight food polymers, such as polysaccharides and proteins, are usually high and the substances tend to decompose at temperatures below T_g. Thus, T_g values of many anhydrous food polymers cannot be experimentally determined (Roos, 1995; Bhandari & Howes, 1999).

Based on the T_g values of maltodextrins, Roos and Karel (1991) predicted a T_g value for anhydrous starch of 243 °C, which was higher than 151 °C predicted by van den Berg (1981), but close to 227 °C reported by Orford *et al.* (1989) (Roos, 1994). The T_g of fructose reported by Bhandari *et al.* (1999) was 14 °C which is higher than that reported by Roos (1993) (5 °C) probably due to a difference in sample preparation and measurement methods. The values of T_g from Tables 2.9 were from DSC heating scan at 5 °Cmin^{-1}. In reporting some of the values of T_g from Table 2.10 did not indicate the experiment details.

The T_g of most water soluble food components such as carbohydrate and protein are high and increase with molecular weight. Amorphous carbohydrates and their hydrolysis products are significantly plasticized by water, which is observed from a rapidly decreasing T_g with increasing water content (Bhandari *et al.*, 1993; 1997; 1999). The detail of this phenomenon is presented in Section 2.2.10.

T_g of dry sugar mixtures

The glass transition temperatures of dry sugar mixtures depend on the individual T_g and the amount of each sugar in the mixtures. The T_g (mid-point) of dry mixtures of fructose and sucrose and dry mixtures of fructose and glucose using DSC at a heating rate of 10 °Cmin^{-1} from Finegold *et al.* (1989) are in Table 2.11. Increasing fractions of sugar with lower T_g in the mixture resulted to decrease T_g of mixtures. The data from Table 2.11 show that fructose, which has the lowest T_g among the three sugars, seems to be a plasticizer in the mixtures with glucose and sucrose. From Table 2.11 it was shown that the T_g of the same sample gave different values. For the 0.75 mole fraction of fructose in sucrose the variation in T_g values of the same material ranged from 28 to 37 °C.

Table 2.11 T_g of dry mixture of fructose and sucrose, and fructose and glucose (Finegold *et al.*, 1989)

Mixture of dry fructose and glucose		Mixture of dry fructose and sucrose	
Mole fraction of fructose	T_g(°C)	Mole fraction of fructose	T_g(°C)
0.00	38	0.00	57
0.25	28	0.10	57
0.50	22	0.15	53
0.75	17	0.25	52
1.00	16	0.25	51
		0.50	45
		0.50	44
		0.75	37
		0.75	32
		0.75	28
		1.00	18

Table 2.12 shows T_g of sugars from various literature source. The variation of the data is very obvious. Roos (1995) had reported T_g onset of fructose, glucose and sucrose at 5, 31 and 62 °C respectively. Various researchers had reported a range of the T_g of materials. The T_g of sucrose had been reported in a range of 52 to 70 °C. The T_g of glucose varies from 20 to 38 °C and that of fructose had found between 5 to 16 °C.

Table 2.12 T_g of anhydrous sugars from various literature sources

Sugars	T_g (°C)	References
fructose	5	Roos (1993)
	7	Walstra (2003)
	10	Levine & Slade (1988); Ablett *et al.*(1993)
	14	Bhandari *et al.* (1997)
glucose	16-18	Finegold *et al.*, 1989)
	31	Levine & Slade (1988);
	31	Walstra (2003); Roos (1993);
	31	Bhandari *et al.* (1997)
	20 to 35	Ollett & Parker (1990)
sucrose	38	Finegold *et al.*, 1989)
	52	Levine & Slade (1988)
	57	Finegold *et al.*, 1989)
	62	Roos (1993); Bhandari *et al.* (1997)
	67	Ollett & Parker (1990)
	70	Walstra (2003)

T_g of some fruit juice

Most of the studies of T_g of fruit juices have been conducted for juice solutions. This study concerns T_g of anhydrous and low moisture content of spray dried fruit juice mixed with carriers. Aguilera *et al.* (1998) reported the T_g of freeze dried apple and apple juice at 11 °C detected by DSC at 10 °C min^{-1}. Wang *et al.* (2008) used the Gordon-Taylor model to predict the glass transition temperature of anhydrous freeze dried Chinese gooseberry (kiwi fruit) and reported the value of 23.2 °C with k = 5.72.

2.2.11 Water plasticiser in foods

A plasticizer is a small molecule which will get in between the polymer chains, and space them out from each other (mobility enhancer). This action is called free volume increasing. When polymers have more free volume they can slide past each other more easily. When they slide past each other more easily, they can move around at lower temperatures than they would without the plasticizer. Thus a plasticizer can lower the T_g of a polymer (Sperling, 2006; Roos, 1995; Slade & Levine, 1991; Walstra, 2003).

The physical state of the food component compounds are affected by water content. Food solids become soft if the water content is increased (Slade & Levine, 1993; Roos, 1995; Bhandari & Howes, 1999). Food materials may form supersaturated amorphous or partially amorphous non-equilibrium structures in the processes in which water is rapidly removed by evaporation or sublimation (Roos, 1995).

Water decreases drastically the T_g of food polymers and even traces of water may significantly decrease T_g values. It is obvious that T_g of substances varies with determination methods. T_g of fructose, glucose and sucrose reported by various researchers are broadly different. T_g of sucrose by DSC heating scan at 5 °Cmin^{-1} by Roos and Karel (1990) are in Table 2.13. T_g of sugar mixture (sucrose 87.5% and fructose 12.5%) at different moisture content by Soesanto and Williams (1981) are in Table 2.14. T_g of glucose by DSC heating scan at 5° Cmin^{-1} by Chan *et al.* (1991) are in Table 2.15. Data from these three tables shows that a small change of moisture content in materials could make a significant decrease in glass transition values.

Table 2.13 T_g of sucrose at different moisture contents (Roos & Karel, 1990)

Moisture contents of sucrose(mass fraction)	T_g (°C)
0.000	56.6
0.015	37.4
0.039	27.9
0.044	9.7
0.065	-6.8

Table 2.14 T_g of mixture of sucrose (87.5%) and fructose (12.5%) at different moisture contents (Soesanto & Williams, 1981)

Moisture content (mole fraction)	T_g (°C)
0.29	15
0.39	7
0.52	0
0.56	-5
0.60	-7

Table 2.15 T_g of glucose at different moisture contents (mass fraction) (Chan, *et al.*, 1991; Oh *et al.*, 2006; Noel *et al.*, 1996)

Moisture (fraction)	T_g (°C) (Chan *et al.*, 1991)	Moisture (fraction)	T_g(°C) (Oh *et al.*, 2006)	Moisture (fraction)	T_g(°C) (Noel *et al.*, 1996)
0.000	29	0.03	13	0.00	30
0.111	-22	0.06	-7	0.05	3
0.177	-27	0.09	-22	0.07	-8
0.429	-72	0.12	-28	0.12	-21
		0.15	-38		

In state diagrams the decrease of T_g with increasing water content is shown by a continuous T_g curve. Various studies found that water plasticization is typical of low molecular weight carbohydrates, oligosaccharides, polysaccharides, proteins and also water plasticizable polymers (Roos, 1995). The effect of water on T_g of various food materials has been predicted by equation 2.1, which originally was reported to describe composition-dependence of T_g of binary blends of miscible polymers. Figure 2.12 shows T_g values of common mono- and disaccharides as a function of water content. Experimental T_g values are indicated with symbols. The T_g curves are calculated with equation 2.1 using T_g = -135 °C for water.

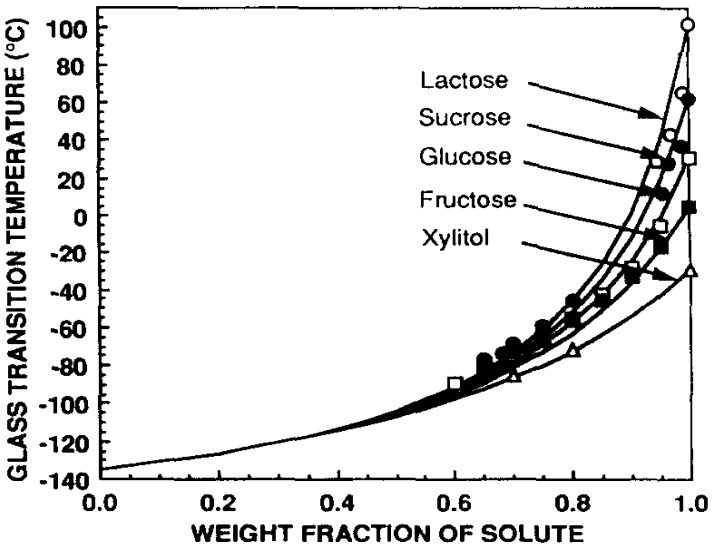

Figure 2.12 T_g of common mono- and disaccharides as a function of water content. Experimental T_g values are indicated with symbols. The T_g curves are calculated with equation 2.1 using T_g = -135 °C for water (Roos, 1995).

A study of the glass transition occurring in aqueous fructose solutions by Ablett *et al.* (1993) also found that the T_g of fructose varies with concentration. The data is shown in Table 2.16. These T_g values are a little different from data reported by Roos (1993) shown in Figure 2.12.

Table 2.16 T_g of various aqueous fructose solutions (onset and midpoint) (Ablett *et al.*, 1993)

Fructose (%w/w)	T_g onset (°C)	T_g midpoint (°C)
60.2	-	-85
65	-	-78
70	-75	-69
74	-68	-63
76	-61	-57
78.5	-55	-50
80.1	-51	-46
82	-42	-38
90	-	-17
95	-	4
100	-	10
100	5 (Roos, 1995)	10 (Roos, 1995)
100	-	16-18 (Finegold *et al*., 1989)

Slade and Levine (1991) indicated that water not only affected the T_g values of completely amorphous polymers but also affected both the T_g and T_m values of partially crystalline polymers. The sugar crystals melt at lower temperature when water is present.

Moreover, Slade and Levine (1991) reported that foods could be divided into three categories according to their water plasticizing related characters. These are: a water compatible monomer with a completely glass curve, a water-compatible solute with practical glass curve, and a water-sensitive solute with a practical glass curve. Typical complete glass curves are shown in Figure 2.12 have values of T_g that trend to move downward to the T_g of water. The practical glass curve for a water-compatible solute levels off when an unfrozen water matrix surrounds ice crystals in the maximally freeze-concentrated aqueous point (T_g') < 0 °C. The practical glass curve for a water-sensitive solute levels off, at lower moisture content, well above 0 °C. Examples of these are the

plasticizing effect of water on T_g of hemicellulose and lignin, the two major amorphous components of fibre. Hemicellulose (similarly to starch, gluten, and elastin) exhibits the characteristic behaviour common to all water compatible, glass-forming solutes. The practical limit to the extent of plasticization is determined by the phase separation of crystalline ice below 0 °C, so that the minimum T_g achievable during slow cooling in a practical time frame is the solute-specific T_g' (with the corresponding maximum content of plasticizing moisture). Accordingly, the glass curve shown for hemicellulose in Figure 2.13 is typical of the "practical glass curve for a water-compatible solute" that levels off at T_g'< 0 °C, rather than continuing along the monotonic descent of the "complete glass curve" to the T_g of water itself. For lignin which is water-sensitive rather than water-compatible, the glass curve started at about 200 °C for the dry solid and decreases by more than 10 °C/w% water. The glass curve for lignin is typical of the practical glass curve for water-sensitive solute. These characters are common to all water-sensitive glass forming solutes which are large polymers that are relatively hydrophobic. The practical limit to the extent of plasticization by water is determined by its much more limited water-solubility and thermodynamic compatibility, leading to the phase separation of liquid water (as clusters of water molecules) above 0 °C, which would subsequently freeze on further cooling to 0°C. Thus the minimum T_g achievable during cooling of a lignin-water mixture is not T_g', but some higher T_g>T_m of ice (about 50 °C as shown in Figure 2.13), because T_g cannot be depressed to T_g' by clustered water in a separate (non-plasticizing) liquid phase.

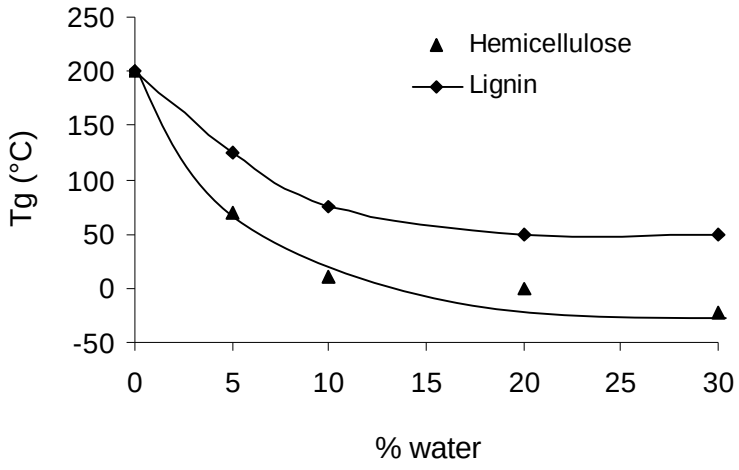

Figure 2.13 "Glass curves" of hemicelluloses and lignin as a function of mass fraction of water up to 30% (modified from Slade & Levine, 1991).

2.3 Spray drying

Spray drying is used to produce a wide range of products including heat sensitive materials (Crowe, 1971; William-Gardner, 1971). The flexibility of drier designs provides opportunities to produce the powders that consistently meet industrial specifications (Huntington, 2004; Sharma *et al.*, 2000). The production capacity can be expanded to over 25 tonnes of product per hour (Masters, 1997). The process is continuous and easily automated which can reduce labour costs (William-Garner, 1971; Sharma *et al.*, 2000). There are less sticking and corrosion problems in spray drying if the material does not contact the equipment walls until it is dry (Gupta, 1978). It is a powerful tool for delivering cost effective, high quality products (Masters, 1997).

The products produced by spray drying include: pharmaceutical, such as antibiotics, analgesics, vaccines, vitamins and catalysts; chemicals, such as, carbides, ferrite, nitrides, tannins, fine organic/inorganic chemicals detergent and dyestuffs; ceramic, including advanced ceramic formulations; and foods such as, milk and milk products, food colour, food supplement, soup mixes, spice and herb extracts, coffee, tea and sweetener. Spray dried food products are appealing, retain nutritional qualities and are convenient to consume (Masters, 1972).

2.3.1 Spray drying processes

Spray drying is a dehydration process in which a concentrated solution, suspension, emulsion or pumpable paste is sprayed, dried and collected. The particles are dried while they are suspended in the hot drying media. The dried products can be in the form of powder, granules or agglomerates depending on physical and chemical properties of the feed, the drier design and the drying operation (Masters, 1972).

There are four processes in spray drying including atomization of the feed into a spray; mixing of the spray and drying medium (air); drying of the spray or evaporation; and product recovery by separation of product and air (Masters, 1972; Marshall, 1954).

There are many different designs for the four processes. The primary concern in the designs of a spray drying system is that the products should be sufficiently dry before contacting the chamber wall (Crowe, 1971). The atomizer, chamber size and drying-gas

temperature must be selected to meet this design constraint at the design feed rate. Masters (1994) suggested that when selecting an overall spray drier design to achieve a specific type of spray dried product, the operation of the atomizer, air disperser, drying chamber and powder collection systems should all be considered.

2.3.1.1 Atomization

The atomizer is the critical component, and atomization is a very complex process in spray drying (Crowe, 1971; Masters, 1997). The atomizer sprays the liquid feed into a stream of hot air or other gas. The droplet size depends on the liquid properties and the atomizer's operating parameters such as pressure drop and flow rate (Crowe, 1971). The choice of atomizer type depend on the properties of liquid such as, concentration and viscosity as well as the droplet size distribution desired (Saravacos & Kostaropoulos, 2002).

The liquid feed and drying gases can enter the chamber in the same direction (co-current) or in opposite directions (counter-current) or a combination of both directions (Masters, 1997). The counter-current option is not applicable to food drying because the hottest air will contact the driest particles and will result in unacceptable heat damage in the product (Masters, 1997).

There are three basic atomizer types: a single-fluid pressure nozzle, a two-fluid (also known as pneumatic) nozzle, and a rotary atomizer (also known as a spinning disc or centrifugal atomizer).

Single-fluid pressure *nozzle*

A single-fluid pressure nozzle is the most common atomization device which produces a narrow size distribution of droplets (Saravacos & Kostaropoulos, 2002). The pressure energy within the liquid feed is converted into the kinetic energy of a moving thin liquid sheet, which is then forced through an orifice. Variation of feed pressure and nozzle type can control the particle size of liquid feed (Masters, 1972). Single-fluid nozzles can be selected and installed to provide a range of spray angles and directions (Crowe, 1971).

Two-fluid or pneumatic nozzle

A two-fluid or pneumatic nozzle is suitable for a more viscous or abrasive feeds. High velocity compressed air or gas impacts the liquid feed. The particle size varies depending on the ratios of the atomizing gas and feed (Masters, 1972).

Rotary or centrifugal atomizer

The rotary atomizer is considered by some to be the most flexible atomizer; it is suitable for a wide range of products including fruit juices with discrete pieces of pulp. The liquid feed is accelerated to speed between 5,000 – 25,000 rpm in the atomizer wheel and is ejected from the rim of the centrifugal atomizer at 60-200 m s^{-1} and droplets break down into smaller particles. Rotary atomizer produces large, easily dissolved dried particles (Saravacos & Kostaropoulos, 2002). However, the liquid feed needs to be homogenized before atomizing to reduce clogging problems (William-Gardner, 1971).

2.3.1.2 Mixing of spray and drying medium

The feed is atomized directly into the hot air stream. As the droplets pass through the hot air flow, the moisture evaporates rapidly. The time and distance required to complete the drying of the droplet spray depends on the rate of heat and mass transfer between the droplets and the drying medium (Crowe, 1971). Heat and mass transfer during drying occur in the air and vapour films surrounding the droplet. There is the protective envelope of vapour, which keeps the particle at the saturation temperature and, as long as the particle does not become completely dry, evaporation still takes place. Thus, heat-sensitive products can be spray dried at relatively high air temperatures without being harmed (Mermelstein, 2001).

2.3.1.3 Evaporation

At the evaporation stage, the concentration difference of the vapour at the droplet surface and in the drying gas is the driving force for mass transfer. A higher drying gas temperature causes higher rates of heat transfer to the droplet. Heat transfer is essential to provide the energy for evaporation which, in turn, establishes a vapour concentration gradient for mass transfer. Then the mass transfer results in size reduction and/or changes in the density of the droplet material which affect the droplet motion (Crowe, 1971).

All transfer mechanisms are interactive precluding the development of simple analytic expression to describe the variation of droplet properties throughout the entire drying period. Evaporation in the spray dryer is almost instantaneous; the drying medium temperature undergoes rapid reduction and the dried material is not raised above this terminal medium temperature. The extremely high evaporation rates obtainable in spray drying are due to high ratio of surface area to mass of the droplets produced in the atomizing device (William-Gardner, 1971). Drying chamber design can create optimum air flow conditions and provide sufficient residence time for the particle formation and drying to be completed (Masters, 1994).

Figure 2.14 shows the flow of hot air and feed droplet and temperature profiles in a co-current spray drier (data from Barbosa-Canovas & Vega-Mercado, 1996). The air inlet temperature was initially at 350 °C then dropped abruptly to 180 °C at the upper part of the drier where about 50% of evaporation took place. The initial feed temperature was 20 °C and increased to 40 °C at the atomizer. This is normal practice to decrease feed viscosity and increase the efficiency of the drier. The air temperature in the drier chamber continued to decrease until it was around 120 °C at the outlet port while the product temperature out of the chamber was around 95-100 °C.

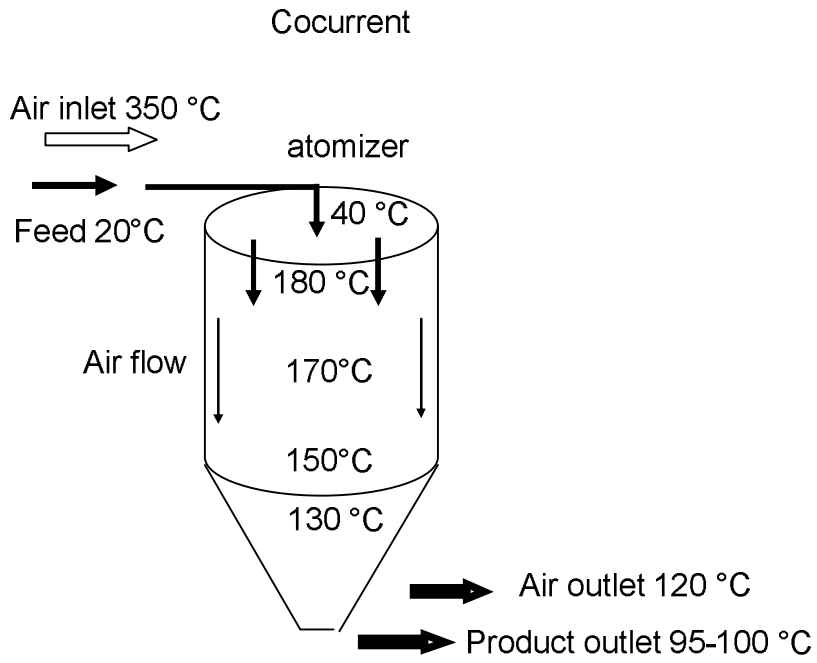

Figure 2.14 Flow direction and temperature profile in co-current flow spray drier (Modified from Barbosa-Canovas & Vega-Mercado, 1996).

2.3.1.4 Separation of dried product

Separation of dried product from the air is the final phase of spray-drying. After evaporation, the large particles fall to the bottom of the chamber and are collected while the fine particles are entrained with the exhaust air and are generally collected by passing the air through a series of external cyclones, electrostatic precipitator, scrubbers or bag filters. Fines are bagged or returned to an agglomeration process in the drier (Masters, 1994). Spray dried powders do not fully retain the spherical shape of the droplets created at the atomizer. Due to variations in air temperature, air velocity and air humidity throughout the drying chamber volume, all droplets are subjected to different local drying conditions and thus have individual drying histories, some particles being spherical or near spherical in shape, others more misshapen, collapsed or, expanded (Masters, 1994).

2.3.2 Physical changes of food droplet during spray drying process

As explained earlier, heat and mass exchange occur while droplets are travelling in the hot air. At the initial phase of evaporation, the temperature, and the evaporation rate change rapidly but the droplet soon achieves a constant evaporation rate (Vehring *et al.*, 2007). The temperature of particle approaches the wet bulb or saturation temperature of the drying air.

During spray drying, the glass transition temperature of the atomized product increases as the water content is reduced. When the temperature of the droplet is above T_g, it influences the structural characteristics of the product. When drying approaches the end state, particles temperatures get closer to the outlet air temperature. The temperature of the droplets increases and the physical properties of droplet continue to change as the water content decreases. If the cooling rate is very fast then amorphous solidification occurs instead of crystallization (Master, 1985; Bhandari *et al*., 1997).

Figure 2.15 shows a schematic representation of physical changes of droplet during co-current spray drying. At the upper part of the spray drier, the initial step of dehydration takes place and the droplet temperature remains at the wet bulb temperature of the hot air. At this stage the surface of particle is in “rubbery” or plastic form. The moisture content decreases to approximately half of the value of the initial moisture content. At the middle part of the drier the evaporation continues and the moisture content of the droplet

becomes less than 10% of its initial value. The temperature of the droplet increases toward the temperature of the air. The droplet's surface starts to become sticky if the surface temperature is higher than T_g of the droplet. At the lower part of spray drier the drying process is completed. The powder temperature is approximately lower than the air temperature at the outlet port. The moisture content of the droplet is down to 2-4% wet basis. When the particle surface temperature is lower than T_g +20 °C, the powder is not sticky (see Section 2.2.6).

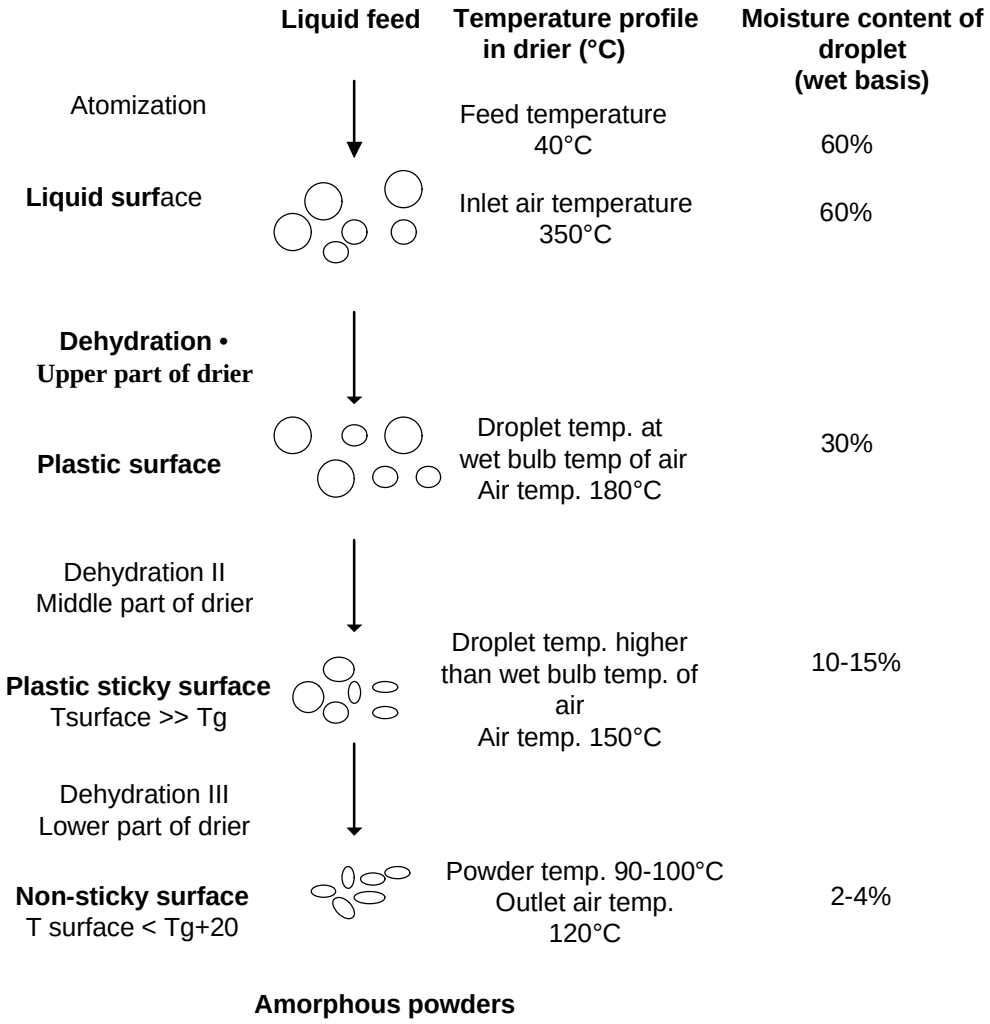

Figure 2.15 Schematic representation of physical changes in droplets at 40% total solid in a co-current spray drying process (dehydration I, II III show the arbitrary stages of dehydration). T_g is the glass transition temperature, $T_{surface}$ is the surface temperature of drying particle. Temperature and moisture content profiles are approximated from Saravacos & Kostaropoulos, (2002); Toledo (1991). Schematic presentation modified from Bhandari *et al.* (1997).

2.3.3 Spray drying of fruit juice

Among food-stuffs, fruit juice is the most difficult substance to be spray dried so as to retain as many as possible of the natural properties and qualities in the final powder such as colour, flavour, test and texture (Adhikari *et al.*, 2000; 2001; Bhandari *et al.*, 1993). Owing to the thermoplastic and hygroscopic nature characteristics of the fruit and vegetable powders special attention needs to be paid to the chamber design, the inlet and outlet temperature, total solid content of the fruit juice to be spray dried, a suitable drying aid, the handling of the dried particles and the packaging of the product after drying (Dolinsky *et al.*, 2000; Goula & Adamopoulos, 2003).

Fruit juice containing acids are more difficult to dry than the same materials with lower acidity. Bhandari *et al.* (1993) found it more difficult to dry orange juice or acid lactoserum than when those materials had lower acidity. During the spray drying process, fruit juice may remain either as syrup or stick on the drying chamber wall (Bhandari *et al.*, 1997; Bhandari *et al.*, 1999; Adhikari *et al.*, 2003).

The main difficulties in fruit juice spray drying were sticking of the powder in the drying and collecting zones, and scorching of the product (Al-Kahtani & Hassan, 1990). The recovery of product from a spray drier is strongly affected by powder stickiness (Bhandari *et al.*, 1997; Boonyai *et al.*, 2004). The continuous airflow in a spray drier can prevent the collisions of the highly viscous particles in the drier chamber, but they might contact each other at the bottom of the drier, or in the cyclones and collection ducts to form unwanted agglomerates (Adhikari *et al.*, 2003). Cooling of fruit juice powders after drying can help to prevent sticking or caking but juice powders with less than 2% moisture were non-caking (Gupta, 1978, Van Arsdel, 1973).

2.3.4 Glass formation in spray drying

During the spray drying process, dehydration of the atomized liquid particles proceeds from the particle surface to the inner core. A layer of concentrated solutes is formed on the particles surface and there is a decrease in the particle temperature due to evaporative cooling. The extremely rapid removal of water increases the viscosity of the remaining solution. The particle surface may approach the glassy state before colliding with other particles or drier walls. Downton *et al.* (1982) found that a critical surface viscosity resulting in stickiness and caking is $> 10^7$ Pa.s (Downton *et al.*, 1982). The general

accepted value for the viscosity of glassy materials is > 10^{12} Pa.s (Sperling, 2006, Roos, 2002, Allen, 1993) which is an ideal viscosity for non-sticky powders. The vitrification of the particles surface in spray drying is essential in allowing the free flow of the particles through the drying chamber and avoiding caking of particles with each other and on the drier surfaces. At the end of the drying process, the particle temperature and water content should support the solid, glassy state (Roos, 2002).

A study of spray drying of concentrated fruit juices, including blackcurrant, apricot and raspberry, with different maltodextrins as drying-aid agents, found that the volatile compounds were encapsulated in carriers at the amorphous glassy state (Bhandari *et al.*, 1993). If the temperature of the products is higher than T_g then collapse or sometimes crystallization occurred, releasing encapsulated volatiles, but if the difference between the material temperature and T_g was not too large, the glassy state might be stable (Roos & Karel, 1991). This might present good conditions for spray drying of fruit juices aromas. On the other hand, the crystalline state might be preferred for low hygroscopicity in fruit juice powder (Bhandari *et al.*, 1993).

2.3.5 Additives in spray drying

Other than the operational techniques, such as cooling the drier wall and blowing with cold air, an additive or drying aid can be used to reduce stickiness during fruit juice spray drying (Kudra, 2002; Gupta, 1978). A drying aid is added for many purposes such as improving the drying rate, stickiness prevention, reducing hygroscopicity, maintaining flowability of the dry powder and maintaining quality of the powder in storage (Langrish *et al.*, 2007). There are many materials used as carriers. Tricalcium phosphate was used as a carrier in the concentrated extract of *Possiflora edulis* leaves (Linden *et al.*, 2002). Soybean proteins, pectins and hemicelluloses have been used as structural element in powders (Bhandari *et al.*, 1993). Maltodextrins at different dextrose equivalence values (DE) are the most common carriers in spray drying of fruit juice (Gupta, 1978; Masters, 1985; Roos 1995; Bhandari *et al.*, 1997; Rodriguez-Hernandez *et al.*, 2005; Langrish *et al.*, 2007). According to Gupta (1978) the addition of carrier to orange juice for spray drying should not exceed 40% of the total solid content of the juice. If the fruit juice makes up less than 60% of the total solid in the powder the juice flavour is unacceptable.

2.3.6 Maltodextrins and spray drying

Maltodextrins are digestible carbohydrates made from several different cereal sources, including corn, potato, rice and tapioca (Deis, 1997). The processes to produce maltodextrins involve cooking of starch followed by acid and/or enzymatic hydrolysis to break the starch into smaller chains. These chains are composed of several oligosaccharides molecules along with polysaccharides of larger molecular weight (Avaltron *et al.*, 2004; Venom, 2005).

Maltodextrins are commonly used as a spray drying aid because of their relative cheapness with no colour and little taste. Maltodextrins are amorphous and tend to inhibit sugar crystallization. Maltodextrins are soluble in water and have a high T_g after drying (Kenyon, 1995). Wang and Wang (2000) stated that maltodextrins exhibited higher viscosities than syrups and were thus preferred to be used with respect to cohesive and foam stabilizing properties for specific applications. Addition of maltodextrins significantly reduced the stickiness of fructose solutions, showing its use as an effective drying aid (Adhikari *et al.*, 2003). Maltodextrins are frequently used to overcome the stickiness of low molecular weight sugars and organic acids. The T_g value of maltodextrins varies from 100 to 188 °C depending on their dextrose equivalent property (DE) (detail in Table 2.9) (Bhandari *et al.*, 1997).

Dolinsky *et al.* (2000) suggested that 30-55% maltodextrin should be added to the fruit and vegetable juice in order to obtain the powder. However, up to 75% dry basis of maltodextrins was added in many fruits juice such as oranges, lemons, apricots and strawberries in order to obtain satisfactory results when spray drying (Masters, 1979). A 1:1 ratio was good for spray drying of honey + maltodextrin and pineapple + maltodextrin (Bhandari *et al.*, 1997). Truong (1994) found good spray dried powder from 45% maltodextrin (solid content) in tamarind juice. Maltodextrins (10 and 20 DE) at concentrations of 180 to 230 gL^{-1} were used in spray drying of cactus pear juice (Rodriguez-Hernandez *et al.*, 2005). The degrees of polymerization of the maltodextrins and the interaction between inlet air temperature and atomizing air pressure had a great effect on the moisture content of powder and on the retention of vitamin C in the reconstituted product. The maltodextrin concentration affected the colour of the final products but there was no significant effect of the type of maltodextrin on the hygroscopicity of the powder of cactus pear juice. Maltodextrin at low dextrose

equivalent (DE) were found to cause higher collapse temperatures than that of high DE at the same concentration when applied as drying aids for orange juice (Tsourouflis *et al.*, 1976). Even though very high amounts of maltodextrins were needed in spray drying of most fruit and vegetable juice, Quek *et al.* (2007) produced a good watermelon spray dried powder with 3-5% maltodextrin (DE 8-12). Adding more than 10% maltodextrin to watermelon juice was found to produce powders with less of their attractive red-orange colour. Shrestha *et al.* (2007) also had found that maltodextrin decreased the lightness, redness and yellowness parameters of orange juice powder.

In various confection industries, glucose syrup which is physically similar to maltodextrin was widely used to prevent crystallization of sugars (Walstra, 2003).

Roos and Karel (1991a) had found that addition of maltodextrins to sucrose caused a fairly small and almost molecular weight independent increase of the T_g up to a concentration of 50% (w/w). Thus, in practice, the dehydration of fruit juice needs fairly high concentrations of maltodextrin. Shrestha *et al.* (2007) found that under certain spray drying conditions 60% maltodextrin was the maximum amount to get a good yield from orange juice. It was found that increasing maltodextrin from 50 to 60% resulted in a significant increase in orange juice yield up to 78%. Further increases in maltodextrin in the juice were found to slightly increase the yield. Adhikari *et al.* (2004) predicted surface stickiness of mixture of sucrose + glucose + fructose drops during spray drying at 63 and 95 °C and found that the 50% maltodextrin in the solid failed to overcome the stickiness. It was also found that lower outlet temperatures in spray drying reduced the stickiness of sugar-rich foods.

The interaction of maltodextrin mixtures in the drying process might affect the dried product properties. Adhikari *et al.* (2004) showed the morphological changes of drops of sucrose + maltodextrin and fructose + maltodextrin at 63°C at fractions of 4:1, 1:1 and 1:4 (Figure 2.16). The drop deviated from sphericity for sucrose + 20% maltodextrin but not for fructose + 20% maltodextrin. The pure sucrose and pure fructose remained spherical in these drying conditions. When the amount of maltodextrin in drops of sucrose or fructose is 50%, the drops elongated after five minutes of drying. It was stated that this shape allowed more water to leave the drop and acted to offset the resistance to moisture diffusion caused by the formation of a skin on the surface. The drop with 80%

maltodextrin had shown the morphological features of surface folds, wrinkles and deviation from spherical shape reported for a pure maltodextrin drop. The surface was less rugged and the surface troughs were shallower. The surface appeared to be much softer than the maltodextrin drop which indicated that it was easier for the moisture to diffuse out from the softer surface (Adhikari *et al.*, 2004).

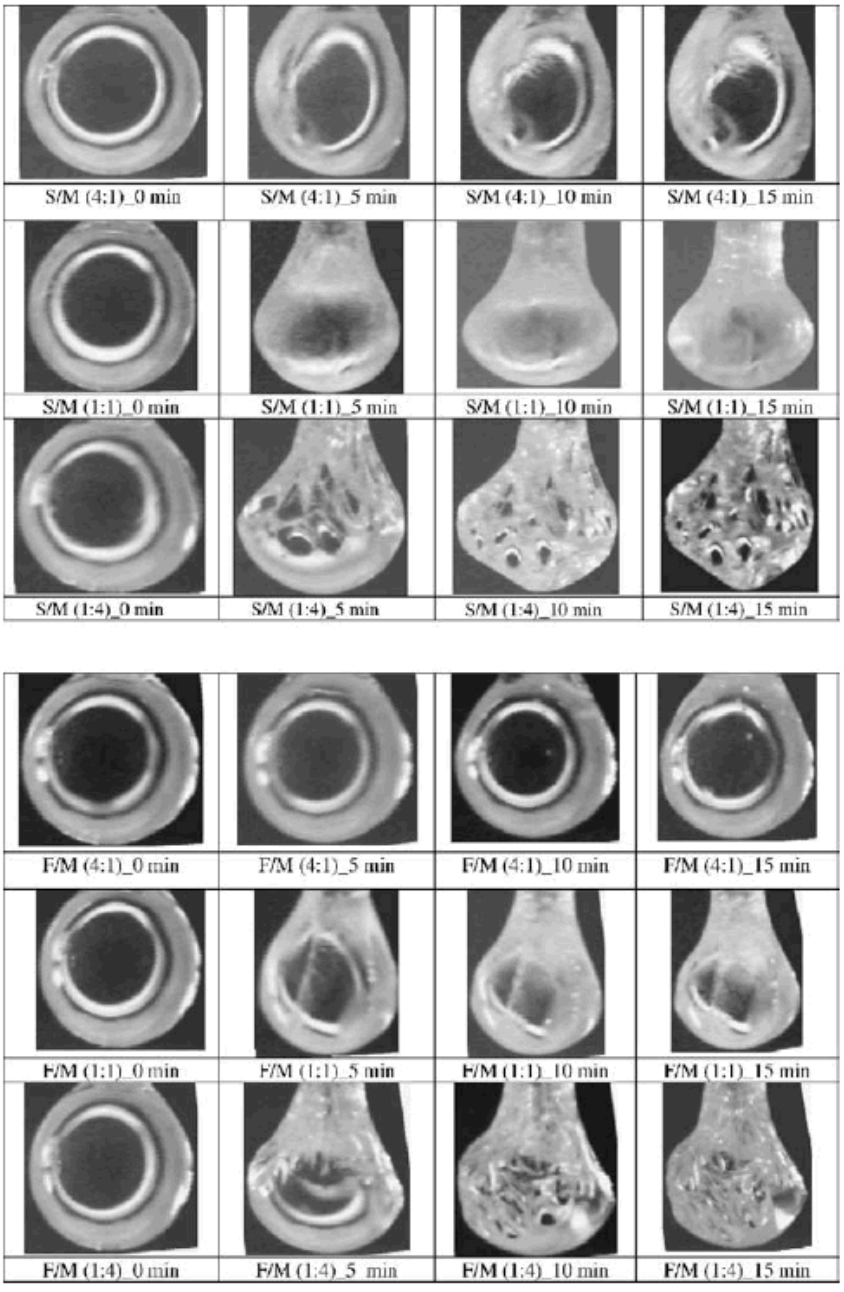

Figure 2.16 Morphology of drops of sucrose + maltodextrin (S/M) and fructose + maltodextrin (F/M) at 4:1, 1:1 and 1:4 ratio drying at 63 ±1 °C, 1 m/s velocity and 2.5±0.5% relative humidity. The time on the image is the capture time (Adhikari *et al.*., 2004).

The morphology of drops of fructose + glucose + sucrose + maltodextrin (F+G+S/M) and citric acid + fructose + glucose + sucrose + maltodextrin (C+F+G+S/M) at 4:1, 1:1 and 1:4 ratio drying at 63 ±1 °C, 1 m/s velocity and 2.5±0.5% relative humidity are shown in Figure 2.17. It was found that the surface of drops containing sugar + maltodextrin or citric acid + maltodextrin at the ratio of 1:4 was softer or more thermoplastic at 95 °C than at 63 °C which meant that the surface of the drops became more plastic at higher temperature (Adhikari *et al.*, 2004).

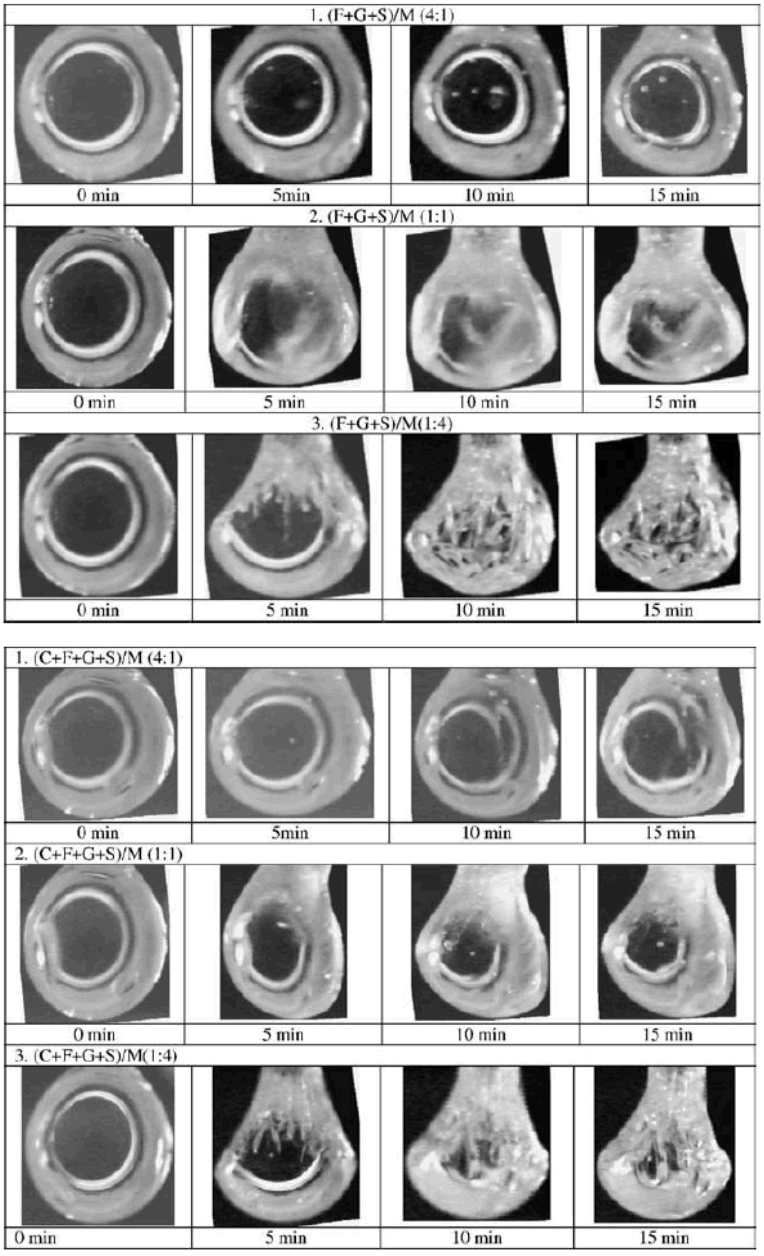

Figure 2.17 Morphology of drops of fructose + glucose + sucrose + maltodextrin (F+G+S/M) and citric acid + fructose + glucose + sucrose + maltodextrin (C+F+G+S/M) at 4:1, 1:1 and 1:4 ratio

drying at 63 ±1 °C, 1 m/s velocity and 2.5±0.5% relative humidity. The time on the image is the capture time (Adhikari *et al.*, 2004).

It was found that starches in maltodextrin swell differently when expose to a range of temperature. Difference source of maltodextrin shows different swelling power when exposes to temperature. Cassava starch has a stable swelling power at around 23% from 65 °C until 95 °C but the swelling power of corn starch increase from 10 to 20 % at 75 to 95 °C (Figure 2.18).

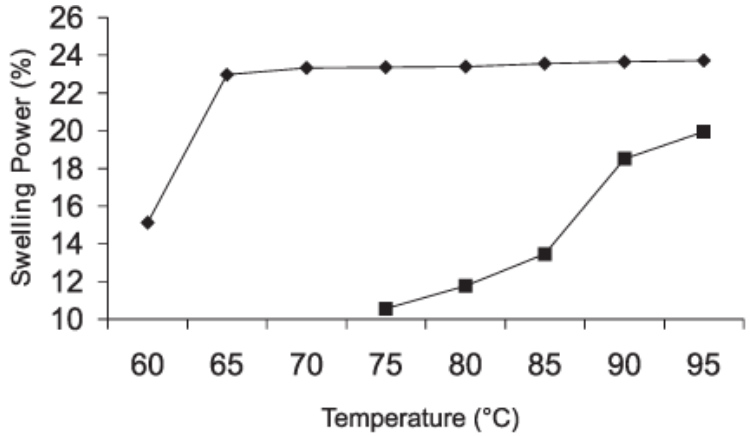

Figure 2.18 The swelling power of corn and cassava starch in maltodextrin at a temperature range (Moore *et al.*, 2005).

2.3.7 Fruit and vegetable fibre as carriers in spray drying

Practically, fruit and vegetable juice powder can be spray dried when a sufficiently high concentration of natural fibres remains in the juice. The edible fibre components are mostly parts of the cell wall of plants. The use of fibres, obtained from fruit or vegetable processing, as carriers to produce free flowing powder in spray drying offers a great potential to utilise waste materials. The use of fibre as a carrier in spray drying could also be applied to other food products as a natural alternative to the carriers used presently. However, the particle sizing and characterization of the fibre to be added in fruit juices could be a critical factor for determining the characteristics of juice powder such as taste, texture, colour, transportation and storage stability (Edwards & Langrish, 2004). Edwards and Langrish (2004) found that fibre particles from apple and orange products had an irregular shape, but were not highly elongated and had a wide size range from 2 to 500 µm. The surface-volume mean diameter measurement is significant in relation to spray drying as it is desirable to maximize the surface to volume ratio, thus increasing the

available surface area for drying. The microstructure of the fibres showed that the particles had a very heterogeneous surface and in some cases had long surface channels which appear to open towards the centre of the particle. The particle size and shape of the fibres indicated that it might be possible to adsorb fruit extract onto the interior surfaces of the fibre particles. This might enhance the usefulness of the fibre particles as carriers by allowing them to act more like encapsulants, trapping the valuable material inside the fibre particle during spray drying.

Langrish and Chiou (2008) found that the fine milled citrus fibre was able to induce crystallization in spray dried extract of hibiscus. The powder from the combination with fibre was found to have stable moisture content.

Previous works on spray drying of fruit juice

Shrestha *et al.* (2007) had found that the product yield at the cyclone of spray dried orange juice + maltodextrin at 50:50 was very low. These powders were highly sticky and caked within 24 hours of storage in vacuum packed plastic bag. Increasing the ratio of maltodextrin in orange juice from 50 to 60% was found to increase the product yield at the cyclone by more than 50%. The recovery of sugar rich products during spray drying is a direct function of the temperature and moisture of outlet air. Towards the end of the spray drying, the particle temperature gets close to the outlet air temperature. This study set the condition of spray drying at 160/65 °C inlet/outlet temperature. The powder contained more than 4% moisture and the T_g of anhydrous 50:50 orange juice + maltodextrin was found by DSC to be 66.4 °C.

By studying the effect of carriers on microstructure Cano-Chauca *et al.* (2005) found that cellulose played an important role of sugar crystallization induction in mango powder. The microstructures of mango juice powder with waxy starch and cellulose showed a high degree of uniformity but without a strong adherence among the particles. The microscopy analysis showed crystalline surfaces. X-ray diffraction of powders of mango juice with maltodextrin and cellulose at levels of 0, 3, 6 and 9% showed that the sample without cellulose had a totally amorphous structure. However, the samples with cellulose addition contained partially crystalline material with the peaks matching that of crystalline cellulose. There were no completely crystalline sugars. This might have been due to the characteristics of the drying process, which is not sufficiently long for the

sugar molecules to arrange into a crystalline form. X-ray diffraction of spray dried powder of mixtures of mango juice + arabic gum + cellulose and mango juice + waxy starch + cellulose confirmed the semicrystalline structure of the powders. It was discussed that the occurrence of semicrystalline material in the mixture with waxy starch without cellulose was because of the formation of semicrystalline amylose and amylopectin. Figure 2.19 shows micrographs of particles of powder of mango juice obtained by electronic microscopy of mango juice + maltodextrin + cellulose. Figure 2.20 shows that of mango juice + gum arabic + cellulose. Figure 2.21 shows that of mango juice + waxy starch + cellulose.

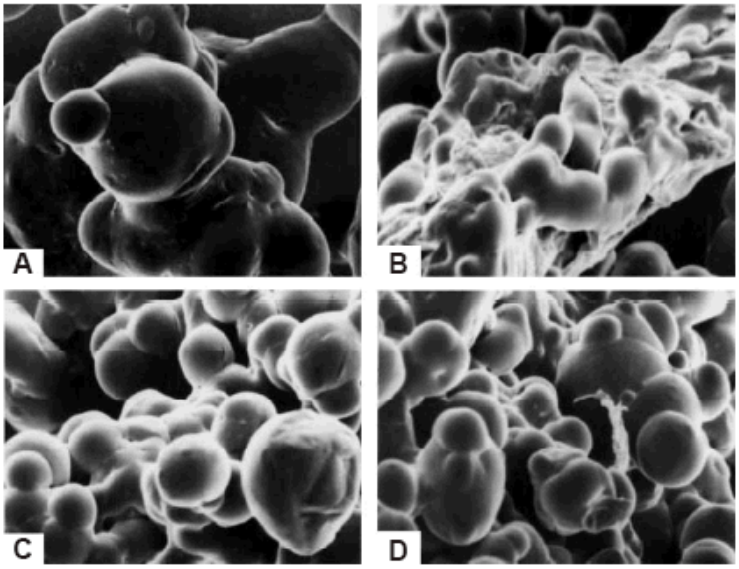

Figure 2.19 Micrographs of mango juice powder obtained by electron microscopy, magnification of 1500-10kV. (A) mango juice + maltodextrin, (B) mango juice + maltodextrin + cellulose 3%, (C) mango juice + maltodextrin + cellulose 6% and (D) mango juice + maltodextrin + cellulose 9% (Cano-Chauca *et al.*, 2005).

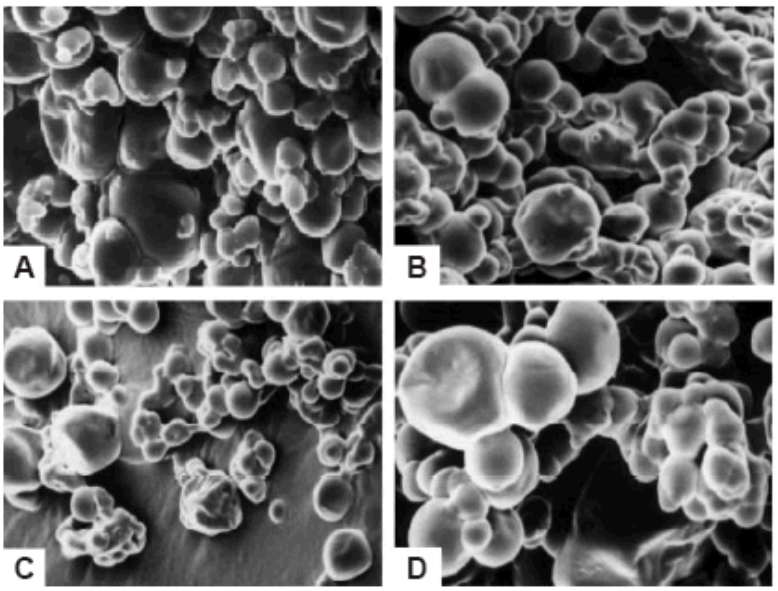

Figure 2.20 Micrographs of mango juice powder obtained by electron microscopy, magnification of 1500-10kV. (A) mango juice + gum arabic, (B) mango juice + gum arabic + cellulose 3%, (C) mango juice + gum arabic + cellulose 6% and (D) mango juice + gum arabic + cellulose 9% (Cano-Chauca *et al.*, 2005).

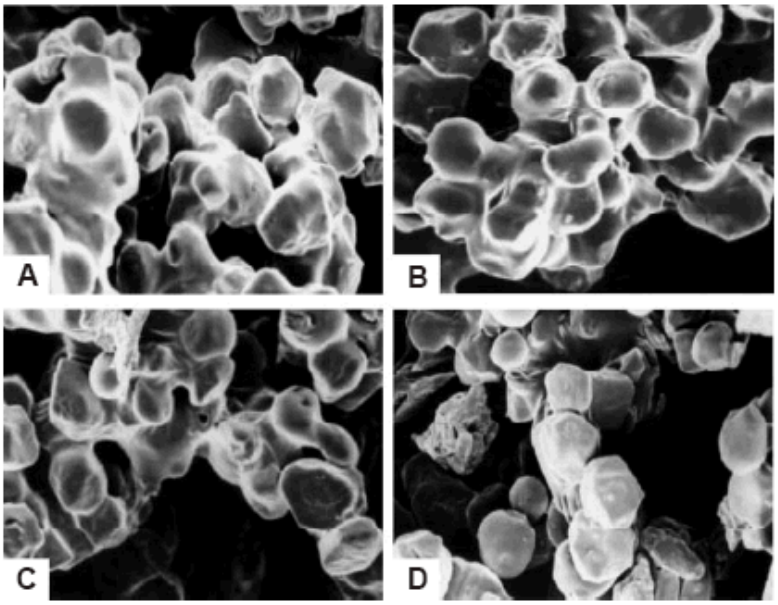

Figure 2.21 Micrographs of particles of mango juice powder obtained by electron microscopy, magnification of 1500-10kV. (A) mango juice + waxy starch, (B) mango juice + waxy starch + cellulose 3%, (C) mango juice + waxy starch + cellulose 6% and (D) mango juice + waxy starch + cellulose 9% (Cano-Chauca *et al.*, 2005).

Figure 2.22 shows the stickiness of mango juice powder as a function of cellulose with maltodextrin, gum arabic and waxy starch. The stickiness of powder with maltodextrin decreased with cellulose concentration. For the waxy starch the stickiness value was low compared to the maltodextrin and the addition of cellulose slightly decreased the stickiness. The stickiness was determined according to the Chen and Hosney (1995) method by using a texture analyser (Model TA.XT2 from Stable Micro Systems) and Smc/Chen-Hosney dough stickiness probe. The samples were mixed with glycerol to form homogeneous doughs. The data were from triplicate values (Cano-Chauca *et al.*, 2005).

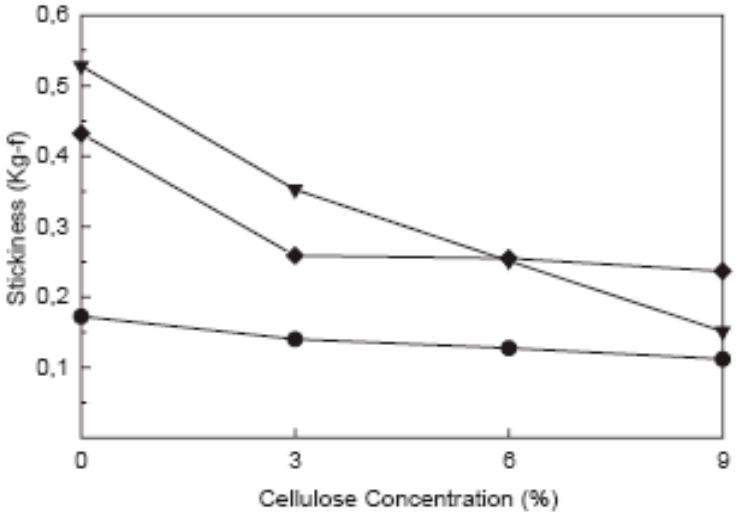

(▼ maltodextrin; ♦ arabic gum; ● waxy starch).

Figure 2.22 The stickiness values of mango juice powders as a function of cellulose concentration with maltodextrin, gum arabic and waxy starch (Cano-Chauca *et al.*, 2005).

2.4 Background of experimental measurements

2.4.1 Sugar determination methods in fruit juice

The methods use for sugar determination in fruit juice include, the enzymatic method, enzyme membrane method and high performance liquid chromatography (HPLC).

Enzymatic method

The enzymatic method includes many steps such as deproteinizing and spectrophotometric analysis. The kit to carry out the sucrose/ glucose/ fructose test is available from Boehringer Mannheim. Cat. No. 716-260 (Linskens & Jackson, 1995).

The enzymatic measurement of sugar in fruit juice is a very specific method. Bergmeyer (1983) indicated that in most cases the volume measurement of reagents and samples is the main determinant of imprecision. Table 2.17 shows the pipetting errors and the consequences of enzymatic measurement.

Table 2.17 Pipetting errors and consequences (Bergmeyer, 1983)

Solution	Volume		Volume error (%)	Error in measured result (mol/l)
	Protocol ml	Pipette ml		
Buffer	1.00	1.09	+9	+3%
Coenzyme	0.10	0.115	+15	+0.5%
Sample	0.10	0.12	+20	+20%
Water	1.60	1.45	-10	-5%
Enzyme	0.20	0.40*	+100	+6.7%

* gross errors from wrong pipette

The accuracy of enzymatic methods depends on the activity and specificity of the enzyme used, and on their purity. Bergmeyer (1983) specified that these three variables cannot be separated because they influence each other. A certain amount of activity is necessary to bring the reaction to completion and thus avoid lack of recovery. Specificity of enzyme means that the enzyme converts only a certain substrate and not similar compounds (for example homologues). Impurity means that the enzyme preparation contains contamination enzymes (not pure enzyme) or other by-products. Non-specificity or impurity causes simultaneous conversion of several compounds in the sample. By using high quality enzymes, one can detect incorrect results, the repetition of measurements in the same cuvette is needed (Bergmeyer, 1983).

YSI Enzyme membrane method

The YSI enzyme membrane (YSI incorporated, Ohio, USA) coupled with an electrochemical probe method for sugar analysis is the most convenient method. It is able to give a result in 30-60 seconds, but there is no membrane to detect fructose. The principle is that the substrate passes through a polycarbonate membrane and encounters an extremely thin layer of the appropriate oxidase enzyme. The reaction occurs as

$$\text{Substrate} + O_2 \xrightarrow[\text{oxidase}]{} H_2O_2 + \text{byproduct}$$

The H_2O_2 is detected by an electrochemical probe (YSI Biochemistry Analyser User's Manual, 2006).

To measure the sample containing both sucrose and glucose by the enzyme membrane method requires simultaneous measurement by a dual channel enzyme membrane probe. Mason (1983) stated that when glucose and sucrose are present in the same sample, the sucrose membrane alone cannot be used. This was because the response would be a weighted sum of the glucose and sucrose present. Sucrose can be determined in the presence of glucose by measuring the glucose before and after the hydrolysis of sucrose. The details are shown as follow:

Glucose:

$$\bullet\text{-D-glucose} + O_2 \xrightarrow[\text{glucose oxidase}]{} H_2O_2 + \text{Gluconic acid}$$

Sucrose:

$$\text{Sucrose} + H_2O \xrightarrow[\text{Invertase}]{} \text{Fructose} + \bullet\text{-D-glucose}$$

$$\bullet\text{-D-glucose} \rightleftharpoons \bullet\text{-D-glucose}$$

$$\bullet\text{-D-glucose} + O_2 \xrightarrow[\text{glucose oxidase}]{} H_2O_2 + \text{Gluconic acid}$$

Mason (1983) determined the sugar content in cereals using the YSI model 27 industrial analyzer equipped with immobilized enzyme membranes. The samples were also assayed by the official AOAC HPLC method for sucrose and glucose. The sucrose content from the enzyme membrane method lower than that from the HPLC method, and that of

glucose was higher than from the HPLC (by about 30%). The details are shown in Table 2.18.

Table 2.18 Sucrose and glucose concentration (%) in cereals by enzyme electrode and HPLC by Mason (1983)

Samples	Enzyme electrode		HPLC	
	Sucrose(%)±SD	Glucose(%)±SD	Sucrose(%)	Glucose(%)
A	35.0 ± 0.6	1.24 ± 0.05	36.0	0.96
B	22.4 ± 0.4	1.52 ± 0.06	23.1	1.52
C	21.4 ± 0.4	0.85 ± 0.03	22.2	0.50
D	5.40 ± 0.09	1.03 ± 0.03	6.07	0.70

Temperature plays a critical part in biosensor analysis. Choi and Yiu (2004) studied the analytical performance of a hydrogen peroxide biosensor of catalase-immobilized eggshell membrane and had found that it was the temperature dependent. The response of the hydrogen peroxide biosensor on exposure to 0.3 mM H_2O_2 was studied over the range 5-55 °C. The result shows in Figure 2. 23.

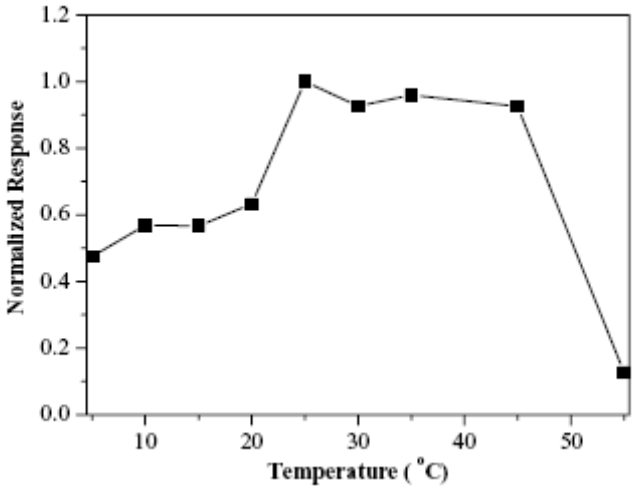

Figure 2.23 Effect of temperature on the normalized response of a hydrogen peroxide biosensor upon exposure to 0.3 mM hydrogen peroxide at various temperatures (Choi & Yiu, 2004).

Choi and Yiu (2004) explained that the activity of an immobilized enzyme is governed by the kinetics of the enzymatic reaction. The reaction rate is faster with higher temperature. However, the rate of reaction dropped dramatically when the temperature was higher than 45 °C because of denaturisation of the enzyme.

High performance liquid chromatography (HPLC) method

The HPLC method is simple and more suitable with chromatographic output of results. This method is attractive for a fast and quantitative separation of the main organic acids and sugars in fruit juice (Chinici *et al.*, 2005). In HPLC, a solution containing the compound(s) of interest is injected into a loop which has been calibrated to contain a specified volume (a 20 µL loop injector is a commonly used size). The valve switch is then rotated, allowing a sample stream of mobile phase (the eluent) to sweep the sample from the loop onto a column, packed with a suitable stationary phase, where the separation occurs. The eluent is delivered from a pump at a constant rate at a pressure sufficiently high to overcome the backpressure of the column. The separation efficiency is inversely proportional to the particle size of the column packing material. A calibration curve from different standard concentration of sugars is needed. See details in the Appendix.

2.4.2 Differential Scanning Calorimetry (DSC)

The differential scanning calorimeter (DSC) is the most common apparatus used to find the T_g of materials (Seymour, 1971; Franks, 1993; Roos, 1995; Champion *et al.*, 1997; Takiyama *et al.*, 2002; Foster *et al.*, 2005). The equipment measures the differential temperature or heat flow to or from a sample as compared with a reference material. The results are displayed as a function of temperature or time. This technique can differentiate between two types of thermal scans, endothermic or taking up heat, and exothermic or a giving off heat (Bhandari *et al.*, 1997, Roos, 1995; Nielsen, 2003). Figure 2.24 shows a simple schematic diagram of a DSC.

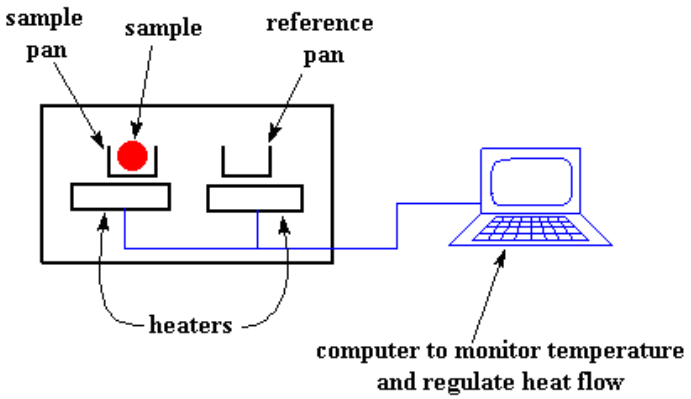

Figure 2.24 A simple DSC system (Otles & Otles, 2005).

A DSC can determine the temperature at which specific chemical or physical changes occur. Physicochemical changes give rise to endothermic and exothermic transitions, as well as a step changes in heat capacity of a material.

Endothermic events that occur over a narrow temperature range indicate crystalline rearrangement, crystalline melting (heat of fusion), or solid state transitions of pure materials. A broad transition indicates that the events relates to dehydration, temperature-dependent phase behaviour, or polymer melt (Nielsen, 2003). Exothermic transitions relate to processes without decomposition caused by a decrease in enthalpy of a phase or chemical system. Narrow exotherm results from crystallization (ordering or freezing) of a metastable system, whether under cooled organic, inorganic, amorphous polymer, or liquid, or annealing of stored energy resulting from mechanical stress. Broad exotherms result from solid-solid phase transitions, chemical reactions, polymerization, or curing of polymers. On the other hand exothermic transitions relating to decomposition can be narrow or broad, depending on kinetic behaviour of substances (Nielsen, 2003). Figure 2.25 shows a typical change in a DSC output for a glass transition and melting.

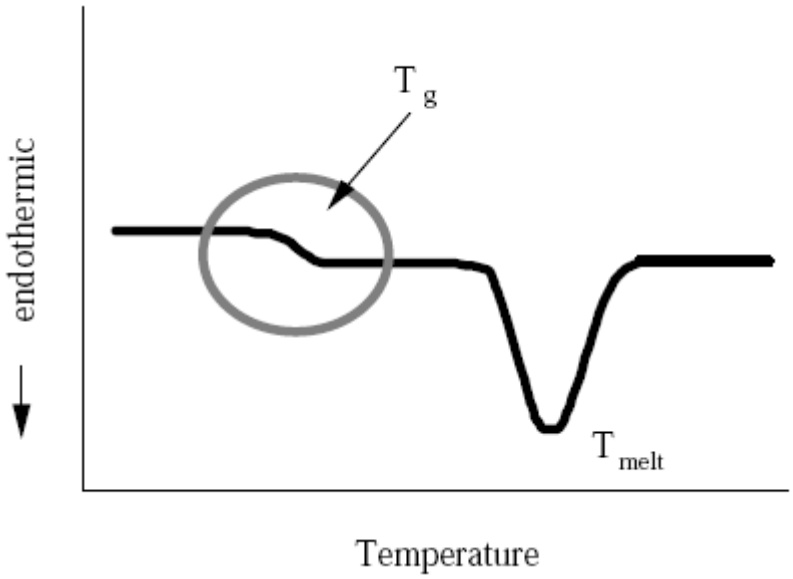

Figure 2.25 Typical changes in DSC thermogram at T_g and melting temperature (Otles & Otles, 2005).

Step changes in the heat capacity of a material can be seen as a small change in heat flow (change in the baseline) with no well-defined peak being produced. This change is a

character of a glass transition (Nielsen, 2003). It is often difficult to determine the T_g of mixed systems. Many low moisture foods are mixtures of polymers, water and several other small molecule components. In practice a narrow transition range rather than a sharp transition point is often observed (Walstra, 2003).

The experimental conditions influencing the thermograms include sample pan size, heating rate of scan, placement of sample pan inside sample holder, sample size, particle size and the position of sample inside the sample pan (Roos, 1995; Nielsen, 2003).

The measured T_g value of a single sample also depends on the sample thermal history and even the same analytical method may give different T_g values (Walstra, 2003, Roos, 1995; Nielsen, 2003). Usually T_g values reported are either onset or midpoint temperatures of the T_g temperature range (Roos, 1995a). Some researchers suggested that due to the kinetic character of the transition, the T_g value should always be provided with the experimental conditions (heating/cooling rates) (Roudaut *et al.*, 2004). Figure 2.26 shows various curve styles, from DSC scans which the heat capacity versus temperature.

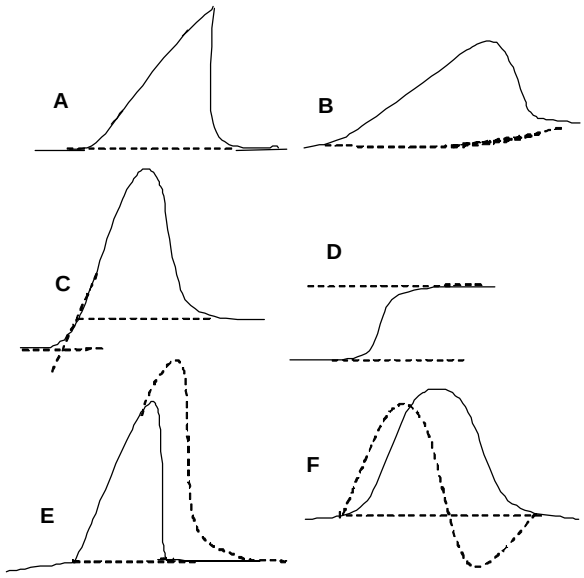

Figure 2.26 Stylized curves apparatus of heat capacity versus temperature from DSC scans. (A) Curve with no change in heat capacity, (B) a broad transition (baseline may not be flat), (C) a transition with a concomitant change in heat capacity, (D) heat capacity change during a glass transition, (E) the effect of an increase in sample size (dashed line) on the transition, (F) comparison of a primary thermogram and its first derivative (dashed line) (Nielsen, 2003)**.**

A number of researchers reported that T_g values measured by differential scanning calorimetry (DSC) shift to higher values with the increase of heating rate but with negligible effect above 20° C min^{-1} (Bai *et al.*, 2001).

Previous work of food materials with a DSC

Studies of the glass transition temperature of a single component material with a DSC is not too complicated, even though a variety of T_g values can be obtained for the same material by different researchers. Researchers have found that it was more complicated to get glass transition temperatures from DSC scans of food materials. Gidley *et al.* (1993) stated that the T_g of anhydrous polysaccharides was difficult to detect because of the decomposition of the material below T_g. Aguilera *et al.* (1998) explained that one of the reasons for having smaller transition in the DSC scans of foods was that the step change in specific heat in the thermogram depends on the fraction of the amorphous phase present. Thus, if the material is semicrystalline and the amorphous fraction is small the step change in the DSC scans will be small. Aguilera *et al.* (1998) scanned five different preparations of anhydrous apple cell wall material and detected a wide endothermic peak at between 118-122 °C (onsets) from the first heating scan but the peaks disappeared after rescanning. These endothermic transitions actually were related to water evaporation which was also found in samples of wood (endothermic peaks 120-125 °C) and dextran (130 °C). The explanation on this phenomenon was that if the T_g was hidden under the endotherm it would have appeared as a step change on rescanning. The reduction of sample weight after scanning is the evidence of this phenomenon.

Shrestha *et al.* (2007) found that T_g of mixture of orange juice + maltodextrin at different ratios seemed to under estimate the actual values. The increase in maltodextrin proportion from 60 to 75% in orange juice + maltodextrin mixture caused a relatively lower increase in T_g value compared to the increase of 50 to 60% maltodextrin. The glass-rubber temperature ($T_{g\text{-}r}$) from the thermal mechanical compression test (TMCT) were measured to compare the results from the DSC of the same mixtures (Table 2.19).

Table 2.19 Glass transition temperature (T_g) and glass rubber transition temperature ($T_{g\text{-}r}$) of orange juice + maltodextrin powders (Shrestha *et al.*, 2007)

Orange juice: maltodextrin	T_g (DSC) (°C)	$T_{g\text{-}r}$ (TMCT) (°C)	Difference
25: 75	97.3±0.3	161±1	63.7
30: 70	90.6±0.9	145±1	54.4
35: 65	87.4±1.2	141±0	53.6
40: 60	86.4±0.8	125±1	38.6
50: 50	66.4±0.6	106±0	39.6

The conclusion from this study was that the DSC resulted in better estimation of T_g values when the material had higher sugar and acid concentrations. With higher maltodextrin concentrations, the ability of DSC to accurately measure the T_g was diminished as a less defined enthalpic shift took place in the macromolecules. The endothermic relaxation peak associated with T_g became broader with increase in maltodextrin concentration in the mixtures. It was likely that the T_g values of the mixtures might have been underestimated by DSC when maltodextrin concentration was high. The TMCT was found to give a resonable results for high molecular weight components.

2.4.3 Moisture content determination of foods

The technique of moisture content measurement depends on the nature of the food being analysed and the reason the information is needed. The moisture content is used for predicting the behaviour of foods and its interaction with food ingredients during processing (Pomeranz & Meloan, 1994, Nielsen, 2003; Sablani *et al.*, 2007). In spray drying of foods, moisture content is one of the main product properties that affect stickiness or free flowing behaviour (Gupta, 1978; Bhandari *et al.*, 1997).

Food materials containing sugars and acids have a very low T_g. A small amount of moisture decreases the T_g of foods (Roos, 1995). Moisture content is considered to be a primary cause of stickiness.

Water presence in materials

The water present in materials is held in a number of different ways. The bonding of the water within a material can be divided into three groups: free water (bulk water, capillary water, or trapped water), physically bound water (or adsorbed water) and chemically

bound water (or water of hydration) (Slight, 1989; Pomeranz & Meloan, 1994; Nielsen, 2003).

Free water

Within free water, each molecule is free from any other constituents and surrounded only by other water molecules (Slight, 1989 and Pomeranz & Meloan, 1994). Free water is present in the intergranular spaces and within the pores of material (Pomeranz & Meloan, 1994). Some molecules of free water are held as trapped water in narrow channels between certain components by capillary forces. Some molecules are held in spaces that are surrounded by a physical barrier, preventing the water molecules from easily escaping. The physicochemical properties of these waters are the same as those of pure water or aqueous solutions, including melting point, boiling point, density, compressibility, heat of vaporization, electromagnetic absorption spectra. This free water serves as a dispersing agent for colloidal substances and as a solvent for crystalline compounds (Pomeranz & Meloan, 1994).

Physical bound water

Physically bound water is a significant fraction of the water molecules in many foods. It is not completely surrounded by other water molecules, but is in molecular contact with other constituents. It may be occluded in cell wall protoplasm such as, proteins, carbohydrates or minerals. This water is closely bound to absorbing molecules by forces of absorption, which are thought to be Van der Wals forces or hydrogen bonding (Slight, 1989; Pomeranz & Meloan, 1994).

Chemically bound water

Chemical bound water is bonded chemically between water molecules in food components. The physicochemical properties are different from the bulk water such as, melting point, boiling point, density, compressibility, heat of vaporization, electromagnetic absorption spectra (Pomeranz & Meloan, 1994; Nielsen, 2003).

Drying method

Drying is the standard method for determining the moisture content of materials. The material is heated under carefully specified conditions and the loss of weight is taken as a measure of the moisture content of the sample. Drying methods are simple, relatively

rapid, and provide the simultaneous analyses of large numbers of samples (Pomeranz & Meloan, 1994).

In moisture analysis, sampling, sample handling and storage are the greatest potential source of error. Any exposure of a sample to the open atmosphere should be as short as possible (Nielsen, 2003). Researchers found that for shredded cheddar cheese at 50% relative humidity, the moisture loss was 0.01% in 5 seconds, and at 70% relative humidity this amount of moisture was lost in 10 seconds. The moisture loss was linear over the 5 minute study interval. This information shows the importance of control during handling the samples when weighing before drying (Nielsen, 2003).

In practical experiments, heating of a moist organic substance also causes volatilization of other materials and of gaseous products formed by irreversible thermal decomposition of organic components. Weight losses should result from quantitative and rapid volatilization of water only (Pomeranz & Meloan, 1994; Mendonca *et al.*, 2007). For accurate moisture determination foods should be dried at the lowest possible temperature, but without a prolonged drying time (Pomeranz & Meloan, 1994).

The factors affecting the accuracy of moisture determinations are drying temperature, relative humidity, and air movement in the drying chamber. The depth and particle size of the samples, the number and position of samples in the oven, surface of the material being dried and the rate of diffusion of water vapour in the drying substance are involved in the accurate of moisture determination (Pomeranz & Meloan, 1994). The extent of variation in the oven should be determined before relying on data collected from it (Nielsen, 2003).

The drying temperature ranges from 70 to 155 °C depend on the tested material (Pomeranz & Meloan, 1994). Some moisture is retained by biological systems up to temperatures as high as the critical temperature of water at 365 °C. The typical average time of drying is from 1 to 6 hours. Food material can be dried for moisture determination for either a selected period of time or until two successive weightings show a negligible loss in weight, generally less than 2 mg for a 5 g sample at one hour intervals (Pomeranz & Meloan, 1994). The drying time is inversely related to the drying temperature but increasing the temperature increases loss of weight to a level that cannot be attained even

by prolonged heating at lower temperatures. Drying at temperatures higher than 80 °C sometimes causes weight loss resulting from decomposition.

Nielsen (2003) described the relationship of decomposition of food samples and temperatures resulting in the incorrect moisture content. The decomposition occurs when the time is extended too much or the temperature is too high. Carbohydrates decompose at about 100 °C, and the moisture generated in carbohydrate decomposition is not part of the moisture content of foods. Sucrose hydrolysis can result in utilization of moisture, which would reduce the moisture for measurement. A consistent error can be from the loss of volatile constituents, such as acetic, propionic, butyric acid, alcohols, esters and aldehydes. Weight gains can occur due to oxidation of unsaturated fatty acids and certain other compounds. High temperatures are used to obtain rapid results and can be justified on pragmatic grounds only. Pomeranz and Meloan (1994) however, suggested that drying temperature can be reduced by using vacuum ovens, and drying times can be shortened by adding drying agents or by means of dry air passing through the sample in the oven.

A common source of error in moisture content determination of foods explained by Pomeranz and Meloan (1994) is the formation of a crust that is impervious to evaporation of moisture within the dried sample. This phenomenon occurred in samples rich in sugars. The effects of crust formation can be reduced by moistening with water and thorough mixing with a known mass of sand or asbestos to increase the exposed surface or by top drying of thin layers under infrared heat lamps. For some plant materials, two-step drying is needed: drying first at a relatively low temperature to prevent crust formation and further drying at a higher temperature until the end.

Pomeranz and Meloan (1994) further discussed the effects of high temperature on the sugar component of foods. Honey and fruit syrups which have a high fructose fraction decompose at high temperature. The drying of fructose, glucose or sucrose solutions is faster and the tendency to decompose is less if the pH is below 7. Fructose solutions decompose at temperature above 70 °C while glucose is relatively stable at 98 °C. Sucrose solutions dry very slowly in an oven. In a vacuum oven, slightly acidic fructose solutions on pumice adsorbent were found to dry in 4 hours at 70 °C, and in 7-9 hours at 60 °C.

Nielsen (2003) suggested that an aluminium pan normally about 5.5 cm diameter with cover is used for drying. This pan can be reused but has to be cleaned. The pan cover is sometimes necessary to control the loss of sample by spattering. The metal cover must be slipped to one side during drying to allow moisture evaporation. Slipping of the cover allows the possibility of spattering with product loss, producing erroneous results and large standard deviations. A disposable pan is a better choice with glass fibre discs for covers.

Vacuum oven method

The vacuum oven method gives a reproducible estimate of true moisture content (Pomeranz & Meloan, 1994). The rate of drying can be increased by lowering the vapour pressure by using vacuum.

The rate of drying can be increased by lowering the vapour pressure in the air by using vacuum. The normal vacuum oven method involves drying to constant weight at a pressure below 6.7 kPa (50 mmHg) (Pomeranz & Meloan, 1994) or 3.3-1.3 kPa (25-100 mmHg) (Nielsen, 2003). Drying to constant weight requires rather long periods for most foods. Drying temperatures specified for most vacuum oven methods are 98-102 °C indicating the accuracy of ±2 °C. Foods rich in levulose and high sugar products as fruits must be dried at 70 °C or below (Pomeranz & Meloan, 1994; Nielsen, 2003). In a vacuum, heat is not conducted well, so the pans must be placed directly on the metal shelves to conduct heat (Nielsen, 2003).

Moisture content determination of sugar

The moisture content determination of samples with a high percentage of fructose, glucose, sucrose and acids requires a more complicated method. For fructose, Browne and Zerban (1941) suggested 60 °C in a vacuum oven with a pressure of not more than 6.7 kPa until the weight no longer changes. For glucose, there is a possibility of losses its water of crystallization at 60 °C, so to prevent this a vacuum oven at 9.2 kPa and 55 °C was recommended for moisture content determination of sugar and mixtures with glucose. The duration of 48 hours was enough to dry the samples (Browne & Zerban, 1941). The vacuum oven at 50 °C for 24 hours was used to dry samples with lactose (Haque & Roos, 2005, 2006).

2.4.4 Dielectric analysis of foods near T_g

Dielectric analysis (DEA) is a thermo-electro analytical method, which is used for studying molecular mobility of polar biopolymers. It detects dielectric, i.e. capacitive and conductive, properties of a material in a periodic electrical field. Researchers found that the dielectric properties are not only closely correlated with water content and temperature but also state changes in a material. They are related to the physical state and are significantly affected by phase transitions, such as melting of ice and the glass transition.

Noel *et al.* (1992) indicated that by dielectric spectroscopy, peaks which correspond to characteristic relaxation processes within the sample can be observed. The primary relaxation (also known as • -relaxation) which is observed at the highest temperature (or lowest frequency), has been generally associated with the increase in molecular mobility which occurs on heating through the glass transition. Secondary relaxations (or • -relaxations) are also observed in many materials at lower temperatures (or higher frequencies) than • -relaxations. However, the reasons for these phenomena are still not clear. Laaksonen and Roos (2000) asserted that the glass transition measured by dielectric analysis was dependent on frequency, because the glass transition phenomenon is a second-order transition.

Dielectric relaxation spectroscopy detects molecular motion of polar molecules when exposed to a weak external alternating electric field. As the electric field frequency is increased, it reaches a relaxation frequency when the polar molecule can no longer rotate with the electric field. Dielectric properties change markedly around this relaxation frequency. Dielectric properties not only depend on water binding in food material but also on food composition. For a given molecular composition, the dielectric spectrum will change with molecular binding. In real material, complexity of molecular composition, presence of ions, electrical charges on proteins and pH variations lead to a complex dielectric spectrum with the contribution of several phenomena (Clerjon *et al.*, 2003).

Kinetic factors determine the temperature of the T_g which depends on the time scale of the observation or conversely on the frequency characteristics of the experimental probe. The glass transition is also accompanied by a change in the rate of molecular translational

and rotational diffusion. By dielectric spectroscopy, peaks which correspond to characteristic relaxation processes within the sample can be observed.

From measurement of the frequency and temperature dependence of dielectric relaxations, it is possible to obtain estimates of the activation energies of the physical processes from which the relaxation arise. These energies may in turn provide information on the processes themselves or even, perhaps, on the molecular structure or arrangement. In general, it is found that energies related with • -relaxations are greater than those of • -relaxations, sometimes by an order of magnitude. Various interpretations have been put forward for the occurrence of these relaxation processes. Johari (2002) had proposed a model whereby structural non-uniformity within a glass leads to "islands of mobility" which are responsible for the secondary relaxation, while the primary relaxation is due to larger, cooperatively rearranging regions. According to this model, specific details of molecular structure are not required for the interpretation. A slightly different approach which depends more on the specific molecular structure proposes that • - and • -relaxations depend on the average free volume and the free volume fluctuations, respectively. In this latter model, fluctuations in free volume provide the space necessary for motion of bulk side groups to occur (Noel *et al.,* 1992).

Studies of molecular dynamics in low water content amorphous carbohydrates using dielectric, mechanical and NMR relaxation techniques showed several features in common with other polyhydric alcohols such as glycerol and glucitol, and with glass forming materials in general. Noel *et al.* (1992) found that some motions give rise to frequency-dependent dielectric and mechanic properties. At temperatures below the calorimetric T_g, the peak relaxation time exceeds experimental time scales (10^2-10^4 s) and non-equilibrium glassy state occur. Further secondary or • -relaxation is observed at temperature close to T_g and in the glassy state. The relaxations typically occur over a wide temperature range and have an Arrhenian temperature dependence, $\bullet_{max} = A\ exp(E_a/RT)$ (Noel *et al.*, 1992).

Practical work in DEA

DEA measures capacitance, and conductance as a function of temperature, time and frequency. It evaluates permittivity or dielectric constant (• '), the loss factor (• "), and dissipation factor (*tan* •) which corresponds to the ratio of loss factor to permittivity

(Laaksonen & Roos, 2000, 2001). Roos (1995) stated that the dielectric constant, dielectric loss and dissipation factor can be measured by placing a sample between parallel place capacitors with an alternating electric field. Polar groups in the sample respond to the alternating electric field and an absorption maximum is obtained at the frequency that equals the molecular motion. A number of researchers have used DEA to analyse sub-zero and sub-T_g relaxations in different carbohydrate models and to characterise phase and state transitions in wheat dough (Lievonen & Roos, 2003). Figure 2.27 shows *tan* • of frozen wheat dough as a function of temperature measured by DEA at various frequencies from the work of Laaksonen and Roos (2000). From Figure 2.27 the authors claimed that the water (ice) in wheat dough started to melt at -21, -24 and -24 °C at 0.1, 0.5 and 1 Hz, respectively. The ice melting peaks were found to shift closer to 0 °C with increasing frequency. The 1000 Hz response showed a melting peak at 0 °C. The figure shows the glass transition temperature only at low frequencies (-25 °C at 0.5 Hz and -33 °C at 0.1 Hz) because at increasing frequencies, the glass transition coincided with melting.

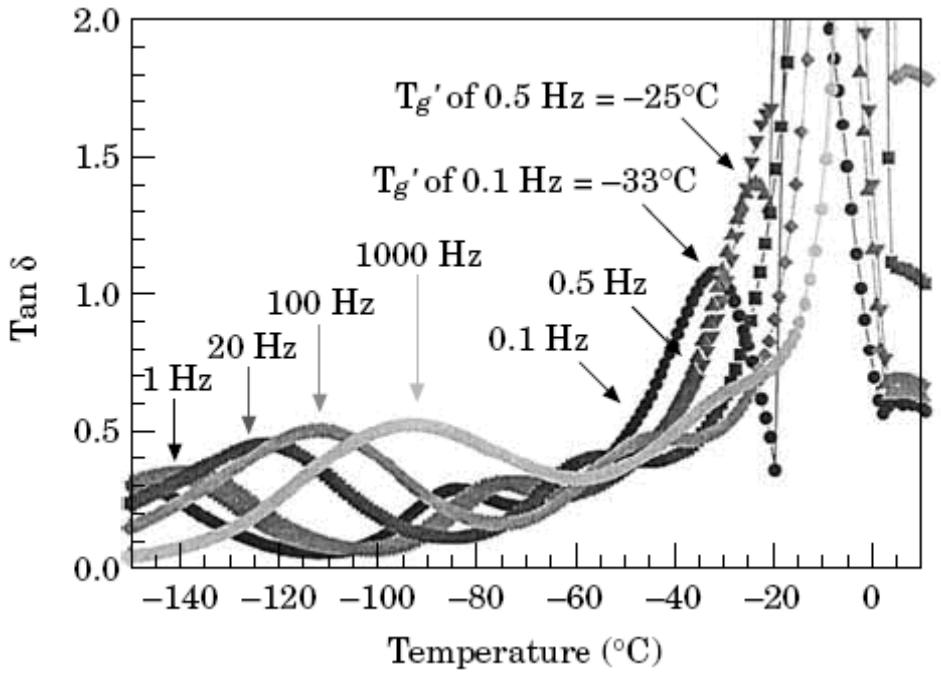

Figure 2.27 Tan • of frozen wheat dough, as a function of temperature, measured by DEA at 0.1, 0.5, 1, 20, 100 and 1000 Hz (Laaksonen & Roos, 2000).

Dielectric measurements provide a low-cost alternative to expensive DSC scans to determine T_g in food material (Kilmartin *et al.*, 2000).

Kilmartin *et al.* (2000) and Goff (1995) stated that, with the aid of a dielectric thermal analyser, the dielectric constant or permittivity (•') can be obtained from the capacitance (*C*).

$$•' = C/C_0$$

where C_0 is the capacitance of free space.

The dielectric loss factor (•") associated with the loss of electromagnetic energy (related to electrical resistance) during molecular motion. Goff (1995) indicated that this value is proportional to conductance at low frequencies.

The loss tangent which estimates the relative contributions of •' and •", defined as

$$tan\ • = •"/•'$$

Kilmartin (2000) stated that these values vary with measurement frequency, temperature and moisture content. In addition for polymers the value of •' generally increases with temperature, while after a glass transition the response can change sharply as the underlying mobility is altered. The T_g was taken from the peak derivative of $d•'/dt$ which is proportional to the derivative of capacitance over temperature.

Chan *et al.* (1986) found with concentrated glucose solutions that the DSC T_g values corresponded with a rapid increase in •", but these were less than the temperature giving the peak in •". Figure 2.28 shows a plot of •" against temperature at 1 kHz of anhydrous glucose (a), 10 wt % water-glucose mixture (b) and 15 wt% water-glucose mixture from the work of Chan *et al.* (1986). The arrows indicate the glass transition temperature from DSC.

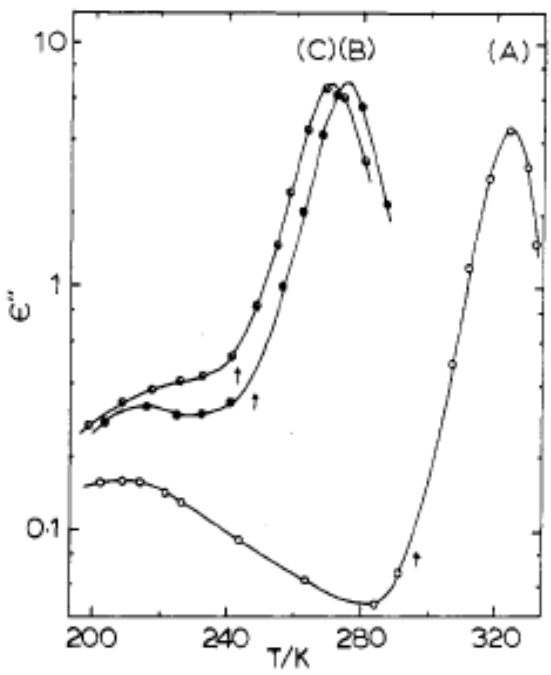

Figure 2 28 A plot of •" against temperature at 1kHz for (A) pure glucose, (B) a 10 wt % water-glucose mixture and (C) 15 wt % water-glucose mixture. The arrows point to T_g from DSC.

The T_g of dilute sucrose solutions by Goff (1995) showed a frequency-independent peak in *d•"/dt* was linked to the main DSC transition. Figure 2.29 shows the first derivative of loss factor as a function of temperature when the frequency range was between 0.1-50 Hz of the 20% aqueous sucrose solution from the work of Goff (1995). From the figure the lowest peak maximum temperature at 0.1 Hz was -53 °C and the second transition from the same frequency appeared at -28 °C. The lower transition showed frequency dependence which was given as evidence that this transition contained a significant second-order relaxation which was the glass transition.

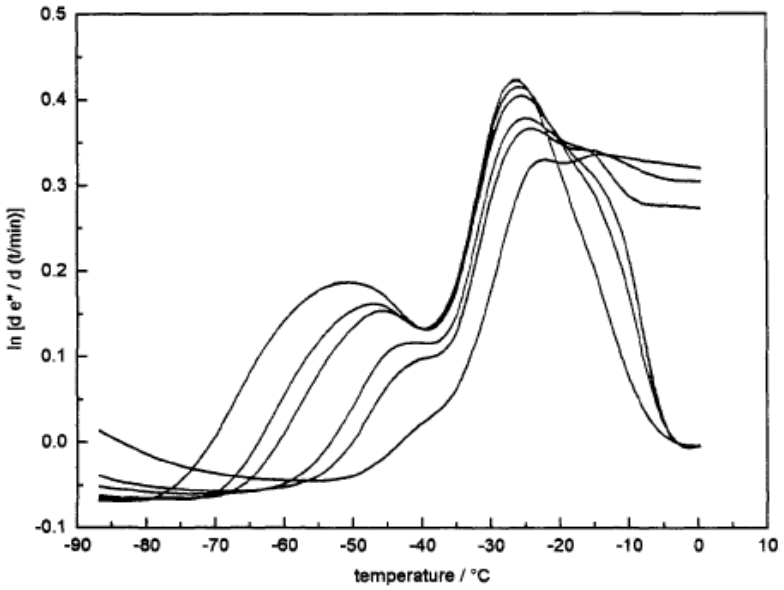

Figure 2.29 First derivative of the loss factor (•”) as a function of temperature (frequency from 0.1 to 50 Hz) determined by dielectric analysis for a 20% aqueous sucrose solution (Goff, 1995).

Noel *et al.* (1996) presented the plot of dielectric constant (•’) and dielectric loss (•”) of glucose and maltose and their mixture with water at 10 kHz as shown in Figure 2.30 and 2.31 respectively. They found that the •-relaxation of anhydrous glucose and maltose were observed as peaks in •” at temperatures above the calorimetric T_g values and the •-relaxation were observed as peaks in •” below the calorimetric T_g. These studies also found that in each case a secondary sub-T_g •- relaxation was also observed and the peak in •” occurred at lower temperatures and was more marked at lower frequencies. The continuation of molecular motion associated with the •- relaxation has been linked to the motion of water and to various hydroxyl groups or has been seen to defined the glass transition occurring at these lower temperature.

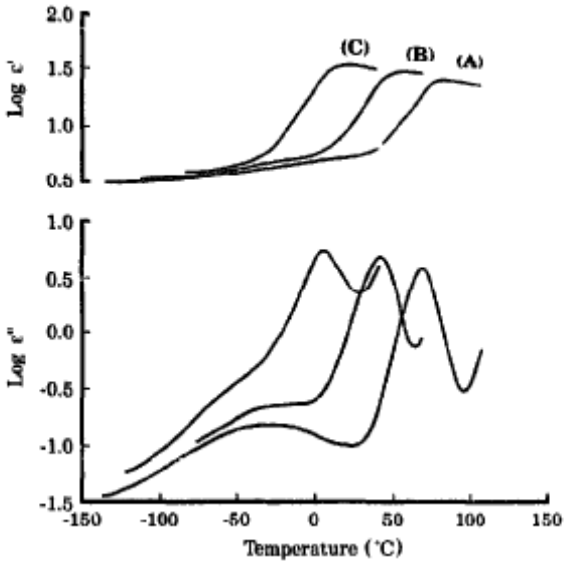

Figure 2.30 The dielectric constant (•') and dielectric loss (•") with temperature at 10 kHz for (A) pure D-glucose, (B) a 5.0% w/w water-glucose mixture and (C) a 12% w/w water glucose mixture (Noel *et al.*, 1996).

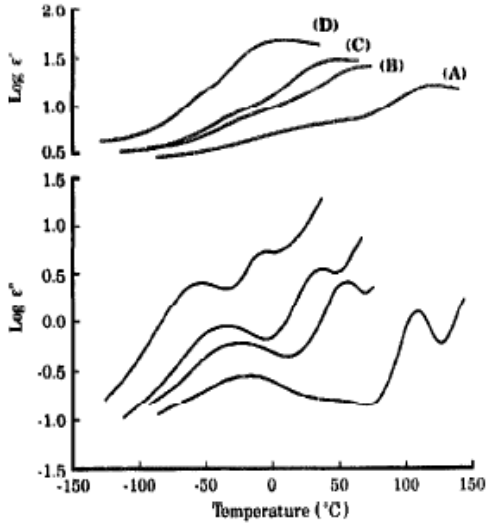

Figure 2.31 The dielectric constant (•') and dielectric loss (•") with temperature at 10 kHz for (A) pure maltose, (B) a 7.0% w/w water-maltose mixture and (C) a 11.5% w/w water maltose mixture (Noel *et al.*, 1996).

Noel *et al.* (1996) studied the dielectric relaxation behaviour of glucose, maltose and their mixtures with water up to a concentration of 12.0 and 23.0% w/w respectively, at frequency range 10^2 to 10^5 Hz found that the primary relaxation was observed at temperatures above the T_g and a secondary relaxation below T_g. The addition of water shifted the primary relaxations to lower temperatures. Water + glucose mixtures

increased the strength of the secondary relaxation and resulted in a merging of the primary and secondary relaxations. The increase in strength of the secondary relaxation was much more marked for the maltose + water mixtures and, in this case, the relaxations remained separate over the range of frequency and water contents in this study. The dependence of the strength of the secondary relaxation on the water content in maltose + water mixtures was bilinear with a change in gradient at around 10% w/w water. The sub-T_g relaxation was thought to arise from motions of pendant hydroxymethyl groups attached to the hexose rings and from the reorientation of water molecules. The difference in the secondary relaxation behaviour of glucose and maltose indicates that structural factors, in addition to the presence of hydroxymethyl groups, are also important.

Kilmartin *et al.* (2004) found that a sharp increase in the rate of charge in permittivity of maltodextrin solutions corresponded to DSC T_g values. The transition was broader with the lower DE maltodrextrins. The mixtures of shorter and longer oligomers might give rise to a more gradual glass transition region. A broad sub-T_g maximum in the permittivity was observed which may have its origin in the continued motion of hydroxyl groups in the glassy matrix. Adding NaCl (0.1 mol kg^{-1}) into maltodextrin solutions causes the T_g to reduce by around 4-6°C.

Experimental set up for DEA

In the experimental set up for DEA of foods by Kilmartin *et al.* (2000) the resistance, inductance, capacitance (RLC) metre connected with round parallel plates of very small clearance functioned well. The sample was placed in between the parallel plates after the capacitance of the empty cell had been measured. The frequency and temperature range were made to be able to match the T_g value of samples from a DSC (Moates *et al.*, 2001; Kilmartin *et al.*, 2000, 2004). Dow Corning high vacuum grease was used to give a paste with no air pockets in the solid samples. The grease has a negligible dielectric response and is thermally stable in the temperature range from -140 to 200 °C (Butler & Cameron, 2000).

Chapter 3 Materials and Methods

3.1 Materials

Fresh apples and carrots were purchased from the fruit and vegetable shop. The apples used in the preliminary study (Section 4.2) were Braeburn, Granny Smith and Royal Gala. The Royal Gala is a crisp sweet and aromatic variety. The Braeburn is a sweet-tart flavour apple. The Granny Smith is a tart apple.

Fresh carrots (*Daucus carota*) were purchased separately from time to time. The two lots of fresh carrots for the production of carrot fibre powders in the experiments were purchased during autumn (April 2006) and summer (January 2007) and were assumed to be freshly harvested. All carrots were cleaned and had their tops removed before processing.

Apple juice concentrate was purchased from ENZAFOODS New Zealand Limited. The juice had been de-pectinised, clarified, and concentrated with separate aroma recovery. The concentrate did not contain additives, preservatives, acidity regulators, added sugars, colourings or flavourings. The concentrate was specified as 70 °Brix with acidity of 1.2-3.5 malic acid, colour < 0.35 absorbance at 420 nm at 12 °Brix, pH 3.0-4.0, specific gravity was 1.35 at 20 °C, crystal clear clarity and completely free from haze. The total soluble solid content was 75%, with 44% fructose, 16% glucose and 22% sucrose (HPLC method). The tritratable acid was 1.99%.

Maltodextrin (DE 9.8 max.) produced by the controlled hydrolysis of corn starch (Fieldose 10C-AP) provided by Penford Australia Limited was used. The sugar profile (% w/w dry basis) was 2.0% monosaccharide, 4.0% disaccharide, 6.0% trisaccharide and 88.0% tetra and higher.

D-fructose, D-glucose, D-sucrose and malic acid were purchased from Sigma Aldrich (Australia).

Deionised reverse osmosis (DI) water was used in all experiments.

Acetronitrile (HPLC grade) purchased from VWR International Ltd. England was used in the HPLC sugars determination method.

The kit for the enzymetic sucrose/ glucose/ fructose analysis was purchased from Boehringer Mannheim (Cat. No. 716-260). All the reagents used for this analysis were included in the kit.

3.2 Methods

3.2.1 Sugars content determination

All juices were passed through a vacuum filter with a glass microfibre filter (Whatman® Cat no. 1821 150) three times to remove solid particles before all types of sugar determination.

Enzymatic methods

The method described with the kit from Boehringer Mannheim (Germany) was followed. The glucose content was determined by the hexokinase/glucose-6-phosphate dehydrogenase method. After determination of glucose the fructose content of the same sample was determined by the hexokinase/phosphoglucose isomerise/glucose-6-phosphate dehydrogenase method. The sucrose content was determined using the invertase hydrolase method with the enzyme • -fructosidase. The sugar contents of fresh carrot juice and fresh apple juice were determined by these enzymatic methods. The results were the average of two replicates.

Determination of glucose and fructose

The juice solution was deproteinized with ice-cold 1 N perchloric acid in the proportion of 1:1, centrifuged and the supernatant was immediately neutralized with 2 M KOH. It was left for 20 min in an ice-bath and the precipitated potassium perchlorate was removed by filter. The ideal concentration for the analysis was 0.4-0.8 g glucose + sucrose per litre; stronger solutions were diluted.

Reagents

Triethanolmine buffer (Tra buffer). 11.2 g triethanolamine HCl and 0.2 g $MgSO_4\,7H_2O$ were dissolved in 150 mL of distilled water, adjusted to pH 7.6 with approximately 4 mL

of 5 M NaOH, then made up to 200 mL with distilled water. The temperature of the buffer was brought to 20-25 °C before use. The buffer was stable for 4 weeks when stored at 4 °C.

Nicotinamade-adenine dinucleotide phosphate solution (NADP). 50 mg NADP-Na_2 was dissolved in 5 mL of distilled water. This solution was stable for 4 weeks when stored at 4 °C.

Adenosine-5' – triphosphate solution (ATP). 250 mg of ATP- Na_2H_2 and 250 mg $NaHCO_3$ were dissolved in 5 mL of distilled water. The solution was stable for 4 weeks when stored at 4 °C.

Hexokinase/glucose-6-phosphate dehydrogenase (HK/G6P-DH). 0.5 mL of hexokinase solution (2mg/mL) was mixed with 0.5 mL of glucose-6-phosphodehydrogenase solution (1 mg/mL). The solution was stable for 1 year when stored at 4 °C.

Phosphoglucose isomerase (PGI). The suspension was used undiluted 2 mg/mL. It was stable for 1 year when stored at 4 °C.

Procedure

The spectrophotometer (model 101, Hitachi, Japan) was zeroed using distilled water, before and after each sample was measured. 3 mL of triethanolamine buffer at 20-25 °C was pipetted into a cuvette (1 cm path length) and 0.10 mL of NADP solution was added, followed by 0.10 mL of ATP solution and 0.20 mL of sample. The contents were mixed by inversion and the absorbance (optical density) was measured at 340 nm (E_1). 0.02 mL of HK/G6P-DH suspension was added and, after mixing, the reaction was allowed to go to completion (10-15 min), and then the optical density was measured again (E_2). If the reaction had not reached completion after 15 min, the absorbance was read at 2-min intervals until absorbance was stable over the 2-min period. 0.02 mL PGI solution was added and mixed, and the absorbance was read after 10 min (E_3).

The concentrations of glucose and fructose were calculated from the absorbance differences:

$E_{glucose}$ (density change due to glucose) = E_2-E_1

$E_{fructose}$ (density change due to fructose) = E_3-E_2

The concentrations [g L^{-1}] were calculated from

$C_{glucose} = E_{glucose}$ x 0.495 F

$C_{fructose} = E_{fructose}$ x 0.495 F

where F was the dilution factor.

Determination of Sucrose by Invertase Hydrolase

The protein was removed by the addition of 1 N perchloric acid in the proportion of 1:1.

Reagents

Acetate buffer. 6.7 mL of 1 M NaOH and 13.5 mL of 1 M acetic acid were added to 180 mL of water. The pH of the buffer was 4.6. The temperature of the buffer was 20-25 °C before use. The solution was stable for 1 year when stored at 4 °C.

Beta–fructosidase solution. 10 mg of beta-fructosidase lyophilisade was dissolved in 2 mL of distilled water. The solution was stable for 1 week when stored at 4 °C.

The following buffers and solutions were the same as for glucose and fructose determination: triethanolmine buffer (Tra buffer), nicotinamade-adenine dinucleotide phosphate solution (NADP), adenosine-5' – triphosphate solution (ATP), hexokinase/glucose-6-phosphate dehydrogenase (HK/G6P-DH) and phosphoglucose isomerase (PGI).

Procedure

0.20 mL of sample was mixed with 0.50 mL of acetate buffer and 0.002 mL of the beta-fructosidase solution in a cuvette (1 cm path-length) and left to stand for 15 min at 20-25 °C. Then 2.50 mL of Tra buffer was added, followed by 0.10 mL of the NADP solution and 0.10 mL of the ATP solution. After mixing, the absorbance was measured at 340 nm (E_1). Then the 0.02 mL HK/G6P-DH solution was added and left for 10-15 min before measuring the absorbance again (E_2). If the reaction was not completed at this time, the absorbance was measured at 2 min intervals until the increase per interval was constant. E_2 was extrapolated back to the time of addition of the hexokinase and this value was used in calculations.

The calculation of the sucrose concentration, C_{sucr} [g L^{-1}] was as follows:

$$C_{sucr} = [(\text{sucrose} + \text{glucose}) - \text{free glucose}] \times 2 \times 0.95$$

$$C_{sucr} = [(E_2 - 0.497E_{1(\text{sucrose test})}) - (E_2 - 0.495E_{1(\text{glucose test})})] \times 2 \times 0.95$$

Enzyme membrane method (YSI 2700 SELECT)

A YSI 2007 SELECT (YSI incorporated, Ohio, USA) was used for glucose and sucrose measurement. The glucose and sucrose dual channel enzyme membrane probe was used. The equipment limits were: the combined total of glucose and sucrose could not exceed 25 gL^{-1}, and the glucose concentration could not exceed 10 gL^{-1}.

Sample preparation was based on the results of sugar determination in carrot juice by the enzymatic method and the sugar content in carrot juice from literature. The samples were diluted to have a glucose solution concentration less than 10 gL^{-1}.

The samples used in this method included freeze dried blanched carrot fibre, freeze dried untreated carrot fibre (detail in Section 3.2.3), fresh carrot fibre, extracted fresh carrot juice, blended fresh carrot juice, extracted fresh carrot juice + blanched fibre, extracted fresh carrot juice + untreated fibre, blended fresh carrot juice + untreated fibre, and extracted fresh carrot juice + 20% fresh carrot fibre (wet weight basis).

DI water was added to the freeze dried carrot samples to bring the total solids content to its original value, and these mixtures were put in a water bath at 40 °C for two hours. The clear solution on the top was used without filtering out the solid content. D-glucose, D-sucrose and DI water were used for sugar concentration standards calibration. The standard solution of glucose was 4.8%. The standard solution for sucrose was 8.3%. The calibration errors were in the range of 4.8 + 0.51% to 4.8 + 0.69% for the glucose standard concentration and 8.3 - 0.13% to 8.3 - 0.99% for the sucrose standards. The results were determined and the averages of 2-5 replicates were presented.

HPLC and RID method

The HP 1100 series HPLC with a refractive index detector (RID 1047A, Agilent Technologies, CA, USA) and a 35101 Prevail carbohydrate ES column (Alltech Assoc, IL, USA) were used. The solvent was 75% acetonitrile in DI water. D-fructose, D-glucose and D-sucrose were used for sugar concentration standards. The flow rates with retention

time, peak height and peak area were determined. The retention times of standards were the indicator of each sugar from the HPLC results. The relationship of peak height and peak area to the concentration of the standards was graphed. The linear relationships of both peak height and peak area with standard concentrations were used to find the concentration of the sugars in the samples. The detail procedure for the HPLC, including the chromatograms of some standards, is in the Appendix.

The solid particles were removed. The 35101 Prevail carbohydrate ES column was used with clear juice without deproteinisation. The clear samples were then injected through a 2.2 µm filter into HPLC vials. The samples vials were put in the HPLC autosampler tray.

The samples used in this method were freeze dried heat treated carrot fibre, freeze dried unheated carrot fibre (December), freeze dried carrot fibre (January), freeze dried fresh carrot juice, extracted fresh carrot stored at -20 °C, extracted fresh carrot juice (1) and (2), fresh apple juice (Braeburn), and apple juice concentrate. The results were determined and the averages of two replicates were presented.

A number of practical hints were followed to optimize the use of the RID HP 1047A (detail in Appendix A). The HPLC procedure was followed (detail in Appendix A).

3.2.2 Preparation of carrot fibre powder

Fresh carrots were passed through a juice extractor (Juice Fountain JE95, Breville, Australia) without any heat treatment. The fibres (retained by the extractor) were freeze dried (the freeze drying method is in Section 3.2.3). The vacuum oven at 45 °C and -85 kPa was used to further dry the fibres before they were processed in a centrifugal mill (ZM 100 Retsch, Germany) at 14,000 rpm with sieve #0.2. The carrot fibre powder was packed in polyethylene bags to protect them from moisture absorption and stored at −20 °C for further analysis. The frozen carrot fibre powder was then dried in the vacuum oven at 45 °C for 48 hours and kept in sealed desiccators with silica gel as a desiccant for all further processes and analysis. The particle size distribution was determined using a Microtrac-x100 (Microtrac Inc., Florida, USA) particle size analyser with water as a fluid media. An Olympus BX60 Optical microscope was used to view the carrot fibre powders. The carrot fibre powder shape and appearance was reanalysing by a Wild M37

Kombistereo microsope with a Meiji Infinity 1 digital camera. The software driving the camera was Lumenera Infinity Capture.

3.2.3 Freeze drying experiments

The samples were frozen at -30 °C overnight before being freeze dried in a VirTis 12 SL (model 24Dx24, Virtis Co., New York, USA) freeze drier. The temperature of the sample chamber was -25 °C and the temperature of condenser was -53°C. The freeze drying continued until the final weight of the samples was stable for 24 hours. The total time to dry depended on the character of each sample. All the freeze drying experiments in this study were carried out by the same method.

Freeze drying of blended fresh apple juice + carrot

Fresh apples (Braeburn, Granny Smith and Royal Gala) were separately cleaned and the seeds were removed before passing through the juice extractor. Fresh carrots were sliced into thin slices. Each type of the apple juice was mixed with slice carrots at ratios of 1:1, 1:0.75, 1:0.50 and 1:0.25 (wet weight). The mixtures were blended in a blender (liquidiser) until the mixtures appear to be homogenous then freeze dried. These mixtures are referred to later as blended juice. Freeze dried samples of pure apple juice from each variety was used as a control for comparing properties of the freeze dried material. The results are in Section 4.2.

Freeze drying of blanched and untreated carrot fibre

The fresh carrots were passed through the juice extractor. The fibre retained from the extractor was separated into two parts. The first part was blanched by soaking in hot water at 80 °C and maintained at 80 °C for 20 minutes. The blanched carrot fibre was rinsed with cold water three times before being freeze dried. The other part of the fibre was freeze dried without any further treatment, immediately after extraction. The freeze dried product of these two types of carrot fibre were then ground and sieved to obtain a particle size of not more than 180 µm. The fibre powder was kept in sealed plastic bags (Whirl pack bags 540 mL sterile 115x230 mm 2.5 mm thick 18 oz Catalogue Number NASB00736WA). The samples were kept at -20 °C for further analysis.

Freeze drying of carrot juice

The juice was extracted from carrots on the day of purchasing and after storage for 10 days in a refrigerator. Juice samples from both types of carrots were freeze dried. To have more samples for comparison the carrot juice + fresh fibre and carrot juice + dry fibre were freeze dried. They were the fresh carrot juice + 20% wet basis of fresh fibre retained from the extractor (blended in a blender and freeze dried), the extracted juice + 5% dry weight of the blanched carrot fibre, and the extracted juice + 5% dry weight of the untreated fibre.

Freeze drying of fructose solutions

Fructose solutions of various concentrations were freeze dried to study the freeze drying performance. D-fructose was first vacuum dried. Deionised (DI) water was used to prepare 50, 60, 70, 80, 90 and 95% fructose solutions. The container of fructose + DI water was put in a hot water bath at 60-80 °C and manually stirred until all the fructose crystals had melted. The solutions were then freeze dried.

Freeze drying of fructose + carrot fibre

Dried D-fructose and DI water were used to prepare the fructose + carrot fibre mixtures. An aqueous solution containing 50% fructose solution was mixed with dried carrot fibre powder to obtain suspensions of 14, 21, and 28% carrot fibre on a dry mass basis. The samples were freeze dried.

Freeze drying of fructose + carrot fibre + malic acid

Dried D-fructose and DI water were used to prepare the amorphous fructose + carrot fibre mixtures. An aqueous solution containing 50% fructose solution was mixed with dried carrot fibre powder to obtain suspensions of 50, 60, and 70% carrot fibre on a dry mass basis. The samples were freeze dried. The freezes dried samples of fructose + carrot fibre then were blended. Malic acid at 1, 2, and 3% w/w dry basis were made into a solution with DI water and mixed with the blended freeze dried 50, 60 and 70% carrot fibre in fructose and mixed. The mixtures of blended fructose + carrot fibre + malic acid solution were freeze dried and vacuum dried.

Freeze drying of fructose + Maltodextrin

A procedure similar to that of freeze drying fructose + carrot fibre was used to obtain mixtures of fructose + maltodextrin (Fieldose 10C AP maltodextrin, DE 9.8 max). The mixtures of 50, 60 and 70% maltrodextrin in fructose were freeze dried.

3.2.4 Spray drying experiment

A Niro Mobile Minor spray drier (Niro, Denmark) with a 0.6 m diameter x 1.8 m high chamber, a rotary atomizer pneumatically-driven at 600 kPa, and 1.5 kg hr^{-1} feed rate was used in all spray drying experiments. Aqueous mixtures containing 40% total solids were spray dried and the powder was collected by a cyclone. The temperatures used for spray drying of fructose + carrot fibre and apple juice concentrate + carrot fibre were 165 °C inlet and 75 °C outlet (denoted as 165/75 °C). The spray drying temperatures for mixtures of fructose + maltodextrin and apple juice concentrate + maltodextrin solution were raised to 175/85 °C in an attempt to achieve a greater yield of dry powder. The moisture content of the powder and DSC analysis were obtained immediately after spray drying. Samples used for further DSC analysis were removed from the dryer and immediately placed in sealed plastic bags in a freezer at -20 °C.

Spray drying of mixtures of fructose + carrot fibre and fructose + maltodextrin

Dried D-fructose and DI water were used. An aqueous solution containing 35% fructose (weight by volume) was mixed with dry carrot fibre powder to obtain suspensions of carrot fibre 40, 50, 60, and 70% on a dry basis. DI water was used to adjust the total soluble solids content of the mixture to 40% before spray drying.

A similar method was used for the mixtures of fructose + maltodextrin at 50, 60 and 70% dry basis.

Spray drying of mixtures of apple juice concentrate + carrot fibre and apple juice concentrate + maltodextrin

Samples of apple juice concentrate + carrot fibre powder at 30, 40, 50, 60, and 70% (w/w dry basis) were prepared. DI water was used to adjust the total soluble solids content of the mixture to 40% before spray drying.

Samples of apple juice concentrate + maltodextrin at 50, 60, and 70% (w/w dry basis) were prepared by the same method.

3.2.5 Moisture content determination

A vacuum oven at 45 °C for 48 hours was used to determine moisture content of all samples. The wet basis moisture was calculated using equation 3.1.

$$\text{Moisture (w/w)} = \frac{W_w - W_d}{W_w} \tag{3.1}$$

where W_w is the mass of sample before drying and W_d is dry mass of sample after drying.

3.2.6 Visualization of phase transition in sugars

Crystalline D-sucrose, D-glucose and D-fructose and mixture of two and three of these sugars at different ratios were melted. The physical changes during the heating and cooling were observed. The glass transition behaviour during cooling and heating amorphous sugars and the relationship of the phenomenon with the temperature of each sugar and mixtures were observed and recorded. A thermocouple (connected to a Fluke 52 K/J thermometer) was used in the observation trials. The sample of 2.5 grams of sugar was melted in a glass plate on the hot plate at the rate of around 5 °C per minute until all sugar crystals became a liquid. The samples prepared by this method were cooled down and checked for crystals (the sugar crystals that was not properly melted and still showed being partial crystals) using a polarized light microscope. The melting method that produced no crystals was applied to further observations.

The liquid sugar was then cooled down until it could be completely wrapped around the thermocouple tip with a 2 mm thickness. The rubbery sugar broke off the thermocouple tip when it became glassy sugar. The temperature was noted at the moment the sugar changed to a glassy solid and this was recorded as the T_g of the sample. The amorphous solid sugar then was heated and cooled down to repeat the record. At least four tests for each sample were performed to get the average T_g of each sample. The thermocouple was calibrated with boiling water and ice everyday.

3.2.7 Measurement of *Tg* by DSC

A CSC 4100 multi-cell Differential Scanning Calorimeter (Calorimetry Sciences Corporation, Utah) with MC-DSCRUN v. 2.2.0 software was used to obtain thermograms and estimates of T_g. The equipment was calibrated with sapphire and DI water. The samples were filled into hastelloy-C ampoules, and sealed with lids and were cooled to –25°C, annealed for 40 minutes then heated at 0.1 °C min^{-1} to get the heating scan thermograms. For all sugar samples the scans were set to anneal at 110 °C for 40 minutes then to cool at the same rate to get the cooling thermograms. The annealing temperature for the sample with carrot fibre and maltodextrin was at 80 °C for 40 minutes. Only heating scans could be done for samples with carrot fibre and maltodextrin.

T_g of melted sugars and their mixtures

Dried D-fructose, D-glucose and D-sucrose were used to prepare melted amorphous sugars. A temperature controllable stove was used to heat the sugars to not more than the melting temperature of each one (to minimise degradation) until all crystals were melted. The temperature used to melt fructose, glucose and sucrose were 105 °C, 150 °C and 185 °C respectively (literature melting points are given in Table 2.6). After melting the resolidified sugars were checked for micro-crystals under a polarized light microscope. This confirmed no microcrystalline material in the samples so this melting method was applied to all samples before immediately filling and sealing in DSC ampoules for analysis.

T_g of freeze dried fructose

Freeze dried fructose prepared from a 95% (w/w) solids solution was used. The sample of 0.2 grams in sheet form was put into a DSC ampoule immediately after freeze drying to prevent moisture absorption. The samples were annealed, and scanned with heating and cooling.

T_g of freeze dried fructose + carrot fibre

The freeze dried fructose + carrot fibre powders at 14, 21, and 28% dry mass basis were used. DI water was added to the samples to alter the moisture content to 2 and 5% and they were held for 2 weeks in a closed container to equilibrate moisture content. A vacuum oven (45 °C 48 hours) was used to determine moisture content before DSC

analysis. A sample of 0.2 grams was immediately put into a DSC ampoule to prevent moisture absorption. The samples were scanned during heating.

Samples of 2.5-3.2 grams of the freeze dried samples of fructose + carrot fibre (50, 60 and 70% dry weight basis) + malic acid (1, 2, and 3% dried weight basis) were scanned during heating.

Samples of 0.3-0.5 grams of the freeze dried of fructose + maltodextrin were scanned during heating.

Samples of 2.5-3.2 grams of spray dried apple juice concentrate + carrot fibre were scanned during heating.

Samples of 0.2-0.3 grams of spray dried apple juice concentrate + maltodextrin were scanned during heating.

3.2.8 Dielectric analysis

A Fluke PM 6306 Programmable Automatic RCL meter was used to measure the capacitance. A cell, provided and described by Kilmartin (2004) was modified to make it easier to hold the sample as shown in Figure 3.1. A sample was placed in between two 50 mm diameter aluminium discs of 1 mm clearance. The cell was then immediately closed and held in a vacuum oven at 20 °C for 30 minutes. Then all the connecting parts were coated with Dow Corning high vacuum grease to prevent moisture loss or gain during testing. The cell was placed in a temperature-controlled air bath. A Microsoft Visual Basic program was used to record the capacitance at frequencies from 200 Hz to 1 MHz every 30 seconds as the temperature measured at the cell was ramped up from 5 °C to 105 °C over 3-6 hours. The data were analysed and filtered in an Microsoft Excel spreadsheet using a moving average method ($x_n = 0.1(x_n) + 0.9x_{n-1}$) to reduce noise. The factor 0.1 was chosen to reduce the noise to a reasonably level without altering the underlying signal. The peak of the derivative of capacitance with respect to temperature was considered as T_g of the samples. The T_g value from DSC for each sample was used as a guide to find a matching frequency for the DEA T_g. The vacuum oven at 45 °C for 48 hours was used to determine the moisture content of sample before and after DEA.

Figure 3.1 DEA cell filled with the blended freeze dried fructose + carrot fibre and the Dow Corning high vacuum grease (left), the DEA cell with temperature probe inserted in the cell to read the temperature of the cell during the capacitance measurement (right).

Sugars and mixtures

Freeze dried fructose and melted glucose and sucrose were used in DEA analysis of each single component. The melted mixtures were used in the analysis of two and three components.

Freeze dried fructose + carrot fibre

The freeze dried fructose + 14, 21 and 28% carrot fibre powders and these samples at 2 and 5% moisture content (wet basis) were tested. The DSC T_g of each sample was used as a guide to find the frequency of DEA that had T_g matching the value found from the DSC.

Chapter 4 Results

4.1 Sugar content determination

4.1.1 Enzymatic method

The enzymatic method for sugar content determination was difficult to use and required experimental skill. The sugar content of carrot juice determined by the enzymatic method was found to be approximately 2.5% fructose, 3% glucose and 6% sucrose (Table 4.1). The sugar content of apple juice (Braeburn) was approximately 9.5% fructose, 2.5% glucose and 5% sucrose (Table 4.1). These values are almost two times those found by Campo *et al.* (2006) (see Section 2.1.1).

Table 4.1 Sugar content in carrot and apple juice determined by the enzymatic method

Materials	Fructose (%)±SD	Glucose (%)±SD	Sucrose (%)±SD	Total(%)
Carrot	2.53± 0.02	3.14±0.01	6.36±0.06	12.03
Apple	9.69±0.014	2.59±0.014	4.77±0.13	17.05

The enzymatic method was confirmed to be specific for the different sugars. The process included many steps; each step had specific conditions such as temperature, purity of enzyme and time of reaction which could introduce errors. Bergmeyer (1983) showed that any small incorrect amount of solution used, due to pipetting errors, would create errors in the measured result. The error could be either an under or over estimation of the measured results. A pipetting error of just 0.02 mL could produce an error of up to 20% (see detail in Table 2.16, Section 2.4.1.)

This method required a single determination for each component and hence was time consuming and had a high cost. It was concluded that this was not a good practical method for analysing a lot of samples.

4.1.2 YSI enzyme membrane method

The YSI enzyme membrane method was used to check the concentration of glucose (4.8%) and sucrose (8.3%) standards. The average and uncertainties (±SD) of measurement on each of three days of sugar determination are shown in Figure 4.1. The

average values were lower than the standard concentration value. On the other hand, the results for the glucose standard showed high values for all readings above the standard.

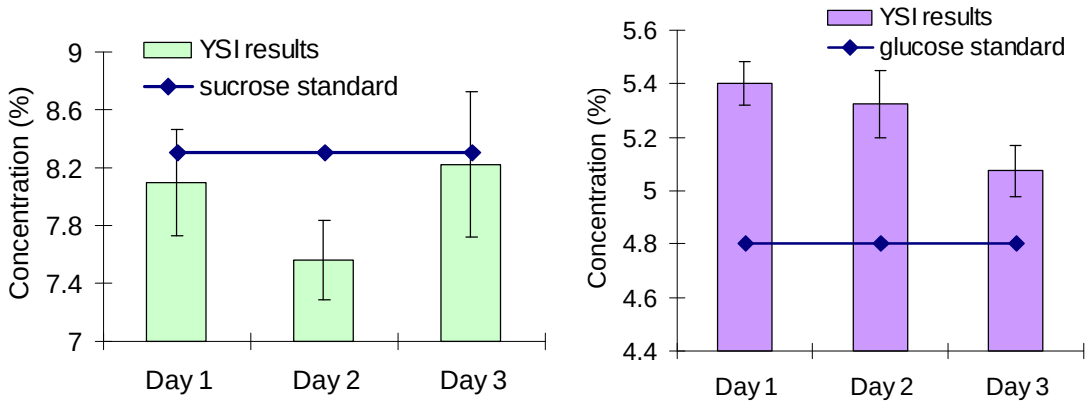

Figure 4.1 The error from YSI results of sucrose (8.3%) and glucose (4.8%) standard during three days analysis. (Error bars indicate ± SD of five replicates).

Mason (1983) gave a comparison of sucrose and glucose in cereal determined by the YSI model 27 and the HPLC method (next section). It was observed that the sucrose data from the enzyme membrane method were lower than that from HPLC method. The glucose data from the enzyme membrane method were around 30% higher than that from the HPLC (see Table 2.17, Section 2.4.1).

Sugar content in carrot fibre

Table 4.2 shows sucrose and glucose content in carrot juice and carrot fibre from YSI method. Blanching and rinsing the carrot fibre before freeze drying was found to reduce the amount of sugars in the fibre. The total amount of sucrose and glucose in blanched carrot fibre was found to be approximately 0.13% which was around 8 times less than that of the untreated fibre (approx. 1.0%). The sucrose and glucose content of fresh fibre was a little bit higher than that of untreated freeze dried carrot fibre (1.2%). Figure 4.2 shows the sucrose and glucose content in blanched, untreated and fresh carrot fibre found by the YSI method.

Table 4.2 Sugars in carrot fibres and sugars content in carrot juice when added to the heat treated and the untreated carrot fibre

Materials	Sucrose (%)±SD	Glucose (%)±SD	Sucrose+ glucose (%)
1. Freeze dried blanched carrot fibre	0.10±0.02	0.03±0.00	0.13
2. Freeze dried untreated carrot fibre	0.82±0.04	0.19±0.01	1.01
3. Fresh carrot fibre	0.83±0.02	0.38±0.01	1.21
4. Extracted fresh carrot juice	8.23±0.13	8.18±0.02	16.41
5. Blended fresh carrot juice	8.15±0.04	7.15±0	15.30
6. Extracted fresh carrot juice + blanched fibre	8.83±0.04	5.11±0.02	13.94
7. Extracted fresh carrot juice + untreated fibre	8.04±0.68	4.92±0.21	12.96
8. Extracted fresh carrot juice + fresh fibre	8.45±0.04	9.25±0.03	17.70
9. Blended fresh carrot juice + untreated fibre	9.18±0.16	8.05±0.01	17.23

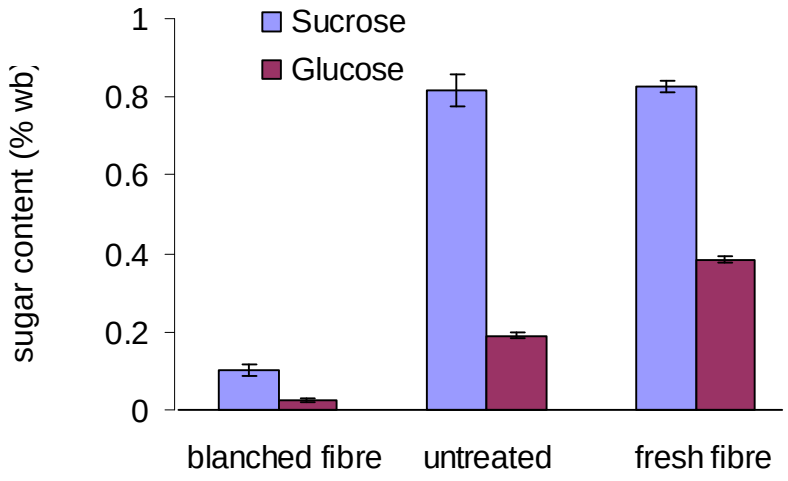

Figure 4.2 Sucrose and glucose content of blanched freeze dried fibre, untreated freeze dried fibre and fresh carrot fibre from the YSI method. Error bars indicate ± SD of triplicate data).

Even though the amount of sugar in blanched carrot fibre was found to be less than that of the untreated fibre, the addition of the same amount of the blanched and untreated fibre to

carrot juice gave only slightly different totals of glucose and sucrose in the mixed juice (approx.13.5% and 13% respectively, number 6 and 7 in Table 4.2). This might have been because the sugar content of carrot fibre retained by juice extractor was very low (less than 1%), and while the blanching further decreased the sugar content, it was not significant when compared to the variations in the carrot juice. The variation between sample 6 and 7, which originated from the same batch of extracted juice, indicated that the uncertainties in Table 4.2 are underestimated. This result was suggested that the carrot fibre for use as the additive in spray drying experiments could be either the fresh fibre or untreated freeze dried fibre.

The different methods of preparation of carrot juice showed a small affect in the sugars content of the juice. The extracted carrot juice had a slightly (around 1%) higher content of the glucose than that of the blended juice (juice from blending the fresh carrot and filtering out the residue).

These results show that the sugar content in carrot juice from the extraction and blending together with that in fresh and untreated fibre were not much different. Therefore, the extracted fresh juice + fresh fibre and the blended fresh juice + untreated fibre were used to compare the sugar content in the mixtures. The results showed that the amount of sugars in both mixtures again were not much different (number 8 and 9 in Table 4.2). Thus, these results confirmed that either fresh carrot fibre or freeze dried untreated carrot fibre would alter the sugar content in the mixture similarly when used as a carrier.

Variation of sugars in fresh carrot juice and the juice from short storage carrot

The sucrose and glucose contents of the reconstituted freeze dried carrot juice were measured over five days to determine if storage time was important. The results are shown in Tables 4.3 and 4.4 and in Figures 4.3, 4.4 and 4.5. The two sugar contents were stable for the first two days but were almost zero after the fifth day. These results clearly show that the product is degraded quickly and should be processed or analysed on the day it is made.

Table 4.3 Variation over five days of sucrose in reconstituted freeze dried fresh carrot juice and carrot juice from carrot that had been stored for 10 days in a refrigerator.

Source of juice	Sucrose content in juice (% wet weight)±SD				
	Day1	Day2	Day3	Day4	Day5
Freeze dried extracted fresh carrot	8.30±0.20	9.11±0.07	2.8±0.35	0.24±0.12	0.06±0.02
Freeze dried extracted stored carrot	10.68±0.64	9.59±0.65	0.47±0.10	0.09±0.01	0.04±0.10
Freeze dried blended stored carrot	6.82±0.14	7.10±0.05	0.51±0.06	0.06±0.01	0.02±0.10

Table 4.4 Variation over five days of glucose in reconstituted freeze dried fresh carrot juice and carrot juice from carrot that had been stored 10 days in a refrigerator.

Source of juice	Glucose content in juice (% wet weight)±SD				
	Day1	Day2	Day3	Day4	Day5
Freeze dried extracted fresh carrot	1.77±0.04	1.94±0.01	0.07±0.02	0.06±0.02	0.03±0.02
Freeze dried extracted stored carrot	4.04±0.28	3.8±0.27	2.1±0.23	1.9±0.24	1.9±0.27
Freeze dried blended stored carrot	3.27±0.04	3.42±0.03	1.23±0.07	1.21±0.03	1.16±0.02

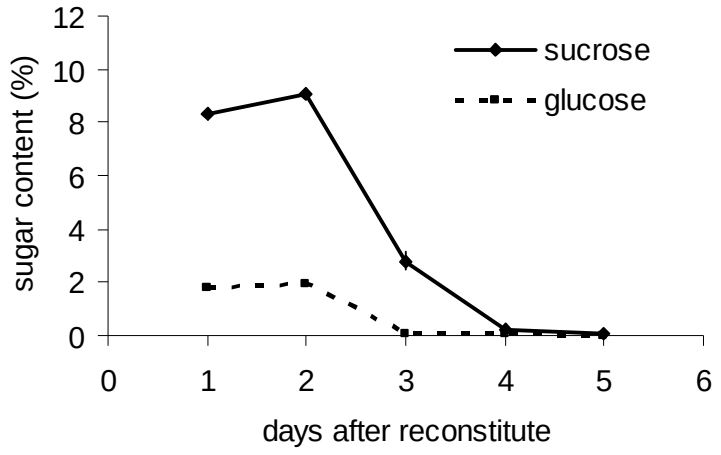

Figure 4.3 The variation of sucrose and glucose in reconstituted freeze dried extracted fresh carrot juice during five days at room temperature. (Error bars indicate ± SD of triplicate data).

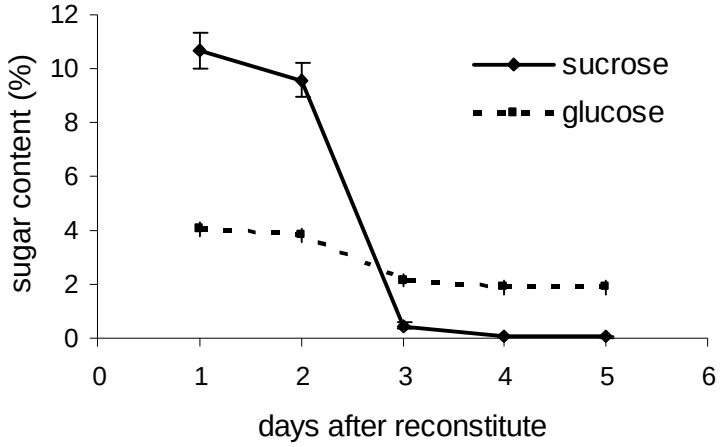

Figure 4.4 The variation of sucrose and glucose in reconstituted freeze dried extracted storage carrot juice during five days at room temperature. (Error bars indicate ± SD of triplicate data).

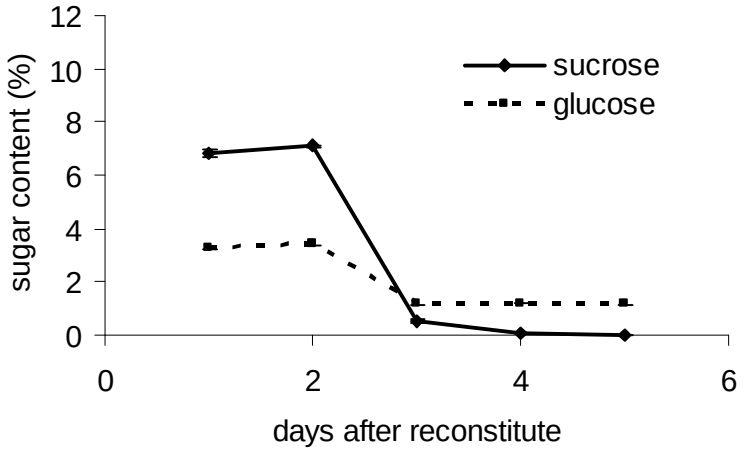

Figure 4.5 The variation of sucrose and glucose in reconstituted freeze dried blended storage carrot juice during five days at room temperature. (Error bars indicate ± SD of triplicate data).

4.1.3 HPLC and RID method

In this section various results obtained while developing the HPLC method are given and discussed. The trials with the HPLC and RID showed that the preparation of acetonitrile to use as the isocratic solvent in the experiments could be a source of error. Catalan *et al.* (2003) stated that acetonitrile was completely water soluble throughout the mole fraction range but appeared to form heterogenous mixtures with water. The physico-chemical properties of acetonitrile consisted of structurally different regions.

The preparation of 75% acetonitrile solvent by (1) adding 750 mL acetonitrile to 250 mL water and (2) by adding 250 mL water to 750 mL acetonitrile solution gave different concentrations of volatile compounds in solution when measured by a GC (Table 4.5). The retention times for peaks of water and sugars in the HPLC showed big differences when using the solvents from two different methods of preparation (Table 4.6). The RID worked with isocratic analyses for which the composition of mobile phase should remain constant during the elution process.

Table 4.5 Differences of volatile compounds concentration in 75% acetonitrile solvent prepared in the opposite ways determined by gas chromatography

Time after injection in GC (minutes)	Volatile compound concentration (%)	
	Solution from 250 mL water in acetonitrile	Solution from 750 mL acetonitrile in water
1.69	21.06	31.91
3.69	78.14	68.09

Table 4.6 Change in retention time in the HPLC with RID results using different solvent preparation

Components	Retention times of component(minutes)	
	Solvent from 250 mL water in acetonitrile	Solvent from 750 mL acetonitrile in water
Water	1.65	2.48
Fructose	5.54	8.37
Glucose	7.68	11.62
Sucrose	10.81	16.21

In subsequent experiments the solvent was prepared by adding 250 mL water in acetonitrile because the retention times of water and sugars were lower.

Analysis of sugar standards by HPLC

The trial on the effect of the flow rate on retention time of sugars showed that the retention times for fructose, glucose and sucrose decreased when the injection flow rate was increased (Figure 4.6). It has been a common technique to reduce the retention time of a substance by increasing the flow rate to a certain limit (Slimestad & Vagen, 2006).

The peak heights of fructose and sucrose decreased when the mobile phase flow rate was increased. The peak heights of glucose however, increased with flow rate (Figure 4.7). This was unexpected and confirmed by repeating twice but the cause of this was not investigated. The peak areas of fructose, glucose and sucrose increased when the mobile flow rate was increased. The trend of increasing peak area with flow rate was clearly seen for glucose (Figure 4.8). This trial was done with the solvent prepared by adding 750 mL of acetonitrile into 250 mL water. The retention times for all sugars were high. Later with the solvent prepared by adding 250 mL water into 750 mL acetonitrile, the retention times were too low with a high mobile phase flow rate. The results are not shown here.

From these results it was decided that a mobile flow rate of 1.0 ml min^{-1} was the most suitable for further experiments because of a shorter retention time. The peak height of glucose appeared at the lowest level among the three sugars at 1 ml min^{-1}. This phenomenon was also found by Slimestad & Vagen (2006).

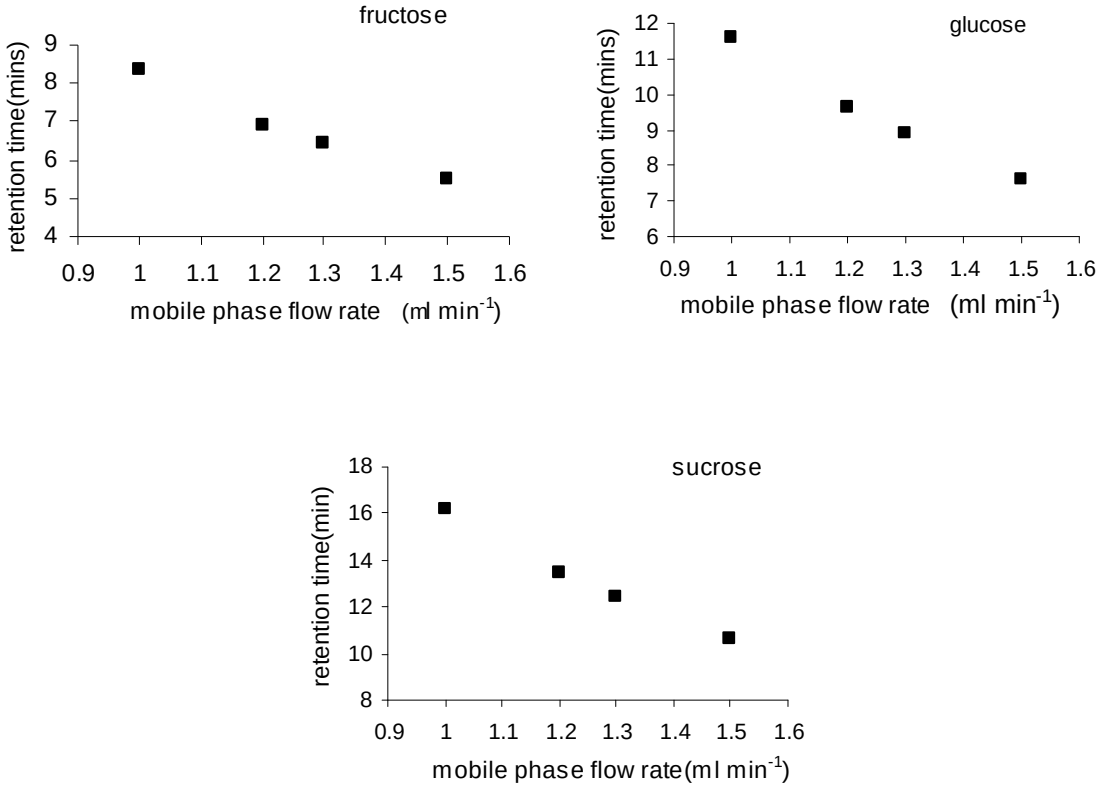

Figure 4.6 The retention times decrease with the mobile phase flow rate of fructose glucose and sucrose.

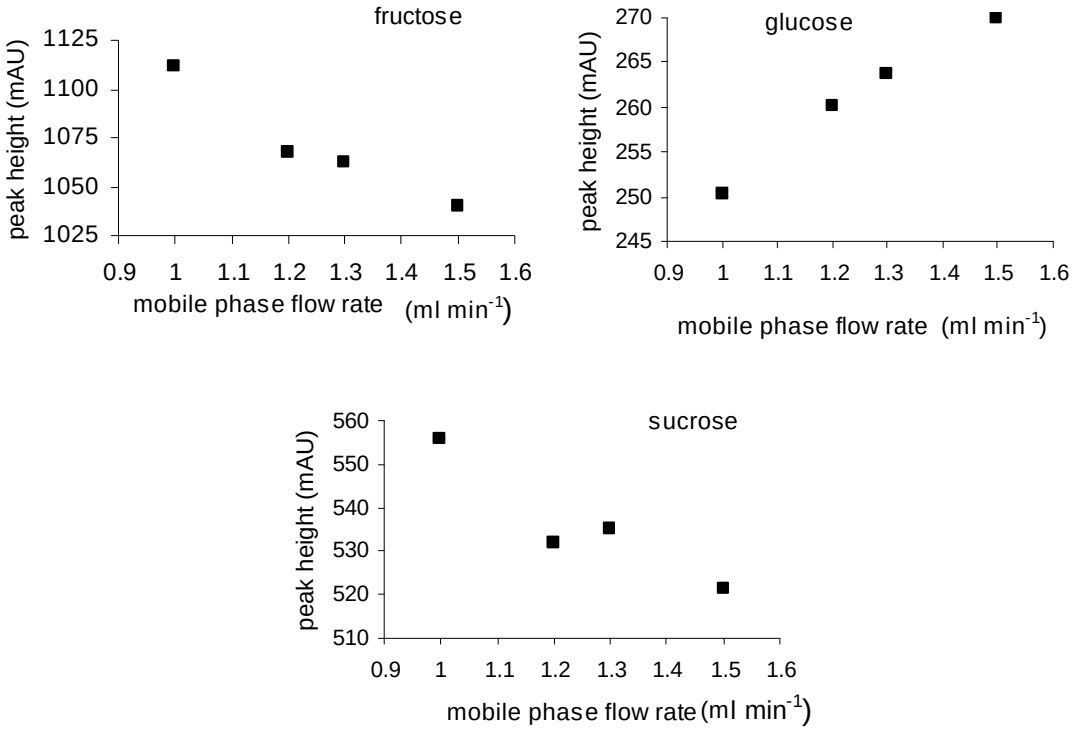

Figure 4.7 The peak heights of fructose and sucrose decreased when the mobile phase flow rate was increased while the peak height of glucose increase with increasing flow rate.

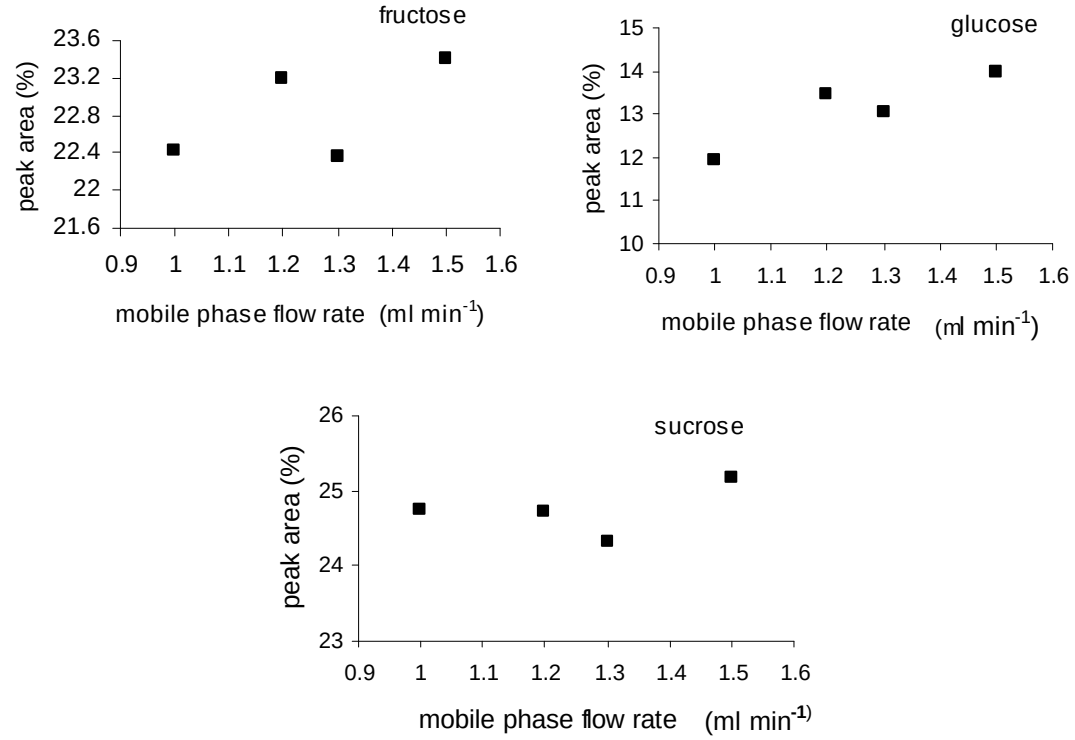

Figure 4.8 The peak areas of fructose, glucose and sucrose appeared to increase with the mobile phase flow rate.

The variation of retention time, peak height and peak area of sugar standards

To check the stability of the HPLC columns and the RID detector, a number of sequential analyses of the sugar standards were performed. The standards were left at room temperature (about 10-20 °C) for the three days of the experiment. Figure 4.9 shows the variation of retention times from the sequential analyses. The retention times increased with runs but levelled off after 8 to10 runs on some days.

Figure 4.10 and 4.11 shows the variation of peak heights and peak areas for the same set of runs. The peak heights of all three sugars showed smaller fluctuations than the peak area. Both peak height and peak area were clearly seen to decrease with time (days) during analysis. This indicated that the standard needed to be prepared freshly or protected by refrigerated or added preservative chemicals when doing the analysis of samples. Some of the values of peak height and area deviated significantly from the expected values. This showed that more than one analysis was required for each sample.

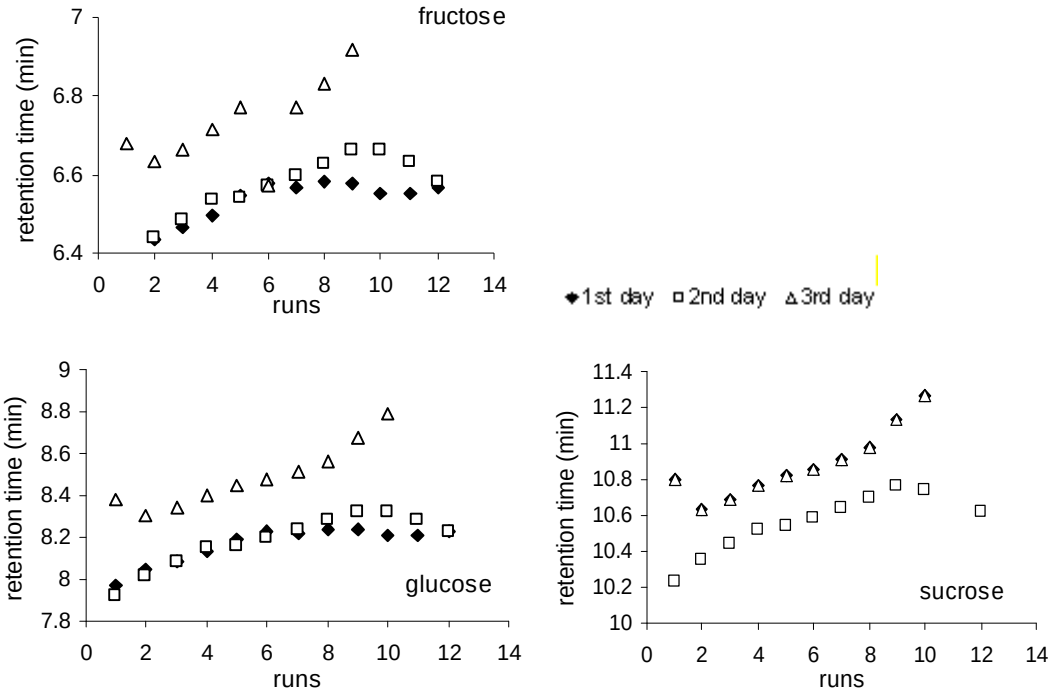

Figure 4.9 The variation of retention time of water, fructose, glucose and sucrose from several subsequent runs during three days analysis. The standard deviations of retention times were 0.07, 0.08, 0.13 for fructose; 0.09, 0.1, 0.1 for glucose and 0.1, 2.6, 0.2 for sucrose on the 1st, 2nd and 3rd day respectively.

Figure 4.10 and 4.11 shows the variation of peak heights and peak areas for the same set of runs respectively. Even though the peak heights of all three sugars showed smaller fluctuations than the peak area, the standard deviation values of variation of peak height over runs shows high variation especially on the third day when all sugars show a spread of data. Both peak height and peak area were clearly seen to decrease with time (days) during analysis. This indicated that the standard needed to be prepared freshly or protected by refrigerated or added preservative chemicals when doing the analysis of samples. Some of the values of peak height and area deviated significantly from the expected values. This showed that more than one analysis was required for each sample

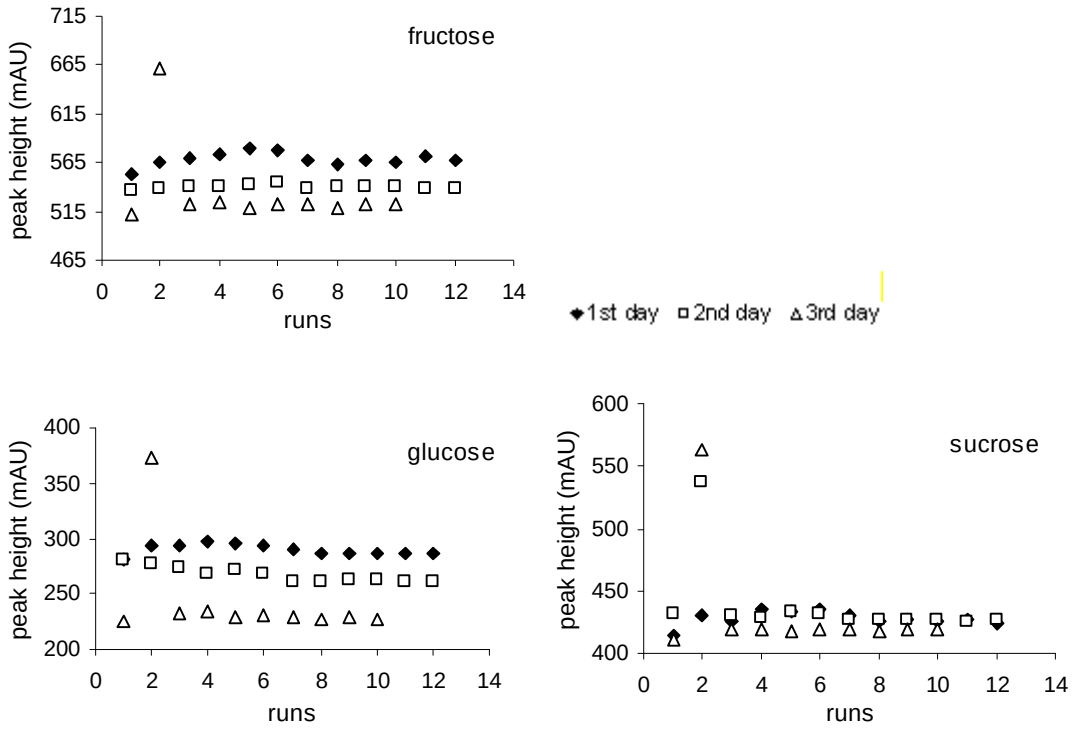

Figure 4.10 The variation of peak height of water, fructose, glucose and sucrose from several subsequent runs during three days analysis. The standard deviations of peak height were 6.7, 2.3, 44.6 for fructose; 4.7, 7.2, 45.6 for glucose and 5.9, 31.7, 45.9 for sucrose on the 1st, 2nd and 3nd day respectively

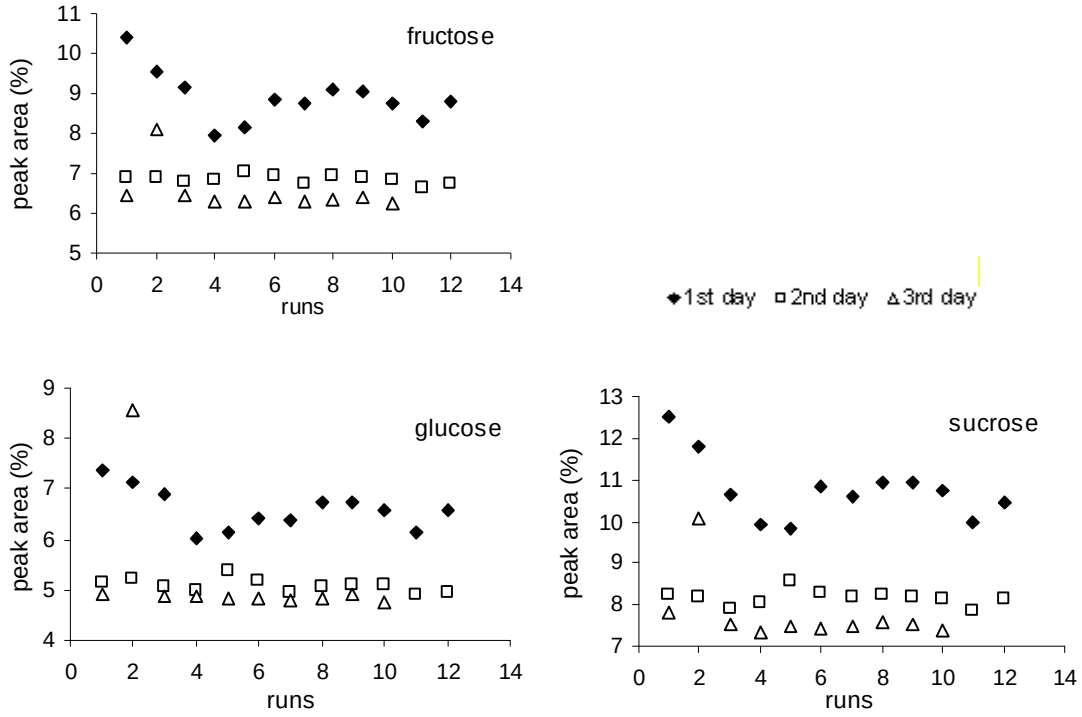

Figure 4.11 The variation of peak area of water, fructose, glucose and sucrose from several subsequent runs during three days analysis. The standard deviations of area were 0.6, 0.1, 0.6 for fructose; 0.4, 0.1, 1.2 for glucose and 0.8, 0.2, 0.8 for sucrose on the 1st, 2nd and 3nd day respectively

The relationship between standard concentration with peak height and peak area

After the stability tests, a range of standards were used to calibrate concentration to peak height and peak area. Figures 4.12 to 4.18 show calibration results of peak height and peak area for the fructose, glucose and sucrose standards. Two ranges of concentration are presented. It was clear that the calibration could not be described by a single line, so two different lines were fitted. The first line with higher slope was maintained over the concentration range lower than 1.0 or 1.25%. The second line with a lower slope was maintained over the concentration range of 1.0 to 10.0% (w/v) for the three sugar standards. The peak height had less fluctuation than the peak area of all sugars. Among the three sugars, glucose showed the most fluctuation of peak height and peak area. The calibrations based on both peak height and peak area were used to determine the sugar contents of samples.

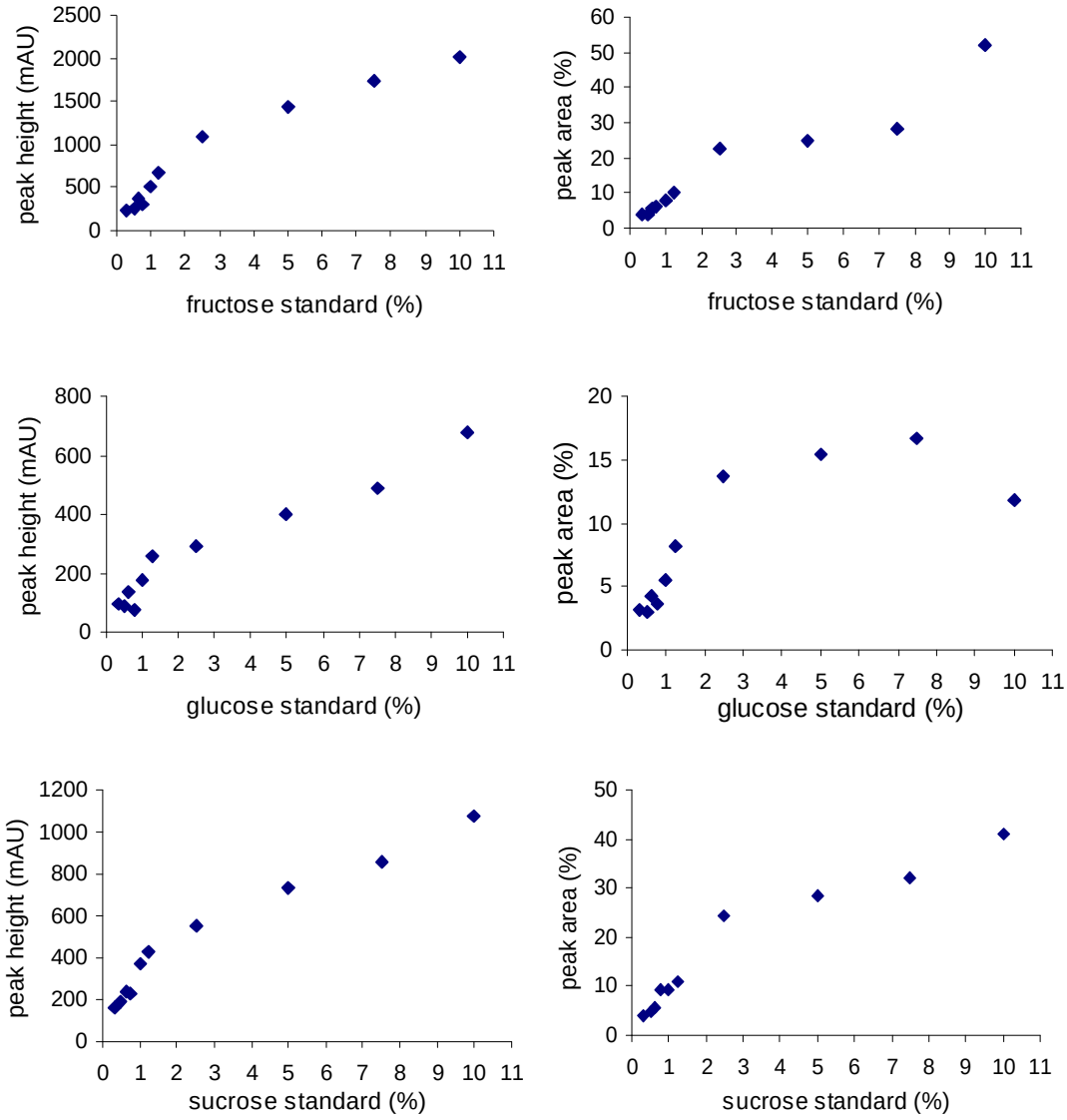

Figure 4.12 Calibration of peak height and peak area for fructose, glucose and sucrose standard.

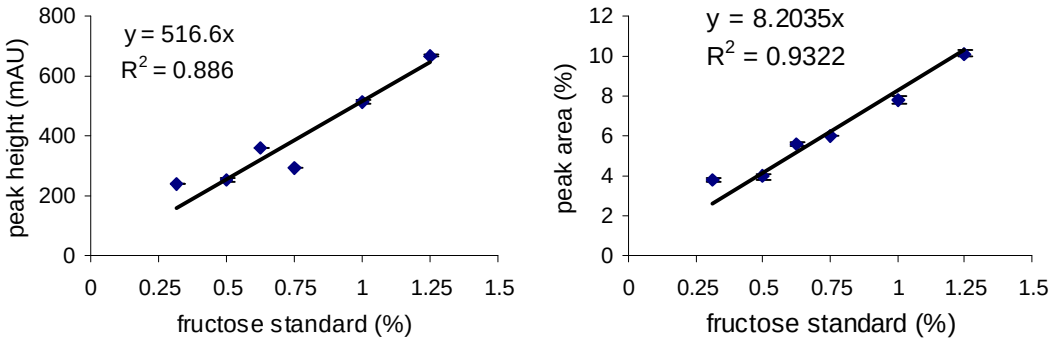

Figure 4.13 Best linear fit peak height and peak area at low concentrations of fructose.

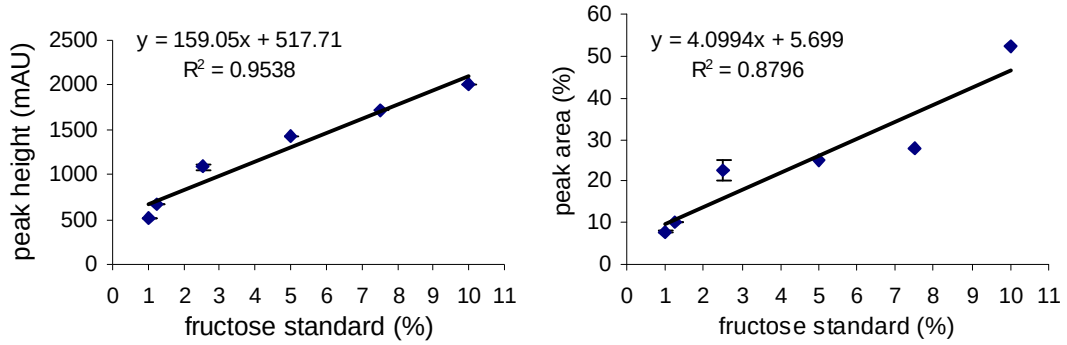

Figure 4.14 Best linear fit of peak height and peak area at the high concentrations of fructose.

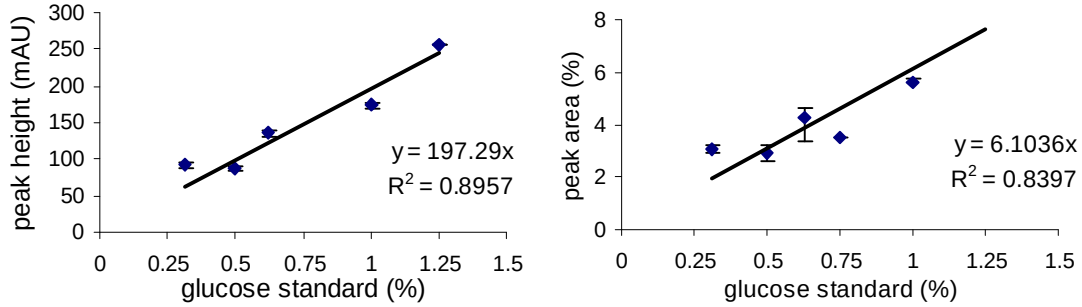

Figure 4.15 Best linear fit of peak height and peak area at low concentrations of glucose.

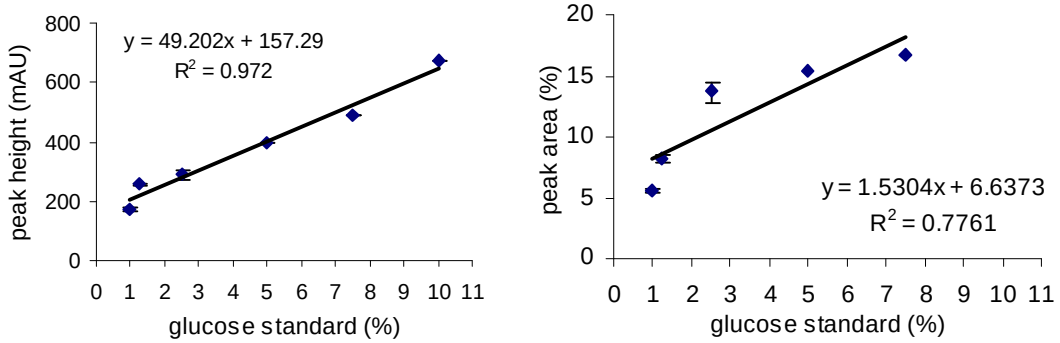

Figure 4.16 Best linear fit of peak height and peak area at the high concentrations of glucose.

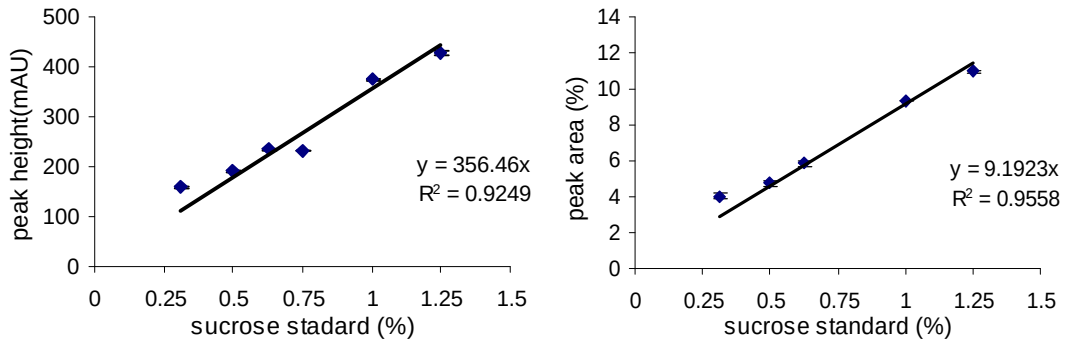

Figure 4.17 Best linear of peak height and peak area at low concentrations of sucrose.

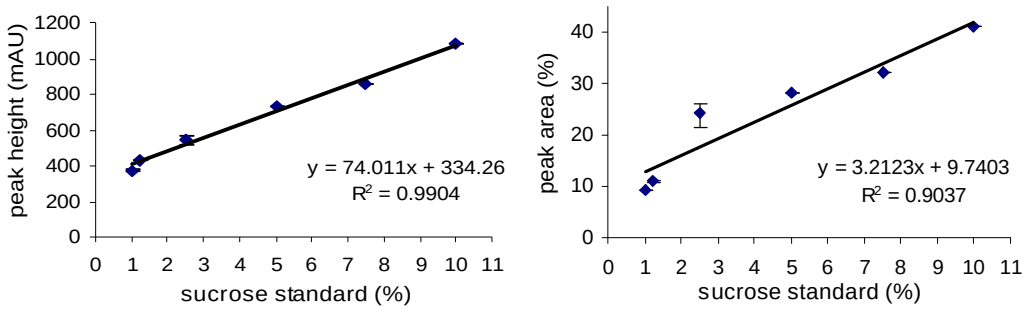

Figure 4.18 Best linear of peak height and peak area at high concentrations of sucrose.

It was concluded that the standards and samples needed to be analysed on the same day they were prepared. Repeats of the analyses were required to get reliable average values. Calibration with both peak heights and peak areas might be needed to get an estimate of the uncertainties of the sugar content.

HPLC analysis of samples

The sugar contents of samples determined from peak height and peak area were different. The results for freeze dried fresh carrot juice are shown in Figure 4.19. It is clearly seen that the peak area gave higher values of all the sugars in carrot juice.

The results for carrot juice, carrot fibre and apple determined by peak height are in Table 4.7. The sugar content of carrot juice, carrot fibre and apple determined by peak area are in Table 4.8. The sugar contents of heat treated fibre were higher than the untreated fibre when determined from peak height. This is unlikely to be true. In addition the total sugars in all carrot juice determined by peak height were lower than from other methods (see next section). It was therefore concluded that the results for sugars in carrot fibre and carrot juices determined by peak areas were more reliable than those from peak height.

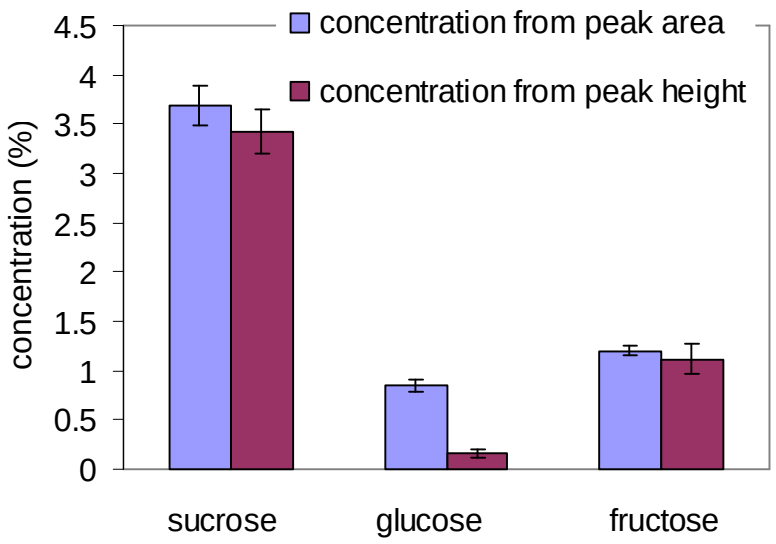

Figure 4.19 Sugar content in freeze dried fresh carrot juice when compared value to the peak height and peak area standard. The error bars indicate ± SD of 3 replicates.

Table 4.7 Sugars content in carrot fibre, carrot juice and apple juice determined by HPLC from peak height standard

Materials	Sugars (% wet weight) ±SD			
	fructose	glucose	sucrose	total
Freeze dried heat treated carrot fibre	0.24±0.03	0.20±0.02	0.82±0.02	1.26
Freeze dried unheated carrot fibre	0.11±0.02	0.10±0.04	0.24±0.02	0.45
Freeze dried carrot fibre (January)	0.06±0.02	0.10±0.02	0.79±0.02	0.95
Freeze dried fresh carrot juice	1.20±0.5	0.80±0.06	3.7±0.2	5.7
Extracted fresh carrot stored at -20 °C	0.69±0.08	0.54±0.16	0.56±0.20	1.79
Extracted fresh carrot juice (1)	1.03±0.11	0.65±0.09	1.15±0.07	2.83
Extracted fresh carrot juice (2)	0.37±0.04	0.31±0.07	0.72±0.11	1.40
Juice from heated carrot	0.23±0.02	0.20±0.02	0.82±0.06	1.25
Fresh apple juice (Braeburn)	8.12±0.06	0.71±0.02	5.25±0.02	14.08

Table 4.8 Sugars content in carrot fibre, carrot juice and apple juice determined by HPLC from peak area standard

Materials	Sugars (% wet weight)			
	fructose	glucose	sucrose	total
Freeze dried heat treated carrot fibre	0.07±0.01	0.08±0.01	0.12±0.01	0.27
Freeze dried unheated carrot fibre	0.19±0.02	0.16±0.01	0.44±0.05	0.79
Freeze dried carrot fibre (January)	0.16±0.01	0.10±0.02	0.69±0.05	0.95
Freeze dried fresh carrot juice	1.10±0.02	0.20±0.04	3.4±0.2	4.7
Extracted fresh carrot stored at -20 °C	1.43±0.03	1.28±0.02	1.39±0.04	4.10
Extracted fresh carrot juice (1)	1.74±0.16	1.24±0.02	2.43±0.17	5.41
Extracted fresh carrot juice (2)	0.90±0.01	0.90±0.02	2.56±0.22	4.36
Juice from heated carrot	0.58±0.07	0.63±0.09	3.51±0.12	4.72
Fresh apple juice (Braeburn)	9.6±0.6	0.90±0.1	5.81±0.2	16.31

4.1.4 Comparison of sugar determination methods

The uncertainties of sugar values from the three different methods are in Table 4.9. The enzymatic method was found to have the smallest uncertainty. The YSI enzyme membrane method had the biggest uncertainty with over-estimated values for glucose. The HPLC method could be able to determine the sugar with very little to medium uncertainty.

Table 4.9 Uncertainties of sugar determination by different methods

Methods	Uncertainty (SD)
Enzymatic	0.01 to 0.02
YSI enzyme membrane	0.01 to 0.7
HPLC & RID	0.01 to 0.6

The YSI method was the fastest for determining glucose and sucrose. However, it was found that the sucrose and glucose content of carrot juice from this method were much higher than value from the other methods. The sugars in fibre from the YSI and HPLC (peak area) methods were similar. The sugars in apple juice from the enzymatic and HPLC methods were very close. These details from some samples are in Table 4.10.

Table 4.10 Comparison of fructose (F), glucose (G) and sucrose (S) in some samples from three different methods

Materials	Enzymatic method			YSI method			HPLC & RID (peak height)			HPLC & RID (peak area)		
	Sugars (%)			Sugars (%)			Sugars (%)			Sugars (%)		
	F	G	S	F	G	S	F	G	S	F	G	S
Carrot juice	2.5	3.1	6.4	-	8.2	8.2	1.0	0.7	1.2	1.7	1.2	2.4
Blanched fibre	No experiment			-	0.03	0.1	0.2	0.2	0.8	0.07	0.08	0.1
Untreated fibre	No experiment			-	0.2	0.8	0.1	0.1	0.2	0.2	0.2	0.4
Apple juice (Braeburn)	9.7	2.6	4.8	No experiment			8.1	0.7	5.3	9.6	0.9	5.8

In conclusion, each method used for sugar content determination in this experiment has its own advantages and disadvantages. By assuming that the enzymatic method has the least error of the three methods, the YSI enzyme membrane method might show the accurate value when dealing with low sucrose and glucose content. The HPLC had a variation in calibration with peak heights and peak areas. While the HPLC seemed to be most accurate at low and high sugar contents, uncertainties were greater at intermediate values. Comparisons of the results with the literature data will be discussed later.

4.2 Freeze drying experiments

4.2.1 Freeze dried blended fresh apple juice + carrot

Mixtures of blended fresh apple juice + carrot at different proportions were freeze dried to check the possibility of carrot fibre being used as a drying carrier. The dried mixtures with a higher proportion of carrot in apple juice were observed to be less sticky than those with a lower proportion. They were easy to break into a powder by hand. The best quality powder was obtained from a 1:1 mixture of Royal Gala apple juice and carrot. The freeze dried sample was very easy to mill into fine particles without stickiness. However, the blended powder was hygroscopic and needed to be protected from moisture immediately after blending. The freeze dried pure apple juices from all three varieties were very sticky and appeared as syrup in the container. The dried powders from the three different varieties of apple with carrot were quite different. The freeze dried Braeburn apple juice + carrot was stickier than the mixture of Royal Gala + carrot at the same ratio. The freeze dried Granny Smith apple juice + carrot was the stickiest. Freeze drying of the pure apple

juices from those three varieties produce syrup stuck in the containers. From these results, the chemical component in juice including amount of sugars and acids was thought likely to influence drying performance. The amount of sugars and acids in the three apple juices was not determined. However, the different taste of each apple variety was a simple indicator for the different chemical components of each apple juice. These results confirmed the possibility of carrot as a drying aid of fruit juice.

The freeze dried powders were kept in plastic bottles at room temperature for three years and showed a little fading of the original carrot colour at the surface of the powder only. This result demonstrates the stability of beta-carotene in sugar from freeze drying.

4.2.2 Freeze dried blanched and untreated carrot fibre

The appropriate process to get carrot fibre as an effective drying carrier was initially investigated by comparison of the freeze dried blanched fibre with the untreated fibre. The freeze dried blanched fibre had a “faded” colour and was rough and very difficult to mill into powder. The freeze dried untreated carrot fibre was bright colour, brittle and easy to blend (Figures 4.20 and 4.21). The trials found that grinding the fibre in a kitchen blender did not make carrot fibre powder that was suitable as a carrier because of the hardness of dry fibre. The fibre powder from the grinding was not small enough to spray dry. The mixtures of carrot juice + ground carrot fibre became blocked in the atomizer during the spray drying trials. The attempt to blend carrot fibre into smaller particle damaged the blender.

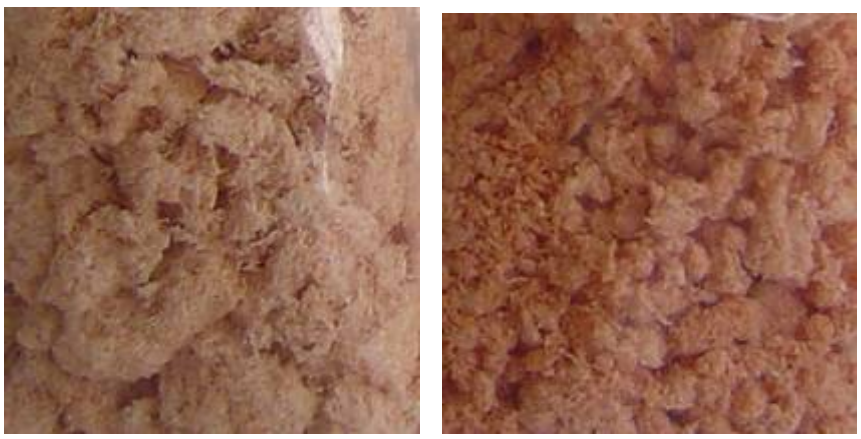

Figure 4.20 The blanched carrot fibre (left) and the untreated carrot fibre (right) after freeze drying.

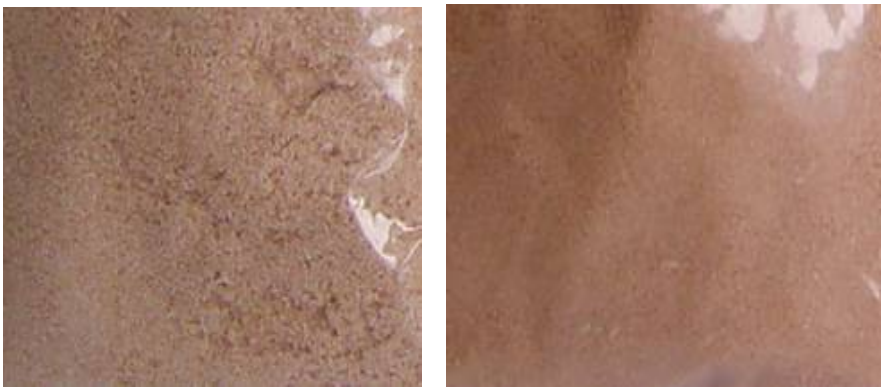

Figure 4.21 The freeze dried blanched carrot fibre (left) and the freeze dried untreated carrot fibre (right) both after size reduction by blending.

4.2.3 Freeze dried carrot juice

The effect of storage time of carrot juice quality was determined by freeze drying. The freeze dried powders of fresh carrot juice and of juice stored for 10 days (before drying), were not significantly different. They were a little sticky, very hygroscopic and absorbed moisture easily. The freeze dried powder of fresh carrot juice is shown in Figure 4.22. The freeze dried powder from fresh carrot juice + fresh fibre was not so sticky, more segregated and easier to blend than the freeze dried pure carrot juice. Figure 4.23 show the freeze dried fresh carrot juice + fresh fibre.

Figure 4.22 The freeze dried fresh carrot juice.

Figure 4.23 The freeze dried fresh carrot juice + fresh fibre.

4.2.4 Freeze dried fructose solution

The freeze dried 50% fructose solution was a very viscous syrup even after more than 10 days in the drier. The 60% fructose solution still showed stickiness but less than that of the 50% solution after 8 days in the freeze drier. The solution of 70 and 80% fructose was successfully dried in 7 to 8 days and was not sticky while in the freeze drier. After being taken out of the freeze drier for 10 minutes, the amorphous solid fructose from 70 and 80% fructose solution became very viscous syrups. The 90% and 95% fructose solutions were dried successfully. The solid was stable during storage in the freezer at -20 °C and still stable until being filled into the DEA cell. The amorphous fructose solid from freeze drying was white and opaque. The reasons for these phenomena will be discussed in Chapter 5.

4.2.5 Freeze dried fructose + carrot fibre and fructose + carrot fibre + malic acid

The mixtures of fructose + carrot fibre at all ratios were successfully dried. They were easy to grind into powder but the powder was hygroscopic. The ground sample is shown in Figure 4.24. The characteristics of freeze dried fructose + carrot fibre + malic acid were similar to the freeze dried fructose + carrot fibre.

Figure 4.24 The blended freeze dried fructose + carrot fibre.

4.2.6 Freeze dried fructose + maltodextrin

During freeze drying the volume of all the mixtures of fructose + maltodextrin expanded more than about five times. They maintained the expanded volume until almost dry at which point the volume reduced. The freeze dried fructose + maltodextrin was very hygroscopic and stuck to the container. Figure 4.25 shows the increase in volume during freeze drying of fructose + maltodextrin.

Figure 4.25 The increase in volume during freeze drying of fructose + maltodextrin (aluminium dish is 14.5 cm diameter).

4.3 Moisture content determination

The standard method for moisture content determination in samples with high sugar contents did not work well. After drying at 60 °C in the vacuum oven for 48 hours, as suggested for moisture analysis of sugars, the final weight still fluctuated. After many

trials it was found that a temperature of 45 °C in the vacuum oven (-85 kPa) until the final weight was stable worked well in these experiments. It took 36-48 hours for each sample to get to the stable weight. The results of the moisture content of particular samples are in the relevant sections on DSC, DEA and spray drying experiments.

4.4 Characteristic of carrot fibre powder

The freeze dried untreated carrot fibre was found to be suitable for use as a drying carrier. The centrifugal milled fibre particles had an irregular shape with most having a length measured by the Microtrac in the range 10-200 μm (Figure 4.26). This was small enough to not block the rotary disc atomizer used in the spray drier. The fibre had a very light creamy orange colour (about RGB: 255, 225, 185) (Figure 4.27).

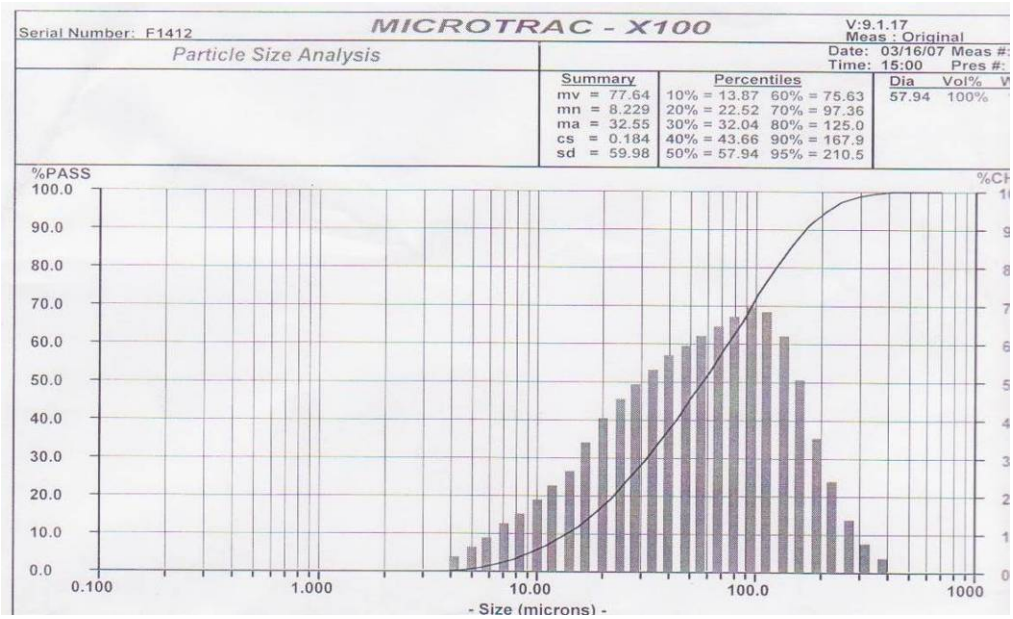

Figure 4.26 Particle size distributor of carrot fibre powder measured by the Microtrac-x100.

Figure 4.27 Carrot fibre powder used in the experiments.

The carrot fibre was found to contain 0.2% fructose, 0.15% glucose, and 0.5% sucrose (wet basis) by the HPLC method. Most of the fibre powder particles under polarised light microscope show very tiny bright spots acting similarly to the crystalline materials. Pictures could not be obtained from polarised light microscope but images were obtained using the Kombistereo (Wild M32 Heerbrugg, Switzerland) with light at right angles from two sources from Global Science/Leica cls 150x connected to a Meiji Infinity 1. Figure 4.28 shows freeze dried carrot fibre before milling. The picture shows that carrot fibre is partially clear and transparent. It is also partially opaque with a carotene colour. Figure 4.29 shows the particle of carrot fibre powder. The arrows point to the spots that appear to be microcrystalline materials under polarised light microscope.

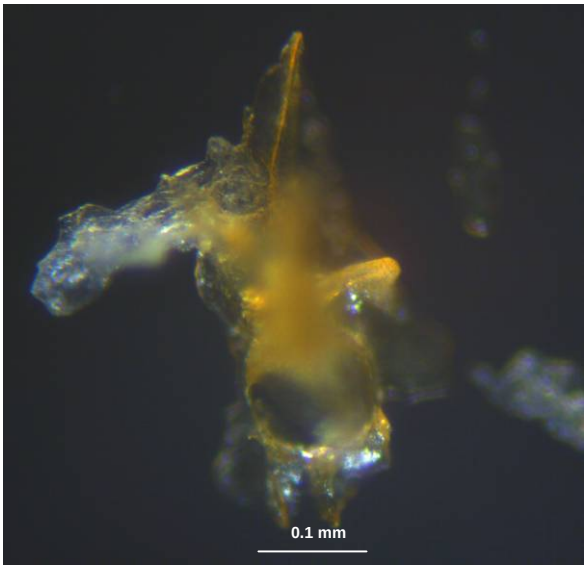

Figure 4.28 Freeze dried carrot fibre before milling.

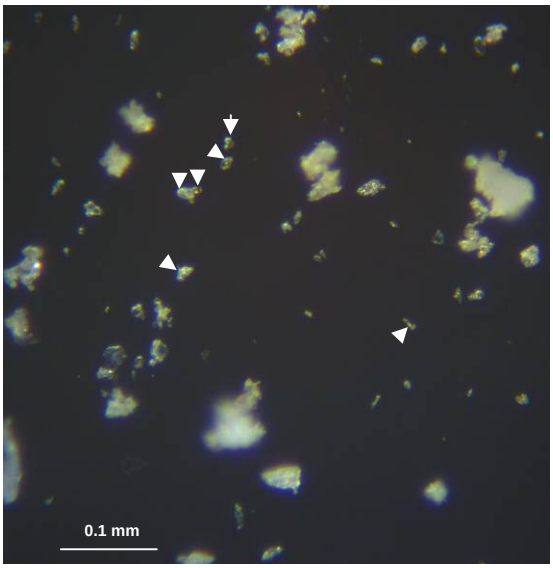

Figure 4.29 Particles of carrot fibre powder. The arrows point to tiny spots that appear to be microcrystalline materials under the polarised light microscope.

4.5 The visual T_g of sugars and mixtures

During the DSC trial of the freeze dried fructose, it was found that the amorphous glass transformed into a liquid when the temperature was higher than 20 °C. No transitions were observed in the DSC thermogram after more than 6 runs. Since the T_g of fructose, glucose and sucrose shown by literature are in the range that can observed in a normal

room temperature, a visual experiment was performed. The transition in sugars was visually observed by melting the sugar then letting it cool down on the tip of a thermocouple to detect the glass transition temperature of the sugar when its texture transformed from rubbery sugar to rigid glassy sugar. The aim of this experiment was to compare the T_g values of sugars from the DSC to the visual appearance of glassy sugars. Fructose, glucose and sucrose and their mixtures were used in this experiment.

It was found that fructose started to melt at around 110 °C and all crystals had melted at around 120-128 °C. Glucose started to melt at around 125 °C. The temperature of melting glucose increased very slowly from 125-138 °C. Most of glucose crystals had melted when the temperature was at around 150 °C. Sucrose started to melt at around 170 °C. The temperature of the melting sucrose was quite stable at 178-179 °C. Most of the sucrose crystals had melted at around 185 °C. The sucrose went brown very easily, as did glucose and fructose but not as quickly.

It was too difficult to record the T_g value during heating of the amorphous solid sugars. That was because, during heating, the amorphous solid sugars transform gradually to rubbery sugars. The physical changed from the hard but brittle glassy solid to the softer and more elastic form occurred over the entire melting temperature range. In addition, when it was at the early rubbery stage, the amorphous sugar was not sticky.

During cooling, the plastic or elastic texture of the sugars lasted until an immediate transformation into a brittle glassy solid. The non-sticky rubbery sugar could be made into any shape before it turned to be a glassy brittle solid up on cooling. This point was recorded as the T_g. The results are shown in Table 4.11. Of the three sugars, fructose has the lowest T_g and sucrose has the highest T_g. The T_g values of amorphous solid fructose, glucose and sucrose were around 22 °C, 48 °C and 61 °C respectively. This is because of the molecular structure and molecular weight differences of the sugars. The molecular weights of fructose, glucose and sucrose are 180, 180 and 342 g mol^{-1} respectively. Lower molecular weight materials tend to have lower T_g values. These results were in good agreement with literature (Roos, 1995; Finegold *et al.*, 1989; Slade & Levine, 1994).

Table 4.11 Cooling T_g of pure melted fructose, glucose and sucrose from visual experiments.

Sugars	T_g (°C)±SD
D-fructose	22.5±0.2
D-glucose	48.4±2.3
D-sucrose	61.3 ±1.5

Figure 4.30 and Table 4.12 show the T_g values of the two-sugar mixtures. The T_g values of mixtures of two sugars at different ratios were higher when a greater fraction of the higher T_g sugar was in the mixtures. On the other hand, when the higher fraction of the lower T_g sugar was in the mixtures, the T_g of mixtures decreased. The visual T_g values of two-sugar mixtures are compared to the DSC T_g values in Section 4.6.8.

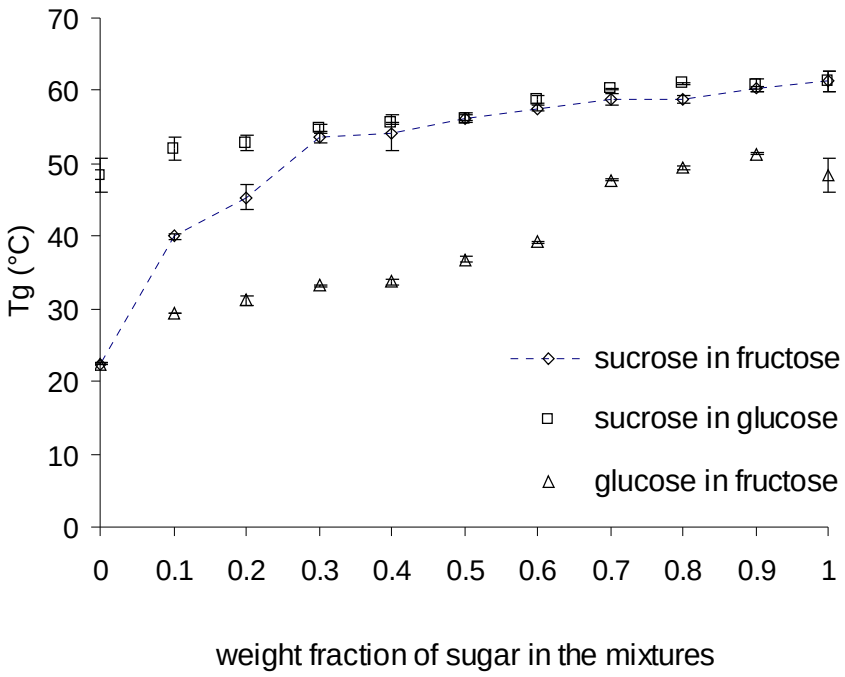

Figure 4.30 Visual T_g of two-sugar mixtures on cooling. (Error bars indicate ± SD of triplicate data).

Table 4.12 Cooling T_g of two-sugar mixtures at different ratios from visual experiments.

		T_g (°C)±SD	
Ratios of mixtures	Sucrose: Fructose	Sucrose: Glucose	Glucose: Fructose
1.0**:** 0.0	61.3±1.5	61.3±1.5	48.4±2.3
0.9**:** 0.1	60.3±0.4	60.8±1.0	51.3±0.1
0.8**:** 0.2	58.8±0.6	61.1±0.1	49.5±0.3
0.7**:** 0.3	58.8±0.7	60.3±0.2	47.7±0.2
0.6**:** 0.4	57.6±0.3	58.9±0.5	39.2±0.2
0.5**:** 0.5	56.3±0.7	56.3±0.3	36.8±0.4
0.4**:** 0.6	54.2±2.5	55.6±0.2	33.7±0.3
0.3**:** 0.7	53.5±0.7	54.9±0.6	33.2±0.1
0.2**:** 0.8	45.4±1.8	52.8±1.1	31.1±0.6
0.1**:** 0.9	40.0±0.4	52.0±1.5	29.4±0.1
0.0**:** 1.0	22.5±0.2	48.4±2.3	22.5±0.2

Table 4.13 shows the T_g values of three-sugar mixtures. The T_g of three-sugar mixtures with uncertainty values are in Figures 4.31, 4.32 and 4.33. It was found that sometimes the glass transition of sugars of mixtures occurred at a temperature lower or higher than that of the lowest or the highest T_g of the individual sugars in each mixture. The visual T_g values of fructose, glucose, and sucrose are compared to the DSC T_g values in Section 4.6.4.

The T_g results of three-sugar mixtures showed that increasing the fraction of sucrose in the mixture increased T_g of the mixtures (Figure 4.31). However, it was not a gradual or a linear increase but stepwise increase of T_g values of the mixtures. The effect of increasing T_g of the mixtures was higher when the fraction of sucrose was at 60-90%. The uncertainties (from repeat) of these T_g appeared to be very low with the maximum average of ±1.00.

Table 4.13 T_g of three-sugar mixtures at different ratios from the visual experiment

		T_g (°C)±SD	
Ratios of mixture	Su: Glu: Fruc	Glu: Fruc: Su	Fruc: Su: Glu
1.0**:** 0.0**:** 0.0	61.3±1.5	48.4±2.3	22.5±0.2
0.9**:** 0.05**:** 0.05	63.5±0.5	47.3±1.2	41.7±0.9
0.8**:** 0.1**:** 0.1	61.4±1.0	49.0±0.6	48.4±0.3
0.7**:** 0.15**:** 0.15	60.9±0.8	47.2±3.2	53.2±0.4
0.6**:** 0.2**:** 0.2	59.1±0.3	45.2±0.4	54.7±0.4
0.5**:** 0.25**:** 0.25	52.2±0.7	50.2±2.1	52.0±1.9
0.4**:** 0.3**:** 0.3	50.3±0.3	48.4±1.7	49.4±1.3
0.3**:** 0.35**:** 0.35	50.1±0.4	52.4±0.6	48.2±3.4
0.33**:** 0.33**:** 0.33	50.3±0.3	50.3±1.0	50.3±1.0
0.2**:** 0.4**:** 0.4	48.8±0.5	55.1±0.9	56.3±2.2
0.1**:** 0.45**:** 0.45	48.0±0.8	59.2±0.3	50.8±0.3

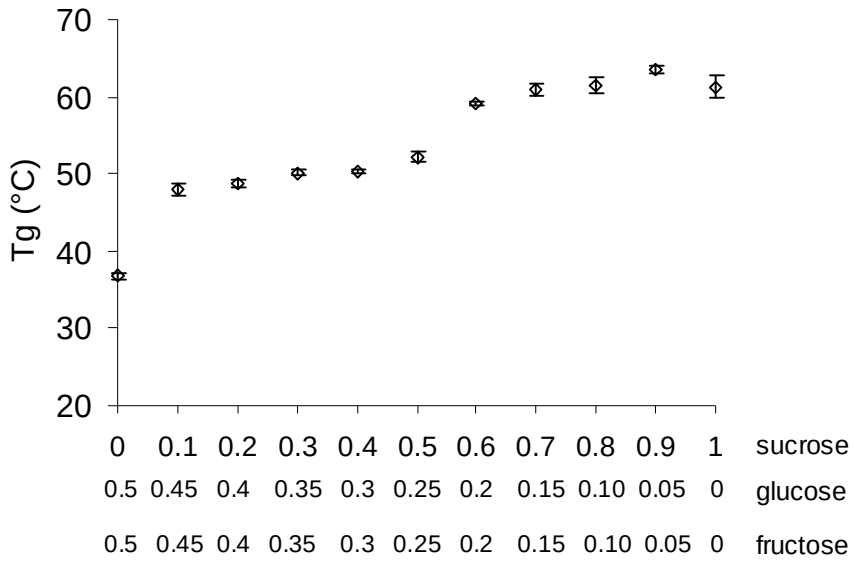

Figure 4.31 T_g values of three-sugar mixtures when the fractions of fructose and glucose were equal. (Error bars indicate ± SD of triplicate data).

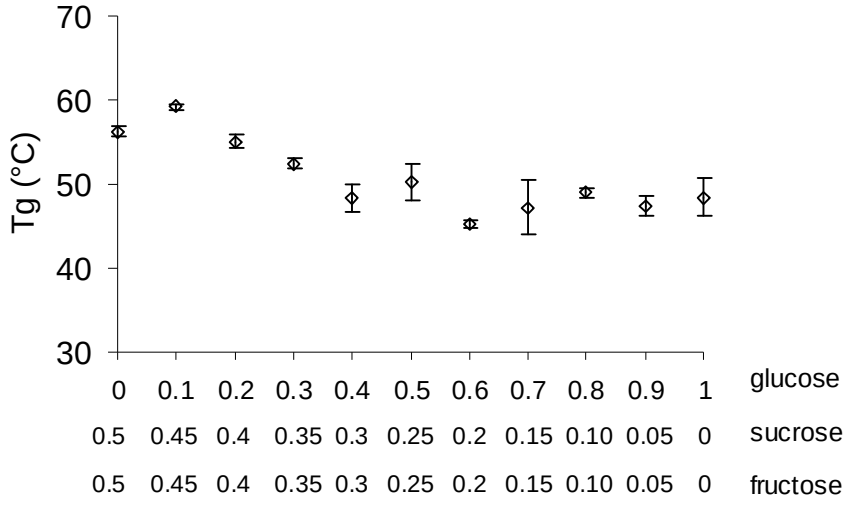

Figure 4.32 T_g values of three-sugar mixtures when the fraction of fructose and sucrose were equal. (Error bars indicate ± SD of triplicate data).

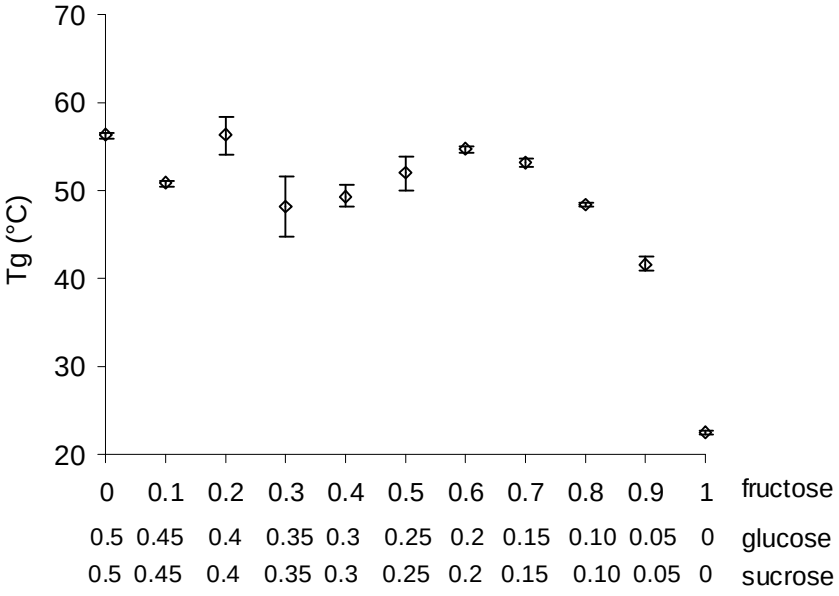

Figure 4.33 T_g values of three-sugar mixtures when the portion of sucrose and glucose were equal. (Error bars indicate ± SD of triplicate data).

Among the three sugars, sucrose is a disaccharide and has the highest molecular weight hence has the highest glass transition temperature. Researchers have found that increasing the higher molecular weight fraction material in the mixtures resulted in increasing T_g of the mixtures. Roos and Karel (1991a) found that the T_g of maltodextrins linearly increases with increasing molecular weight at various relative humidities. The T_g values of mixture

of maltodextrin + sucrose increased with increasing maltodextrin. It was further found that the effect of maltodextrins and their molecular weight at concentration below 50% was small in comparison to the increase at concentrations above 50%. The T_g of maltodextrins + sucrose mixtures was substantially decreased with increasing sucrose concentration.

Increasing glucose in the mixtures gave a fluctuating trend of T_g values with very high uncertainties of some mixtures (Figure 4.32). The maximum uncertainty found was +4.5 and -3.5. It was shown that T_g values decreased when the fraction of glucose was less than 50%. The T_g values of mixtures were more constant when the fraction of glucose in the mixtures was more than 50% onward. The high uncertainty occurred were started when the fraction of glucose was 40% and at the higher fractions. A few of the mixtures with a high fraction of glucose showed lower uncertainties. This might because the T_g value of glucose is in between the T_g of the other two sugars. It was likely to have less effect on the T_g values of the mixtures. It was found from the visual experiment that in the mixtures of glucose + sucrose, glucose had a small effect in decreasing the T_g value of sucrose. Similarly, in the mixtures of fructose + glucose, fructose had a small effect in decreasing the T_g value of glucose. The effect of fructose on decreasing the T_g values of mixtures with sucrose were found to be less when the fraction of fructose in sucrose less than 70%. With an equal amount of sucrose and fructose in the mixture, the T_g appeared at the values close to T_g of sucrose (Figure 4.30, Table 4.12).

Increasing fructose decreased T_g values of the mixtures (Figure 4.33). The uncertainties were very low when the fraction of fructose was more than 50%. The T_g values of mixtures decreased dramatically with the increasing of fructose fraction more than 50%. The uncertainty was high (± 4.00 °C) when almost equal fraction of each sugar presented in the mixture (fructose: glucose: sucrose = 0.3: 0.35: 0.35).

In conclusion, the results of visual T_g of fructose, glucose, sucrose and their mixtures gave the extent of the effect of lower and higher T_g component on the T_g of mixtures. It was shown that fructose had more influence on decreasing T_g of the two mixtures when the fraction was from 50% and above. Glucose seemed to have less effect on the T_g of mixtures because of its intermediate T_g values. Sucrose with the highest T_g among the three sugars seemed to raise the T_g of mixtures to higher values (seen from Figure 4.30 in

which the mixture of sucrose + glucose and sucrose + fructose were very similar when the fraction of sucrose more than 30%, and also seen in Figure 4.31).

4.6 DSC experiments

4.6.1 Calibration of DSC

In this section the results of DSC calibration experiments are presented. The sapphire calibration curves for all three ampoules were normal as shown in Figure 4.34.

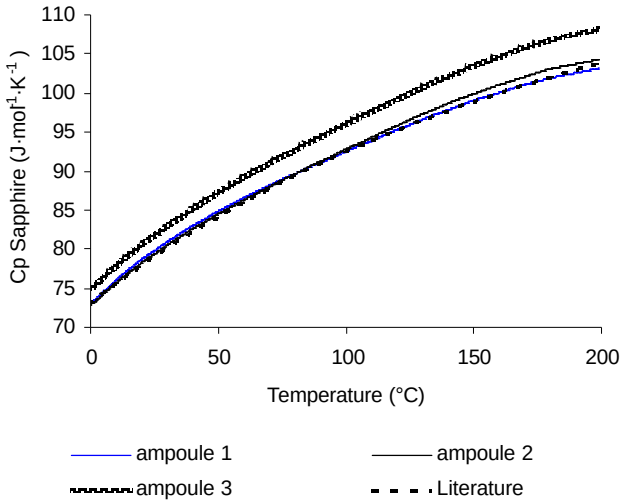

Figure 4.34 Sapphire calibration curves of DSC.

DI water was scanned in the three ampoules and showed endothermic responses on heating with the melting of water crystals starting at around 0.4 °C (Figure 4.35). It was concluded that the DSC was behaving as expected. In Figure 4.35 and others the terms signal 1, signal 2 and signal 3 refer to ampoule 1, ampoule 2 and ampoule 3 respectively.

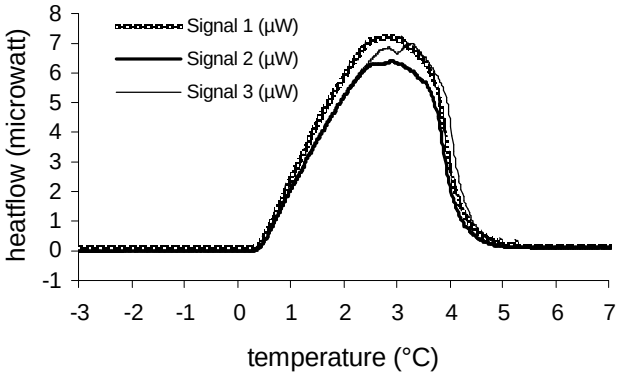

Figure 4.35 DI water calibration shows melting endothermic on upward direction from a DSC heating scan.

4.6.2 DSC trials

The T_g determination of sugars and carrot samples by DSC showed that there were some features of the DSC and samples that affected the appearance of transitions on the thermograms. The factors related to the DSC were the scanning rate, the annealing temperature and the annealing time. The factors related to samples were the texture of samples, the mass of samples put in the ampoules, and the handling of samples during the DSC scan.

The scanning rates of 5 and 2 °C min^{-1} did not produce clear thermograms in this experiment. It was found that a scanning rate of 0.1 °C min^{-1} worked well. The literature shows various DSC scan rate for sugars, such as 4 °Cmin^{-1} (Seo *et al.*, 2006), 5 °C min^{-1} (Roos, 1993; Roos & Karel, 1991) and 10 °C min^{-1} (Finegold *et al.*, 1989; Monica & Blanshard, 1993). Ablett *et al.* (1993) applied a low scan rate (0.1 °C min^{-1}) to measure the temperature of the peak for the ice-melting endotherm of 20-50% w/w fructose solution.

Annealing of samples before scanning helped to get a transition in the thermogram. The annealing temperature not only depended on the material being scanned but also depended on the nature of machine. Trials of annealing at 30 °C above or below the expected T_g of materials as suggested by Roos (1993) did not work well with the DSC used for most of the samples in this experiment. For some reason, which was not known, it was important to cool down the machine to the lowest temperature (-15 °C) before started the scan. An annealing temperature at -15°C for 40 minutes was best for all sugar scans. The fibre mixtures scans needed to be annealed at 70-80 °C for 40 minutes before heating to 150 °C to get good results. Apparently, both annealing temperature and time affect the glass transition temperature of materials. Ablette *et al.* (1993) had found that after annealing a 60% fructose solution at -50 °C for 45 minutes, the T_g values had increased from -84 to -80 °C whereas, the annealing at the same temperature for one hour, the T_g values increases substantially to -53 °C. It was stated that the effect was reproducible but the reason for this behaviour was obscure (Ablette et al, 1993). Israkarn and Charoenrein (2006) had found that using an annealing temperature slightly lower than the expecting T_g gave a clear transition on a DSC thermogram of cooked rice-stick noodles.

In this experiment it was found that some of the scans of samples with carrot fibre showed clear transitions but most of the scans of carrot fibre mixture showed very small transitions. Selected scans from the DSC of these mixtures will be presented in the relevant sections.

During the high temperature heating scan, degradation of samples occurred. Nitrogen was flushed into the DSC ampoules and reduced burning of the samples. In the trial of freeze dried 50% fibre in fructose with N_2 the sample started to burn at around 110 °C while samples without N_2 showed burning at around 90 °C. After the scan, the colour of samples in the ampoules without N_2 was darker indicating greater oxidation.

Application of vacuum to the samples in the ampoules did not give clearer transitions, but it was found to reduce burning of samples during heating scans. The samples in the ampoules were less oxidised, similar to those when N_2 was used.

The best way to get transitions from these trials was to fill the ampoule with as much sample as possible. This method worked well with the samples of carrot fibre mixture. When the sample completely filled the ampoule, N_2 flushing could be omitted. Ablett *et al.* (1993) used a larger sample weight when studying the T_g of fructose glasses and glass-ice mixtures by DSC.

Samples of mixtures with carrot fibre completely changed to a homogeneous black mass after the heating scans (Figure 4.36). This shows that the heat penetrated into all of the well packed sample in the ampoules. The samples probably acted as a single mass during the heating scan and thus facilitated the appearance of transitions.

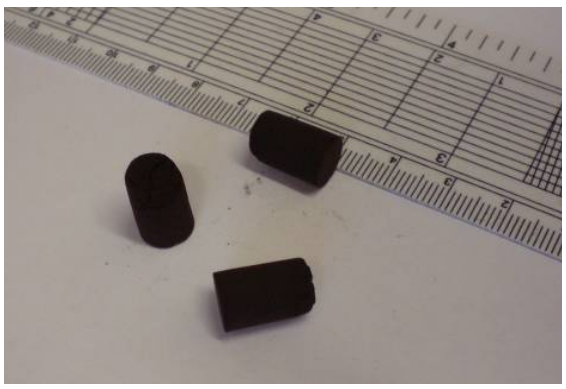

Figure 4.36 The samples of carrot fibre mixture after the DSC heating to 160 °C.

The scan of mixtures with maltodextrin had to be done with a very small amount of sample due to excessive swelling when exposed to high or very low temperature. This was also observed during freeze drying of maltodextrin (Section 4.2.6). During DSC scans of mixtures with maltodextrin, it was found that the samples splashed out of the ampoules and caused the problem of burning in the ampoule holders. Some of the experiments with maltodextrin needed to be omitted to avoid damaging the DSC.

4.6.3 T_g of melted sugars

The transition on the thermogram that occurred after the melting of ice and before melting temperature of the pure sugar was considered to be the glass transition temperature. A range of forms of the glass transitions appeared on DSC scans. Some of the thermograms showed the change in baseline as was indicated as a typical glass transition (as shown in Figure 2.21, Section 2.4.2). Figure 4.37 shows the typical thermograms from heating and cooling scans of melted fructose. Some of the thermograms showed a jump in the curve before moving back to the second baseline on the thermogram (Figure 4.38 heating scan of glucose). This style of the transition always appeared on the thermogram of glucose and glucose mixtures. In Figure 4.37 the onset, midpoint and endpoint of glass transition are indicated on both the heating and cooling thermogram.

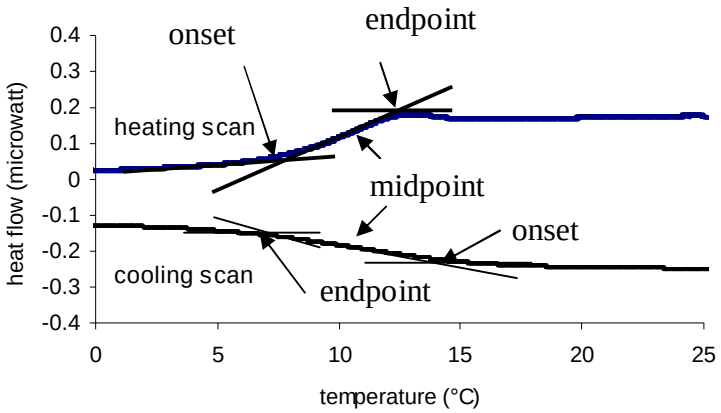

Figure 4.37 DSC heating and cooling scans of melted anhydrous fructose.

The thermogram from heating and cooling scans of melted sugars showed different T_g values for the same sample. Figures 4.38 and 4.39 show heating and cooling scans near T_g of melted, glucose and sucrose respectively.

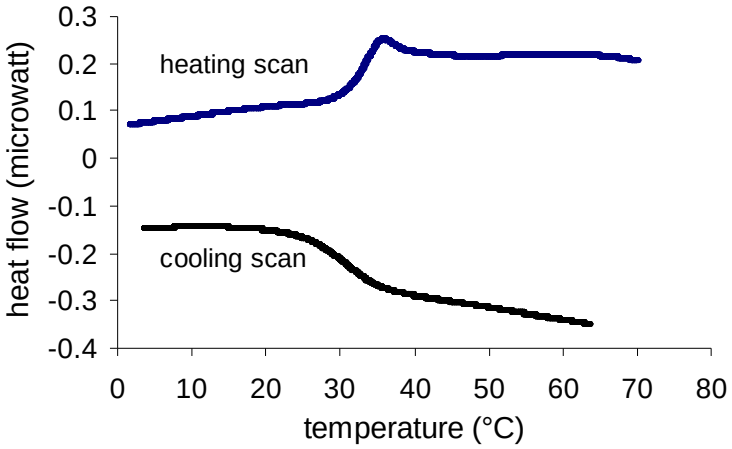

Figure 4.38 DSC heating and cooling scans of melted anhydrous glucose.

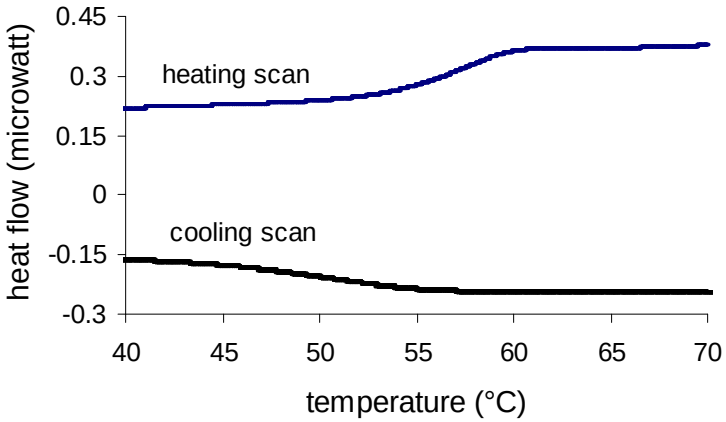

Figure 4.39 DSC heating and cooling scans of melted anhydrous sucrose.

The onset T_g values of fructose, glucose and sucrose on heating scans were 6 °C, 30 C and 54 °C respectively. The onset T_g values on cooling scans were at 15 °C, 35 °C and 53.5 °C respectively. Table 4.14 shows onset, midpoint and endpoint T_g values of heating and cooling scans. Even though the range of transition depended on the amount of sample, it was obvious that the same sugar samples demonstrated different transition ranges for the heating and cooling scans (Table 4.41 shows the values of the transition ranges for the three sugars).

Table 4.14 T_g values of melted anhydrous sugars from DSC heating and cooling scans at 0.1 °C min^{-1}

DSC scans	Heating			Cooling		
Sugars	onset	mid point	end point	onset	mid point	end point
Fructose	6	9	13	15	10	5
Glucose	30	33	35	35	29	24
Sucrose	54	58	60	53.5	50	44

From Table 4.14 the onset T_g of fructose from the heating scan was similar to the end point T_g from the cooling scan. This confirms that it is important to give the direction and scan rate used to obtain the T_g of a material. Upon heating, fructose starting to change from an amorphous glassy solid to rubbery state at 6 °C and the entire process finished at around 13 °C. From the cooling scan of fructose, the state change from rubbery to glassy solid occurred when the temperature cooled down to 15°C and the transition finished at 5 °C. A difference between onset T_g from heating and cooling scans has normally been found in DSC studies of polymers including foods (Pomeranz & Meloan, 1994; Simperler *et al.*, 2006). Simperler *et al.* (2006) demonstrated for glucose that the cooling T_g was 52 °C and the heating T_g was at 61 °C which was 9 °C apart. The discussion from this study indicated that cooling runs were preferred to heating runs as relaxation phenomena are faster at higher temperature for large molecules. Therefore, it was likely that after being at a higher temperature, the long polymer chain would have enough time during cooling to relax. For amorphous compounds of small molecules such as monosaccharides and disaccharides the relaxation process might well be sufficiently fast at lower temperatures. In addition, from the experiments, the cooling run of glucose seemed to show a slightly smaller overestimation of T_g than the heating run (Simperler *et al.*, 2006). Roos (1993) preferred to report onset heating T_g values. He stated that most of the mechanical properties change above the onset T_g (including viscosity and stickiness as well as crystallinity of carbohydrates).

These T_g values were in good agreement with many other literature values even though the scan rates were different. Table 4.15 shows a comparison of T_g values of sugars from literature and this work. There was no clear trend relating T_g to the DSC scan rate. Hurtta *et al.* (2004) found that the onset of endothermic peaks of sucrose increased (from 167.9 to 189.0 °C) when the scan rate increased (from 0.5 to 100 °C min^{-1}). Roos (1995)

stressed that the T_g value of a single sample also depends on the sample thermal history and even the same analytical method may give different T_g values. The detail on the different DSC T_g values of the same material from different researchers will be discussed more in the discussion chapter.

Table 4.15 DSC scans and T_g values of sugars

Scan rate	T_g fructose (°C)		T_g glucose (°C)		T_g sucrose (°C)		Reference
(°Cmin^{-1})	onset	mid point	onset	mid point	onset	mid point	
10	-	13	-	38	-	57	Finegold *et al.*, 1989
10	5	16	31	36	-	-	Wungtanagorn & Schmidt, 2001
5	5	10	31	36	62	67	Roos, 1993
4	-	-	-	32	-	69	Seo *et al.*, 2006
0.1	6	9 (13)	30	33(35)	54	58(60)	This work (heating)
0.1	15	10(5)	35	29(24)	53.5	50(44)	This work (cooling)

The values in ( ) are the T_g end points of heating and cooling scans from this experiment

4.6.4 Comparison of the visual T_g with DSC T_g

The physical appearance of fructose was found to change from a rubbery to glassy state at around 22 °C. Similarly, glucose and sucrose were visually found to have T_g values at 48 and 61 °C respectively. A comparison between T_g values from the visual experiment and DSC T_g onset of heating scan and DSC T_g end point of cooling scans of fructose, glucose and sucrose is given in Figure 4.40. The visual T_g and DSC T_g of sucrose were very close. The DSC T_g onset from heating and endpoint T_g from cooling scan of fructose were quite close but they were much lower than the visual T_g. The T_g onset from heating and endpoint from cooling scan of glucose and sucrose were different. However, the DSC T_g onset of heating sucrose was close to the visual value. On the contrary, Wungtanagorn & Schmidt (2001) found that fructose showed the biggest variation of reported DSC T_g values.

These experiments showed that the technique used gave T_g values comparable with previous work and reinforced the need to be precise about the method used to obtain any

quoted T_g. It was very clear that it is unrealistic to assume a material has a single precise T_g.

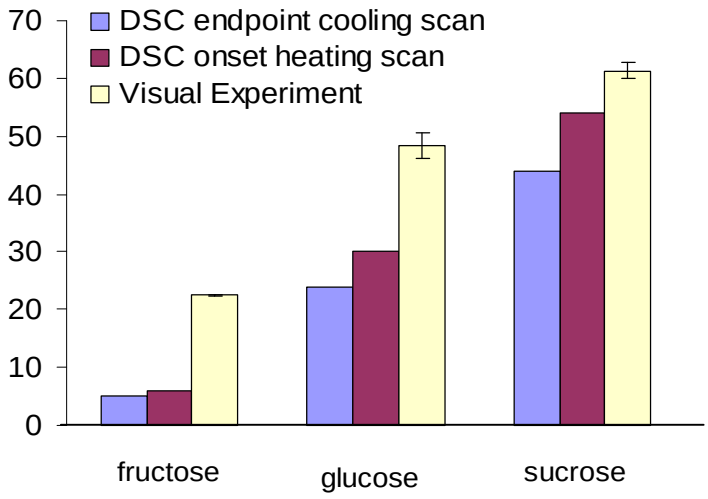

Figure 4.40 Comparison of T_g from the visual experiment and DSC scans of fructose, glucose and sucrose. Error bars indicate ± SD from triplicate data..

4.6.5 T_g of freeze dried fructose

The heating DSC scan of freeze dried amorphous fructose showed the glass transition at quite a high temperature (18 °C) compared to that of melted amorphous fructose (6 °C). The shapes of the DSC thermograms of melted amorphous fructose (Figure 4.37) and freeze dried fructose (Figure 4.41) were different. The thermogram has a narrow transition from which it was not possible to distinguish the onset, midpoint and endpoint of the transition. It was seen that the thermograms of the three samples showed slight changes of base line before 18 °C. It was not immediately clear if it was the glass transition or not. The appearance was checked by holding the three samples in the DSC at 6, 14, 16, 18 and 20 °C overnight for these three samples. The result found no physical change of samples at 6, 14 and 16 °C. The samples became completely rubbery at 20 °C. At 18 °C the sample showed a physical change from an amorphous solid to a rubbery solid. A study of the DSC T_g of freeze dried hydrated amylose and amylopectin at 3 °C per minute by Bizot *et al.* (1997) also found a similar change in the base line before the onset T_g. This transition style did not appear on the DSC scans of melted pure sugars. The stylized curves from DSC scans by Nielsen (2003) did not indicate this style of scan.

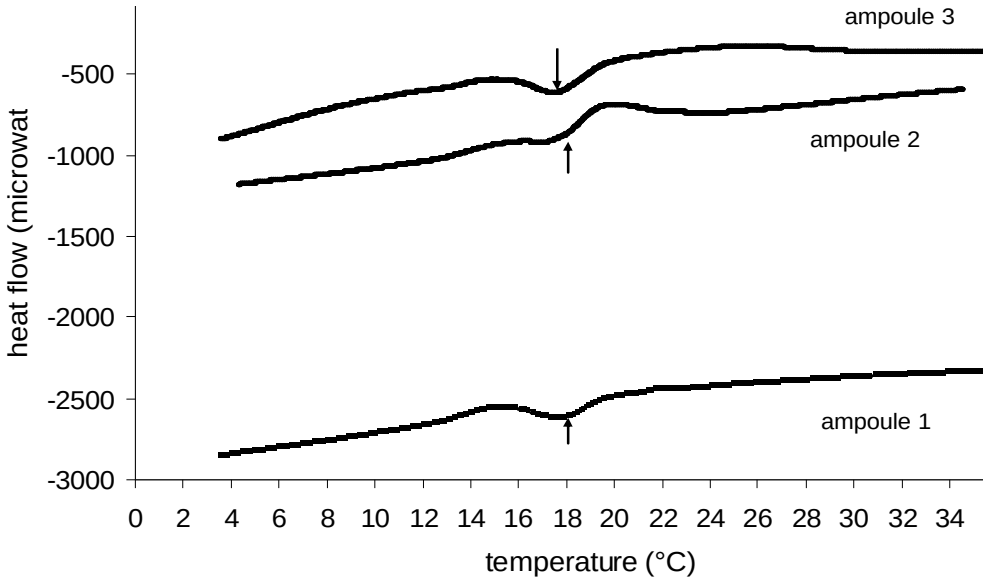

Figure 4.41 DSC heating scan of freeze dried fructose (approximate MC =0.05% wb). The arrows indicate T_g values.

The attempt to find the glass transition of freeze dried fructose on a cooling scan was not successful (Figure 4.42). The only transitions that were seen on these thermograms were endothermic (upward direction) at -8 °C. This indicated that some moisture in the sample was crystallised upon freezing (the samples contained 0.05% moisture).

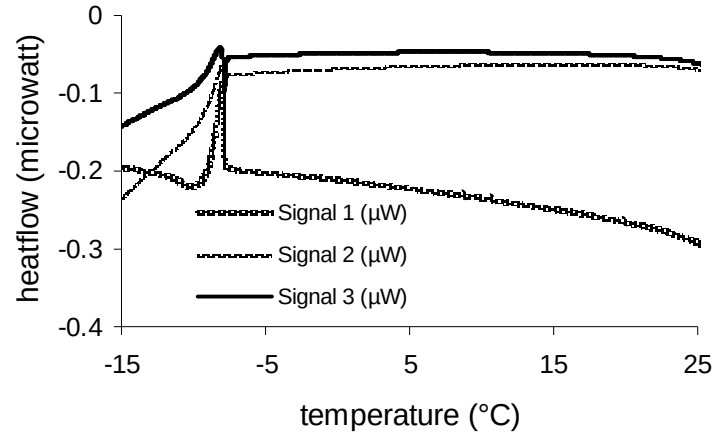

(a)

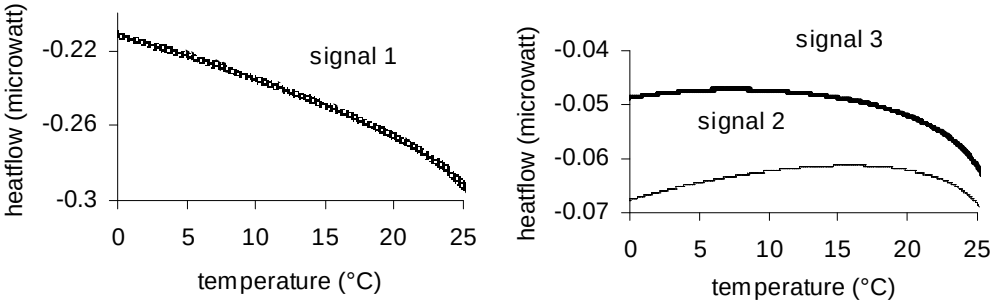

(b) (c)

Figure 4.42 Cooling scan of freeze dried fructose shows crystallisation of moisture at -8 °C (a). No glass transition appeared on the thermograms (b) and (c).

Some DSC scans of samples did not show any transitions. (The reason for this was not understood). Figure 4.43 (a) shows heating scans of freeze dried fructose from -25 °C to 125 °C with no apparent glass transition, even though a transition was expected at about 18 °C. The sample in ampoule 3 (signal 3) showed endothermic transition at around 80 °C which was not related to anything expected in pure amorphous fructose. Figure 4.43(b) shows one of the heating scans of the same sample as in Figure 4.43(a). An endothermic peak was found for the sample in ampoule 1 (signal 1) with an onset temperature at around 45 °C. The samples in ampoule 2 and 3, showed an onset endothermic transition at around 55 °C. These temperatures had no relationship with the samples at all. If there were some semicrystalline material of fructose present in the samples the melting transition should show at around 102-103 °C which is the melting point of fructose. Wide endothermic peaks related to water evaporation in DSC scans

have been found at temperatures much higher than the endothermic transition from this graph (118-122 °C in apple cell wall, 120-125 °C in samples of wood and 130 °C in dextran (Aguilera *et al.*, 1998). Detail is in Section 2.4.2. It was not clear what caused these endothermic transitions in DSC scans of freeze dried fructose.

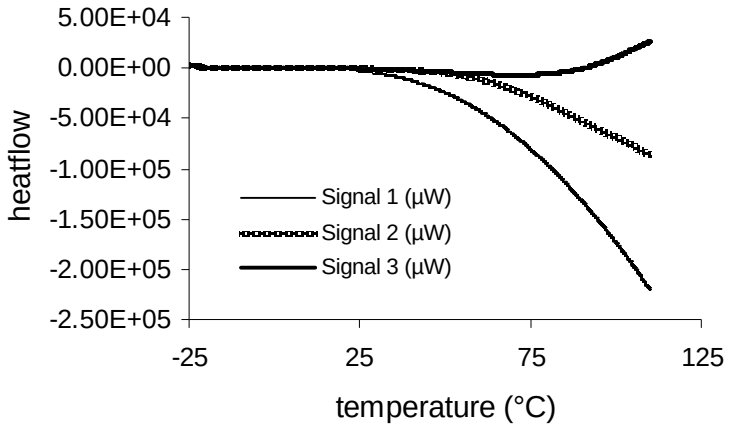

(a)

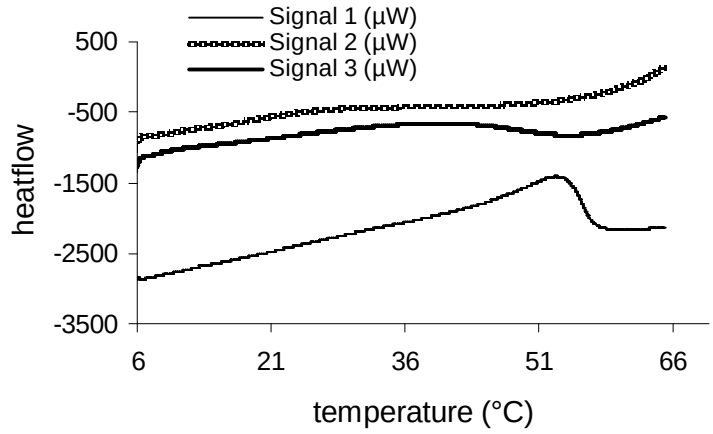

(b)

Figure 4.43 (a) One heating scans of freeze dried fructose without a glass transition. The onset endothermic transition appeared at 80 °C from signal 3. (b) the signal 1 shows an onset endothermic transition at around 45 °C and signals 2 and 3 show the onset endothermic transition at around 55 °C.

4.6.6 T_g of two-sugar mixtures

In this experiment two sugars were mixed at different fractions. The first sugar was melted (higher melting temperature) and left to cool down to around 100 °C and the second sugar was mixed and melted. All of the thermograms from the two-sugar mixtures

showed a broad glass transition. DSC heating scans of mixtures of sucrose + fructose, sucrose + glucose and fructose + glucose at a 1:1 ratio are shown in Figure 4.44. These thermograms show melting of ice at 0 °C and clear glass transitions. Moisture might have entered the ampoules during the transfer of samples from the glassware after the sugars were melted.

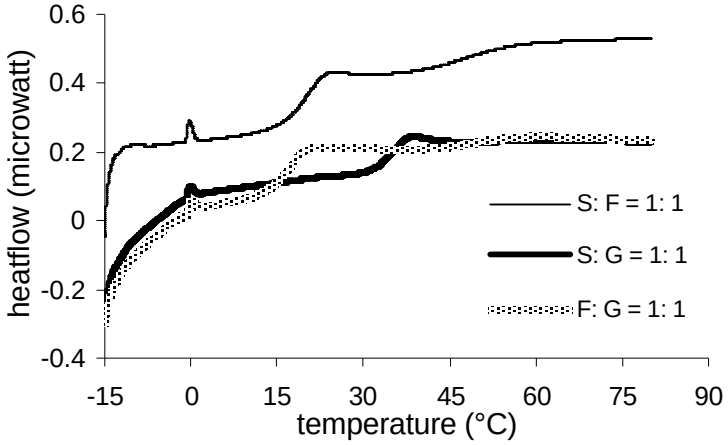

Figure 4.44 DSC heating scan of mixture of two sugars. The endothermic transition at 0 °C is evidence of some water crystals melting.

The cooling scans of the same mixtures are in Figure 4.45. The cooling thermograms confirmed the small amount of moisture in samples with the crystallisation of ice appearing at -8 °C. On cooling, the three samples showed small endothermic transitions (20 °C for sucrose:fructose, 25 °C for sucrose:glucose, and 10 °C for fructose:glucose) but it was not known what caused these.

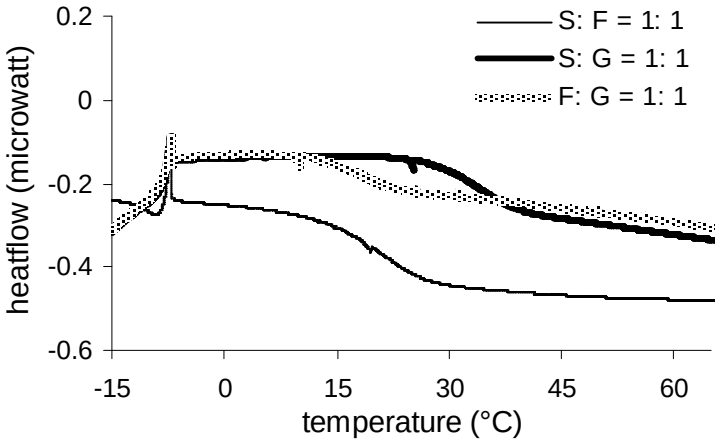

Figure 4.45 DSC cooling scan of two-sugar mixtures with the crystallisation of moisture found at -10°C. There are small endothermic transitions in the three samples.

It was expected that the T_g of different sugar mixtures would show different T_g values. However, some of the DSC scans of sugar mixtures showed the T_g of different sugar mixtures at a very similar temperatures. Figure 4.46 shows that the transitions of two-sugar mixtures with a ratio of 1:3 and 3:1 of sucrose + glucose occurred at very similar temperatures. The mixture of sucrose + fructose at a ratio of 3:1 also had a transition very close to the transition of sucrose + glucose at a ratio of 1:3.

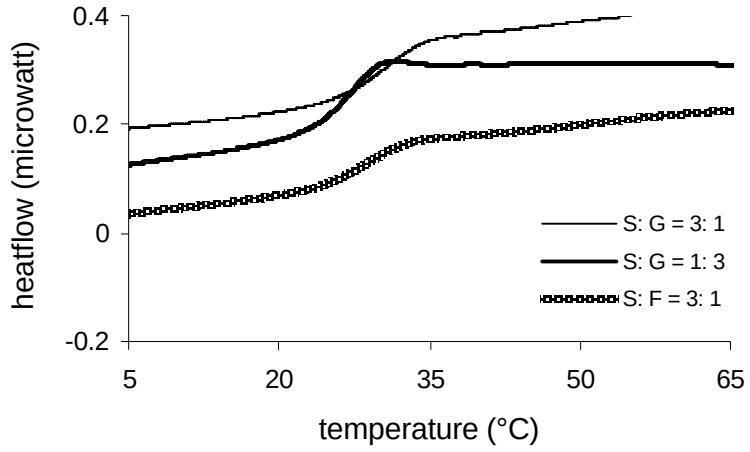

Figure 4.46 DSC heating scan of two-sugar mixture at 3:1 and 1:3 ratio found the transition at almost the same temperature.

4.6.7 Analysis of DSC onset T_g heating scan of two-sugar mixtures by Gordon-Taylor equation

The onset T_g values from DSC heating scan results of the mixtures of two dry melted sugars did not fit the Gordon-Taylor equation well (detail on this equation is in Section 2.2.5). Figures 4.47, 4.48 and 4.49 show the data and equations for mixtures of sucrose + fructose, glucose + fructose and sucrose + glucose, respectively. The curve fitting was by non-linear least squares using Solver in Excel. The end points were obtained from at least three measurements and were found to be consistent with values from literature, so the curve was forced to pass through the end points. The T_g values of mixtures of sucrose + fructose and glucose + fructose showed similar trends with the T_g values from the experiment lower than the Gordon-Taylor equation when the ratios of fructose was in the range 0 to 40%. Above the ratio of 50% fructose the experimental T_g values were higher than the predicted. The presence of moisture in the samples would reduce the T_g, but many of the data points in Figures 4.47 and 4.48 are higher that expected, indicating that moisture was unlikely to be the cause of discrepant results.

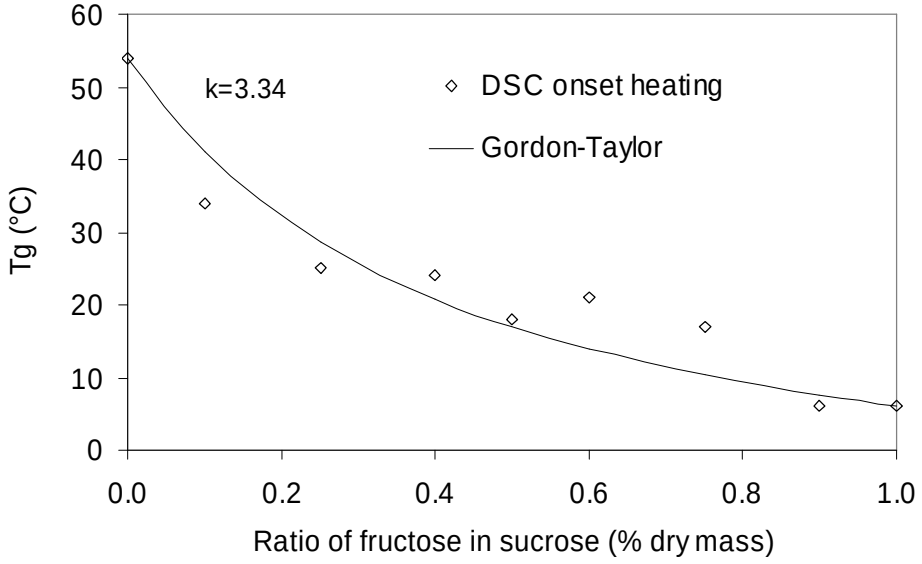

Figure 4.47 Gordon-Taylor plot (k=3.34 for heating scan) and experimental data for the onset T_g values of mixtures of sucrose and fructose.

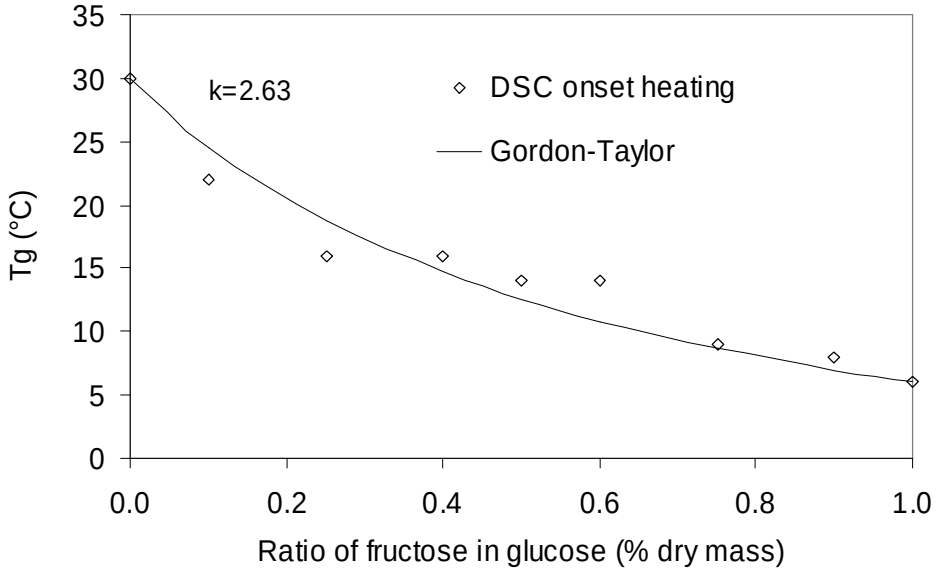

Figure 4.48 Gordon-Taylor plot (k=2.63 for heating scans) and experimental data for the onset T_g values of mixtures of fructose and glucose.

On the other hand, most of the experimental T_g values were lower than the prediction for mixtures of glucose + sucrose (Figure 4.49). One of the possibilities that the experimental T_g values lower than the prediction T_g is the effect of decomposition of sugars during melting process. Fan and Angell (1995) demonstrated that if the melting of sugar samples

was not controlled at the right temperature along the process, decomposition occurred and a decrease of the T_g value was found. Simkovic *et al.* (2003) found that a part of sucrose cleaved to glucose and fructose around the melting temperature. Since all the mixtures were prepared by the same method, the possibility that moisture reduced the T_g of some samples was unlikely.

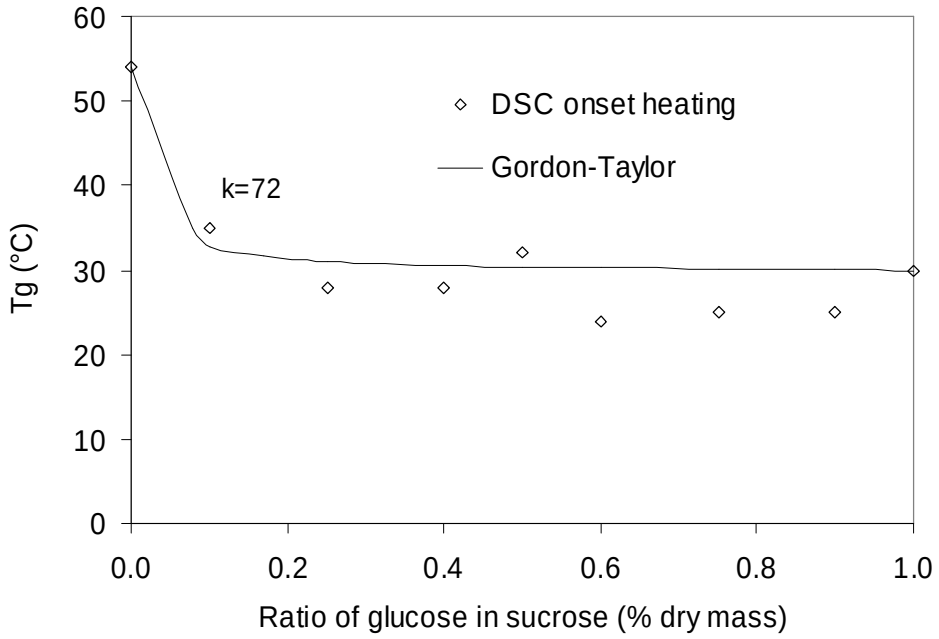

Figure 4.49 Gordon-Taylor plot (k=72 for heating scan) and experimental data for the onset T_g values of mixtures of glucose and sucrose.

Results of Seo *et al.* (2006) for glucose + sucrose and glucose + maltotriose did not fit the Gordon-Taylor equation well (Figure 4.50). These mixtures which showed the greatest deviation, were monosaccharide + disaccharide and monosaccharide + trisaccharide. The researchers concluded that the molecular size and shape of the mixture components affected the T_g.

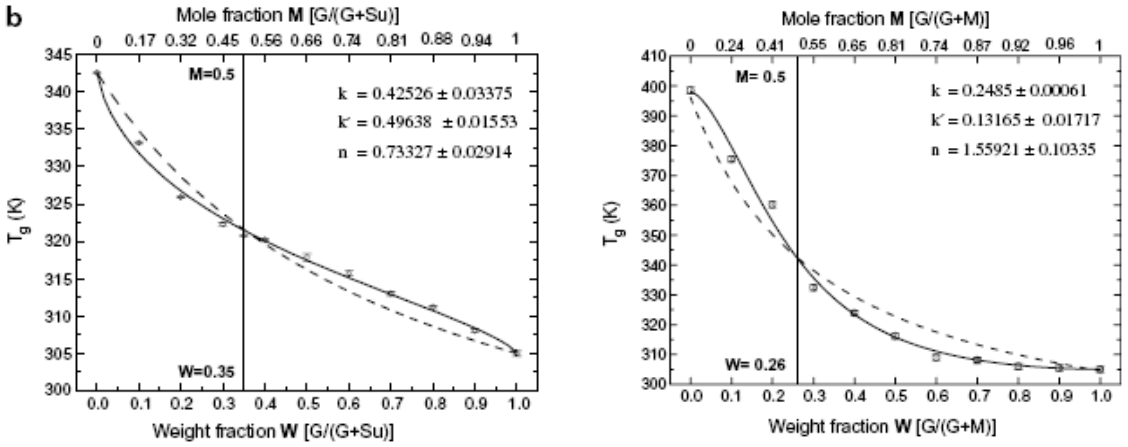

Figure 4.50 Glass transition temperatures of glucose + sucrose mixtures (left) and glucose + maltotriose (right) as a function of weight fraction and mole fraction. The dashed lines are fitted results using the Gordon-Taylor equation and solid lines are fitted results using the modified Gordon-Taylor equation (Seo *et al.*, 2006).

On the other hand, Seo *et al.* (2006) found that the midpoint T_g values of monosaccharide + monosaccharide (sorbitol + glucose) and disaccharide + disaccharide (sucrose + trehalose) could be fitted to the Gordon–Taylor equation well (Figure 4.51).

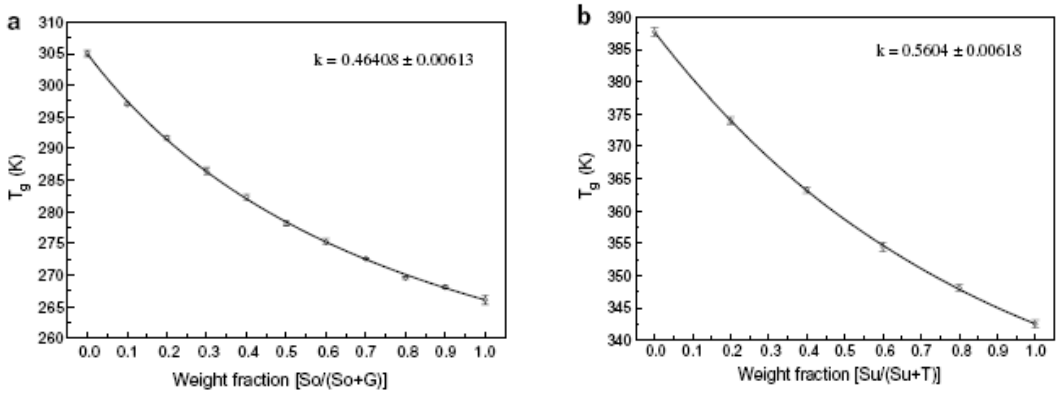

Figure 4.51 Glass transition temperatures of sorbital + glucose mixtures (left) and sucrose + trehalose (right) as a function of weight fraction. The solid lines are fitted results using the Gordon-Taylor equation (Seo *et al.*, 2006).

In this study the T_g values of glucose + fructose still showed variation between the experimental and predicted results but much less than that of sucrose + fructose and sucrose + glucose. As already discussed in the visual T_g experiment (Section 4.5), the apparent T_g values of sugar mixtures were lower than the lower T_g values of the two sugars. A study of T_g (midpoint) of dry mixtures of sucrose + fructose and sucrose +

glucose by Finegold (1989) however, showed very good agreement with the Gordon–Taylor equation (Figure 4.52). For these mixtures the k values for Gordon-Taylor plot of the Finegold *et al.* data and from this experiment are similar. The onset DSC T_g values from cooling scans are very close to the data from Finegold *et al.*

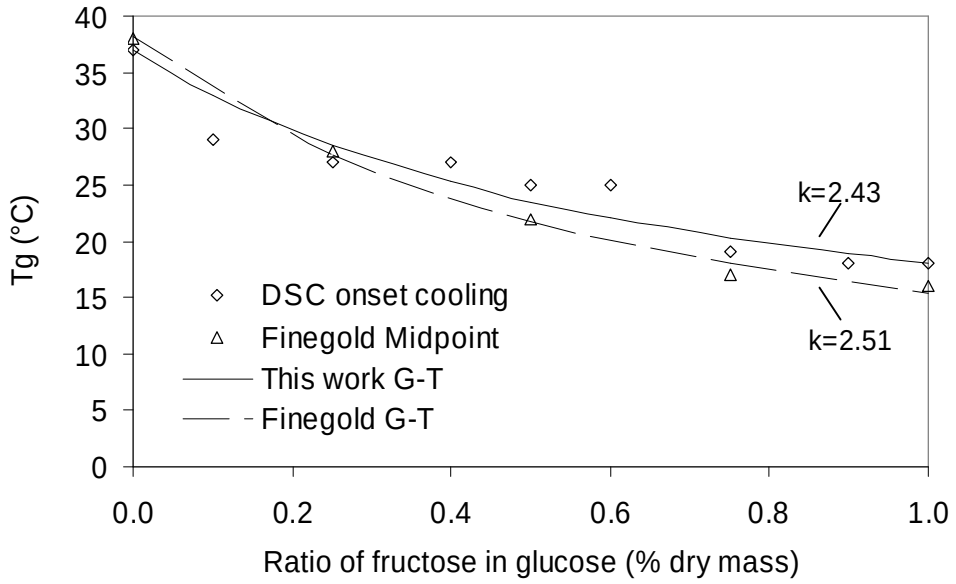

Figure 4.52 Experimental data for T_g values of mixtures of fructose and glucose from Finegold *et al.* (1989) compared to those of the onset cooling DSC scans from this experiment with Gordon-Taylor equations for both

Since the T_g values from Finegold *et al.* (1989) were from the midpoints of the transition, the midpoint T_g values from this experiment were compared as shown in Figure 4.53. It is interesting that the midpoint T_g values from DSC heating and cooling scans were similar and close to values from Finegold *et al.* However, the values from Finegold *et al.* are systematically higher by about 5-10 °C.

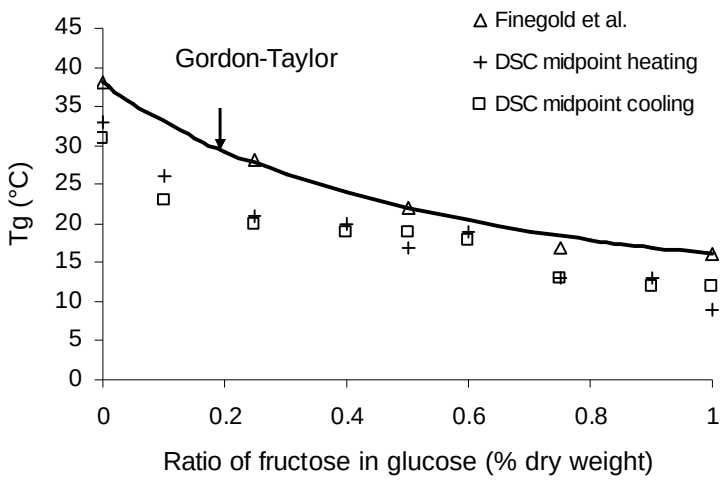

Figure 4.53 The Gordon-Taylor plot and experimental data for T_g values of mixtures of fructose + glucose for data from Finegold *et al.* (1989) compared to those from midpoint heating and cooling DSC scans from this experiment.

Using the Gordon-Taylor equation and k values from Section 2.2.11 the moisture content 0.7 to1.5% would reduce T_g of glucose by 5 to 10 °C. This high level of moisture contaminated was very unlikely given the sample preparation used.

The T_g values of mixtures of fructose + sucrose from this experiment were compared with the data from Finegold *et al.* (1989) (Figure 4.54). Again Finegold's data were higher than those obtained here.

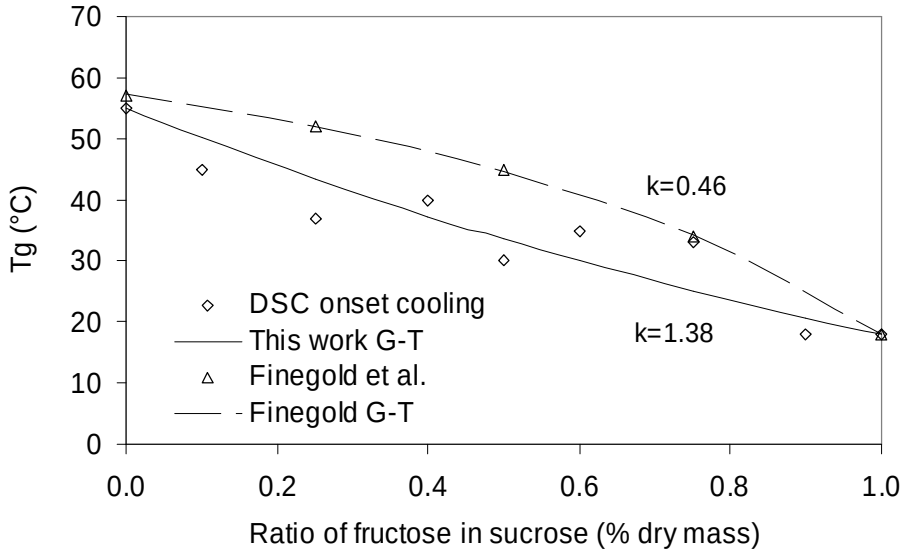

Figure 4.54 Experimental data for T_g values of mixtures of fructose and sucrose from Finegold *et al.* (1989) compared to those of the onset cooling DSC scans from this experiment with Gordon-Taylor equations for both.

All of the onset and midpoint T_g values of fructose + sucrose mixtures from this experiment are lower than the data from Finegold *et al.* (1989). The midpoint T_g values from this experiment are compared to the data from Finegold *et al.* in Figure 4.55. The degradation of samples during melting might be a cause of this variation.

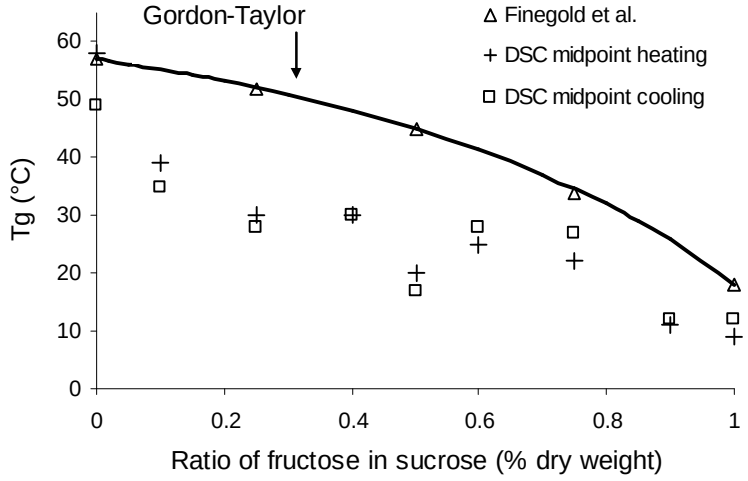

Figure 4.55 The Gordon-Taylor plot and experimental data for T_g values of mixtures of fructose + sucrose from Finegold *et al.* (1989) compared to midpoint values from heating and cooling DSC scans from this experiment.

4.6.8 Comparison of DSC onset T_g of two-sugar mixtures to the visual T_g

The DSC T_g of two-sugar mixtures were much lower than the visual T_g. Figure 4.56 shows the comparison of these T_g values of the mixtures of sucrose + fructose and sucrose + glucose including data from Feingold *et al.* (1989). The figures show that the trend of T_g values from the visual experiment and data from Finegold *et al.* are similar for both types of mixture. The visual T_g values are slightly higher than those of data from Finegold *et al.* The onset T_g values from heating and cooling scans are fairly low when compared to the visual T_g values. Figure 4.57 shows the comparison between the visual T_g values and the onset T_g of glucose + sucrose mixtures. There is more variation in the values from the onset T_g of heating and cooling scans for mixtures of sucrose + glucose and sucrose + fructose compared to mixtures of glucose + fructose. According to Seo *et al.* (2006) this might be because of the effect of differences in size and shape of sugars molecules of sugars in the mixtures.

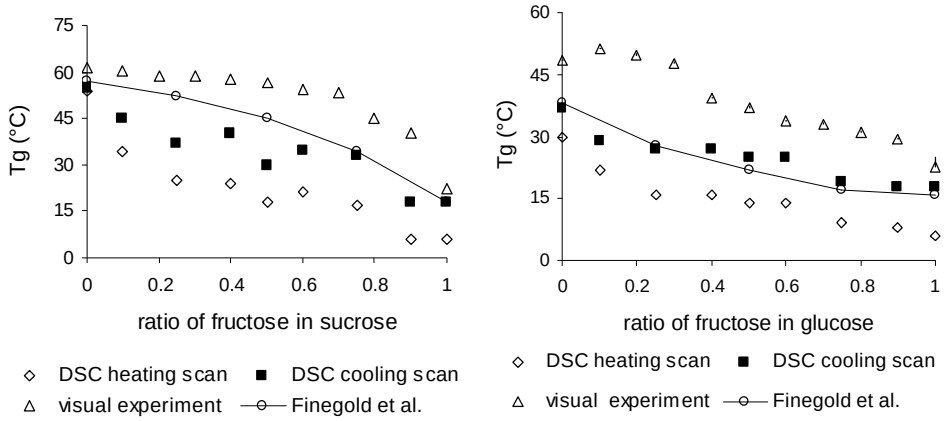

Figure 4.56 Comparisons of DSC onset T_g from heating and cooling scans to the visual T_g and data from Finegold *et al.* (1989) of fructose + sucrose mixtures (left) and fructose + glucose mixtures (right).

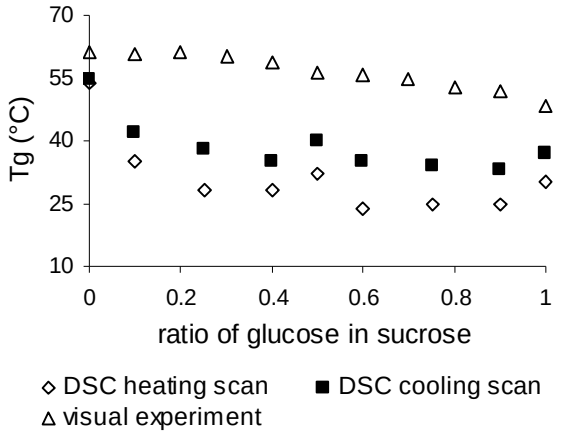

Figure 4.57 Comparisons of DSC onset T_g from heating and cooling scans to the visual T_g of glucose + sucrose mixtures.

The visual T_g of two-sugar mixtures were higher than the onset heating DSC T_g by about 23 to 28 °C. The visual T_g of two-sugar mixtures were higher than the onset cooling DSC T_g in the range 13 to 18 °C. As stated before, the DSC T_g of some sugars and mixtures in this experiments did not show any transition in the DSC results. For many mixtures, the midpoint T_g values from DSC scans can present better T_g values of sugars and their mixtures and reduce the difference between the visual and the DSC results. Details of the difference of visual T_g from DSC onset heating and cooling scan values of the two-sugar mixtures are in Table 4.15.

Table 4.15 The different of visual T_g values from DSC heating and cooling T_g of two-sugar mixtures

Ratios of mixture	Sucrose: fructose		Sucrose: glucose		Glucose: fructose	
	T_{gV}-T_{gH}	T_{gV}-T_{gC}	T_{gV}-T_{gH}	T_{gV}-T_{gC}	T_{gV}-T_{gH}	T_{gV}-T_{gC}
0.0: 1.0	16.45	4.45	18.42	11.41	16.48	4.48
0.1: 0.9	33.95	21.95	27.04	19.04	21.37	11.37
0.25: 0.75	32.4	16.4	28.85	19.85	23.12	13.12
0.4: 0.6	32.45	19.22	31.6	20.6	19.73	8.73
0.5: 0.5	36.22	26.28	24.28	16.28	22.8	11.8
0.6:0.4	32.28	17.55	30.88	23.88	23.23	12.23
0.75: 0.25	34.15	21.775	32.72	22.72	32.63	21.63
0.9:0.1	26.28	15.275	25.82	18.82	29.3	22.3
1.0:0.0	7.31	6.31	7.31	6.31	18.42	11.42
average	27.94	16.57	25.21	17.66	23.00	13.08

4.6.9 DSC T_g of three-sugar mixtures

In this experiment the mixtures of three sugars had various fractions of fructose with equal amounts of glucose and sucrose. The aim was to determine T_g of mixtures similar to those in natural apple juice which is dominant in fructose and has equal amounts of glucose and sucrose (Berüter, 1985).

The detail of onset T_g values from DSC heating and cooling scans of these three-sugar mixtures are shown in Table 4.16. The results showed that increasing the amount of fructose decreased T_g of the mixtures toward T_g of pure fructose. However, the DSC onset T_g from heating scans of mixtures of fructose + glucose + sucrose at 3:1:1, and 4:1:1 appeared at very similar temperatures as shown in Figure 4.58. The heating scans showed endothermic melting transitions at 0 °C for all three samples. The cooling scan (Figure 4.59) of the same sample exhibited very similar T_g values for the mixtures at ratios 3:1:1 and 4:1:1. The crystallisation of moisture in the samples appeared at -10 °C.

Table 4.16 T_g of melted fructose + glucose + sucrose mixtures from DSC heating and cooling scans at 0.1 °C min^{-1}

DSC scans	Heating			Cooling		
Fructose:glucose:sucrose	onset	mid point	end point	onset	mid point	end point
0:1:1	32	36	39	40	34	28
1:1:1	21	25	29	32	27	20
2:1:1	19	24	28	30	25	19
3:1:1	15	19	23	26	20	13
4:1:1	14	18	22	24	18	12
5:1:1	13	15	19	22	16	11
6:1:1	10	12	15	19	13	8
7:1:1	12	18	22	23	17	12
8:1:1	10	13	17	18	13	8
9:1:1	8	13	16	19	12	7
1:0:0	6	9	13	18	12	6

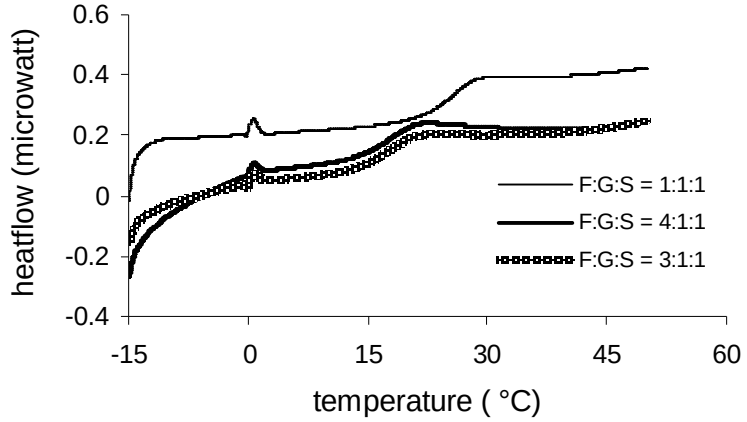

Figure 4.58 DSC heating scans of three-sugar mixtures.

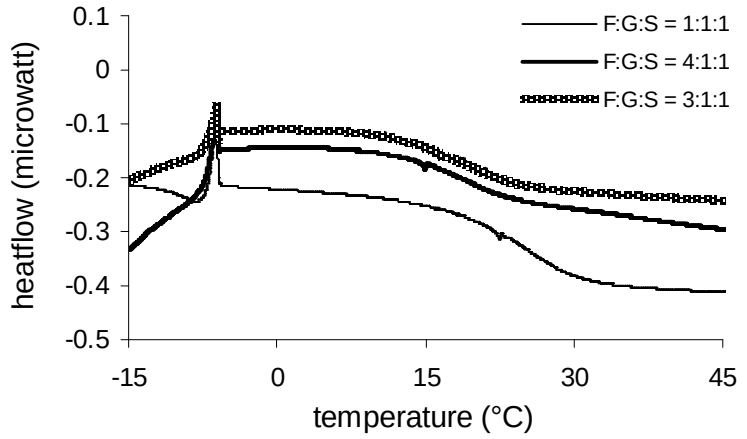

Figure 4.59 DSC cooling scans of three-sugar mixtures.

However, the visual T_g of the 1:1:1 mixture was about 50 °C which was 29 °C higher than the onset T_g from this DSC heating scan result. This discrepancy is consistent with the previous results.

4.6.10 Analysis of three-sugar mixtures by the modified Coachman and Karaze equation

Data from Table 4.16 for the T_g of three-component samples were compared to the predicted values from the modified Coachman and Karaze equation given by Kalichevsky and Blanshard (1992) . This equation used the weight fractions, T_g and • C_p of all component compounds (equation 4.1). The T_g and • C_p of fructose, glucose and sucrose

given by Roos, 1995, were 5 °C, 0.75 J(g °C)$^{-1}$, 31 °C, 0.63 J(g °C)$^{-1}$ and 62 °C, 0.60 J(g °C)$^{-1}$ respectively.

$$T_g = \frac{w_1 \Delta C_{p1} T_{g1} + w_2 \Delta C_{p2} T_{g2} + w_3 \Delta C_{p3} T_{g3}}{w_1 \Delta C_{p1} + w_2 \Delta C_{p2} + w_3 \Delta C_{p3}} \qquad (4.1)$$

This prediction did not work well. However it was noted from Figure 4.49 that 1:1 mixtures of glucose and sucrose had T_g values very similar to 100% glucose. The data was therefore fitted with a two-component equation of the same form as (4.1) in which 1:1 glucose + sucrose was considered to be a single component and fructose was the other component. The least squares fits for both heating and cooling are shown in Figure 4.60. For both curves the value of • C_p of fructose and 1:1 glucose + sucrose were based on Roos (1995) with values of 0.75 J(g °C)$^{-1}$ and 0.63 J(g °C)$^{-1}$. The cooling T_g values of fructose and 1:1 glucose + sucrose were found to be 16.3 °C and 40.8 °C respectively. For heating the corresponding values were 5.6 °C and 31.9 °C.

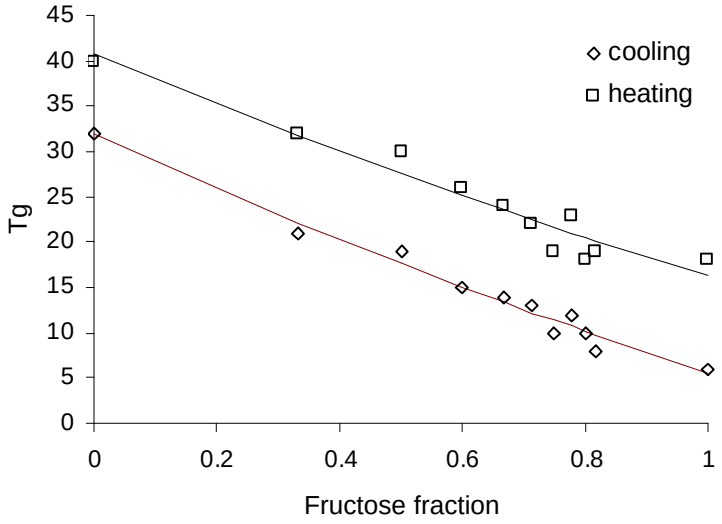

Figure 4.60 Comparison of onset T_g values of three-sugar mixtures with prediction from the modified Couchman and Karaze equation with two components. (The fractions of sucrose and glucose were equal).

4.6.11 Comparison of DSC T_g and visual T_g of three-sugar mixtures

The visual T_g of three-sugar mixtures was around 20-30 °C higher than the DSC T_g values of the cooling scan. Selected T_g values from both experiments are compared in Figure 4.61.

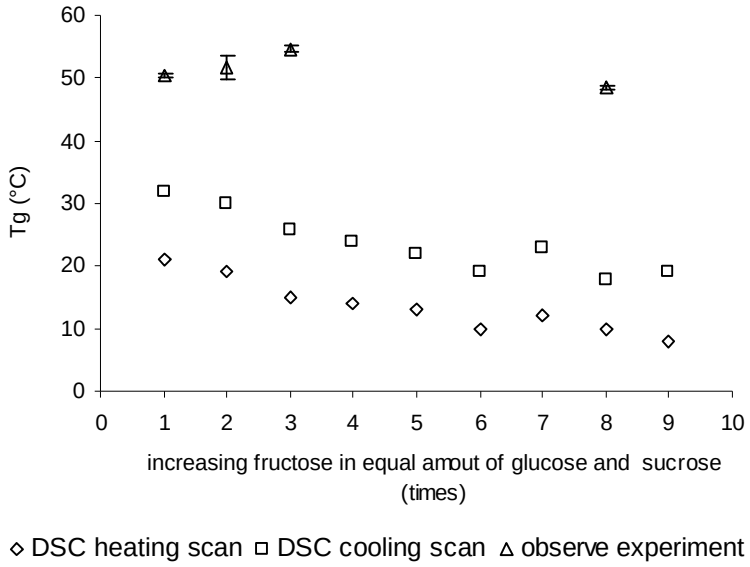

Figure 4.61 Comparison of DSC T_g heating and cooling scans to visual T_g of three-sugar mixtures.

The results of DSC and visual T_g values of sugars and mixtures cast doubt on the validity of the DSC results in predicting the physical response of real samples. The extent of decomposition of the visual and DSC samples was unknown and remains the greatest area of uncertainty.

4.6.12 DSC scans of anhydrous carrot fibre powder and maltodextrin

The cooling scan gave T_g values of sugars closer to the visual T_g values for sugar and their mixtures. However, it was not possible to perform cooling scans of food materials with high T_g values due to oxidation of samples. Thus the DSC scans of all fibre and maltodextrin mixtures from freeze drying and spray drying were performed with heating scans only.

The glass transition thermograms of carrot fibre powder and maltodextrin were quite different from each other. Figure 4.62 shows heating scan of maltodextrin with a decrease of the base line after the transition. The thermogram of carrot fibre powder was similar to that of the heating scan of the glucose (Figure 4.38). This transition style might be because the cellulose and xylan in fibre are composed of glucose, galactose, xylose and arabinose (Dien *et al.*, 2006). Processing might break glycosidic linkages in the dietary fibre polysaccharides, resulting in an increased amount of low molecular fragments. Heat

during milling of fibre might be able to redistribute of high molecular weight components into smaller fragments (Tijskens *et al.*, 1997; Vicenta *et al.*, 2005; Nyman *et al.*, 1993).

The carrot fibre powder samples showed two similar transitions at 173.5 °C and 194 °C as shown in Figure 4.62. The components of carrot fibre were 3.88% pectin, 12.3% hemicellulose, 51.6% cellulose and 32.2% lignin (Nawirska & Kwasniewska, 2005). The T_g values of cellulose, lignin and hemicellulose were found to be 103 °C, 200 °C and 200 °C respectively (Georget *et al.*, 1999). The T_g values of these components reported by Salmen *et al.* (1984) were 220 °C, 205 °C and 220 °C respectively. The two transitions found from this thermogram could possibly be the T_g of cellulose, lignin or hemicellulose.

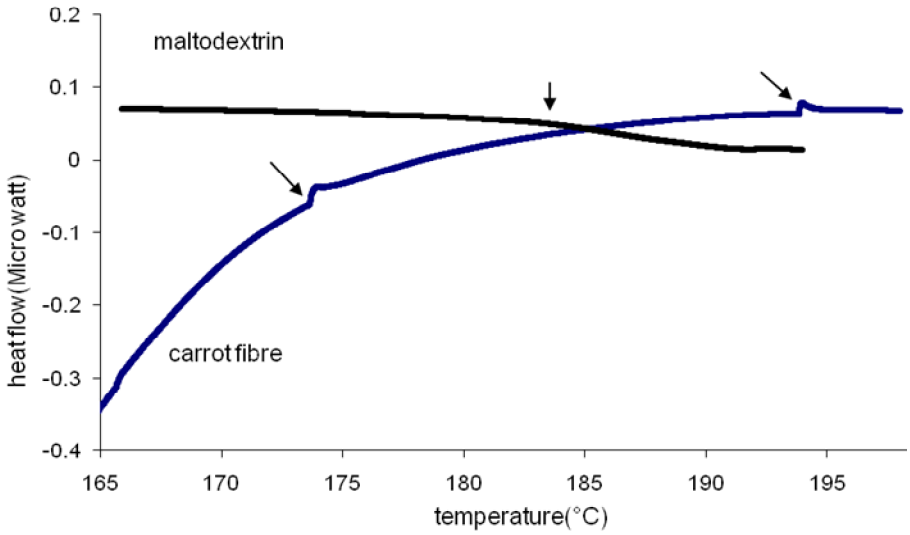

Figure 4.62 DSC heating scan at 0.1 °Cmin^{-1} of carrot fibre powder and maltodextrin (DE max 9.8). The carrot fibre powder thermogram shows two glass transitions at 173.5°C and 194°C. The arrows indicate the T_g values of maltodextrin and carrot fibre.

Figure 4.63 shows the DSC thermogram of dry carrot fibre from 132-157 °C with a small endothermic transition onset at 133 °C follow by a broad endothermic transition with the onset at 138 °C. Since the sample was dried, the small endothermic peak might be the evaporation of a small amount of water in the sample similar to the endotherm of dextran which was found at around 130 °C (Aguilera *et al.*, 1998). Dextran is a branched glucan (polysaccharide) which is also found in cellulose (detail of components in fibre is in Section 2.1.2). The broad endothermic transition found might be caused by the melting of one component present in the carrot fibre. The onset of the melting endotherm was very close to the melting point of glucose which is the main sugar content in fibre. The milling

might break the glucan chains of cellulose and released some glucose. Since the fibre consists of many components there was more than one possibility of the causes of this endothermic transition. This is an interesting point that should further investigated. However, the heating scans of carrot fibre at 5 °C min^{-1} on a Perkin-Elmer DSC which was carried out later shows onset melting point at 140-145 °C for all 5 runs with one run showed an extra melting endothermic at 170 °C. The micro-picture of carrot fibre (Section 4.4) shows the particle shape of carrot fibre under a microscope with many spots appearing as semicrystalline materials under the polarise light.

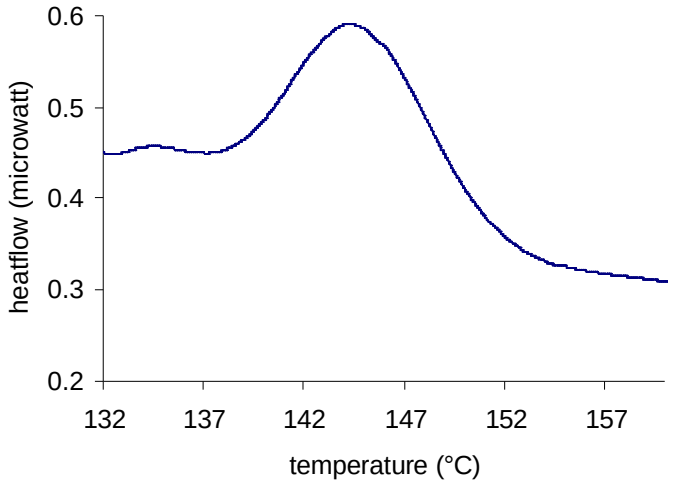

Figure 4.63 DSC heating scan of carrot fibre.

4.6.13 T_g of freeze dried fructose + carrot fibre, fructose + carrot fibre + malic acid

It was quite difficult to get a clear glass transition on the DSC thermogram of most of the samples with carrot fibre. The transition was detected as a very small transition of baseline. This experiment was repeated with 3 to 9 scans for each sample. Some of the DSC thermograms presented here are examples of different transitions that appeared. As discussed by Walstra (2003), in practice a narrow transition rather than a sharp transition point is often observed in DSC scans of food. According to Nielsen (2003) step changes in the heat capacity of a material that can be seen as a small change in baseline with no well defined peak are characteristic of glass transitions (detail in Section 2.4.2). The T_g values of samples presented later were taken from the trace transitions with a slight change of baseline appearing on the thermograms.

Figure 4.64 shows the transition from heating scan of fructose + 50% fibre + 3% malic acid with the transition from the three ampoules appearing clearly at the same temperature. Figure 4.65 shows the transitions from DSC scans of fructose + 50% carrot fibre and that of the mixture with 1, 2 and 3% malic acid.

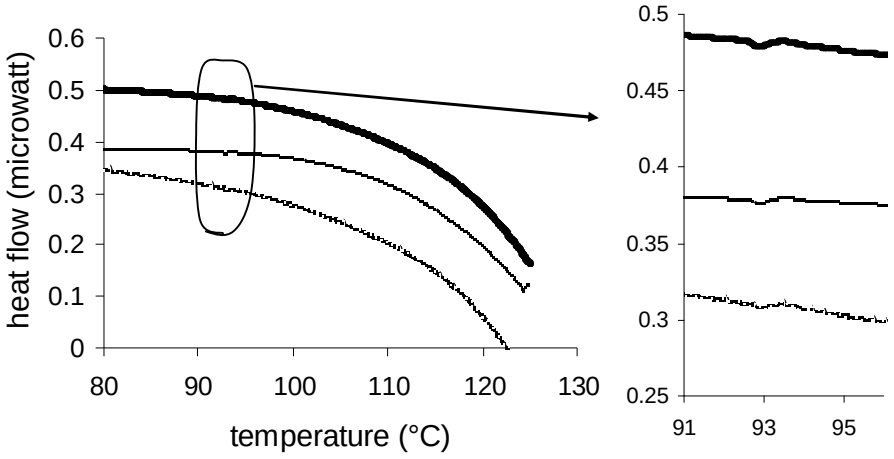

Figure 4.64 DSC scans of fructose + 50% carrot fibre + 3% malic acid with the transition appearing on scans from the three ampoules.

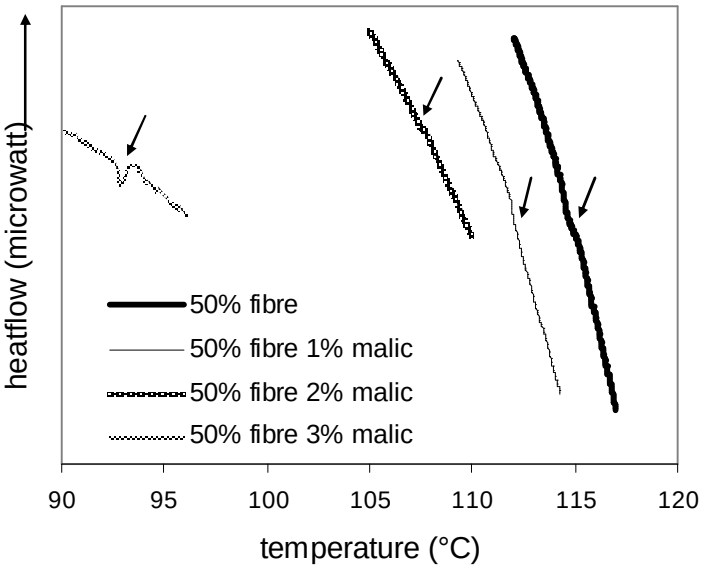

Figure 4.65 DSC scans at the transition of mixtures of fructose +50% carrot fibre and fructose + 50% carrot fibre +1 to 3% malic acid. The arrows point at the transitions.

4.6.14 Various transitions from DSC thermograms

As shown before, the DSC scans of the same sample in different ampoules sometimes showed different thermograms. Figure 4.66 exhibits a transition of the mixture of fructose

+ 60% carrot fibre + 1% malic acid from all three ampoules. The transition appeared at around 141.5 °C with the strange transition style shown in Figure 4.66 (b). This transition might have been due to oxidation or other physical changes. Researchers reported melting point of glucose at the range 135-158 °C (detail in Section 2.2.1). At this transition temperature, most of the samples were already oxidised, so the rescan could not be performed. Thus the validity of this transition is still in doubt.

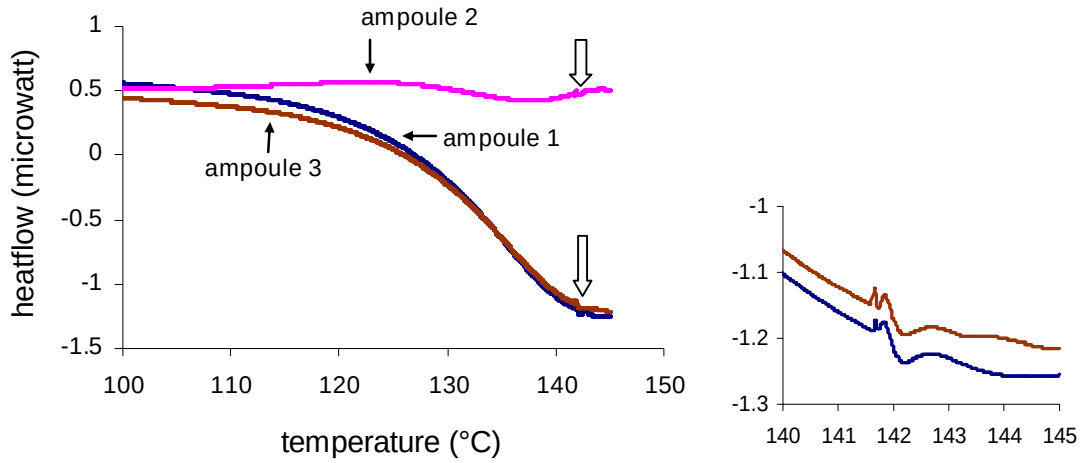

(a) (b)

Figure 4.66 DSC heating scans of fructose + 60% carrot fibre + 1% malic acid.

Figure 4.67 shows the DSC scan of fructose + 60% carrot fibre + 3% malic acid with the transition around 102-104 °C. This temperature was the same as the melting temperature of fructose by DSC method from previous studies (detail in Section 2.2.1). Two endothermic transitions appeared with the first transition being bigger than the second. The second transition immediately after the first transition seemed to either be a melting or glass transition.

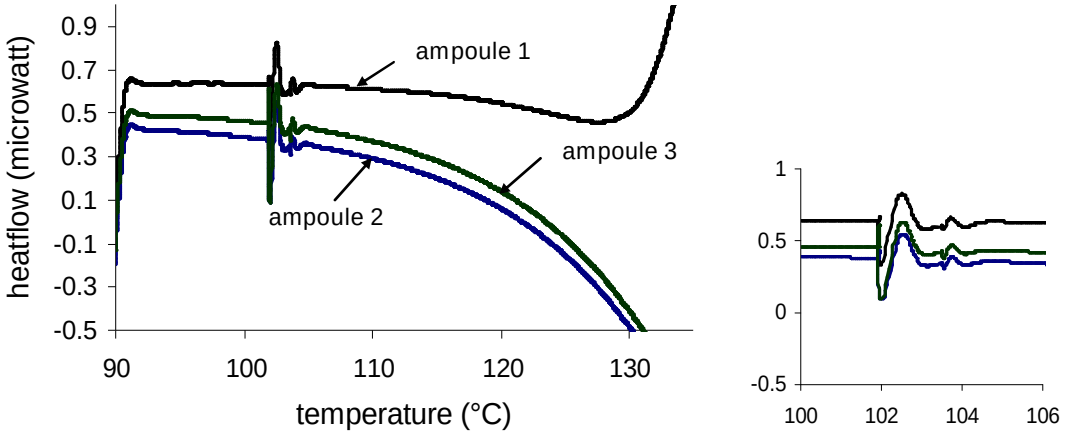

Figure 4.67 DSC scans of fructose + 60% carrot fibre + 3% malic acid.

Some of the DSC scans found melting endothermic transitions at high temperatures. The thermograms of mixtures of fructose + 70% carrot fibre showed this phenomenon clearly. Figure 4.68 shows the thermograms of fructose + 70% carrot fibre and fructose + 70% carrot fibre + 1, 2 and 3% malic acid from different runs. The arrows in the figure indicate the possible point of melting of a component in the mixture. It was obvious that the transition temperatures decrease with increasing malic acid. This confirmed the effect of acid interaction in the mixtures.

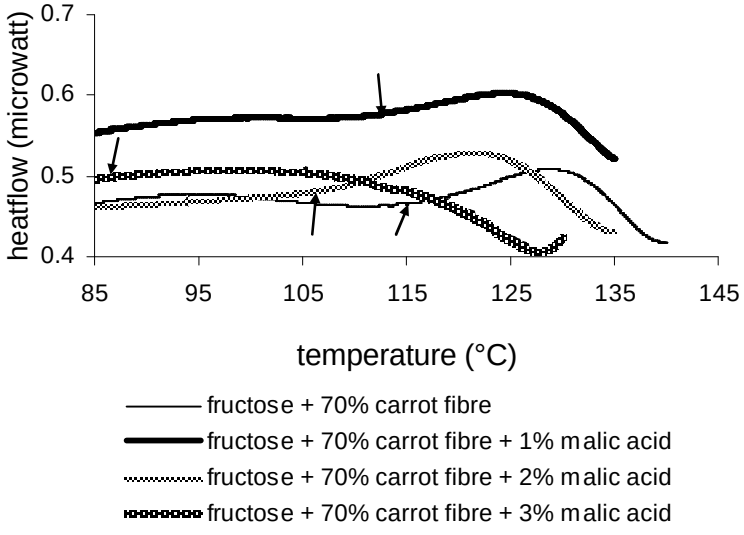

Figure 4.68 DSC scan of fructose + 70% carrot fibre and fructose + 70% carrot fibre + 1, 2 and 3% malic acid from different runs. The arrows indicate the start of melting when exposed to high temperatures.

T_g values of freeze dried mixture of fructose + carrot fibre and fructose + carrot fibre + malic acid at different ratios were found from small transitions of the base line without any clear onset, midpoint and endpoint, and these are summarised in Table 4.17. The values demonstrated that an increase of carrot fibre resulted in an increase of T_g of the mixtures. In the opposite way, an increase in fraction of malic acid decreases T_g of the mixtures.

Table 4.17 T_g of freeze dried mixture of fructose + carrot fibre and fructose + carrot fibre + malic acid at various ratios

% of fibre and malic in fructose	T_g of freeze dried powder(°C)	% of fibre and malic in fructose	T_g of freeze dried powder(°C)	% of fibre and malic in fructose	T_g of freeze dried powder(°C)
50-0	114.5	60-0	122.9	70-0	130
50-1	111.8	60-1	122.25	70-1	122
50-2	107.5	60-2	105.85	70-2	119
50-3	92.6	60-3	96.5	70-3	115

4.6.15 T_g of freeze dried fructose + maltodextrin

The DSC scans of mixtures with maltodextrin were difficult to perform due to the swelling of the mixtures with temperature as shown in Figure 4.25, Section 4.2.6. One of the DSC scans of fructose + 50% maltodextrin is shown in Figure 4.69. The thermograms from the three ampoules were quite different. The sample in ampoule 3 shows an endothermic transition of melting in a component at around 100 °C. The base line of the sample in ampoule 2 moved downward with a transition at around 120 °C. The thermogram of the sample in ampoule 1 also showed a slight endothermic transition at around 100 °C and seemed to show a glass transition at around 124 °C. Repeated scans were carried out until the transition was confirmed.

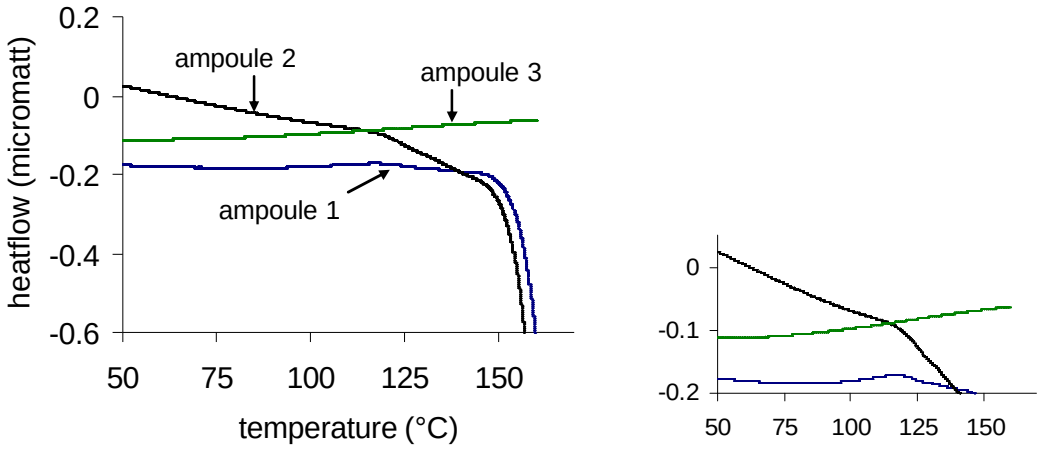

Figure 4.69 DSC scans of fructose + 50% maltodextrin.

One of the DSC scans of fructose + 60% maltodextrin is shown in Figure 4.70 (a) and (b). The sample in ampoule 1 spilled out of the ampoule and burned at around 126 °C. Before this, it seemed to have one transition around 122-125 °C. The sample in ampoule 3 also showed an endothermic transition at around 100 °C. The sample in ampoule 2 showed one transition at around 60 °C and another transition at around 104 °C.

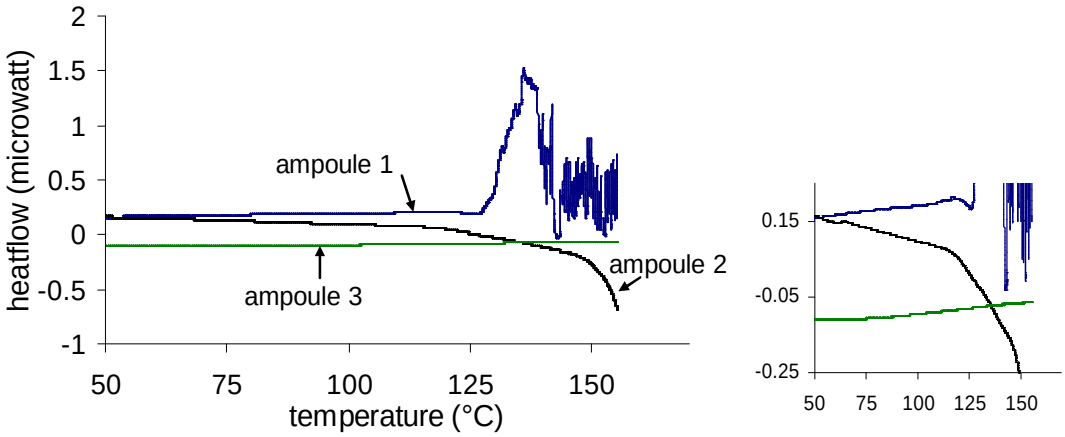

(a) (b)

Figure 4.70 DSC scans of fructose + 60% maltodextrin.

One of the DSC scans of fructose + 70% maltodextrin is in Figure 4.71. The sample in ampoule 3 showed a strange transition before the scan went as normal. The three thermograms were similar types with onset endothermic transitions at around 100 °C.

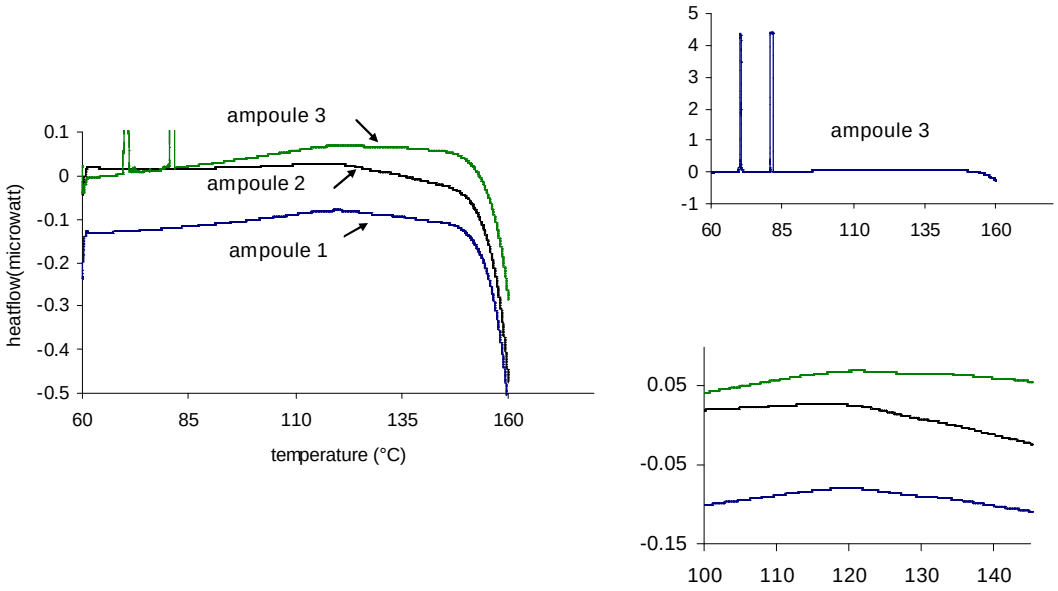

Figure 4.71 DSC scan of fructose + 70% maltodextrin.

The DSC scans of sample of fructose + maltodextrin + malic acid were inconclusive. The samples often swelled and spilled out of the ampoules. This might have led to damage of the equipment. Figure 4.72 shows the scans of a sample when two of the ampoules spilled out and burned.

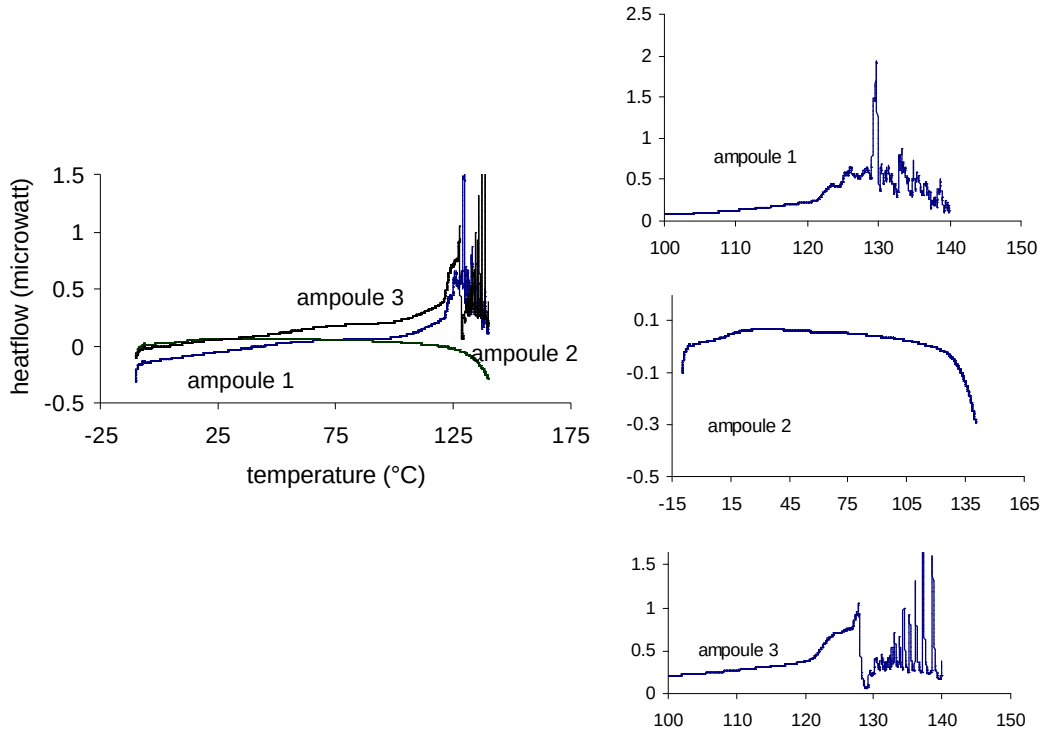

Figure 4.72 DSC heating scan of fructose + 50% maltodextrin + 3% malic acid.

Figure 4.73 shows the burning of a mixture of fructose + maltodextrin + malic acid that was in the DSC ampoule's holder (ampoule 3). This was very difficult to clean and took a very long time. The cleaning needed to be very delicate so as to not disturb the underneath part of the ampoule's holder. Figure 4.74 shows acceptable DSC performance after cleaning up all burnt material stuck in the ampoule's holder.

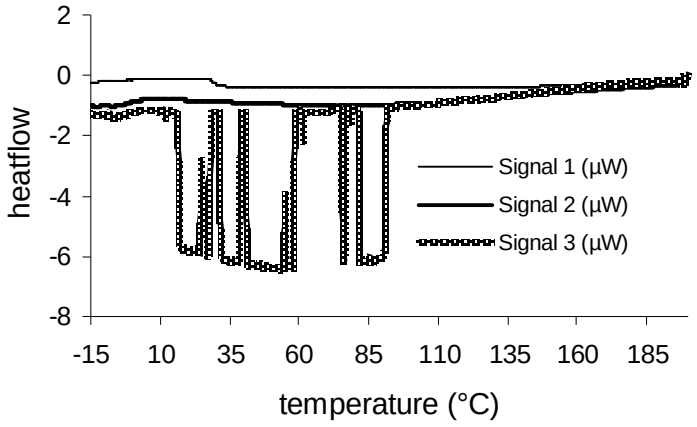

Figure 4.73 DSC scans of empty ampoules after cleaning the burnt ampoules but there was some material stuck in the ampoule's holder.

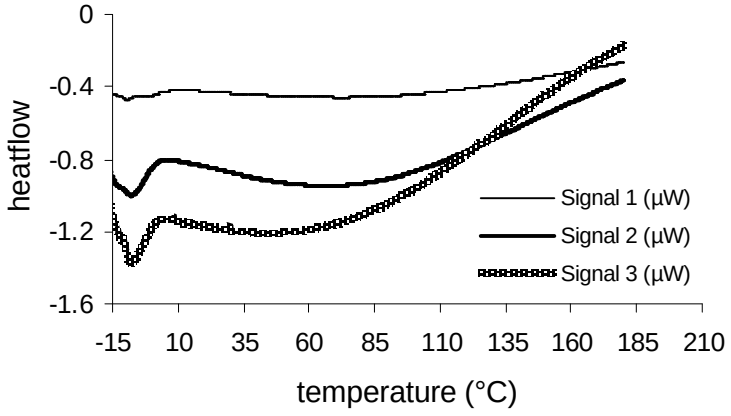

Figure 4.74 DSC scans of empty ampoule after cleaning off the burning of mixture of fructose +maltodextrin +malic acid from the ampoule's holder.

As said before, the T_g values of mixtures with fibre and maltodextrin were taken from the small change in the base line on the DSC thermograms. Some of the T_g values shown in this study might not represent the true T_g values of mixtures but only be noise that appeared in the DSC which has caused a slight change in the baseline. On the other hand it is also possible that the components present in the sample such as crystals might

decrease the transition of the samples. The glass transition is a transition found in amorphous materials. If the samples have less amorphous material, this should also affect the appearance of the glass transition on the thermogram. In this experiment it was found that there was a lot of semicrystalline material in the mixtures with carrot fibre and some semicrystalline material in the mixtures with maltodextrin. This might also have caused the very small transition on the thermograms. The summary of T_g values of fructose + maltodextrin is in Table 4.18.

Table 4.18 T_g of freeze dried fructose + maltodextrin at 50, 60 and 70% dried w/w

% maltodextrin in fructose	T_g of freeze dried powder (°C)
50	119
60	124
70	135

4.6.16 DSC performance of spray dried fructose + carrot fibre and apple juice + carrot fibre

The spray dried powders of the mixtures of fructose + carrot fibre and apple juice + carrot fibre were analysed in the DSC immediately after spray drying or after storage.

A clear transition of spray dried fructose + 50% carrot fibre (moisture content around 2%) was found from the 2 °C min^{-1} scan rate as shown in Figure 4.75. The transition was quite small but it was a clear change in the base line. However, this transition was found from the 2 °C min^{-1} scan rate but not in the scan rate at 0.1 °C min^{-1}. This value was not used in the analysis with the other mixtures. However, this transition was much higher than the T_g of normal amorphous fructose. It was likely to be a glass transition of the carrot fibre which had not previously been observed, or a new transition resulting from interaction between fructose and fibre.

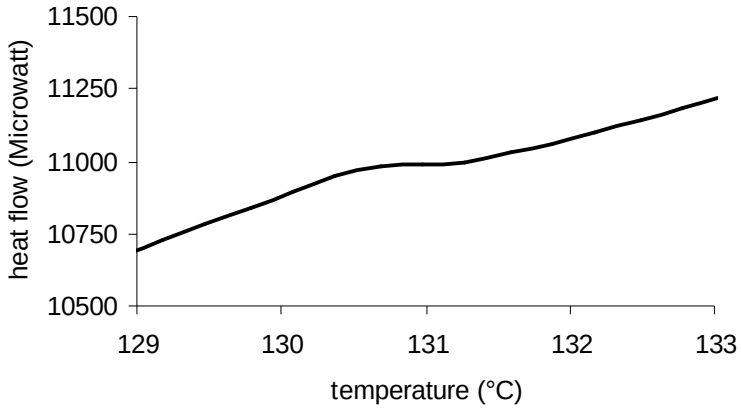

Figure 4.75 DSC scan at 2 °C min^{-1} of spray dried fructose + 50% carrot fibre.

Figure 4.76 shows DSC scan at 0.1 °Cmin^{-1} of dry spray dried powder of fructose + carrot fibre. The thermogram shows a sharply endothermic transition after 130 °C which was probably from the melting of some crystalline material in the sample. A small transition was found at around 146 °C.

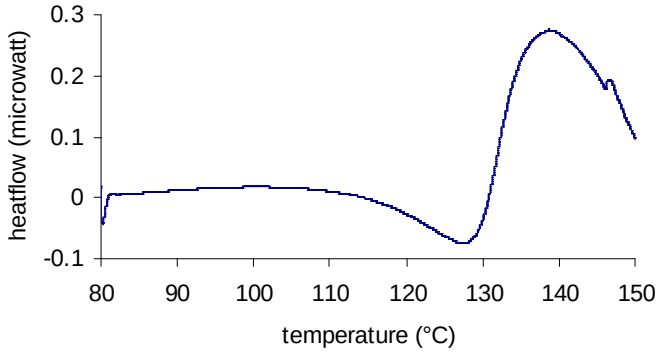

Figure 4.76 DSC scan of spray dried fructose + 50% carrot fibre.

Figure 4.77 shows the transitions of dry apple juice + 30% carrot fibre and apple juice + 50% carrot fibre with endothermic transitions of different amplitude. The bigger endothermic transition from the mixture with 50% fibre shows the higher amount of crystalline material in this sample than that in the sample with 30% fibre. It is obvious that from the same scan of the sample with 40% carrot fibre doesn't show the endothermic transition but oxidation. All the samples in three ampoules after heating scans showed oxidation (see Figure 4.36) but it was strange that the thermograms did not

really present these oxidation from every run. However, the heterogeneity of the samples might be one of the possible causes for this.

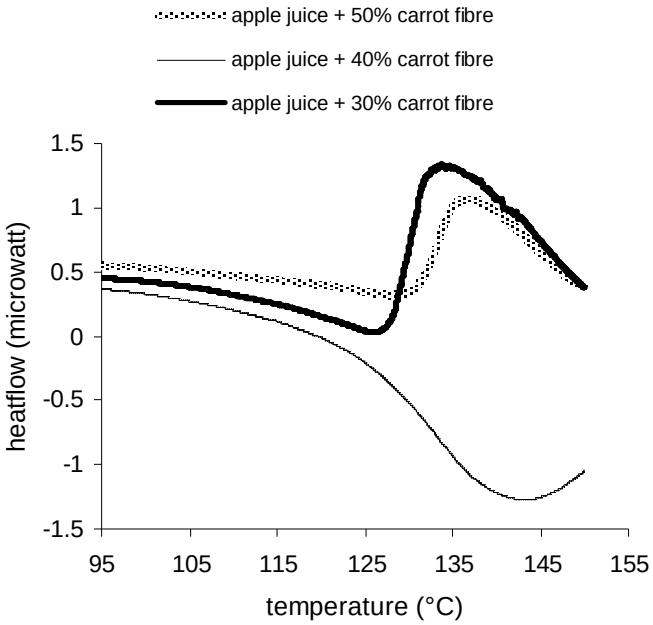

Figure 4.77 DSC scans of dry spray dried powder of apple juice + carrot fibre at different ratios.

Figure 4.78 shows the DSC thermograms of dry spray dried apple juice + carrot fibre at 40, 50 and 60% w/w. The samples were annealed at 130 °C for 40 minutes and scanned from 130 to 170 °C. The sample with 50% carrot fibre again found the endothermic transition above 130 °C while the samples with 40 and 60% fibre only show the oxidation transition.

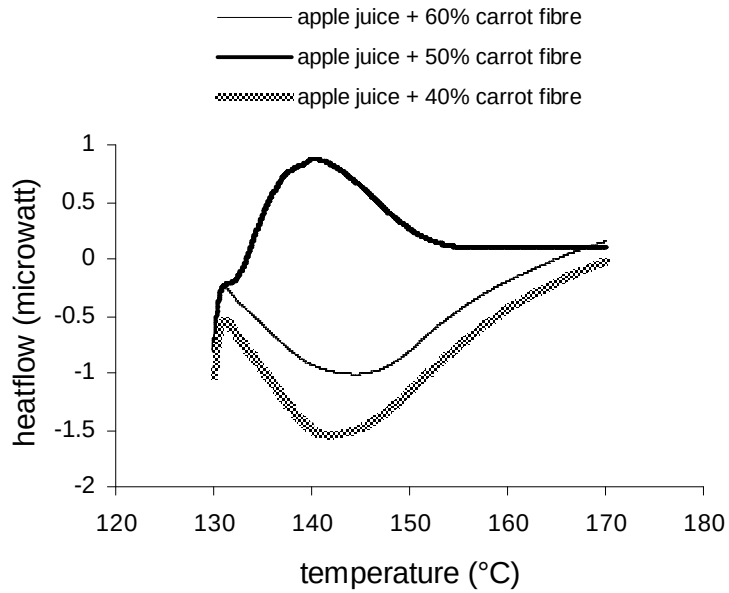

Figure 4.78 DSC scan of dry spray dried apple juice + carrot fibre at different ratios.

Figure 4.79 shows the thermograms of dried spray dried apple juice + carrot fibre at 50, 60 and 70% w/w. All the thermograms show no endothermic transitions but oxidation. The sample with 50% fibre showed a large endothermic transition in the previous figures but none from this scan.

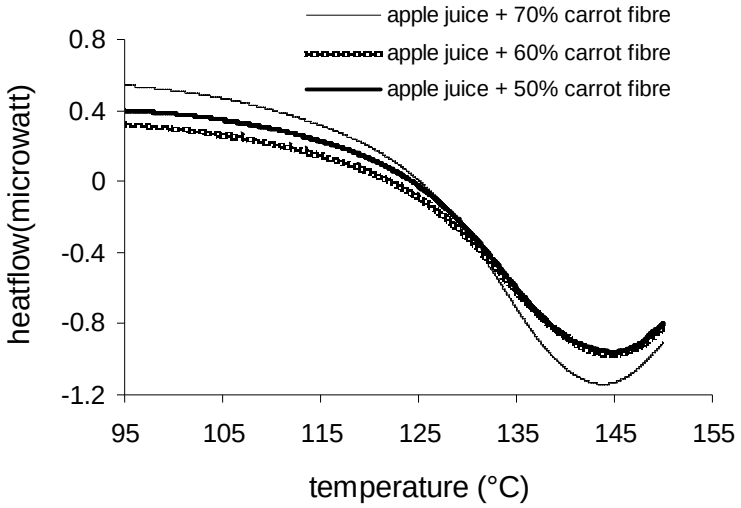

Figure 4.79 DSC scan of dry spray dried powder of apple juice + carrot fibre at different ratios.

4.7 Spray drying experiments

4.7.1 Spray drying trials

Before spray drying fructose + carrot fibre and apple juice + carrot fibre, carrot juice at different total solid contents was spray dried with different drying conditions. The carrot juice sample of 10 and 15% total solid content was spray dried first. It was found that there was no free flowing powder from these samples. The powder appeared as a syrup coating the chamber wall and collection jar. The carrot juice at 50% total solids content was spray dried, and the powder stuck in the drier chamber especially at the atomizer ring. The powder contained a high moisture content. Spray drying a 40% total solids carrot juice gave a good result with free flowing powder and sweepable powder from the chamber walls. Most of the powder stuck to the drier chamber wall. The swept powder was not sticky and had a bright colour. The powder was kept in a plastic bottle and a little agglomeration was observed after a couple of months. The colour changed from bright orange to yellowish in a couple of weeks.

The inlet/outlet air temperatures at 165/75 °C were found to be satisfactory to spray dry carrot juice with added carrot fibre. These temperatures were used to successfully spray dry mixtures of fructose + carrot fibre and apple juice + carrot fibre. The mixtures of fructose + maltodextrin were not successfully dried using these temperatures. The product coated the dryer chamber as a syrup. The product did not dry before contacting the chamber wall and cyclone collection system. The same results were found when 50%, 60% and 70% maltodextrin in fructose were spray dried at 165/75 °C. Increasing the temperature of the spray drier enabled the production of a free flowing powder. The trials found 175/85 °C were the best temperatures to spray dry the mixtures of fructose + maltodextrin.

4.7.2 Spray drying of fructose + carrot fibre and fructose + maltodextrin

Spray drying of fructose + carrot fibre mixtures produced free flowing powder which was mostly deposited as friable sweepable agglomerate on the drier wall. After cooling down to room temperature, it was very easy to sweep the powder from the drier surface. The swept powder had a moisture content of around 2-4% (wet basis) for all mixtures. Figure 4.80 shows powder stuck on chamber wall (a) and roof above the atomizer (b). The clear area on top of the atomizer shows where the powder had been swept from the surface. The powder was hygroscopic and needed to be swept out of the drier immediately after cooling down. The powder left in the dryer for a longer time was more difficult to sweep from the surface. This phenomenon demonstrated stickiness of the powder which resulted from absorption moisture from the ambient air. Figure 4.81 shows spray dried powder of fructose + carrot fibre.

(a) (b)

Figure 4.80 The sweepable powder of spray dried fructose + carrot fibre(a) on the chamber wall and (b) on top of atomizer.

Figure 4.81 Spray dried powder of fructose + carrot fibre.

Spray drying of fructose + maltodextrin produced a little free flowing powder but most was deposited on the drier wall. Some of it appeared to redissolve and form a film on the drier wall but some could be manually swept from the wall with moderate effort. The dissolution of powder was clearer on top of the atomizer. Figure 4.82 (a) and (b) shows powder on the chamber wall and on top of atomizer. The amount of swept powder from all runs of fructose + maltodextrin appeared as shown in Figure 4.83 (b). Figure 4.83 (a) shows the collection bottle of spray dried fructose + maltodextrin before the swept powder was collected. The powder became very sticky after a few minutes exposure to ambient air.

(a) (b)

Figure 4.82 Spray dried powder of fructose + maltodextrin (a) on the chamber wall and (b) on top of atomizer.

(a) (b)

Figure 4.83 The powder of fructose + maltodextrin coated in the collection bottle (a) and the swept powder after the drier cooled to room temperature.

The yield and moisture content of the spray dried powder of fructose + carrot fibre and fructose + maltodextrin at various ratios are in Table 4.20. The minimum fraction of carrot fibre that could facilitate the spray drying was lower than that of maltodextrin. By adding 40% (dry basis) of carrot fibre to fructose solution a yield of around 50% was obtained. Increasing the ratio of carrot fibre to fructose increased the yield. Spray drying of fructose + maltodextrin was not successful when the ratio of maltodextrin in fructose less than 50% dry weight. The mixture of 40% maltodextrin in fructose was sticky in the drier chamber and was not recovered as powder. Fructose + 50% maltodextrin gave a

very low yield (approximately 13%). Increasing maltodextrin ratios in fructose increased the yield. However, the average yield of spray dried fructose + carrot fibre was approximately three times higher than that of fructose + maltodextrin.

Table 4.20 The yield and moisture content of spray dried fructose + carrot fibre and fructose + maltodextrin at different ratios

Carrot fibre: fructose ratio (dry basis)	Moisture content (% wb) ±SD	Yield (%)±SD	Maltodextrin: fructose ratio (dry basis)	Moisture content (% wb) ±SD	Yield (%)±SD
40:60	2.56±0.52	51.5±0.8	40:60	-	-
50:50	2.23±0.10	63.1±0.6	50:50	1.25±0.85	12.9±2.8
60:40	3.05±1.37	65.7±0.7	60:40	1.18±1.1	19.7±3.2
70:30	3.51±0.60	68.0±0.5	70:30	3.42±1.50	27.0±3.1

4.7.3 Particles of spray dried fructose + carrot fibre and fructose + maltodextrin

The particles produced from spray dried fructose + carrot fibre and fructose + maltodextrin were quite different. Figure 4.84 shows that the fructose +carrot fibre powder was irregular and semicrystalline. The powder under polarised light showed many semicrystalline particles dispersed in the powder. The light spots in the pictures are the evidence of semicrystalline particles. The maltodextrin + fructose powder was smoother and possibly more amorphous. The size of particle was much bigger than the particle of spray dried fructose + carrot fibre which was noticeable by eye. This might because of the swelling of the mixtures when exposed to high temperature in the spray drying. Their appearance supports the observation that the carrot fibre based powder was more easily recovered. The DSC scans of fructose + carrot fibre showed melting transitions with only a slight glass transition region. The spray dried powder of fructose + carrot fibre had shown a better quality which was supported by the microstructure and the DSC results when compared to the mixtures with maltodextrin.

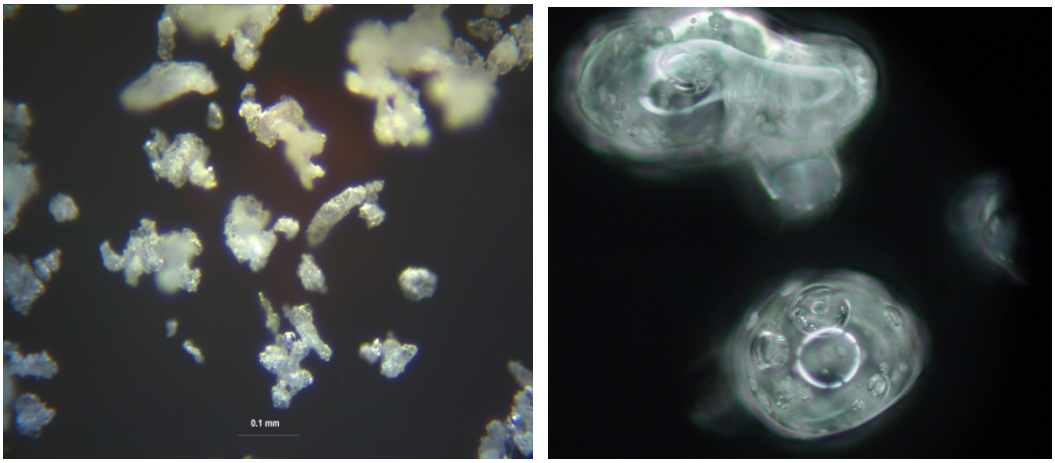

Figure 4.84 Dried powders from spray drying of fructose + carrot fibre (left) and maltodextrin + fructose (right). The white ring appeared in fructose + maltodextrin is the reflection of light from the microscope.

4.7.4 Spray drying of apple juice concentrate + carrot fibre and apple juice + maltodextrin

Spray drying of apple juice + carrot fibre produced powder most of which stuck in the drier. Figure 4.85 shows the powder stuck in the drier chamber but most of the powder was able to be swept out (swept and unswept areas are shown). The powder was hard to sweep out at the ring of atomization (the left upper corner of the picture) which was the shortest distance area from atomizer.

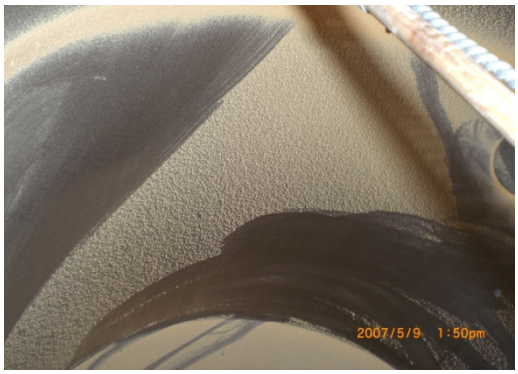

Figure 4.85 The spray dried powder of apple juice + carrot fibre in the drier chamber

Spray drying of apple juice + maltodextrin produced a little free flowing powder and appeared similar to spray drying of fructose + maltodextrin. Figure 4.86 (a) and (b)

clearly shows the different performance of the fibre and maltodextrin product on the chamber roof on top of the atomizer.

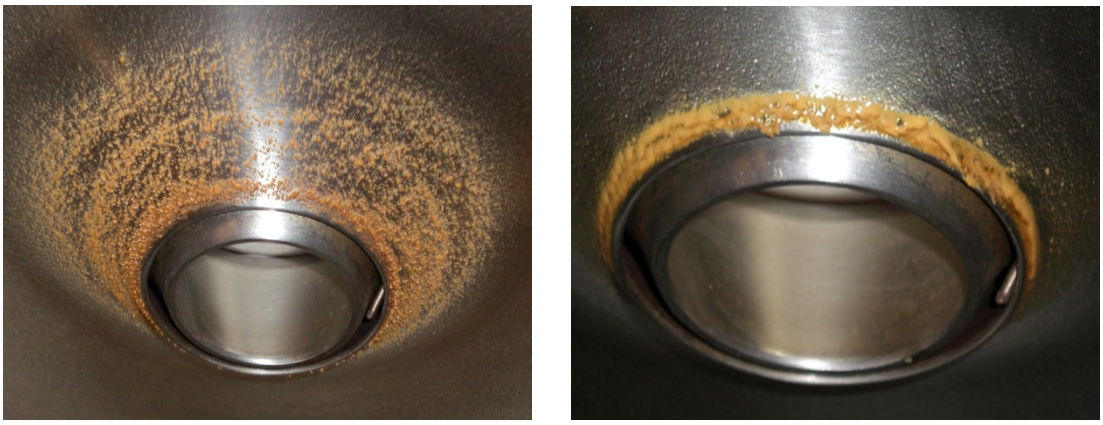

(a) (b)

Figure 4.86 Spray drying of (a) apple juice + carrot fibre and (b) spray drying of apple juice + maltodextrin on top of the atomizer.

The moisture content of free flowing spray dried powder of all apple juice mixtures was found to be approximately 1-5% (wet basis). Values of T_g from the DSC of spray dried powders of apple juice + carrot fibre are shown in Table 4.21. It appeared that the T_g values of powders from mixtures with maltodextrin (Table 4.22) from the spray drier were much higher than that of the mixtures with carrot fibre. The powders from mixtures with fibre were less sticky and less hygroscopic than the powder of mixtures with maltodextrin. Figure 4.87 shows the relationship of yield and DSC T_g values of powders for both types of apple juice mixtures. The yield of swept powders was higher for the carrot fibre + apple juice mixture (approx. 59%) than for maltodextrin + apple juice (approx. 17%). Even though the T_g values of powder from mixtures with maltodextrin were higher, the yield was approximately one third of that from the mixtures with carrot fibre. Given that the product made with carrot fibre had lower T_g than that with maltodextrin, it seems that $T–T_g$ alone is not a good indicator of stickiness as suggested by Roos and Karel (1991).

Table 4.21 DSC T_g values, yield and moisture content of spray dried powder of apple juice concentrate + carrot fibre at different ratios.

Fibre in apple juice concentrate (% dry basis)	Average yield of powders (%) ±SD	Moisture content of powders ex drier (% wet basis) ±SD	T_g of powders ex drier (°C)	T_g of dry powders (°C)
20	Not applicable		-	-
30	37.9±0.5	1.4±0.4	83	128
40	50.7±0.8	0.2±0.2	85.3	143
50	64.2±0.9	1.2±0.2	92.6	145
60	69.7±0.4	1.9±0.5	87.0	158
70	69.9±0.5	4.9±0.7	92.5	168.5

Table 4.22 DSC T_g values, yield and moisture content of spray dried apple juice concentrate + maltodextrin at different ratio

Maltodextrin in apple juice concentrate (% dry basis)	Average of yield (%)±SD	Moisture content of powder ex drier (% wet basis)±SD	T_g of the powder ex the drier (°C)
50	8.7±2.0	1.7±1.2	114.2
60	18.2±1.5	2.7±0.7	124.9
70	23.8±3.2	4.0±3.3	122.2

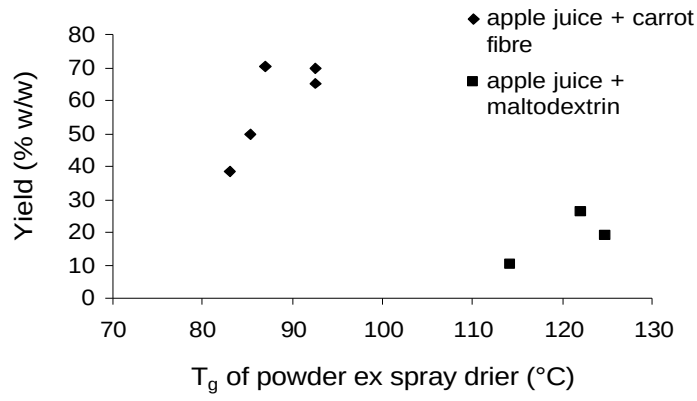

Figure 4.87 The powder yield from spray drying of apple juice + carrot fibre and apple juice + maltodextrin at different ratio versus T_g of the spray dried powders.

4.7.5 Gordon-Taylor equation of spray dried apple juice concentrate + carrot fibre and freeze dried fructose + carrot fibre

Using the results of dry samples from freeze dried carrot fibre + fructose at different ratios and spray dried carrot fibre + apple juice, the Gordon-Taylor equation was fitted (using mass fractions). The results are shown in Figure 4.88. It was found that the value of *k* for spray drying samples (k = 0.18) was much less than that of freeze dried samples (1.29). From these two k values, the Gordon-Taylor equation can be used to predict T_g of dry carrot fibre (176.6 °C) and dry apple juice (18.6 °C). It was reasonable that the T_g of dried apple juice predicted by Gordon-Taylor is approximately 18.6 °C because the DSC T_g of dry melted sugar mixture of fructose: glucose: sucrose at ratio 3: 1: 1 found at the range of 14-22 °C (the apple juice concentrate used in this experiment had the ratio of fructose: glucose: sucrose at around 3:1:1). Even though acids in the juice might be able to reduce T_g values of the dried apple juice, other components in juice such as polysaccharide, pectin, protein, minerals and ash (Lukanin et al., 2003) can increase the T_g of the juice.

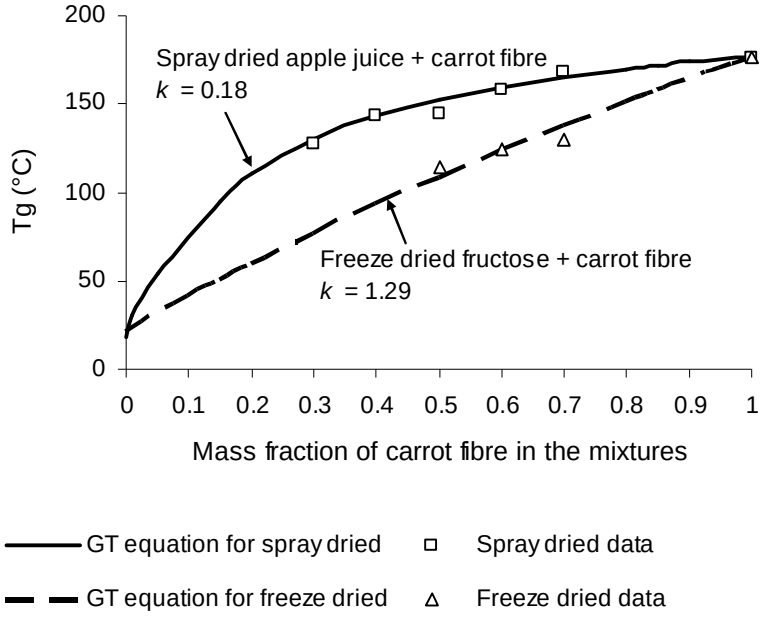

Figure 4.88 Gordon-Taylor plot of T_g of dry powder from spray dried apple juice concentrate + carrot fibre and dry freeze dried fructose + carrot fibre.

4.7.6 Particle of spray dried apple juice + carrot fibre and apple juice + maltodextrin

The particles produced with apple juice mixtures had similarities to, but difference from the corresponding powders from mixtures with fructose. Figure 4.89 (a) shows that the apple juice + carrot fibre powder was more irregular and semicrystalline. The particles

under polarised light showed many semicrystal particles dispersed in the powders. The particles were more transparent than that of fructose mixtures with some orange coloured particles. This is due to the combination of transparent and massive orange coloured part of carrot fibre as shown in Figure 4.28 (Section 4.4). The microstructure of these particles from a scanning electron microscope (SEM) is shown in Figure 4.90. The SEM picture show most of the particle are semicrystals. This supports the DSC scans with the broad melting endothermic transition of dry apple juice + carrot fibre. This might be the reason for the very small DSC glass transition found for these powders. According to Sperling (2006) the glass transition of semicrystalline materials sometimes was hidden. The only portion of the materials that will show a glass transition is the amorphous. Since the spray dried powder of apple juice + carrot fibre shows more semicrystalline form than amorphous form, it is reasonable that the glass transition found from DSC scan was small. There might be some other interactions of components in the powder which affected the appearance of DSC glass transition of the powder. This will be discussed more in the discussion section.

The apple juice + maltodextrin powders were smoother and more amorphous than the fibre based powders. The particles of spray dried apple juice + maltodextrin were round and much bigger than the size of apple juice + carrot fibre particles. This appearance was due to the swelling of maltodextrin during drying as shown in Figure 4.25 (Section 4.2.6).

The appearance of spray dried apple juice + carrot fibre and apple juice + maltodextrin again supports the observation that the carrot based powder was more easily recovered. Given that the product made with carrot fibre had a lower T_g than that with maltodextrin, this cannot confirm that $T–T_g$ alone is a good indicator of stickiness as suggested by Roos and Karel (1991).

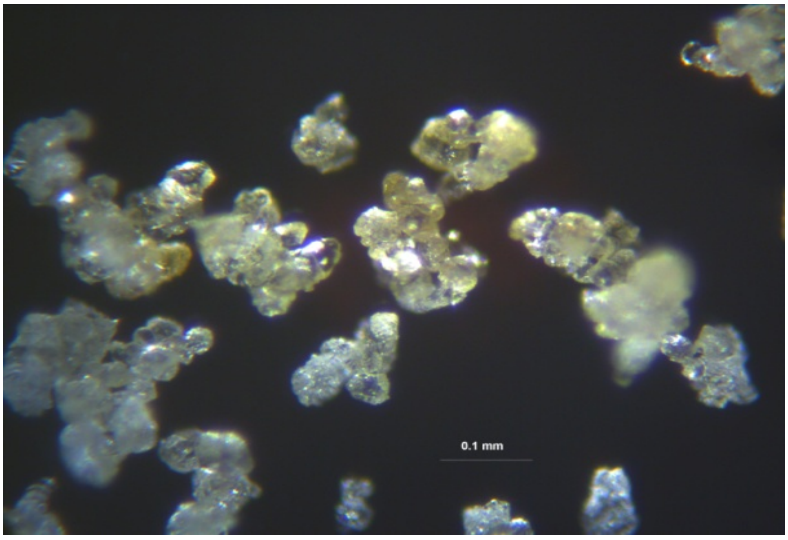

(a)

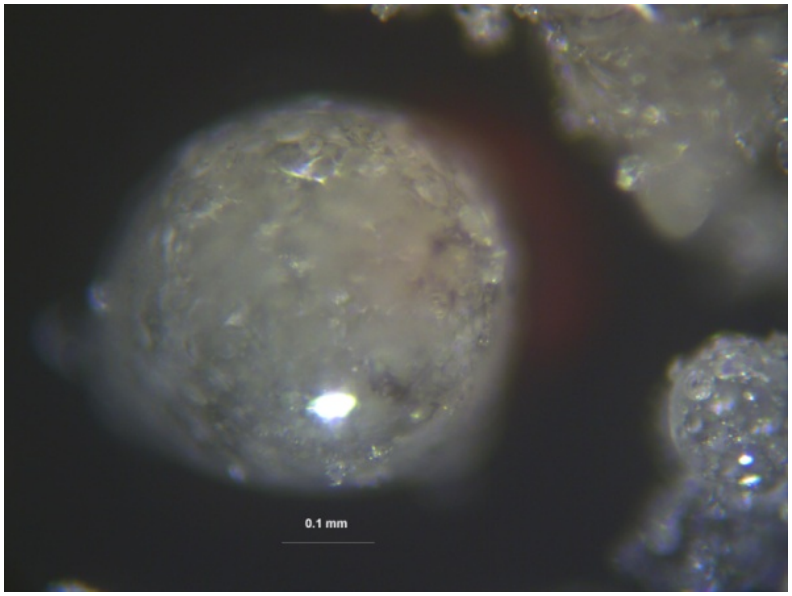

(b)

Figure 4.89 The particle from (a) spray dried apple juice + 70% carrot fibre and (b) spray dried of apple juice +maltodextrin.

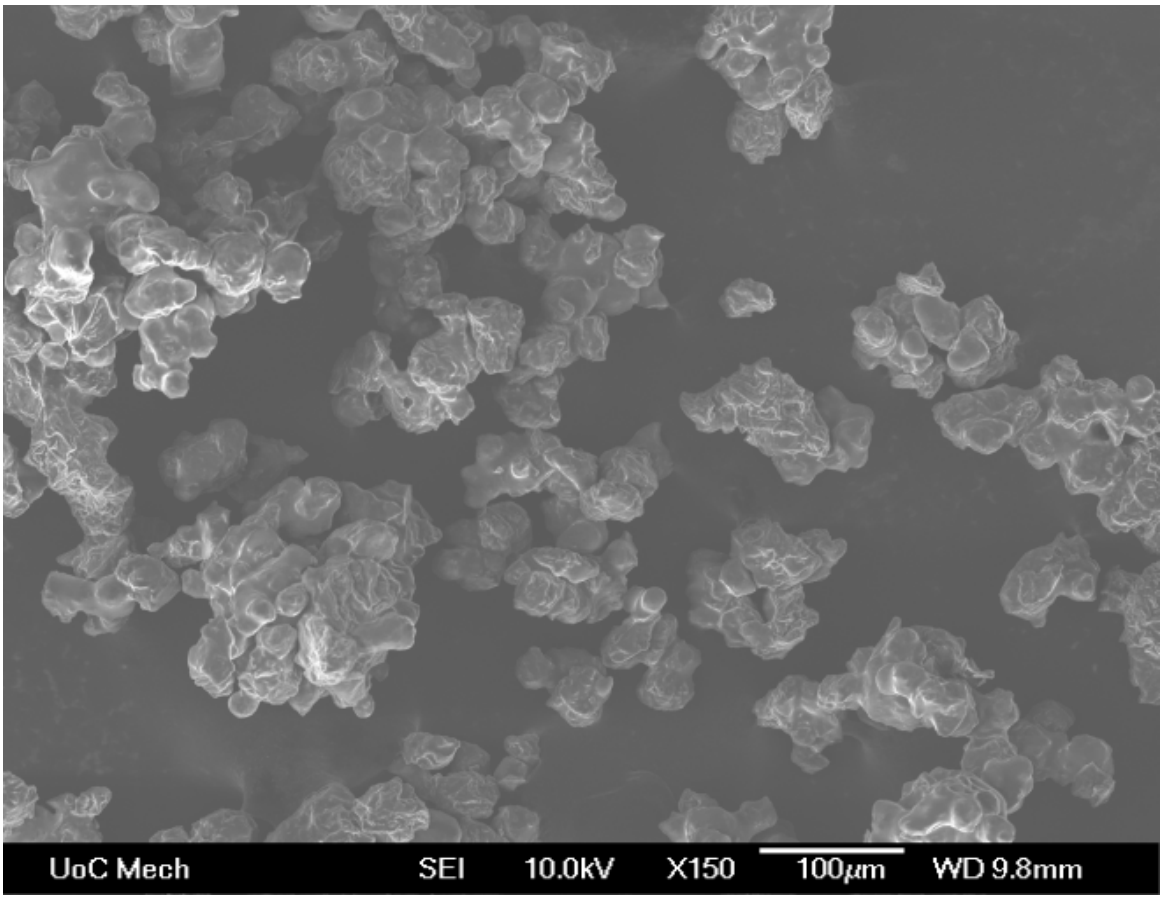

Figure 4.90 SEM of spray dried apple juice + 70% carrot fibre.

4.7.7 Hygroscopicity of powder from apple juice concentrate + carrot fibre and apple juice concentrate + maltodextrin

Figure 4.91 shows the powder of apple juice + carrot fibre and apple juice + maltodextrin after air exposure for 10 minutes (23 °C, RH 65%). The powder with maltodextrin was very sticky and caking while that with carrot fibre was a little bit sticky on the surface. This indicated the possibility of packing the carrot fibre based juice powder in normal environment but with limited moisture exposure.

(a) (b)

Figure 4.91 Hygroscopicity after 10 minutes air exposure of (a) apple juice + maltodextrin and (b) apple juice + carrot fibre.

4.7.8 Spray drying of mixture of carrot fibre + maltodextrin in apple juice

It was shown that 30% of fibre in apple juice was enough to be a spray drying carrier. This experiment was performed to investigate the possibility and effectiveness of maltodextrin as a drying additive in fruit juice with high content of fibre.

The experiment was base on the minimum amount (from this study) of carrot fibre and maltodextrin that could be used as a carrier. A combination of carrot fibre and maltodextrin was added to apple juice at different fractions and spray dried. It was found that the combination of maltodextrin and carrot fibre in apple juice did not increase the yield of products from spray drying. Adding maltodextrin to the mixture of apple juice + 30% carrot fibre and adding carrot fibre in the mixture of apple juice + 50% maltodextrin did not increase the yield in either case. The results are shown in Table 4.23. The juices that contained higher portions of fibre (10 to 20%) produced lower yields when added with 50% maltodextrin. There was no significant increase in yield when maltodextrin was added (Table 4.23). These results seemed to confirm that maltodextrin might not be the best spray drying carrier of fruit juice.

Table.4.23 Yield and moisture content of spray dried apple juice concentrate + maltodextrin +carrot fibre at different ratio

Percentage of maltodextrin + carrot fibre in apple juice (dry weight basis)	Yield from spray drying (% weight)	Moisture content of powders ex drier (% wb) ±SD
50 + 0	8.66	1.7±1.2
50 + 10	8.93	3.6±1.7
50 + 15	7.84	4.1±1.5
50 + 20	4.61	3.6±1.1
0 + 30	37.9	1.4±2.6
10 + 30	37.14	0.4±0.7
12.5 + 30	35.62	0.5±0.2
15 + 30	40.15	1.4±0.4
17.5 + 30	39.00	0.5±0.4
20 + 30	32.45	1.8±1.0

4.7.9 Particle of spray dried apple juice + carrot fibre + maltodextrin

The particles of apple juice + 50% maltodetrin + 12.5% carrot fibre are shown in Figure 4.92. The particles appear to be a combination of particles of apple juice + fibre and apple juice + maltodextrin. The fraction of semicrystalline particles of apple juice + carrot fibre dispersed in the amorphous particle of apple juice + maltodextrin should decrease the stickiness of the product and increase the yield. The result of a lower yield after adding the carrot fibre raised doubts that the spray drying temperatures (185/75) were suitable for this mixture. The interaction between maltodextrin and fibre is also something to investigate to understand the process.

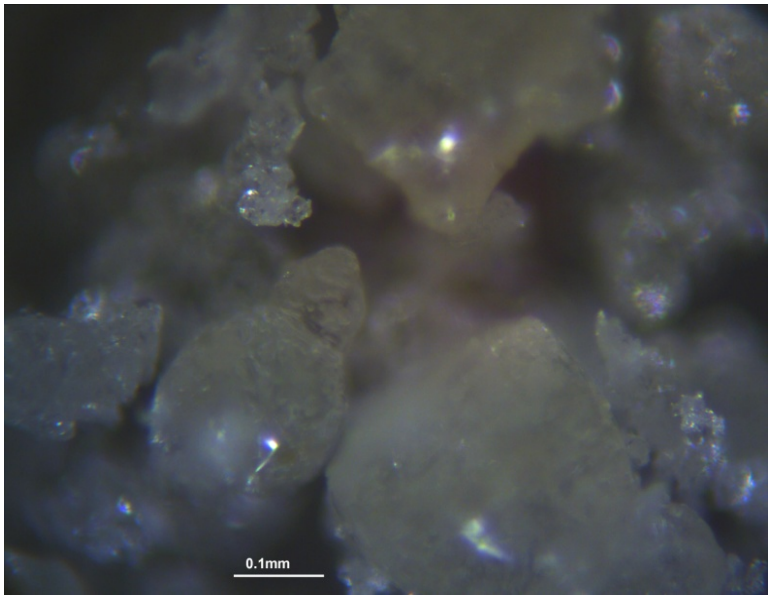

Figure 4.92 The particles of spray dried apple juice + 50% maltodextrin +12.5% carrot fibre.

The particles of spray dried apple juice + 30% carrot fibre + 10% maltodextrin are shown in Figure 4.93. The little amount of maltodextrin moderately modified the appearance of the particles. It was unlikely that the spray drying temperatures of 175/65 °C were suitable for this mixture. However, this result confirmed that using both maltodextrin and carrot fibre as carrier was not better than the fibre alone. Thus fibre alone is the best carrier for fruit juice spray drying.

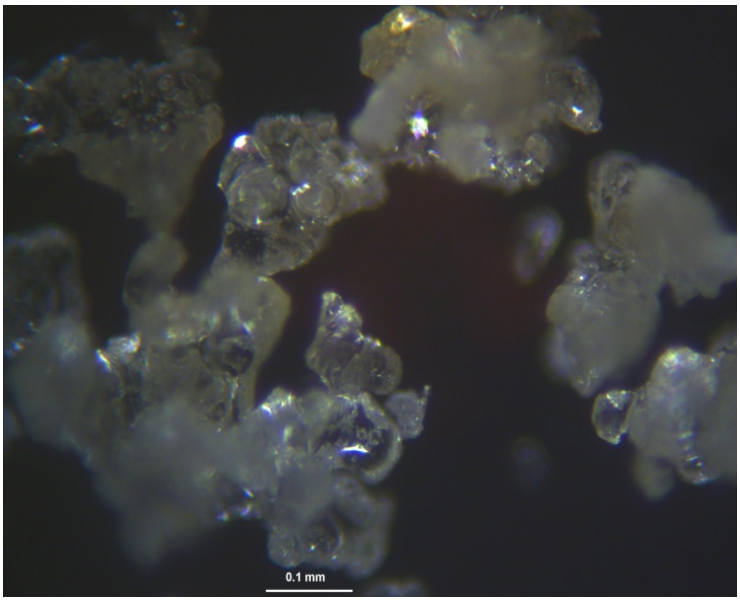

Figure 4.93 The particles of spray dried apple juice + 30% carrot fibre + 10% maltodextrin.

4.7.10 Reconstitution of powder from apple juice concentrate + carrot fibre and apple juice concentrate + maltodextrin

The product made during this work was reconstituted without difficulty though the carrot fibre noticeably started settling out after a few minutes but was not completely settled after 12 hours. Figure 4.94 shows the reconstituted apple juice powder with maltodextrin and carrot fibre. There was very little odour or flavour from the carrot fibre in the reconstituted juice. It is very likely that, with appropriate storage conditions, a fruit juice made in this way would be acceptable. It is possible, in a commercial situation, to extract the carrot fibre by filtration or settling after the juice has been reconstituted, thus producing a fruit juice with very little non-fruit component.

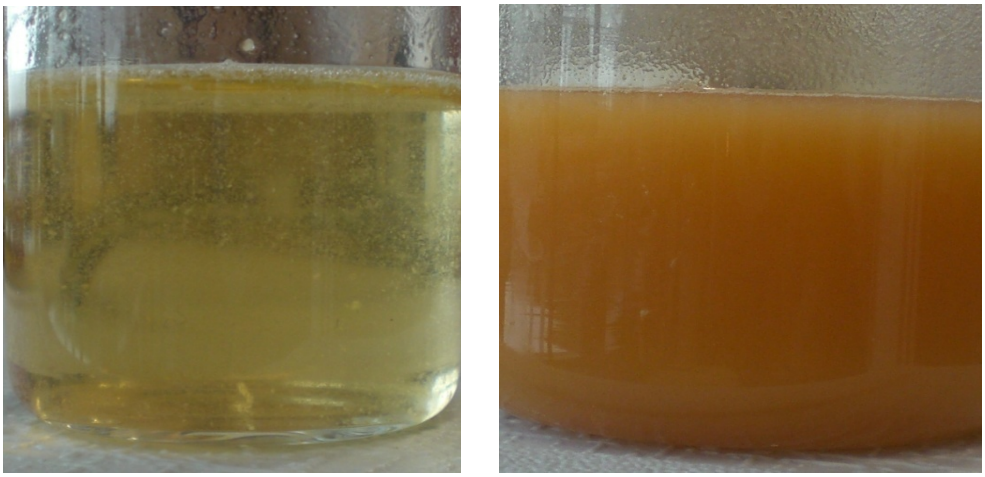

(a) (b)

Figure 4.94 Reconstitute of (a) apple juice concentrate + maltodextrin and (b) apple juice concentrate + carrot fibre.

4.8 DEA experiments

The capacitance measurement of freeze dried fructose at 500 Hz at 10-80 °C is shown in Figure 4.95. It was stable before 40 °C then increased with temperature.

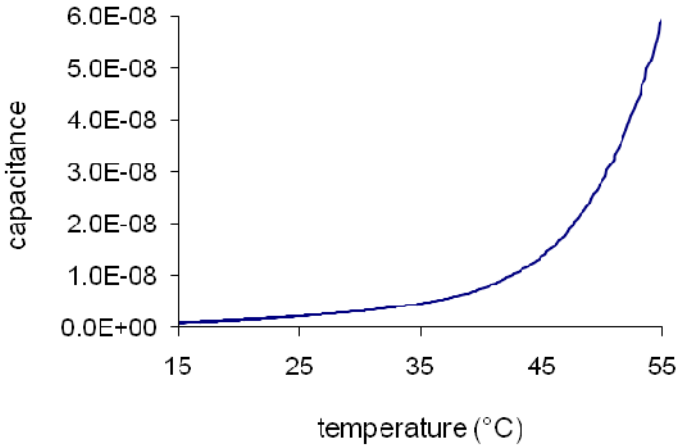

Figure 4.95 The capacitance measurement of freeze dried fructose at 500 Hz.

The derivative of capacitance over temperature range of this measurement before smoothing is shown in Figure 4.96. The derivative of capacitance over temperature range of this measurement after smoothing gave a peak of derivative as shown in Figure 4.97.

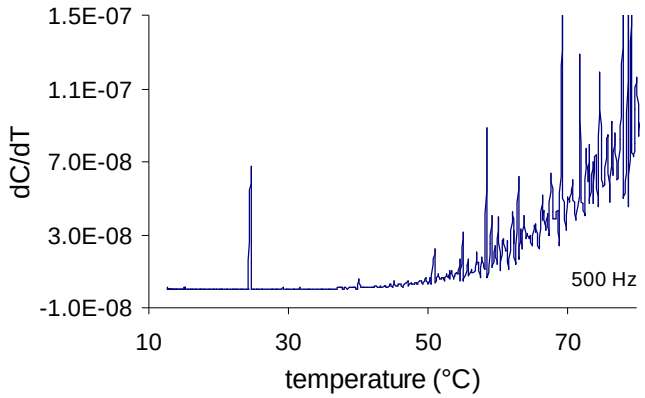

Figure 4.96 Derivatives of capacitance at 500 Hz against temperature for freeze dried amorphous solid fructose without grease or data smoothing.

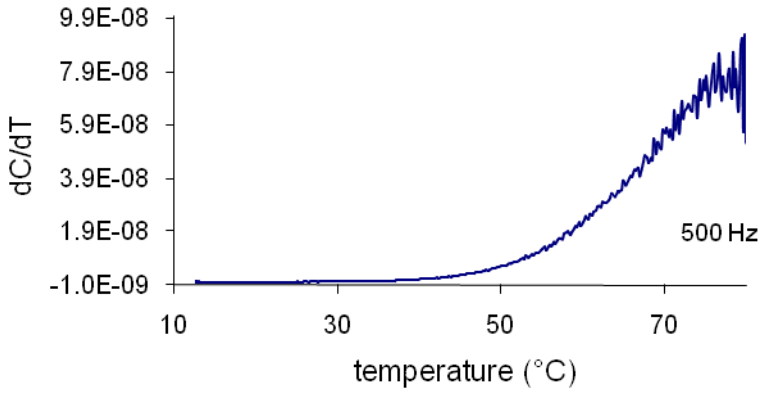

Figure 4.97 Derivatives of capacitance at 500 Hz against temperature for freeze dried amorphous solid fructose with data smoothing.

The moisture content in the samples was found to change during the DEA tests. Dow Corning high vacuum grease was then applied to seal at all connecting parts of the DEA cell. There was no variation of moisture content of samples during DEA tests after application of the grease. The capacitance measurements were smoothed using a moving average. Heating and cooling measurements gave similar results. The results presented here were from heating measurement only. The same sample of freeze dried amorphous fructose showed good trends after smoothing (Figure 4.98). The trial with many materials confirmed the change in peak derivative with the chemical component of materials.

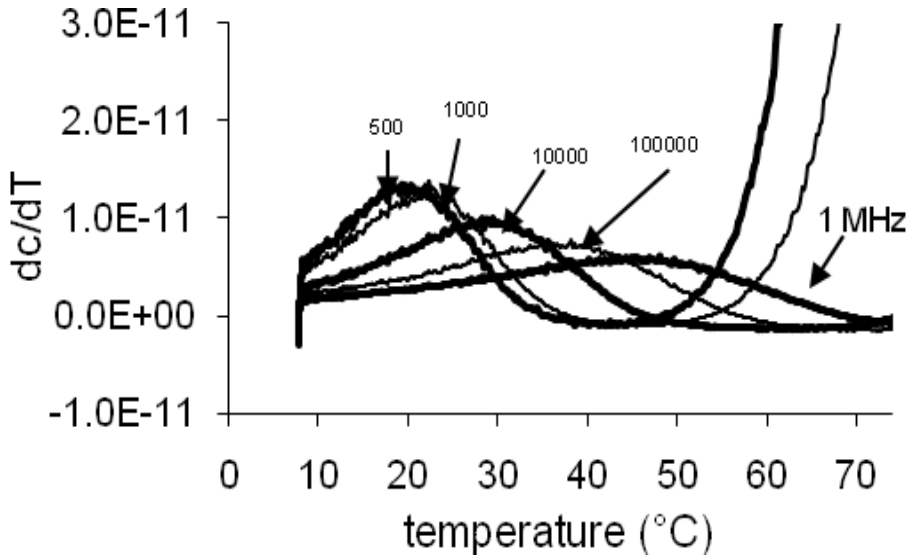

Figure 4.98 Derivatives of capacitance against temperature of freeze dried amorphous fructose when Dow Corning high vacuum grease and data smoothing was used. The peak of derivative at 500Hz matched T_g from DSC.

The melted fructose, glucose and sucrose were analysed to determine T_g. DEA at 200 Hz gave a peak derivative at a temperature very close to the DSC T_g for glucose and sucrose. The DEA results of melted fructose are shown in Figure 4.99. Melted fructose was the most difficult substance to get good curves from DEA. The 200 and 500 Hz curves did not show the peak derivative that matched the DSC T_g. The peak derivative at 500 Hz was around 35 °C.

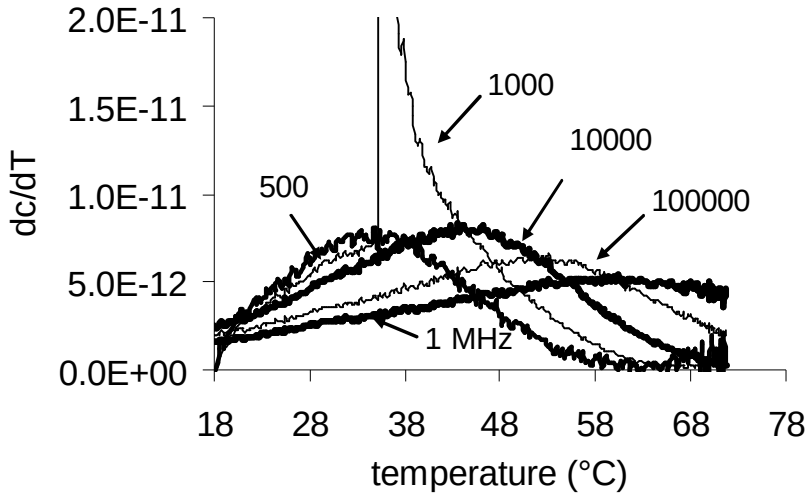

Figure 4.99 Derivatives of capacitance against temperature for melted fructose. The peak of derivative at 500Hz showed a much higher temperature when compare to DSC T_g of melted fructose and freeze dried fructose. The derivative at 1000 Hz showed unusual jump of the capacitance before went back to normal range.

The DEA of melted glucose is in Figure 4.100. The peak derivative of glucose at 200 Hz was found at around 50 °C which matched T_g of this material from the visual experiment. All other peak derivatives at all frequencies including at 200 Hz were at around 37 °C which is very close to onset DSC T_g of glucose from cooling scan (35 °C). This point was also very close to T_g value of glucose at 38 °C reported by Finegold et al. (1989). The work of Ollett & Parker (1990) indicated T_g of glucose in a range of 20-35 °C.

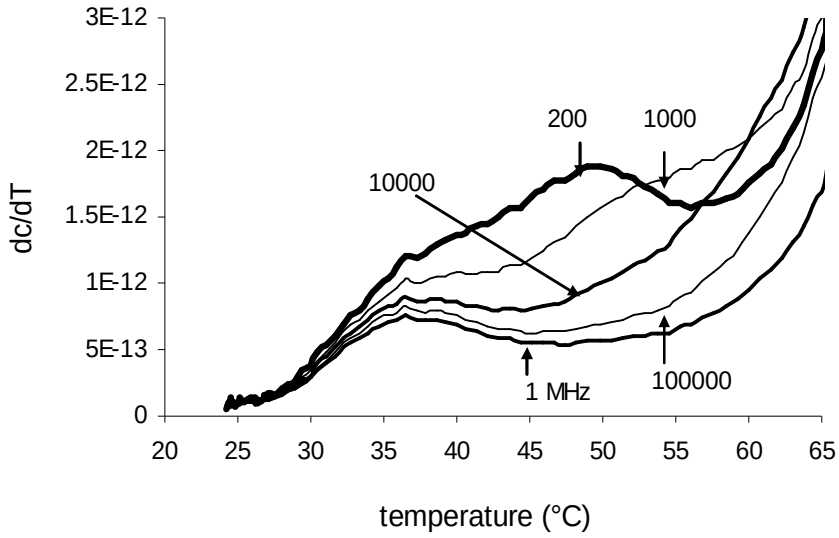

Figure 4.100 Derivatives of capacitance against temperature for melted glucose.

Figure 4.101 shows the derivatives of capacitance with respect to temperature for melted sucrose. The peak derivative of sucrose at 200 Hz found at around 60 °C which matched the T_g of this material from the visual experiment. The DSC onset T_g values from both cooling and heating scans found the transition at around 54 °C. This value was similarly to T_g of dry melted sucrose reported at 56.6 °C by Roos & Karel (1990).

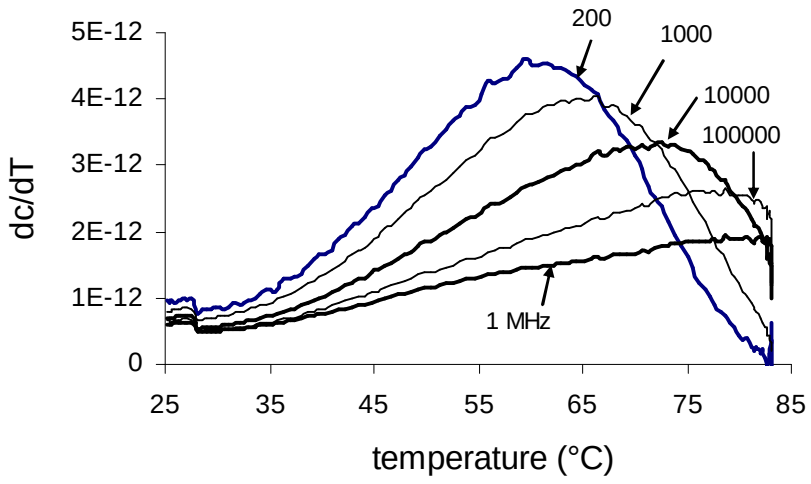

Figure 4.101 Derivatives of capacitance against temperature for melted sucrose.

The DEA trial of a mixture of sucrose: glucose: fructose at a 1: 1: 1 ratio found the peak derivative at 1000 Hz at 50 °C. This value matched the T_g of this mixture from the visual experiment (Figure 4.102). The DSC onset T_g from cooling scan of the same ratio mixture had found at much lower than the values from this measurement (32 °C).

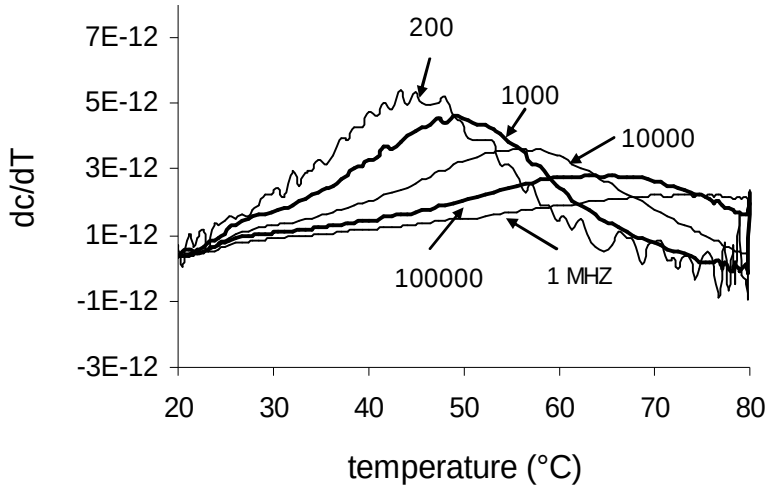

Figure 4.102 Derivatives of capacitance against temperature of melted mixture of sucrose: glucose: fructose at ratio of 1: 1: 1.

The fraction of acid in freeze dried fructose + 50% carrot fibre was changed and it was found that the peak derivative varied with the acid fraction. Figure 4.103 shows the peak derivative (200 Hz) of freeze dried fructose + 50% carrot fibre + 1% citric acid at 70 °C. The peak derivative at the same frequency appeared at around 60 °C when the citric acid in the sample was 3% (dry weight) (Figure 4.104). It was also found that the T_g decreased when adding more citric acid. There was no experiment from DSC of fructose +50% fibre + citric acid to compare to these results.

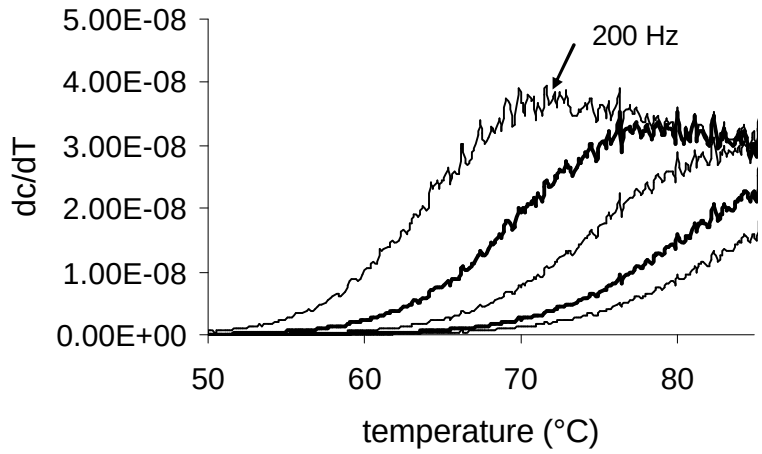

Figure 4.103 Derivatives of capacitance against temperature of freeze dried fructose + 50% carrot fibre + 1% citric acid.

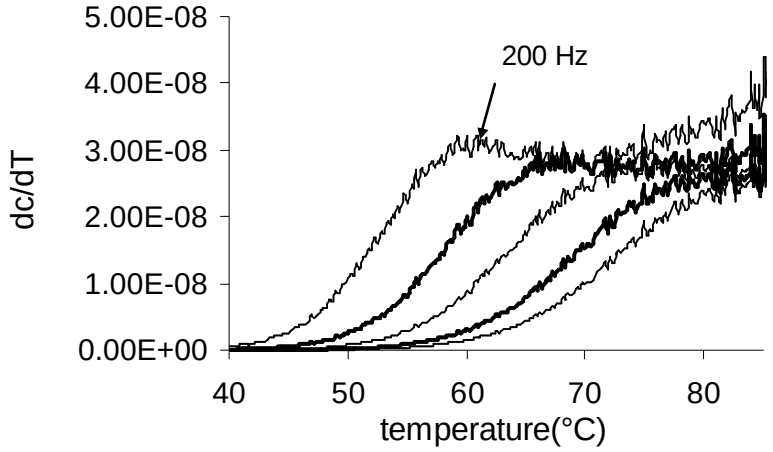

Figure 4.104 Derivatives of capacitance against temperature of freeze dried fructose + 50% carrot fibre + 3% citric acid.

The trial of DEA with fructose + 3% sodium chloride at the temperatures from 10 to 80 °C showed that the first peak derivative might occurred below 10 °C (Figure 4.105). It was shown that DEA at low frequencies had a possibility of measuring the glass transition of a single substance or a few mixed food components.

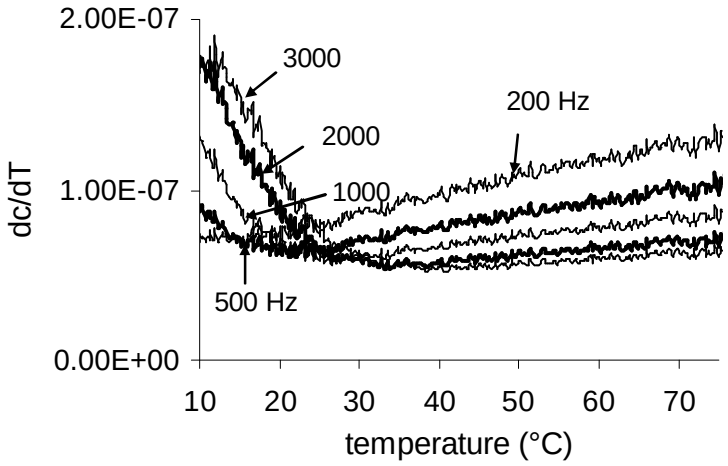

Figure 4.105 Derivatives of capacitance against temperature of freeze dried fructose + 3% sodium chloride.

DSC and DEA of freeze dried fructose + carrot fibre

The results from DSC and DEA of freeze dried mixtures of fructose + carrot fibre are in Table 4.24. It was difficult to match the DSC T_g results and the peak derivative from DEA. The DEA results showed the frequency independence of each sample. The

measurement frequency range was set by guessing the possible performance of each range until it was successfully matched the DSC T_g to the peak derivative of DEA.

Table 4.24 T_g from DSC and corresponding DEA frequencies for carrot fibre in freeze dried amorphous fructose

Carrot fibre: fructose ratio (dry basis)	Moisture content (% wb)	DSC T_g (°C)	DEA frequency for same T_g (Hz)
0:100	0.05	18	500
14:86	5.0	59	1,300
21:79	5.0	69.5	20,000
28:72	5.0	82	6,000
21:79	0.01	98.2	10,000
21:79	2.0	90.5	7,000
21:79	5.0	69.5	20,000

In conclusion the frequency used in DEA was found to vary with the food components. This showed a possibility of DEA to measure the T_g values of a single and double mixed food components. However, when working with DEA, repeating at different range of frequencies until it is matched the results from typical equipments used to measure T_g is required.

Chapter 5 Discussion

5.1 Sugar content determination

5.1.1 Enzymatic method

Theoretically, there are many possible sources of error while conducting sugar content determination by the enzymatic method (detail in Section 2.4.1). From the results of this experiment the average data of two samples showed a very small uncertainty of 0.01-0.02 SD values. This confirmed that enzymatic method was a good method for sugar content determination as long as the experimental technique used is precise. Since the T_g depends on the chemical composition of the material, when dealing with the sugar component of samples the enzymatic should be the best method for sugar content determination. It is suitable for research work which needs very precise data

5.1.2 YSI enzyme membrane method

The YSI method was very convenient and very fast. The results seemed to under estimate the sucrose values and over estimate the glucose values in samples (see Figure 4.1). Choi and Yiu, (2004) indicated that the ability of the enzyme membrane to detect H_2O_2 was affected by temperature. This experiment was carried out at room temperature which varied between 20 and 25 °C. The temperature possibly affected the results to some extent. Mason (1983) found the results similar to this experiment when comparing data from the YSI 2700 and HPLC methods of sucrose and glucose. The sucrose values of cereals determined by the YSI Model 27 Industrial Analyser were slightly lower than the HPLC method. The glucose values were about 30% higher than the HPLC method (detail in Section 2.4.1). This information indicated the probability of incorrect sucrose and glucose values from the enzyme membrane method. This might lead to incorrect conclusions and recommendations. Researchers who need precise data for samples containing both glucose and sucrose should avoid using this method. The determination of concentration of a simple sugar by this method might not have a large error. Mormino (2001) used a YSI glucose analyser to measure the glucose content in glucose medium. The research indicated a daily calibration with 2 and 5 gL^{-1} standards. No problems in using the YSI analyser were reported from that study. In fact the YSI analyser is a very

quick method to use for sugar content determination, if the calibrations of sucrose and glucose show good results. In this experiment, even though the results were under estimated for sucrose and over estimated for glucose, it showed consistent results over a period of five days (Table 4.3 and 4.4). The YSI method might be useful when working with many samples with a limit of time. Calibration including suitable standard concentrations and calibration frequency are needed when working with this equipment. The performance of this equipment might be improved by the development of better membranes to use with samples with sucrose and glucose. However, there is no fructose membrane available for YSI measurement so an alternative method was required as fructose is the dominant sugar in fruit juice.

5.1.3 HPLC and RID method

The most difficult part of the work with the HPLC was that it took a very long time to stabilize the baseline of the RI detector used with the HPLC for sugar determination. Alternatively, the evaporative light scattering detector (ELSD) can be used to detect sugars in the HPLC. Clement *et al.* (1992) reported that, compared with the RI detection, an ELSD showed better sensitivity, more stability of the chromatographic baseline, and no effect of temperature. An ELSD was not available for this study. In this study, it was found that calibrations based on the peak area and peak height gave different results (see Figures 4.12-4.19). The response was not repeatable and part of the problem might be baseline stability. The determination should include more frequent calibration such as injecting the same standard after every five samples. The output of the standard will show the stability of the detector clearly. The variation of the standard with time (see Section 4.1.3 Figures 4.9-4.11) indicated a decay of the standard perhaps due to microbial contamination. However, the preparation of a new standard every time when running the experiment will introduce errors from the measurement of raw materials and the preparation environment. It might be better to use commercial standards which contain a preservative substance to maintain the quality for a longer time. The accuracy of the HPLC method was sufficient to find the sugar composition and hence develop and test model sugar solutions.

5.1.4 Comparison of the sugars determination from the three methods

Uncertainties

The uncertainties of the sugar analysis were lowest for the enzymatic method followed by the HPLC method. The highest uncertainties were obtained using the YSI enzyme membrane method. The low uncertainties from the enzymatic and HPLC methods indicated that these were acceptable methods for sugar content determination in the study. The accuracy was sufficient to obtain reasonable T_g and stickiness relationships for the samples in the later experiments. The high uncertainties of sugar values obtained from the YSI enzyme membrane method indicated that this method was not suitable for this study.

Measurement of sugars in carrots and apples

Even though the sugar content of carrot and apple depends on many factors and is expected to vary greatly, some of the results from the three methods used in this study were very different from the literature (Table 4.10). For the low sugar levels in the fibre samples, the YSI and HPLC showed good agreement. The enzymatic method and HPLC gave good agreement for the high sugars levels in apple juice. The three methods showed variation in the results for the medium sugar levels such as in carrot juice. The enzymatic method gave values similar to those in literature (Suojala, 2000; Alabran & Mabrouk, 1973). The YSI gave high values and the HPLC gave low values. The different values of sugar content in raw materials directly affected the prediction of T_g.

Measurement of sugars in apple juice

The sugar content obtained for apple juice was similar from the enzymatic and HPLC methods. Fructose was found to dominant. These results were in good agreement with the literature (Brause, 1998; Brause & Raterman, 1982). The results from enzymatic method showed the content of sucrose was around two times the concentration of glucose. Some literature showed the glucose content of apple juice was on the other way round from this study (detail in Section 2.4.1). However, the results from HPLC method showed very small concentrations of glucose while the sucrose was found to be around half concentration of fructose. This might be because of the difference in variety, growing condition, harvesting time and storage history. The apple juices used in the enzymatic and HPLC methods were from different sources. It was very likely that the sugar contents of the juices were not the same.

The enzymatic and HPLC methods were suitable for sugar content determination of apple juice. The YSI enzyme membrane method had no membrane to detect fructose which is the major sugar in apple juice and so it was not suitable.

Measurement of sugars in carrot juice

The enzymatic method gave good agreement of sugar values in carrot juice to the literature (Soujala, 2000). Even though the glucose and sucrose values from the YSI method were high, the values were consistent for the whole 5 days of measurement (Tables 4.3, 4.4, Figures 4.3, 4.4 and 4.5). The slight increase in sucrose and glucose values on the second day indicated the possible metabolism of fructose, glucose and sucrose in the juice (Berüter, 2004; Sergeeva & Vreugdenhil, 2002). The suddenly drop of sucrose and glucose in all samples on the third day might be due to bacteria and enzyme reactions in the juice. These data indicated that YSI might be suitable for the measurement of sucrose and glucose in carrot juice. More calibration would yield more accurate results for sucrose and glucose. The attractiveness of the YSI method was its convenience and speed of obtaining results. It helps save a lot of time in experiments with many samples. However, carrot juices also contain fructose (Table 4.1) so the YSI could not be used for all analyses.

In conclusion, the best method for sugar content determination in terms of the accuracy was found to be the enzymatic method, but it was time consuming. The HPLC was found to give reasonable results and was reproducible. The automatic application of this method reduces the time required to analyse many samples. Storage times before analysis must be less than three days to minimise the effects of enzyme reactions on the sugars.

5.2 Sugar content of carrot fibre

The objective of blanching the carrot fibre was to wash the sugar from the carrot fibre as much as possible. The apple juice had a high enough sugar content to make it difficult to spray dry. The fibre which would be a drying additive should not increase the sugar content of the juice. The blanching caused tissue cell membrane disruption (Galindo *et al.*, 2005). The water soluble component in carrot fibre is temperature dependent (Georget *et al.*, 1998). Blanching at 80 °C increased the water soluble component in

carrot but below this temperature it was found that the water soluble and water insoluble component of carrot cell wall remained unchanged (Georget *et al.*, 1998). It was expected that blanching and washing should decrease the sugar in carrot fibre but the blanched carrot showed no significant difference of sugar content from the untreated one. Moreover, the mixtures of carrot juice + blanched fibre and carrot juice + untreated fibre were little different in sugar content. In addition, the blanched carrot fibre had a very faded colour and was more difficult to mill into a fine powder. According to Galindo *et al.* (2005) blanching not only causes tissue cell membrane disruption but also protein denaturation, poor firmness and crispness. The heat treatments also cause loss of colour, flavour and nutrition. The freeze dried blanched carrot pomace in this experiment had a faded colour and very strong fibre. The untreated fibre was easy to break into a fine particle. This result indicates that the soluble, or heat sensitive components of the carrot fibre had maintained the crispness of the dried carrot material. Most of the carrot fibre after blanching and washing could be cellulose, which is the structural frame in the form of cellulose microfibriles in cell walls. The hemicelluloses present in between the microfibril and the lignin (the encrusting substance binding the cell wall together) appeared to degrade with heat (Saka, 2001).

In conclusion, the best way to prepare carrot fibre for use as a drying additive is to use the fibre directly from the juice extraction without any processing.

5.3 Crystal induction by carrot fibre

As shown in Section 4.4, Figure 4.29, the particles of carrot fibre were likely to contain many crystals. The main crystal in carrot fibre is cellulose (Nawirska & Kwansniewska, 2005). deMan (1999) stated that dehydrated carrots increased crystallinity with time and the amorphous gel regions of cellulose can become progressively more crystalline when moisture is removed.

He stated that the crystalline nature of cellulose fibres can be easily seen under a polarizing microscope. In this experiment it was not possible to take carrot fibre pictures from the polarizing microscope. Figure 4.29 and other particle pictures were taken from a Wild M37 Kombistereo microsope with a Meiji Infinity 1 digital camera. The software

driving the camera was Lumenera Inifinity Capture. This camera system presented a better quality picture than from the polarizing microscope.

The crystallinity present in carrot fibre was not only from cellulose, as some degree of crystallinity has been observed in pectic polysaccharides and hemicellulose polysaccharide. Georget *et al.* (1999) found evidence for the contribution of pectin to the crystallinity of the carrot cell wall. They found that wetting and heating at high moisture content and temperature (70%, 30 °C) increased the crystallinity of carrot fibre. In this experiment carrot fibre powder was mixed with fructose solution and apple juice then freeze dried and spray dried. The crystals and amorphous part in the carrot fibre present in the mixtures during freeze and spray drying of fructose and apple juice might be able to induce crystals or semicrystals in the final product (detail in Section 2.2.2).

Bhandari *et al.* (1993) stated that during rapid drying in spray drying the products represented amorphous solids. The rapid drying during spray drying should produce amorphous powder, but the spray dried powder of mixtures with carrot fibre showed some crystalline properties. These were confirmed by the melting endothermic transition of spray dried fructose + 50% carrot fibre (Figure 4.76), and that of spray dried apple juice + carrot fibre in Figure 4.77 and 4.78. Seymour (1971), Williams (1971) and Cahn *et al.* (2005) validated that a polymer can have both a glass transition and a melting temperature, but amorphous portions undergo the glass transition only. The polymer chains that melt are not the chains that undergo the glass transition.

The particles of spray dried powder of fructose + carrot fibre and apple juice + carrot fibre were found to contain crystalline materials (Figures 4.84, 4.89 and 4.50). This demonstrated that the spray dried products of the mixtures with carrot fibre were not really amorphous. The crystal induction by carrot fibre took place during the spray drying of fructose and apple juice but the rapid drying during the drying could not provide enough time for the maturation process of the complete sugar crystals. The DSC performance of these powders with very small transitions (as shown in Figure 4.65) also seemed to confirm that there were only small amounts of amorphous material in the samples. These results were similar to the work of Cano-Chauca *et al.* (2005) who found that the cellulose and carrier was essential to the occurrence of the crystallinity in mango powder (detail in Section 2.3.7). The crystalline state of the product has advantages over

the amorphous form in terms of physical and chemical stability (Walstra, 2003; Roos, 1995; Cano-Chauca, 2005).

In addition, the DSC scan of food mixtures mostly showed very small glass transitions (detail in Section 2.4.2). Lin *et al.* (1991) found a large reduction in the glass transition energy on DSC scans of soybean cell wall when calcium chloride was added to the cell wall but the T_g values increased. They explained that the cross linking and ionic interaction of pectin and Ca^{2+} in the cell wall material increased the glass transition of the mixture (from 52.9 to 60.8 °C in the elongating region cell wall and from 60.1 to 61.7 °C in the mature region cell wall). No explanation on the reduction of the magnitude of the transition was given. However, this study showed that the different parts and age of the cell wall material also gave a variation of T_g.

According to Roos (1995) polymers and sugars with high values for the T_m/T_g ratio tend to crystallize rapidly. Roos (1995) reported T_m/T_g values of fructose, glucose and sucrose at 1.37, 1.37 and 1.33, respectively. T_g values from Orford *et al.* (1990) and melting values from Roos (1995) give T_m/T_g of fructose, glucose and sucrose at 1.36, 1.33 and 1.30 respectively. In this study the values were 1.37, 1.31 and 1.29. Based on the T_m/T_g values of these sugars, fructose has the highest potential to crystallize first, followed by glucose and sucrose. A study of sugar crystallization in honey, however, found that glucose, and not fructose, is the sugar which crystalline (Tchoumboue et al., 2007). Fuisz *et al*. (1993) stated that supersaturation of sugar induced crystallization. Nucleation of sugar crystals during supersaturation converts the remaining portion of the amorphous mass to a crystalline form. In this experiment fructose and apple juice were very saturated when they were almost dried in spray drying and freeze drying. The fibre present in the mixtures acted as nucleation sites in the concentrate, so further removal of water could produce sugar crystals. This showed a possible mechanism for fructose and apple juice to be crystalline. It is likely that the crystals found in spray dried fructose + carrot fibre was a crystal of fructose. The appearance of this particle was quite opaque (Figure 4.84). From Figure 4.89 the appearance of some particles of spray dried apple juice + carrot fibre was opaque and some were very transparent. This indicated that there was more than one type of crystal in the particle of spray dried apple juice + carrot fibre. One of the crystals in this spray dried particle was speculated to be fructose. The other crystals

should be the combination of crystals of the other main sugars and acids in apple juice which are sucrose, glucose and malic acid and others. These crystals can be determined by means of analysis X-ray diffraction. The presence of diffuse and large peaks in X-ray diffraction is from amorphous material. The crystalline materials will show a sharp and defined peak in the X-ray diffraction because of the highly ordered state (Cano-Chauca, 2005). Unfortunately X-ray diffraction was not performed on these particles obtained in this study.

In conclusion, the DSC thermograms and the microstructure of the spray dried powders confirmed that there were crystals in the spray dried powder of fructose and apple juice with added carrot fibre. The crystals present in the powders affected the glass transition by the reduction of magnitude of the energy of the transition. The crystals and/or semicrystals of materials were more stable than the amorphous form (detail in Section 2.2.6). These crystals and/or semicrystals were believed to occur in the spray dried powder by the induction of the components in carrot fibre. Bhandari *et al.* (1993) stated that the crystalline state might be preferred for a low hygroscopicity in fruit juice. Chiou and Langrish (2007) stated that the problem of stickiness in spray drying of foods might be reduced by increasing the crystalline fraction of spray dried powders. Confirmation of semicrystalline material in the spray dried products of fructose + carrot fibre and apple juice + carrot fibre indicated that carrot fibre was a good additive in spray drying of apple juice.

5.4 Freeze drying experiment

5.4.1 Freeze dried fructose solution

The freeze drying temperature used in this experiment was limited to -25 °C (detail in Section 3.2.3). This temperature is lower than the eutectic point of fructose which was found to be -9 °C at 0.48 mass fractions in water (Walstra, 2003). The mass fractions of fructose solution used in the experiment were at least 0.50. If the fructose solution forms a eutectic on freezing (see detail in Section 2.2.4) this temperature should be sufficiently low to completely freeze it. In this experiment 50, 60, 70 and 80% fructose solutions were not successfully dried at -25 °C, but the 90 and 95% fructose solutions were successfully freeze dried. The glass transition of fructose solutions, rather than the eutectic formation

is likely to be dominant in the freeze drying behaviour. As shown in Figure 2.10 and Table 2.15 the T_g of 60% fructose solution is about -85 °C and increases with the concentration to around -17 °C at 90%. In the case of 90 and 95% fructose solution, the freezing temperature at -25 °C was lower than the T_g values and freeze drying was successful. The 50, 60, 70 and 80% fructose solutions became more and more viscous but never formed a very stiff, highly viscous liquid because the freezing temperature was higher than their T_g. In addition, the pre-freezing process might also play a partial role in these results. In this experiment the pre-freezing at -30 °C took place over night. This was a slow freezing rate which created large ice crystals in the fructose solution. In practice a larger ice crystal has a shorter drying time in the subsequent primary drying stage (Song *et al.*, 2005). But the samples with concentration less than 90% took a very long time to dry.

In conclusion, freeze drying of fructose solution was found to be a glass formation type so the drying performance relied on the glass transition temperature not the eutectic temperature. The suitable freeze drying temperature is the temperature lower than T_g of the fructose solution.

The success in freeze drying of pure fructose suggested that it will not be possible to spray dry fructose solution without any additive because of the low T_g value of fructose. Very high concentrations of fructose solution cannot be used in spray drying.

5.4.2 Freeze dried fructose + carrot fibre

In the previous section it was found that fructose solution with an initial concentration of 50% could not be successfully freeze dried at -25 °C. In contrast, freeze drying of fructose solution + 14% carrot fibre was successful at -25 °C. This indicated that fructose + carrot fibre had a higher T_g than pure fructose solution. Carrot fibre increased the T_g of the fructose solution and facilitated the freeze drying of fructose solution. This was confirmed by the DSC T_g results of these dry mixtures. The DSC T_g results of the freeze dried fructose + carrot fibre were found to increase from 59 °C to 82 °C when the fraction of carrot fibre in fructose was increased from 14% to 28% (dry weight). The T_g values of these mixtures were 114.5, 122.9 and 130 °C when the fraction of carrot fibre in fructose were 50, 60 and 70%. Thus increasing the fraction of carrot fibre in fructose increased T_g

of the mixtures. Many researchers have found that when the fraction of material with higher T_g is increased, the T_g of the mixture increases (Roos, 1995; Slade & Levine, 1991, Bhandari *et al.*, 1997). It was expected that when the T_g value of material is high the problem of stickiness and hygroscopic will reduce. Freeze drying of carrot juice (Figure 4.22) and of carrot juice + carrot fibre (Figure 4.23) confirmed that the stickiness of the carrot juice was reduced when the amount of carrot fibre in the juice increased. The freeze dried fructose + 14% carrot fibre (Figure 4.24) was less hygroscopic and less sticky than the pure freeze dried fructose after grinding into the powder form. One of the advantages of freeze dried fructose + carrot fibre is the colour retention. It was found that freeze dried powders were bright orange and the colour lasted for a long time. Tai and Chen (2000) reported 48% loss of carotenoid pigment in daylily flowers from hot air drying at 48 °C while colour loss from freeze drying at -53°C was minimized. Aina and Shopide (2006) reported that the effect of sugar on colour stability was very dominant in freeze dried product but was less in spray dried products.
Thus the carrot fibre showed good performance as an additive in fructose freeze drying by increasing T_g of the mixtures, and reducing the hygroscopicity of the dried product. The fructose improved colour retention of the carrot fibre.

The result from the freeze dried fructose + carrot fibre at various fractions and their high T_g values suggested that these mixtures should be able to be spray dried successfully.

5.4.3 Freeze dried fructose + maltodextrin

The freeze dried fructose + maltodextrin (50, 60 and 70% dry weight) swelled to a very big volume during freeze drying (Figure 4.25). After freeze drying the mixtures of fructose + maltodextrin were found to be hygroscopic and sticky. This result was different from the work of Adhikari *et al.* (2003) who stated that the addition of maltodextrin in fructose solution reduced stickiness. However, the current study did not perform a stickiness test to compare the stickiness value of pure freeze dried fructose and the freeze dried fructose + maltodextrin.

The T_g of fructose + maltodextrin were found very similar to the T_g of fructose + carrot fibre at the same fraction (Table 4.18). The freeze dried fructose + carrot fibre were less hygroscopic and less sticky than the freeze dried fructose + maltodextrin at the same

fraction in the fructose mixtures. The stickiness and swelling of the freeze dried fructose + maltodextrin made it difficult to perform DSC experiments (detail in Section 4.6.15). It was interesting that even though there have been a lot of applications of maltodextrin in spray drying of fruit juice, there is still doubt that, with the high viscosity of the mixture of fruit juice + maltodextrin, it is a good additive. In was found from this study that a mixture with a maltodextrin fraction lower than 50% with fructose failed to freeze dry (and also spray dry). Roos and Karel (1991a) found that addition of less than 50% maltodextrin in sucrose did not significantly increase the T_g values of sucrose, thus it needs more than 50% maltodextrin in practical drying of fruit juice to increase T_g value of the juice to be high enough to spray dry. Adhikari *et al.* (2004) also found that 50% maltodextrin in a mixture of sucrose + glucose + fructose failed to overcome stickiness of the mixture (detail in Section 2.3.6). In this study the maltodextrin used was made from corn. Swelling of corn maltodextrin was found to sharply increase from 10 to 20% with a temperature increase of 20 °C (detail in Section 2.3.6). Unfortunately, there was no work reported on the swelling power of corn maltodextrin during freeze drying to compare with the freeze drying of fructose + maltodextrin in this experiment. Adhikari *et al.* (2004) stated that the swelling of maltodextrin during heating increased the rate of evaporation of water from the maltodextrin droplet. Observations during the freeze drying of fructose + maltodextrin seemed to show that during the swelling the dried crust was likely to block the moisture from diffusing out. It took a long time to freeze dry fructose + maltodextrin solutions.

In this experiment maltodextrin was found to be a poor additive in freeze drying of fructose even though the T_g values of the mixtures after freeze drying were found to be high. This result casts doubt on the usefulness of T_g as a good indicator of the drying ability of materials.

5.5 Spray drying Experiment

5.5.1 Spray dried fructose + carrot fibre

The high yields of dried fructose + carrot fibre from the spray drier (Table 4.20) confirmed that carrot fibre was a good additive. The DSC T_g of spray dried powder of fructose + 50% carrot fibre was found to be around 131 °C (Figure 4.75). This high T_g

values proved that carrot fibre is suitable to be a carrier in spray drying of sugar rich product. In spray drying the outlet temperature is the key parameter for stickiness, and in this experiment the outlet temperature was 75 C which is much lower than the T_g of fructose + carrot fibre. Foster *et al.* (2005) showed sticky point temperatures of sugars and sugars mixtures by presenting the T-T_g value which has a minimum of 19 °C (maltose) and a maximum of 41 °C (fructose + lactose) (detail in Section 2.2.6). Paterson *et al.* (2006) showed the stickiness curve of the whole milk powder is around 37.5 °C above the T_g line of lactose. These studies showed that the sticky point temperatures of pure sugars were closer to T_g values than the sticky point of sugar mixtures and the milk. Jaya and Das (2007) showed sticky point temperature of vacuum dried pineapple + maltodextrin at around 2.5 °C above the T_g values (detail in Section 2.2.6). If the T_g is the indicator for stickiness, the spray dried powder of fructose + 50% carrot fibre was unlikely to have been sticky at a temperature lower than the T_g (131 °C) which is very high for a fructose product. The powder stuck on the drier wall might because of the powder was high moisture and low T_g of powder when touching the wall. This high moisture powders could make a liquid bridge when touching each other at the wall. The evaporation took place until it was cooled down to the outlet temperature (75 °C) and finally cooled to room temperature. This made its sweepability.

In addition the melting endotherm in the DSC scan of this spray dried powder (Figure 4.76) and the presence of crystals-like particles (Figure 4.84) confirmed that the spray dried powder of this mixture was partially crystalline. The crystallinity of the spray dried powder provided good stabilization of the fructose (detail was discussed in Section 5.3).

The spray dried fructose + carrot fibre powder produced in the laboratory scale spray drier was easily swept from the walls and it is believed that a free flowing powder could be produced in a commercial size spray drier. This is because the powder is less likely to reach the chamber wall while it is still moist. The moisture contents of the powders taken from the chamber were found at 2-4 % (wet basis) (Table 4.20) which was consistent with the finding by Gupta (1978) that powder in this range of moisture showed the potential to be free flowing. The good performance of carrot fibre as a drying aid in fructose solutions indicated the possibility of carrot fibre being a drying carrier for fruit juice.

The spray dried fructose + carrot fibre powder had a very faded colour (Figure 4.81). This was in good agreement with the work of Tai and Chen (2000) who showed that a high loss of the carotinoid pigment at high temperature. This result suggested that carrot fibre when used as a spray drying aid of fruit juice will have a minimum effect on the colour of the finish product.

5.5.2 Spray dried apple juice + carrot fibre

The results of spray dried apple juice + carrot fibre were similar to the spray dried of fructose + carrot fibre in terms of the yield, T_g values, DSC performance and appearance of the particles. The hygroscopicity of this spray dried powder was low enough to enable packaging in a normal environment (detail in Section 4.7.7). This could be explained by crystal induction (Section 5.3) but also might be related to the hydrophobic nature of the fibre. deMan (1999) stated that the main components of fibre will not absorb water. For example, the crystalline area of cellulose in the fibre absorbs water poorly and the hemicelluloses in fibre are water insoluble compounds. The high-methoxyl pectins are formed by noncovalent forces and are hydrophobic in the presence of concentrated sugar (55% by weight and acid; pH below 3.6) which will act as a dehydrating agent. These might be the reason for the low hygroscopicity of spray dried apple juice + carrot fibre powder (shown in Figure 4.91b). In addition, Slade and Levine (1991) demonstrated that hemicelluloses and lignin are large polymers that are relatively hydrophobic each with distinct curves for the effect of water on T_g values (detail as shown in Section 2.2.10). It is very likely that the spray dried product of apple juice + carrot fibre could be vacuum packed in a one-serve size. The reconstituted apple juice +carrot fibre in normal water (Section 4.7.9) had the appearance of a healthy quality drink. The fibre in the drink is thought to be useful for the human digestion system. These results reconfirmed the value of carrot fibre as an additive. The evaluation of the nutrition and sensory properties of the dried juice powder after spray drying was beyond the scope of this project and will need to be evaluated to find the acceptable limits for the fraction of fibre in the juice.

5.5.3 Spray dried fructose + maltodextrin

The powder of spray dried fructose + maltodextrin was stickier than that of fructose + carrot fibre. The spray drier temperatures (165/75 °C) that worked well with spray dried

of fructose + carrot fibre did not work when fructose + maltodextrin was dried. Higher temperatures were used to spray dry fructose + maltodextrin (175/85 °C). It was found that the mixtures of fructose + maltodextrin were more viscous than the mixtures of fructose + carrot fibre. The viscosity of maltodextrins was also reported by Wang and Wang (2000) (detail in Section 2.3.6). The higher viscosity of fructose + maltodextrin solution might have caused larger droplets from the drier atomizer which would need more time to dry. The particle size of fructose + maltodextrin powders was found to be bigger than that of fructose + carrot fibre. This supported the idea that the fructose + maltodextrin required higher temperatures for drying in the spray drier. This could be a reason that more powder stuck on the surface wall of spray drier when compared to the drying of fructose + carrot fibre. Moreover, the larger size and round shape of fructose + maltodextrin particles allowed more contact area with each other and with the chamber wall which could increase the stickiness of the powders.

The physical state of maltodextrin is amorphous. Maltodextrin has been used to prevent crystallization in many food processes to prevent crystallization of sugars (Waltra, 2003). The T_g values of freeze dried fructose + maltodextrin were found to be similar to those of fructose + carrot fibre, but the yield of spray dried fructose + maltodextrin was lower than that of fructose + carrot fibre (Table 4.17, 4.18 and 4.20). (Unfortunately, the T_g values of spray dried fructose + carrot fibre and fructose + maltodextrin were not available due to some technical problems during the experiments).

The spray dried particles of fructose + maltodextrin appeared to be more amorphous but the powder of fructose + carrot fibre was more semicrystalline. As discussed before the crystalline powder has the advantage of greater chemical and physical stability than the amorphous form (Langrish & Chiou, 2008).

Thus maltodextrin was not found to be a good additive for spray drying of fructose when compared to carrot fibre.

5.5.4 Spray dried apple juice + maltodextrin

The results of spray dried apple juice + maltodextrin were similar to those of fructose + maltodextrin. The particles of apple juice + maltodextrin powder were amorphous, round

and big when compared to the size of spray dried apple juice + carrot fibre. This showed a disadvantage in terms of stickiness of the powder. The viscosity of maltodextrin might cause this problem as already discussed in Section 5.5.3. Jaya and Das (2007) showed the stickiness point temperature of vacuum dried mango juice, pineapple juice and tomato juice with added maltodextrin + tricalcuim phosphate from 2.5 to 15.5 °C above T_g values (detail in Section 2.2.7). These points were much lower than the sticky point temperatures of sugars and milk reported by Foster *et al.* (2005) and Paterson *et al.* (2006). The stickiness of the products described by Jaya and Das (2007) was possibly from the characteristic of maltodextrin.

In conclusion, even though maltodextrin has many suitable characteristics to be an additive in the dehydration of foods such as, no colour, ease of mixing and making solutions, relatively cheap and a high glass transition temperature (detail in Section 2.3.6), the results from this study indicated that, when compare to carrot fibre, maltodextrin has many disadvantages as an additive in freeze drying and spray drying of fruit juice.

5.6 DSC experiments

Appearance of T_g of sugars and mixtures

The glass transitions on DSC thermograms of single sugars and their mixtures were normal. The glass transitions showed onset, mid-point and endpoint from both heating and cooling scans but at different values. There seemed to be a question of which T_g values should be presented; the onset, mid-point or endpoint T_g. As indicated in Section 4.6.3, Roos (1993) preferred to report onset T_g. Simperler *et al.* (2006) found that the cooling DSC scans gave T_g values of glucose closer to literature values than the heating scans. In this experiment the onset T_g from cooling scans were found to be more similar to literature than the onset T_g from heating scans. The mid-point T_g of both cooling and heating scans were very similar.

The variation of T_g values of pure sugars from literature values (Table 4.15) might be because of the sample preparation. The melting of sugars for DSC analysis in this

experiment was not done in a completely controlled temperature and environment. It was possible that the excess heat might have caused the degradation of sugars during melting. The browning reaction might also have occurred during melting and caused the variation in the T_g of the melted sugars and their mixtures. Wantanagorn and Schmidt (2001) discussed that there could be many factors causing the variation in T_g values from literature. These factors including the initial moisture content of the samples before melting, the moisture content of the glassy sugars after melting and cooling, the method used to form the sugar glasses such as rate of cooling, and the method used to determine and report the T_g values. In addition, Wantanagorn and Schmidt (2001) further discuss that the thermal history and the decomposition of the sample took part in this variation. According to the study of Fan and Angell (1995) the DSC onset T_g value of the "partial melt" fructose was found at 16 °C, that of the "complete melt" fructose was 13 °C, and that of the "relaxed melt" fructose (after complete melting the fructose was in tautomer equilibrium) was 7.2 °C. Wantanagorn and Schmidt (2001) showed the effect of ageing time of amorphous sugars on the DSC T_g values of fructose and glucose. From this experiment the DSC heating onset the T_g of fructose was found at 6 °C which is a slightly lower than the T_g of relaxed melt fructose reported by Fan and Angell (1995). The variation in DSC T_g results from this study and the literature should be because of many possibilities as discussed by Wangtanagorn and Schmidt (2001).

Appearance of T_g of fructose + carrot fibre and apple juice + carrot fibre mixtures

It was very difficult to detect glass transitions in some of the DSC thermograms. This difficulty has been reported by many researchers. Seo *et al.* (2006) reported that the DSC measurement of sucrose and glucose mixtures had to be done more than four times with newly prepared samples. They stated that only one glass transition temperature was observed from the runs. Monica and Blanshard (1993) also indicated that it was difficult to obtain reliable DSC T_g for many samples of fructose + amylopectin solutions. The researchers commented that this was due to a combination of heterogeneity and the low temperatures involved in some cases. Walstra (2003) discussed that in many mixtures, the T_g is uncertain because of the non-equilibrium state of the sample that will depend to some extent on the temperature history of the system. In addition, it is often difficult to determine the T_g of mixed systems such as low moisture foods which are mixtures of

polymers, water and several other small molecules. Prediction of T_g from the composition of mixed systems is generally uncertain.

5.7 The visual T_g

The visual T_g experiment was conducted because it was doubted that the DSC T_g values of some sugars truly represented the glass transition. The visual T_g values were found to be 13 to 28 °C higher than the cooling onset DSC T_g and heating onset DSC T_g of the two-sugar mixtures. The difference of the T_g values by the visual experiment and DSC T_g (Section 4.6.4, 4.6.8, and 4.6.11) indicated that when dealing with T_g of substances more than one method should be used to get more information about the T_g values.

For complex components such as fructose + carrot fibre, fructose + maltodextrin, apple juice + carrot fibre and apple juice + maltodextrin, the transitions were more complicated. The transition might have occurred at high temperatures which were not be able to observed at room temperature by the visual method. The DSC was a better method than the visual method to measure the T_g value of the complex components. However, the difference between the visual and DSC results of sugar and their mixtures, means there is doubt about whether the DSC results for more complex components represent the accurate values. The inaccurately results from DSC was also reported. Shrestha *et al.* (2007) found that the DSC did not accurately measures the effect of proteins on the glass transition temperature of the lactose. The DSC gave better estimation of T_g values when the material had higher sugar and acid concentrations. With higher maltodextrin concentration, the ability of DSC to accurately measure the T_g is diminished as less defined enthalpic shifts take place in macromolecules. It was also found that the endothermic relaxation peak associated with T_g was broader with increased maltodextrin concentration in the mixtures. The thermal mechanical compression test (TMCT) was found to be a better method for T_g of these samples in the study (detail in Section 2.4.2). Gidley *et al*. (1993) however, reported that the T_g values of anhydrous polysaccharide was difficult to be determined experimentally because of thermal decomposition below T_g. Many researchers reported the difficulty of determining T_g of foods (detail in Section 2.4.2). According to Roos (1995) when water is rapidly removed from foods during extrusion, freezing or drying a glassy state may be produced. As discussed in the previous

section, the glassy state is a metastable state, the variable of state with time and environment made difficult to get the certain T_g values of material.

In conclusion it is still doubted that if the T_g values determined by DSC from this experiment really represent the true transition and to which extent that this can be applied to any further particular process.

5.8 The Gordon-Taylor equation of two-sugar mixtures

It was found that the Gordon-Taylor equation was better predicted T_g values of fructose +glucose (Figure 4.47) than those of sucrose +fructose (Figure 4.48) and sucrose +glucose (Figure 4.49). This is in good agreement with the work of Seo *et al.* (2006) who found that the Gordon-Taylor equation was good to predict the T_g values of the mixtures of monosaccharide + monosaccharide and the greatest deviation found from monosaccharide + disaccharide and monosaccharide + trisaccharide. It is obvious that the data from Finegold *et al*. (1989) fitted the Gordon-Taylor equation very well for fructose + glucose, fructose + sucrose and glucose + sucrose. When compared the T_g values from this experiment, less variation was found from fructose +glucose than fructose + sucrose and glucose +sucrose. These results seemed to show that the Gordon-Taylor was a good equation to predict T_g of the less complicate texture components than the complicate ones.

The visual Tg values showed the similar trend to the Gordon-Taylor equation from Finegold *et al*. (1989) data for sucrose + fructose (Figure 4.56) and sucrose + glucose (Figure 4.57) but opposite trend from fructose + glucose. .This deviation is needed more work to support and explain the results.

Gordon-Taylor equation for spray dried and freeze dried apple juice + carrot fibre

The result in Section 4.7.5 showed that when considered the spray dried apple juice + carrot fibre powder and freeze dried fructose + carrot fibre as two mass fractions, the experimental data could be fitted the Gordo –Taylor equation. The *k* value for freeze drying (0.18) is lower than that of spray drying (1.29). By using the Gordon –Taylor

equation the T_g of dried apple juice and dried fibre could be able to predict with the reasonable values (see Section 4.7.5). Miao and Roos (2004) found similar results from the comparison of freeze dried and spray dried carbohydrate. The glass transition temperatures of spray dried samples were higher than those of freeze dried samples at the same water activity.

In conclusion the Gordon-Taylor was found to be an acceptable on the prediction of T_g values of the anhydrous two-sugar mixtures with a better performance from the monosaccharide + monosaccharide. In some extent the Gordon-Taylor could be used to predict the T_g values of anhydrous spray dried and freeze dried mixtures base on the experimental data.

5.9 DEA experiment

The possibility of obtaining T_g values of single and double component materials was shown by low frequency DEA. More experiments, together with other T_g determination methods, are needed in order to indicate the frequency range to predict the T_g of pure components. For food polymers with many components, it was found that the T_g value was not consistently dependent on frequency (Table 4.24). In conclusion, DEA might be an alternative method to study relaxation of a single foods component but it was not be a good method to study that in complex food polymers.

5.10 Feasible drying compositions

From the range of experiments carried out, it is possible to speculate about the feasible range of compositions of carrot fibre + apple juice that could be successfully spray dried. Literature values (Table 2.1) and experimental results (Table 4.10) show that apple juice contains about 5-10% fructose, 2-5% sucrose and 2-3% glucose. Various results (e.g., Figures 4.33, 4.47-4.57) show that variations in sugar composition might lead to a range of about 10 °C in the T_g of mixtures. Figure 4.88 shows the effect of adding carrot fibre to apple juice together with the Gordon-Taylor equation. This equation can be used (with k = 0.18) to predict the effect of changes in the apple juice T_g in the fibre + apple juice mixture. At 30% fibre, the maximum likely variation of ±10 °C in the T_g of apple juice is

predicted to cause a change of ±3 °C in the T_g of the fibre mixture. Thus it can be concluded that apple composition is unlikely to affect the feasibility of the spray drying process. It also shows that initial concerns about the residual sugar concern of carrot fibre (Section 4.2.2) were unfounded.

The effect of moisture content is likely to be much more significant. Figure 2.13 shows the effect of water on the T_g of hemicellulose and Table 4.21 gives experimental results for the T_g values of powders with and without moisture after spray drying. These data are very sensitive to moisture content which leads to uncertainty in the exact effect of moisture on the T_g. However there is sufficient data to show that spray drying is likely to be feasible if the moisture content is kept less than about 2% in the product. At this level the T_g should be high enough to ensure that the product is not sticky.

Chapter 6 Conclusion and Recommendations

6.1 Conclusions

The best method for sugar content determination in terms of the accuracy was the enzymatic method, but this method is expensive and time consuming. The HPLC gave reasonable results and was reproducible. The automatic application of this method reduces the time required to analyse many samples.

The best way to prepare carrot fibre for use as a drying additive was to use the fibre directly from the juice extraction without any processing. Milling of the dried carrot fibre was a good process to produce the suitable fibre powder to use as a drying additive.

The carrot fibre contained crystals of cellulose, hemicelluloses and pectic polysaccharide. These crystals in the fibre induced crystallinity in the freeze dried and spray dried powder of fructose and apple juice. The DSC scans of these products had very small glass transition energies and large endothermic melting transition. The microscope images of these products showed crystalline materials.

The results of T_g values of sugars and mixtures melted showed that the T_g values from heating and cooling scans of fructose, glucose and sucrose were in good agreement with literature. Fructose acted as a plasticizer; an increase in the fructose fraction decreased the T_g of sugar mixtures. Sucrose increased the T_g of the mixtures while glucose seemed to be a stabilizer for the T_g of the three-sugar mixtures. The midpoint T_g from heating and cooling DSC scans gave very similar values. The visual T_g values of sugars and mixtures were 7-28 °C higher than the onset DSC heating and cooling T_g values. The Gordon-Taylor equation did not fit well the T_g values of the dry sugars and their mixtures from this experiment but it showed a better agreement from the mixtures of monosaccharide + monosaccharide than monosaccharide + disaccharide. The variations might have been due to the degradation of sugar samples on the melting process. The Coachman and Karaze equation gave a good prediction of the three-sugar mixtures from this experiment.

Dielectric analysis at low frequency was able to possible detect the T_g of single and double components. For food polymer with many components it was found that T_g value was not consistently dependent on frequency. Dielectric analysis might be an alternative method to study relaxation of a single foods component but it was not be a good method to study that in complex food polymers.

Carrot fibre increased the T_g of freeze dried fructose and decreased stickiness of freeze dried and spray dried fructose. Increasing malic acid fraction decreased T_g of the mixtures. Freeze dried fructose + maltodextrin showed higher hygroscopicity than freeze dried fructose + carrot fibre. It was not possible to determine the T_g of fructose + maltodextrin + malic acid due to the swelling and hygroscopicity of the freeze dried samples. T_g values of freeze dried fructose + carrot fibre and fructose + maltodextrin were found to high enough to allow spray drying of these mixtures.

The minimum fraction of carrot fibre required to facilitate spray drying of fructose and apple juice concentrate was found to be 30%. Mixtures with maltodextrin at a fraction lower than 50% could not be successfully spray dried. When spray drying fructose + carrot fibre, apple juice + carrot fibre, fructose + maltodextrin and apple juice + maltodextrin at the appropriate ratios most of the powder stuck to the drier walls. The powder swept from the wall was free flowing with moisture content of approximately 2-4%. The T_g values of these powder indicated the wall build-up might be avoided in larger scale drying. T_g values of spray dried powder from the mixtures with fibre and maltodextrin were found to be quite similar. The yield from mixtures with carrot fibre was three times higher than those of mixtures with maltodextrin. This cast doubts that T_g alone could be a good indicator for the stickiness of spray dried material. The microscope images and DSC scans of spray dried powders of fructose + carrot fibre and apple juice + carrot fibre showed crystalline materials. The particles of spray dried fructose + maltodextrin and apple juice + maltodextrin were mostly amorphous. The crystalline form is more physically and chemically stable than the amorphous form. Thus carrot fibre is a good additive in spray drying of fruit juice.

6.2 Recommendations

For the analysis of sugars in fruit juice, enzymatic fixation should be used. The comparison of different sugar determination methods should be done on the same lot of raw materials and standards.

Freeze drying of fructose, glucose and sucrose and these sugars with maltodextrin from different sources should be performed to compare the drying performance and swelling property.

For studies of glass transition temperatures and their application more than one method should be used to measure the glass transition temperature of materials.

The crystals induction in spray drying of specific sugars by specific fibre components such as cellulose, hemicelluloses and pectic saccharide should be carried out to find the efficiency of each component on the crystal induction.

The X-ray diffraction analysis of the spray dried particle should be performed to find out the type and fraction of crystals in the spray dried powder.

To confirm the result of the effectiveness of carrot fibre as a spray drying additive for fruit juice, the experiment should be done in a commercial spray drying scale.

References

Ablett, S., Izzard, M.J., Lifford, P.J., Arvanitoyannis, I. & Blanshard, J.M.V., 1993. Carolimetric study of the glass transition occurring in fructose solutions. *Carbohydrate Research*, **246**, 13-22.

Adhikari, B., Howes, T., Bhandari, B.R. & Troung, V., 2000. Experimental studies and kinetics of single drop drying and their relevance in drying of sugar-rich foods: A review. *International Journal of Food Properties*, **3**, 323-351.

Adhikari, B., Howes, T., Bhandari, B.R. & Troung, V., 2001. Stickiness in foods: A review of mechanisms and test methods. *International Journal of Food Properties*, **4**, 1-33.

Adhikari, B., Howes, T., Bhandari, B.R. & Troung, V., 2003. Characterization of the surface stickiness of fructose-maltodextrin solutions during drying. *International Journal of Food Properties*, **21**, 17-34**.**

Adhikari, B., Howes, T., Bhandari, B.R. & Troung, V., 2003a. In situ characterization of stickiness of sugar-rich foods using a linear actuator driven stickiness testing device. *Journal of Food Engineering*, **58,** 11-22.

Adhikari, B., Howes, T., Bhandari, B.R. & Troung, V., 2003b. Surface stickiness of drop of carbohydrate and organic acid solutions during convective drying: Experiments and modelling. *Drying Technology*, **21**, 839-873.

Adhikari, B., Howes, T., Bhandari, B.R. & Troung, V., 2004. Effect of addition of maltodextrin on drying kinetics and stickiness of sugar and acid-rich foods during convective drying: experiments and modelling. *Journal of Food Engineering*, **62**, 53-68**.**

Adhikari, B., Howes, T., Lecomte, D. & Bhandari, B.R., 2005. A glass transition temperature approach for the prediction of the surface stickiness of a drying droplet during spray drying. *Powder Technology*. **149,** 168-179.

Aguilera, J.M., Cuadros, T.R. & del Valle, J.M., 1998. Differential scanning calorimetry of low moisture apple products. *Carbohydrate Polymers*, **37**, 79-86.

Aina, J.O. & Shodipe, A.A., 2006. Colour stability and vitamin C retention of roselle juice (Hibiscus Sabariffa L.) in different packaging materials. *Nutrition & Food Science,* **36(2),** 90-95.

Alabran, D.M. & Mabrouk, A.F., 1973. Carrot Flavour. Sugars and free nitrogenous compounds in fresh carrots. *Journal of Agricultural and Food Chemistry,* **21(2)**, 205-208.

Albersheim, P., Darvill, A., Roberts, K., Staehelin, A. & Varner, J.E., 1997. Cell wall polysaccharide synthesis. *Plant Physiology,* **113**, 1-3.

Allen, G., 1993. A history of the glassy state. In *The Glassy State of Foods.* Blanshard, J.M.V. & Lillford, P.J. (editors), Nottingham University Press. UK.

Al-Kahtani, H.A. & Hassan, B.H., 1990. Spray drying of roselle (*Hibiscus sabdariffa L.*) extract. *Journal of Foods Science,* **55**, 1073-1076.

Ang, H.G., Kwik, W. L., Lee, C. K. & Theng, C.Y., 1986. Ultrafiltration studies of foods: Part 1- The removal of undesirable components in soymilk and the effects on the quality of the spray-dried powder. *Food Chemistry*, **20**, 183-199.

Arvanitoyannis, I., & Blanshard, J.M.V., 1994. Rates of crystallization of dried lactose-sucrose mixtures. *Journal of Food Science,* **59**, 197-205.

Avaltroni, F., Bouquerand, P.E. & Normand, V., 2004. Maltodextrin molecular weight distribution influence on the glass transition temperature and viscosity in aqueous solutions, *Carbohydrate polymer*, **58**(3), 323-334.

Azoubel, P.M., Cipriani, D.C., El-Aouar, A.A., Antonio, G.C. & Murr, F.E.X., 2005. Effect of concentration on the physical properties of cashew juice. *Journal of Food Engineering,* **66**, 413-417.

Bai, Y., Rahman, M.S., Perera, C.O., Smith, B. & Melton, L.D., 2001. State diagram of apple slice; glass transition and freezing curves. *Food Research International*, **34**, 89-95.

Barbosa-Canovas. G. & Vega-Mercado, H., 1996. *Dehydration of Foods,* Chapman & Hall International Thomson Publishing, New York.

Barbosa-Canovas. G., Ortega-Rivas, E., Juliano, P.& Yan, H., 2005. *Food Powders*: *Physical Properties, Processing and Functionality*. Springer, New York.

Burnett, D.J., Thielman, F. & Booth, J., 2004. Determining the critical relative humidity for moisture-induced phase transitions. *International Journal of Pharmaceutics*, **287(1-2)**, 123-133.

Bartolomé, A., P. & Rupérez, P., 1995. Polysaccharides from the cell walls of pineapple fruit. *Journal of Agricultural Food Chemistry*, **43**, 608-612.

Bates, R.P., Morris, J.R. & Crandall, P.G., 2001. *Principles & practices of small and medium scale fruit juice processing*. FAO Bulletin no 146.

Berüter, J., 1985. Sugar accumulation and changes in the activities of related enzymes during development of the apple fruit. *Journal of Plant Physiology*, **121**, 331-341.

Berüter, J., 2004. Carbohydrate metabolism in two apple genotypes that differ in malae accumulation. *Journal of Plant Physiology*, **161**, 1011-1029.

Bergmeyer, H.U. (editor), 1983. *Methods of Enzymatic Analysis*, 3rd edition. Verlag Chemie GmbH, Weinheim, Germany.

Bhandari, B.R. & Howes, T., 1999. Implication of glass transition for the drying and stability of dried foods. *Journal of Food Engineering*, **40**, 71-79.

Bhandari, B.R., Datta, N. & Howes, T., 1997. Problems associated with spray drying of sugar rich foods. *Drying Technology*, **15**, 671-684.

Bhandari, B.R., Senoussi, A, Dumoulin, E.D. & Lebert, A., 1993. Spray drying of concentrated fruit juices. *Drying Technology*, **11**, 1081-1092.

Bhimte, N.A. & Tayade, P.T., 2007. Evaluation of microcrystalline cellulose prepared from sisal fibres as a tablet excipient: A technical note. *AAPS PharmSciTech*, **8(1)**, 1-7.

Boonyai, P., Bhandari, B., & Howes, T., 2004. Stickiness measurement techniques for food powders: A review. *Powder Technology*, **145**, 34-46.

Brause, A.R., 1998. Detection of apple juice adulteration. *Fruit Processing*, **7**, 290-297.

Brause, A.R. & Raterman, J.M., 1982. Fruit and vegetable products, Verification of authenticity of apple juice. *Journal of Association Official Analysis Chemistry*, **65(4),** 846-849.

Briggner, L-E., Buckton, G., Bystrom, K. & Darcy, P., 1994. The use of isothermal microcalorimetry in the study of changes in crystallinity induced during the processing of powders. *International Journal of Pharmaceutics*, **105**, 125-135.

Browne, C.A. & Zerban, F.W., 1941. *Physical and Chemical Methods of sugar analysis. A Practical and Descriptive Treatise for Use in Research, Technical and Control Laboratories.* 3rd edition, John Wiley & Sons,Inc New york.

Boyer, R. F., 1977. in *Encyclopedia of polymer science and Technology, Suppl. Vol. 2,* Bikales, (editor), Interscience, New York.

Butler, M.F. & Cameron, R.E., 2000. A study of the molecular relaxation in solid starch using dielectric spectroscopy. *Polymer*, 41, 2249-2263.

Camerlingo, C., Zenone, F., Delfino, I.D., Diano, N., Mita, D.G. & Lepore, M., 2007. Investigation on clarified fruit juice composition by using Visible Light Micro-Raman Spectroscopy. *Sensors*, **7,** 2049-2061.

Campo, G., Berregi, I, Iturriza, N & Santos, J.I., 2006. Ripening and changes in chemical composition of seven cider apple varieties. Food *Science and Technology International*, **12(6)**, 477-487.

Cano-Chauca, M., Stringheta, P.C., Ramos, A.M. & Cal-Vidal, J., 2005. Effect of carriers on the microstructure of mango powder obtained by spray drying and its functional characterization. *Innovative Food Science and Emerging Technologies*, **6,** 420-428.

Canovas, G.V. & Vega-Mercado, H., 1996. *Dehydration of Foods.* International Thomson Publishing, Florence, USA.

Cassano, A., Drioli, E., Galaverna, G., Marchelli, R., Di Silvestro, G. & Cagnasso, P., 2003. Clarification and concentration of citrus and carrot juices by integrated membrane processes. *Journal of Food Engineering*, **57**, 153-163.

Catalan, J., Diaz, C. & Garcia-Blanco, F., 2003. Characterization of binary solvent mixtures: the water-acetonitrile mixture. *Organic and .Biomolecular.Chemistry*, **1**, 575-580.

Caulfield, D.F. & Moore, W.E., 1974. Effect of varying crystallinity of cellulose on enzymatic hydrolysis. *Wood Science*, **6(4)**, 375-379.

Cahn, R.W., Haasen, P. & Kramer, E.J. (editors)., 2005. *Materials Science and Technology*. Vol. 9, Wiley-VCH, Germany.

Champion, D., Hervet. H., Blond,G., Le Meste, M. & Simatos, D., 1997. Translational Diffusion in sucrose solutions in the vicinity of their glass transition temperature. *Journal of Physical Chemistry*, **101**, 10674-10679.

Chegini G.R., & Ghobadian, B., 2005. Effect of spray-drying conditions on physical properties of orange juice powder. *Drying Technology*, **23(3)**, 657-668.

Chegini G.R., Ghobadian, B., & Barecatin, M., 2005.The study of effective parameters on deposit wall in spray-drying conditions of orange juice powder. *Drying Technology*, **23(3)**, 657-668.

Chegini, G.R., Khazaei, J., Ghobadian, B. & Goudarzi, A. M., 2008. Prediction of process and product parameters in an orange juice spray dryer using artificial neural networks. *Journal of Food Engineering*, **84**, 534-543.

Chen, A.C.C., Mead, B., Lang, C.E., Graham, C.P. & Rizzuto, A.B., 1982. Crystallized, readily water dispersible sugar product. *United State Patent No. 4,338,350*, 1-10.

Chen, W.Z. & Hoseney, R.N., 1995. Development of an objective method for dough stickiness. Lebensmittel-Wissenschaft und-Technologie, 28(5). 467-473.

Chinici, F., Spinabelli, U., Riponi, C & Amati, A., 2005. Optimization of the determination of organic acids and sugars in fruit juices by ion-exclusion liquid chromatography. *Journal of Food Composition and Analysis*, **18**, 121-130.

Chiou, D. & Langrish, T., 2007. Development and characterisation of novel nutraceuticals with spray drying technology. *Journal of Food Engineering*, **82**, 84-91.

Choi. M.M.F & Yiu, T.P., 2004. Immobilization of beef liver catalase on egg shell membrane for fabrication of hydrogen peroxide biosensor. *Enzyme and Microbial Technology*, **34**, 41-47.

Christensen, K.L., Pedersen, G.P. & Kristensen, H.G., 2002. Physical stability of redispersible dry emulsions containing amorphous sucrose. *European Journal of Pharmaceutics and Biopharmaceutics*, **53,** 147-153.

Cinar, I., 2004. Carotenoid pigment loss of freeze dried plant samples under different storage conditions. *Lebensm.-Wiss.u.-Technol*. **37**, 363-367.

Clerjon S., Daudin, J.-D. & Damez, J.-L., 2003. Water activity and dielectric properties of gel in the frequency range 20 MHz – 6 GHz. *Food Chemistry*, **82**, 87-97.

Clement, A., Yong, D. & Brechet, C., 1992. Simultaneous identification of sugars by HPLC using eveaporative light scattering detection (ELSD) and refractive index detection (RI). Application to plant tissues. *Journal of Liquid Chromatography*, **15(5)**, 805-817.

Crowe, C.M., 1971. *Chemical Plant Simulation: An Introduction to Computer-aided Steady-state Process Analysis.* Prentice-Hall international series in the physical and chemical engineering sciences, New York.

deMan, J.M., 1999. *Principles of Food Chemistry.* An Aspen Publication. Maryland, USA.

Dmitrovsky, M., Heights, R. & Kokke, A.H., 1976. Continuous crystallization. *United State Patent No. 3,981,739*, 1-10.

Dolinksky, A., Maletskaya, K. & Snezhkin, Y., 2000. Fruit and vegetable powders production technology on the bases of spray and convective drying methods. *Drying technology*, **18(3)**, 747-758.

Downton, G.E., Flores-Luna, J.L. & King, G. J., 1982, Mechanism of stickiness in hygroscopic, amorphous powders. *Industrial Engineering and Chemistry Fundamentals,* **21(4)**, 447-451.

Edwards, K. & Langrish, A.G., 2004. Characterisation of fruit fibre particles for use as carriers in spray drying. *Chemeca Conference*, 1-4.

El-Sayed, M., Wallack, D.A. & King, C.J., 1990. Change in particle morphology during drying of drops of carbohydrate solutions and food liquids 1 Effects of composition and drying condition. *Industrial & Engineering Chemistry Research,* **20(12)**, 2346-2354.

Fan, J. & Angell, C.A., 1995. Relaxational transitions and ergodicity breaking within the fluid state: the sugars fructose and galactose. *Thermochimica Acta*, **266**, 9-30.

Fennema, O.R.(editor), 1996. *Food Chemistry.* Marcel Dekker, Inc. New York.

Finegold, L., Franks, F., & Hatley, H.M., 1989. Glass/rubber transitions and heat capacities of binary sugar blends. *Journal of the Chemical Society, Faraday Transactions I***, 85**, 2945-2951.

Foster, K.D., Bronlund, J.E., & Paterson, A.H.J., 2005. The Prediction of moisture sorption isotherms for dairy powders. *International Dairy Journal*, **15,** 411-418.

Foster, K.D., Bronlund, J.E. & Paterson, A.H.J., 2006. Glass transition related cohesion of amorphous sugar powders. *Journal of Food Engineering*, **77(4)**, 997-1006.

Frank, F & Murase, N., 1992. Nucleation and crystallization in aqueous systems during drying: Theory and practice. *Pure & Applied Chemistry*, **64(11)**, 1667-1672.

Franks, F., 1993. Solid aqueous solutions. *Pure & Applied Chemistry*, **65(12)**, 2527-2537.

Fuisz, R.C., Battist, G.E. & Myers G.L., 1993. Method of making crystalline sugar and products resulting therefrom. *United State Patent No. 5,597,416*, 1-19.

Fujita, M. & Harada, H., 2001. Ultrastructure and formation of wood cell wall. In *Wood and Cellulosic Chemistry*. Hon, D.N.-S. & Shiraishi, N. (editors). Marcel Dekker, Inc., New York. USA.

Galindo, F.G., Toledo, R.T. & Sjöholm, I., 2005. Tissue damage in heated carrot slices. Compariing mild hot water blanching and infrared heating. *Journal of Food Engineering*, **67**, 381-385.

Georget, D.M.R., Smith, A.C. & Waldron, K.W., 1998. Low moisture thermo-mechanical properties of carrot cell wall material. *Thermochmica Acta*, **315**, 51-60.

Georget, D.M.R., Ng. A., Smith, A.C. & Waldron, K.W., 1998. The thermomechanical properties of carrot cell wall material. *Journal of Science Food Agriculture*. **78**, 73-80.

Georget, D.M.R., Smith, A. C. & Waldron, K.W., 1999. Thermal transitions in freeze-dried carrot and its cell wall components. *Thermochimica Acta*, **332,** 203-210.

Georget, D.M.R., Cairns, P., Smith, A.C. & Waldron, K.W., 1999a. Crystallinity of lyophilised carrot cell wall components. *International Journal of Biological Macromolecules*, **26,** 325-331.

Georget, D.M.R., Smith, A.C. & Waldron, K.W., 2004. The role of mannitol in affecting the thermal transitions in carrot tissue. *Thermochimica Acta*, **417**, 245-249.

Gidley, M.J., Cooke, D. & Ward-Smith, S., 1993. Low moisture polysaccharide systems: Thermal and spectroscopic aspects. In *Glassy State of Foods*, Blanshard, J.M.V., Lillford, P.J. (editors). Nottingham University Press, Nottingham, England.

Goff, H.D., 1995. The use of thermal analysis in the development of a better understanding of frozen food stability. *Pure and Applied Chemistry*, 67(11), 1801-1808.

Goula, A.M. & Adamopoulos, K.G., 2003. Spray drying performance of a laboratory spray dryer for tomato powder preparation. *Drying Technology*, **21**, 1273-1289.

Goula, A.M. & Adamopoulos, K.G., 2005a. Spray drying of tomato pulp in dehumidified air: Part I, The effect on product recovery. *Journal of Food Engineering*, **66,** 25-34.

Goula, A.M. & Adamopoulos, K.G., 2005b. Spray drying of tomato pulp in dehumidified air: Par II The effect on powder properties. *Journal of Food Engineering*, **66,** 35-42.

Goula, A.M., Karapantsios., T.D., Achilias, D.S. & Adamopoulos., K.G., 2008. Water sorption isotherms and glass transition temperature of spray dried tomato pulp. *Journal of Food Engineering*, **85**, 73-83.

Gozlekci, S. & Kaynak, L., undated. Physical and chemical changes during fruit development and flowering in pomegranate (*Punica granatum L.*) cultivar Hicaznar grown in Antalya region. *CIHEAM-Options Mediterraneennes*, 79-85.

Greensmith, M, 1998. *Practical Dehydration*. Woodhead Publishing Limited, Cambridge England.

Gunko, S., Verbych, S. Bryk, M. & Hilal, N., 2006. Concentration of apple juice using direct contact membrane distillation. *Desalination*, **190**, 117-124.

Gupta, A.S., 1978. Spray drying of citrus juice. *American Institute of Chemical Engineers*, 7th Annual meeting, paper no.55f.

Haque, M. K. & Roos, Y.H., 2004. Water sorption and plasticization behaviour of spray-dried lactose/ protein mixtures. *Journal of Food Engineering and Physical Properties,* **69(8),** 384-391.

Haque, M. K. & Roos, Y.H., 2005. Crystallization and X-ray Diffraction of crystals formed in water-plasticized amorphous spray-dried and freeze dried lactose/protein mixtures. *Journal of Food Engineering and Physical Properties,* **70(5),** 359-366.

Haque, M. K. & Roos, Y.H., 2006. Differences in the physical state and thermal behaviour of spray-dried and freeze-dried lactose and lactose/protein mixtures. *Innovative Food Science and Engineering Technologies*,. 7(1-2), 62-73.

HP 1047A Refractive Index Detector User's Guide,1994. Hewlett Packard, Third Edition.

HP 1047A RID Service Manual Version 12/2001 Agilent Technologies Online Service. Publication number: 01047-90100.
http://www.chem.agilent.com/scripts/literaturepdf.asp?iWHID=26377

Huang, L.X., Han, L., Wang, Z. L. & Hou, Y. F., 2001. Study on preparation of modified edible micro-crystalline cellulose power by spray drying. *Chemistry and Industry of Forest Products*, **21**, 1-5.

Hui, Y.H., 2005. *Handbook of Food Science, Technology, and Engineering*. CRC Press.

Huntington, D.H., 2004. The influence of the spray drying process on product properties. *Drying technology*, **22(6)**, 1261-1287.

Hurtta, M. Pitkänen, I & Knuutinen, J., 2004. Melting behaviour of D-sucrose, D-glucose and D-fructose. *Carbohydrate Research*, **339**, 2267-2273.

Ikeda, S., Kumagai, H. & Nakamura, K., 1997. Dielectric analysis of food polysaccharides in aqueous solution. *Carbohydrate Research*, **301**. 51-59

Imai, T., Sugiyama, J. & Itoh, T., 1997. Structure determination of cellulose microfibrils in the cell wall of *Cladophora*. *47th Annual Meeting of the Japan Wood Research Society*. 28-30.

Israkarn, K. & Charoenrein, S., 2006. Influence of annealing temperature on T_g' of cooked rice-stick noodles. *International Journal of Food Properties*, **9(4)**, 759-766.

Ivin, K. J.,1977. Transitions and relaxations in *Encyclopedia of Polymer Science and Technology, Suppl. Vol. 2,* Bikales, N. M. (editor), Interscience, New York.

Jackman. R.L. & Stanley, D.W., 1995. Perspectives in the textural evaluation of plant foods. *Trends in Food science & Technology*, **6**, 187-194.

Jaya, S. & Das, H., 2007. Glass transition and sticky point temperatures and stability/mobility diagram of fruit powders. *Food Bioprocess Technology*, 1-7.

Jayaraman, K. S. & Das Gupta, D. K., 2007. Drying of fruit and vegetables in *Handbook of Industrial Drying,* 3rd edition, Mujumdar, A. S.(editor), CRC Press, New York.

Jouppila, K. & Roos, Y. H., 1994. Water sorption and time-dependent phenomena of milk powders. *Journal of Dairy Science*, **77(7),** 1798-1808.

Keit, A. & King, C. J., 1985. Factors governing surface morphology of spray-dried amorphous substances. *Drying Technology*, **3**, 321-348.

Kalichevsky, M.T., Jaroszkiewicz, E.M. & Blanshard, J.M.V., 1993. A study of the glass transition of amylopectin-sugar mixtures. *Polymer*, **34(2),** 346-358.

Kenyon, M.M., 1995. Modified starch, maltodextrin, and corn syrup solids as wall materials for food encapsulation. *ACS Symposium Series*, **590**, 42-50.

Kilmartin, P. A., Reid, D.S. & Samson, I., 2000. The measurement of the glass transition temperature of sucrose and maltrose solutions with added NaCl. *Journal of the Science of Food and Agriculture*, **80**, 2196-2202.

Kilmartin, P. A., Reid, D.S. & Samson, I., 2004. Dielectric properties of frozen maltodextrin solutions with added NaCl across the glass transition. *Journal of the Science of Food and Agriculture*, **84**, 1277-1284.

Kittaka, S., Kuranishi, M., Ishimaru, S. & Umahara, O., 2007. Phase separation of acetonitrile-water mixtures and minimizing of ice crystallities from there in confinement of MCM-41. *Journal of Chemical Physics*, **126**, 091103-1 - 091103-4.

Klages, K., Donnison, H., Wünsche, J & Boldingh, H., 2001. Diurnal changes in non-structural carbohydrates in leaves phloem exudates and fruit in Braeburn apple. *Australia Journal of Plant Physiology*, **28**, 131-139.

Kudra,T., 2003. Sticky region in drying - Definition and identification. *Drying Technology*, **21(8)**, 1457-1469.

Kuprovskyte, K., Pranaityte, B. & Padarauskas, A., 2002. Isocratic HPLC determination of preservatives in beverages. *Chemija (Vilnius),* **13(3),** 160-163.

Laaksonen, T. J. & Roos, Y. H., 2000. Thermal, dynamic-mechanical and dielectric analysis of phase and state transitions of frozen wheat doughs. *Journal of Cereal Science*, **32,** 281-292.

Laaksonen, T. J. & Roos, Y. H., 2001. Dielectric relaxations of frozen wheat doughs containing sucrose, NaCl, Ascorbic acid and their mixtures. *Journal of Cereal Science*, **33,** 331-340.

Langrish, T.A. & Wang, E., 2006. Crystallisation of powders of spray-dried lactose, skim milk and lactose-salt mixtures. *International Journal of Food Engineering*. **2**(4), 1-15.

Langrish, T.A.G., Chan, W.C. & Kota, K., 2007. Comparison of maltodextrin and skim milk wall deposition rates in a pilot-scale spray dryer. *Powder Technology*, **179**, 84-89.

Langrish, T.A.G. & Chiou, D., 2008. Stabilization of moisture sorption in spray-dried bioactive compounds by using novel fibre carriers to crystallize the powders. *International Journal of Food Engineering*, **4(1)**, 1-7.

Levine, H. & Slade, L.A., 1986. A polymer physic-chemical approach to the study of commercial starch hydrolysis products (SHPs). *Carbohydrate Polymer*, **6**, 213-244.

Liapis, A. I. & Bruttini, R., 2007. Freeze drying. In *Handbook of industrial drying*, 3rd edition, Mujumdar, A. S. (editor), CRC Press, New York.

Linskens, H.F., & Jackson, J. F. (editors), 1995. *Modern Methods of Plant Analysis, Volume 18, Fruit Analysis.* Springer-Verlag Berlin Heidelberg, Germany.

Liao, X., Raghavan, G.S.V. & Yaylayan, V.A., 2002. Dielectric properties of aqueous solutions of • -D-glucose at 915 MHz. *Journal of Molecular Liquids*, **100(3)**, 199-205.

Liao, X., Raghavan, G.S.V., Dai, J. & Yaylayan, V.A., 2003. Dielectric properties of aqueous solutions of • -D-glucose at 2450 MHz. *Food Research International*, **36**, 485-490.

Lievonen, S.M. & Roos, Y.H., 2003. Comparison of dielectric properties and non-enzymatic browning kinetics around glass transition. *Innovative Food Science and Emerging Technologies*, **4**, 297-305.

Lin, L-H, Yuen, H.K. & Varner, J.E., 1991. Differential scanning calorimetry of plant cell walls. *Proc. Natl. Acad. Sci. USA*, **88**, 2241-2243.

Lockemann, C.A., 1999. A new laboratory method to characterize the sticking properties of free flowing solids. *Chemical Engineering and Processing*, **38,** 301-306.

Lukanin, O.S., Gunko, S.M., Bryk, M.T., Nigmatullin, R.R., 2003. The effect of content of apple juice biopolymers on the concentration by membrane distillation. *Journal of Food Engineering*, **60**, 275-280.

Marshall, W.R., 1954. *Atomization and Spray Drying*. American Institute of Chemical Engineers. Lancaster, Pennsylvania, the Science Press.

Mason, M., 1983. Determination of glucose, sucrose, lactose and ethanol in foods and beverages, using immobilized enzyme electrodes. *Journal of Associate Official Analytical Chemistry*, **66(4),** 981-984.

Masters, K., 1972. *Spray Drying: an Introduction to Principles, Operational Practice and Applications,* Chemical and process engineering series. London: L. Hill.

Masters, K., 1980. Foodstuffs - Where spray drying plays a role. *Chemical Engineering*, **354**, 145-148.

Masters, K., 1985. *Spray Drying*, 4th edition., Longman Sci. and Techn., John Wiley and Sons, New York.

Masters, K., 1994. Modern developments in spray drying particle structure and safety. Seminar paper in modern developments in industrial drying technology centre for continuing education. University of Canterbury. New Zealand.

Masters, K., 1997. *Industrial Drying of Foods; Spray Drying*. Baker, C G J.(editor), Blackie Academic & Professional London.

Masters, K., 2004. Applying spray drying to customize powder manufacture. *Chinese Journal of Chemical Engineering*, **12(6),** 744-749.

Mendonca, J.C.F., Franca, A.S. & Oliveira, L.S., 2007. A comparative evaluation of methodologies for water content determination in green coffee. *LWT*, **40 ,**1300-1303.

Mermelstein, N. H, 2001. Products and technologies processing; Spray drying. *Food Technology*, **55** (4).

Miao, S. & Roos Y.H. 2004. Comparison of nonenzymatic browning kinetics in spray dried and freeze dried carbohydrate-based food model system. *Journal of Food Science*, **69(7),** 322-331.

Monica, T.K. & Blanshard, J., 1993. The effect of fructose and water on the glass transition of amylopectin. *Carbohydrate polymers*, **20**, 107-113.

Moore,G.R.P., Canto, L.R., Amante, E.R. & Soldi, V.C., 2005. Cassava and corn starch in maltodextrin production. *Quim Nova* [online], **28(4)**, 596-600.

Mormino.R., 2001. Cellulose production in a RBC. In *Chemical Engineering*. Troy, NY: Rensselaer Polytechnic Institute, New York.

Nawirska, A. & Kwasniewska,M., 2005. Dietary fibre fractions from fruit and vegetable processing waste. *Food Chemistry*, **91**, 221-225.

Newey, C. & Weaver, G. (editors), 1991. *Material Principles and Practice*. Butterworth Scientific, UK.

Nielsen, S.S. (editor), 2003. *Food Analysis*, 3rd edition, Kluwer Academic/ Plenum Publishers, New York.

Niro powder technology, nd. *Small-scale Spray Drying from the Industry's Leading Supplier For R&D and Small Scale Production*.

Noel, T.R., Ring, S.G. & Whittam, M.A., 1992. Dielectric relaxations of small carbohydrate molecules in the liquid and glassy states. *The Journal of Physical Chemistry*, **96(13)**, 5662-5667.

Noel, T.R., Parker, R. & Ring, S.G., 1996. A comparative study of the dielectric relaxation behaviour of glucose, maltose, and their mixtures with water in the liquid and glassy states. *Carbohydrate Research*, **282**, 193-206.

Noel, T.R., Parker, R. & Ring, S.G., 2000. Effect of molecular structure and water content on the dielectric relaxation behaviour of amorphous low molecular weight carbohydrates above and below their glass transition. *Carbohydrate Research*, **329**, 839-854.

Nyman, M., Nylander, T. & Asp, N-G., 1993. Degradation of water-soluble fibre polysaccharides in carrots after different types of processing. *Food Chemistry*, **47**, 169-176.

Ollett, A.-L & Parker, P., 1990. The viscosity of supercooled fructose and its glass transition temperature. *Journal of Texture Studies*, **21**, 355-362.

Orford, P.D., Parker, R., Ring S.G., & Smith, A.C., 1989. Effect of water as a diluents on the glass transition behaviour of malto-oligosaccharides, amylase and amylopectin. *International Journal of Biological Macromolecules*, **11(2),** 91-96.

Otles, S. & Otles, S., 2005. Glass transition in food industry-characteristic properties of glass transition and determination techniques. *Electronic Journal of Polish Agricultural Science (Food Science and Technology)*, **8(4)** #69.

Otsuka, H. & Take, T., 1969. Sapid components in carrot. *Journal of Food Science,* **34(5)**, 392-394.

Ozmen, L. & Langrish, T.A.G., 2003. An experimental investigation of the wall deposition of milk powder in a pilot-scale spray drier. *Drying Technology*. **21,** 1253-1272.

Passonneau, J.V. & Lowry, O.H., 1993. *Enzymatic Analysis, A Practical Guide*. Humana Press, New Jersey, USA.

Paterson, A.H., Bronlund, J.E., Zuo, J.Y. & Chatterjee, R., 2006. Analysis of particle-gun-derived dairy powder stickiness curves. *International Dairy Journal*, doi:10.1016/j.idairyj.2006.08.013.

Peleg, M., 1993. Mapping the stiffness-temperature-moisture relationship of solid biomaterials at and around their glass transition. *Rheological Acta*, **32**, 575-580.

Phatak, L., Chang, K.C. & Brown, G., 1988. Isolation and characterisation of pectin in sugar-beet pulp. *Journal of Food science*, **53(3)**, 830-833.

Pomeranz, Y. & Meloan, C.E., 1994. *Food Analysis Theory and Practice*. 3rd edition, Chapman & Hall, One Penn Plaza New York.

Quek, S.Y., Chok, Ng. K. & Swedlund, P., 2007. The physicochemical properties of spray-dried watermelon powders. *Chemical Engineering and Processing*, **46**, 386-392.

Rahman, M.S., 1995, *Food Properties Handbook*. Boca Raton, CRC Press. Florida, USA.

Ramos, A.M. & Ibarz, A., 1998. Density of juice and fruit puree as a function of soluble solids content and temperature. *Journal of Food Engineering*, **35**, 57-63.

Ramula, P. & Rao, P.U., 2003. Dietary fibre content of fruit and leafy vegetables. *Nutrition News*, **24**, 1-6.

Reid, D.S., Kerr, W. & Hsu, J., 1994. The glass transition in the freezing process. *Journal of Food Engineering*, **22**, 483-494

Rodriguez-Hern Rodriguez-Hernandez, G. R., Abud-Archila, M., Gonzalez-Garcia, R., Grajales-Lagunes, A. & Ruiz-cabrera. M .A., 2005. Spray drying of cactus pear juice (*Opuntia streptacantha*): Effect on the physicochemical properties of powder and reconstituted product. *Faculty of Chemical Engineering, University of Autonoma de San Luis Potosi,* Maxico.

Roos, Y.H., 1993. Melting and glass transitions of low molecular weight carbohydrates. *Carbohydrate Research*, **238**, 39-48.

Roos, Y.H., 1995. *Phase Transitions in Foods.* Academic Press, New York, USA.

Roos, Y.H., 2002. Importance of glass transition and water activity to spray drying and stability of dairy powders. *Lait,* **82(4),** 475-484.

Roos, Y.H. & Karel, M., 1990. Differential scaning calorimetry study of phase transitions affecting the quality of dehydrated materials. *Biotechnology Progress,* **6(2),** 159-163.

Roos, Y.H. & Karel, M., 1991. Plasticizing effect of water on thermal behaviour and crytallization of amorphous food models. *Journal of Food Science*. **56**, 38-43.

Roos, Y.H. & Karel, M., 1991(a). Phase transition of mixtures of amorphous polysaccharides and sugars. *Biotechnology Progress,* **7**, 49-53.

Roos, Y.H. & Karel, M., 1991(b). Water and molecular weight effects on glass transitions in amorphous carbohydrates and carbohydrate solutions. *Journal of Food Science.* **56(1)**, 1676-1681.

Roos, Y.H. & Karel, M., 1992. Crystallization of amorphous lactose. *Journal of Food Science,* **57(3),** 775-777.

Roos, Y.H. & Karel, M., 1993. Effects of glass transition on dynamic phenomena in sugar containing food systems. In Blanshard, J.M.V. & Lillford, P.J. (editors), *The glassy states in foods*. Nottingham University Press. London, UK.

Roudaut, G., Simatos, D., Champion, D., Contreras-Lopez, E., & Meste, M. Le., 2004, Molecular mobility around the glass transition temperature: A mini review. Innovative Food Science and Emerging Technologies, 5, 127-134.

Sablani, S.S., Kasapis, S & Rahman, M.S., 2007. Evaluating water activity and glass transition concepts for food stability. *Journal of Food Engineering*, **78**, 266-271.

Saka, S., 2001. Chemical composition and distribution. In Wood and cellulosic chemistry. Hon, D.N.-S. & Shiraishi, N. editors. Marcel Dekker Inc. New York, USA.

Salmen, L., Back, E. and Alwarsdotter, Y.,1984. Effects of non-aqueous plasticizers on the thermal softening of paper, *Journal of Wood Chemistry and Technology*, **4**(3), 347-365.

Sano, Y., 1992. Drying of polymer solution. *Drying Technology*, **10**, 591-622.

Saravacos, G.D. & Kostarropoulos, A.E., 2002. *Handbook of processing equipment*. Kluwer Academic/Plenum Publishers. New York, USA.

Schols, H.A. & Voragen, A.G.J., 1994. Occurrence of pectic hairy regions in various plant cell wall materials and their degradability by rhamnogalacturonase. *Carbohydrate Research*, **256**, 83-95.

Senoussi, A., Dumoulin, E. & Berk, Z., 1995. Retention of diacetyl in Spray-drying and storage. *Journal of Food Science*, **60(5),** 905-912.

Seo, J., Kim, S.J., Kwon, H., Yang, Y.S., Kim, H.K. & Hwang, Y., 2006. The glass transition of sugar mixtures. *Carbohydrate Research*, **341**, 2516-2520.

Sergeeva, L.I. & Vreugdenhil, D., 2002. In *situ* staining of activities of enzymes involved in carbohydrate metabolism in plant tissues. *Journal of Experimental Botany*. **53(367)**, 361-370.

Seata, G., 2006. Determination of sugars in Royal jelly by HPLC, *Apidologie Journal*, **37**, 84-90.

Sharma, S.K., Mulvaney. S.J. & Rizvi, S.S., 2000. *Food Process Engineering: Theory and Laboratory Experiments*. Wiley-interscience A John Wiley & Sons, inc., Publication. New York, USA.

Shamsudin, R., Daud, W.R.W., Takriff, M.S. & Hassam, O., 2007. Physicochemical properties of the Josapine variety of pineapple fruit. *International Journal of Food Engineering*, **3(5),** 1-9.

Shashirekha, M.N., Baskaran, R., Rao, L.J., Vijayalakshmi, M.R. & Rajarathnam, S., 2008. Influence of processing conditions on flavour compounds of custard apple (*Annona squamosa* L.). *LWT*, **41**, 236-243.

Shlieout, G., Arnold, K. & Müller, G., 2002. Powder and mechanical properties of microcrystalline cellulose with different degrees of polymerization. *AAPS PharmSciTech*, **3(2)**, 1-10.

Shrestha, A.K., Ua-arak, Th., Adhikari, B.P., Howes, T. & Bhandari, B.R., 2007. Glass transition behaviour of spray dried orange juice powder measured by differential scanning calorimetry (DSC) and thermal mechanical compression test (TMCT). *International Journal of Food Properties*, **10**, 661-673.

Simperler, A., Kornherr, A., Chopra, R., Arnaud Bonnet, P., Jones, W., Samuel Motherwell, W.D. & Zifferer, G., 2006. Glass transition temperature of glucose, sucrose and trehalose: An experimental and in Silico Study. *Journal of Physical Chemistry*, **110**, 19678-19684.

Šimkovic, I., Šurina, I & Vri•an, M., 2003. Primary reactions of sucrose thermal degradation. *Journal of Annalysis Applied Pyrolysis*, **70**, 493-504.

Slade, L. & Levine, H., 1988. Non-equilibrium behaviour of small carbohydrate-water systems. *Pure & Apply Chemistry*, **60(12)**, 1841-1864.

Slade, L. & Levine, H., 1991. Beyond water activity: Recent advances based on an alternative approach to the assessment of food quality and safety. *Critical Reviews in Food Science and Nutrition*, **30(2-3)**, 115-360.

Slade, L. & Levine, H., 1993. Glass transition and water-food structure interactions. In Taylor, L. & Kinsella, J.F.(editors). *Advances in Nutrition and Food Research*. Academic Press, San Diego, 103-269.

Slade, L., Levine, H., Ievolella, J. & Wang, M., 1993. The glassy state phenomenon in applications for the food industry: Application of the food polymer science approach to structure-function relationships of sucrose in cookie and cracker systems. *Journal of the Science and Food Agriculture*. **63(2):** 133-176.

Slight, H.A., 1989. The measurement of moisture content. *Measurement + control*, **22(2)**, 42-44.

Slimestad, R. & Vagen, I. M., 2006. Thermal stability of glucose and other sugar aldoses in normal phase high performance liquid chromatography. *Journal of Chromatography A.*, **1118**, 281-284.

Soesanto, T. & Williams, M.C., 1981. Volumetric interpretation of viscosity for concentrated and dilute sugar solutions. *Journal of Physical Chemistry*, **85**, 3338-3341.

Song, C.S., Nam, J.H., Kim, C.-J. & Ro, S.T., 2005. Temperature distribution in a vial during freeze-drying of skim milk. *Journal of Food Engineering*, **67**, 467-475.

Sperling, L.H., 2006. *Introduction to Physical Polymer Science*. 4th edition, Wiley Publisher, USA.

Stevens, B.J.H. & Selvendran, R.R., 1984. Structural features of cell wall polymers of the apple. *Carbohydrate Research*, **135**, 155-166.

Sun, R. & Hughes, S., 1998. Fractional extraction and physico-chemical characterization of hemicellulose and cellulose from sugar beet pulp. *Carbohydrate Polymers*, **36**, 293-299.

Suojala, T., 2000. Variation in sugar content and composition of carrot storage roots at harvest and during storage. *Scientia Horticulturae*, **85**, 1-19.

Tai, c.-Y. & Chen, B.H., 2000. Analysis and stability of carotenoids in the flowers of Daylily (*Hemerocallis disticha*) as affected by various treatments. *Journal of Food Chemistry*, **48**, 5962-5968.

Takiyama, H., Suzuki, H., Uchida, H. & Matsuoka, M., 2002. Determination of solid-liquid phase equilibria by using measured DSC curves. *Fluid Phase Equilibria*, **194-197**, 1107-1117.

Tchoumboue, J., Awah-Ndukum., J., Fonteh, F.A., Dongock.N.D., Pinta, J. & Mvondo Ze. A., 2007. Physico-chemical and microbiological characteristics of honey from the sudano-guineanzone of West Cameroon. *African Journal of Biotechnology.* **6(7),** 908-913.

Tijskens, L.M.M., Waldron, K.W., Ng, A., Ingham, L. and van Dijk, C., 1997. The kinetics of pectin Methyl Esterase in Potatoes and carrot during blanching, *Journal of Food Engineering*, **34**, 371-378.

To, E.C., & Flink, J.M., 1978. Collapse, a structural transition in freeze dried carbohydrates II. Effect of solute composition. *Journal of Food Technology,* **13,** 567-581.

Toledo, R.T., 1991. *Fundamentals of food process engineering*. 2nd edition An Aspen Publication. Maryland, USA.

Truong, V., Bhandari, B.R. & Howes, T., 2005.Opimizaion of co-current spray drying process of sugar-rich foods. Part I – Moisture and glass transition temperature profile during drying. *Journal of Food Engineering,* **71**, 55-65.

Tsourouflis, S., Flink, J.M. & Karel, M., 1976. Loss of structure in freeze dried carbohydrate solusions: Effect of temperature, moisture content and composition. *Journal of the Science of Food and Agriculture,* **27**, 509-519.

U.S. Department of Health and Human Services Public, 1996. *Standardized Method for HPLC Identification of Mycobacteria.*

Vaillant, F., Jeanton, E., Dornier, M., O'Brien, G. M., Reynes, M. & Decloux, M., 2001, Concentration of passion fruit juice on an industrial pilot scale using osmotic evaporation. *Journal of Food Engineering,* **47**, 195-202.

Van Arsdel, W.B., 1973. *Food Dehydration*. 2nd edition. Vol. 2, Westport. Connecticut, USA.

Vehring, R., Foss, W.R. & Lechuga-Ballesteros, D., 2007. Particle formation in spray drying. *Journal of Aerosol Science,* **38**, 728-746.

Venkatest, M.S. & Raghavan, G.S.V., 2005. An overview of dielectric properties measuring techniques. *Canadian Biosystems Engineering,* **47**, 7.15-7.30.

Voragen, G.J., Timmers, P.J., Linssen, P.H., Schols, A. & Pilnik, W., 1983. Methods of analysis for cell wall polysaccharides of fruit and vegetables. *Zlebensm Unters Forsch*.**177**, 251-256.

Wallack, D.A. & King, C.J., 1988. Sticking and agglomeration of hygroscopic, amorphous carbohydrate and food powders. *Biotechnology Progress***, 4**, 31-35.

Wallack, D.A., El-Sayed, M., & King, C.J., 1990. Change in particle morphology during drying of drops of carbohydrate solutions and food liquids 2 Effects of drying rate. *Industrial & Engineering Chemistry Research,* **20(12)**, 2354-2357.

Waldron, K.W., Parker, M.L. & Smith, A.C., 2003. Plant cell walls and food quality. *Comprehensive Review in Food Science and Food Safety*, **2**,101-119.

Wang, H., Zhang, Sh. & Chen, G., 2008. Glass transition and state diagram for fresh and freeze dried Chinese gooseberry. *Journal of Food Engineering*, **84**, 307-312.

Wang, Y-J. & Wang, L., 2000. Structures and properties of commercial maltodextrins from corn, Potato, and rice starches. *Starch/Stärke*, **52**, 296-304.

Walstra, P., 2003. *Physical Chemistry of Foods*. CRC Press, USA.

Weimer, P. J., Hackney, J. M. & French, A.D., 1995. Effects of chemical treatments and heating on the crystallinity of cellulose and their implications for evaluating the effect of crystallinity on cellulose biodegradation. *Biotechnology and Bioengineering*, **48**,169-178.

William-Gardner, A., 1971. *Industrial Drying*. Chemical and Process Engineering Series. Leonardo Hill. London, UK.

Wosiacki, G., Nogueira, A., Denardi, F. & Vieira, R.G., 2007. Sugar composition of depectinized apple juice. *Semina: Ciências Agrárias, Londrina*, **8(4)**, 645-652.

Wungtanagorn, R. & Schmidt, S.J., 2001. Thermodynamic properties and kinetics of the physical aging of amorphous glucose, fructose and their mixture. *Journal of Thermal analysis Calorimetry*, **65**, 9-35.

Yildiz, S. & Gümü•kaya, E., 2007. The effects of thermal modification on crystalline structure of cellulose in soft and hard wood. *Building and Environment*, **42**, 62-67.

Youn, K.-S, Hong, J.-H, Bae, D.-B, Kim, S.-J & Kim, S.-D., 2004. Effective clarifying process of reconstituted apple juice using membrane filtration with filter-aid pretreatment. *Journal of Membrane Science*, **228**, 179-186.

Appendix: Sugars determination in fruit and vegetable juice by HPLC 1100 series and RID HP 1047A

Introduction

The information about HPLC and RID appears in this part is the summary from various sources as indicated in the references.

High Performance Liquid Chromatography (HPLC) is a chemistry based tool for quantifying and analyzing mixtures of chemical compounds. It's used to find the amount of a chemical compound within a mixture of other chemicals, based on a variety of chemical interactions between the substance being analyzed and the chromatography column. It is an analytical technique for the separation and determination of organic and inorganic solutes in any samples especially biological, pharmaceutical, food, environment, industrial, etc.

The fundamental basis for HPLC consists of passing a sample (analytic mixture) in a high pressure solvent (the mobile phase) through a steel tube (column) packed with sorbents (the stationary phase). As the analytic mixture pass through the column they interact between the two phases, mobile and stationary phase, at different rates. The difference in rates is primarily due to different polarities for the analytes. The analytes that have the least amount of interaction with the stationary phase or the most amount of interaction with the mobile phase will exit the column faster. Repeated interactions along the length of the column effect a separation of the analytes.

The stationary phase is usually in the form of small-diameter (5-10 mm) uniform particles, packed into a cylindrical column, to allow certain sized analytes to pass through at different rates. The typical column is constructed from a rigid material (stainless steel or plastic) and generally 5-30 cm long and the internal diameter is in the range of 1-9 mm, to allow different sample sizes to be analyzed.

Various mixtures of analytes can be analyzed by changing the polarities of the stationary phase and a mobile phase. Changing in the polarity of the mobile phase is another variable that can affect the efficiency of HPLC separation. The mobile phase polarity is generally the opposite of stationary phase. The multisolvent delivery system allows the polarity of

the mobile phase to be changed during the course of the HPLC run. The rate at which the polarity is changed defines the “gradient”. This gradient technique helps to further separate mixtures of variously polar analytes. The gradient elution can be done by progressively increasing the proportion of organic solvent or salt buffer with time. When the solvent composition remains constant throughout the analysis the elution is called isocratic. The basic system component of HPLC is shown in figure1. The chromatogram processes occur in a column is shown in figure 2.

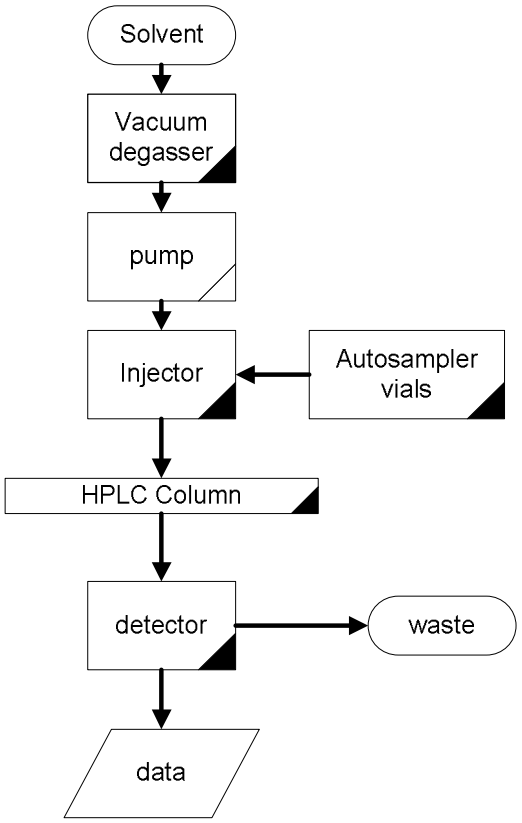

Figure A.1. Basic system component of HPLC

Function of each component

Solvent delivery system**:** pushes the solvent stream through the instrument at a constant flow rate. The solvent delivery system is equipped with an inline filter. Check the solvent filter to see if it is choked up; wash it if it is. All solvents use in HPLC system must be HPLC grade and use only the same barcode from the beginning until finish the whole analysis. Solvents used include any miscible combination of water or various organic liquids. The most common solvents are methanol and acetonitrile. Water may contain buffers or salts to assist in the separation of the analyte components.

Vacuum Degasser**:** preventing of foaming with the dissolution gas in liquid and curtailment of the chemical, physical, and biological influence of the dissolution gas in liquid itself, or stabilization. Degassing removes and prevent obstacle at the time of measurement and quantification, maintain precision during the use of HPLC or precision analysis vessel, prevention of oxidization / decomposition of substance during extract of dissolved oxygen, and prevention of underwater microbe propagation.

Autosampler vials**:** introduces the sample into the liquid stream of the instrument.

Column**:** a stainless steel tube packed with silicon beads that separate what we are looking for from other compounds.

Detector**:** an optical sensor that detects changes in the characteristics of the solvent stream

Data System: a means of controlling the system components and storing, processing and displaying data

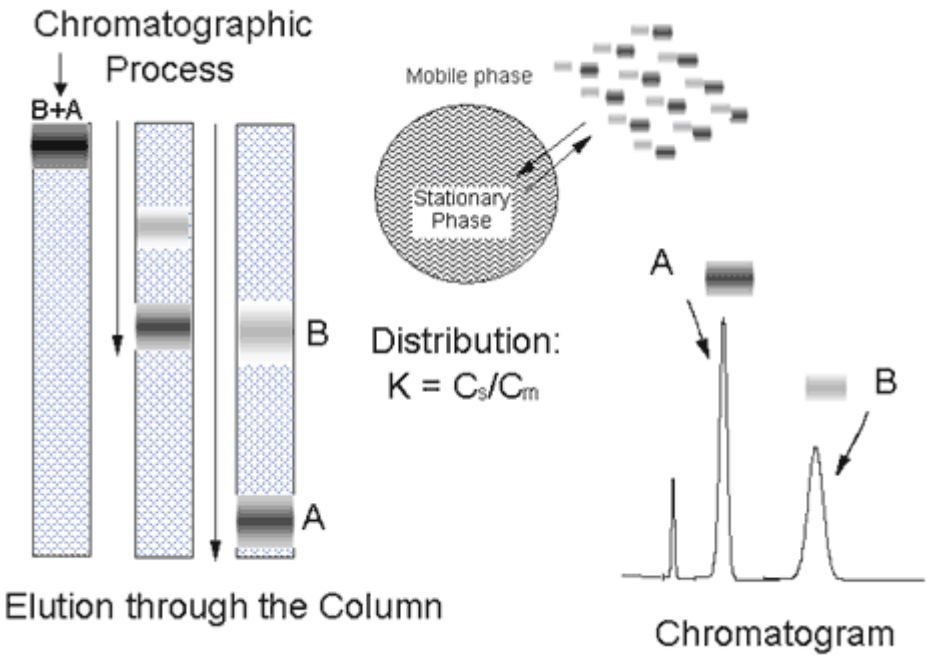

Separation can be achieved by controlling and manipulating these interactions, which effect the relative retention times of the various sample components. C_s = concentration of a solute in the stationary phase, C_m = concentration of a solute in the mobile phase

Figure A.2. Chromatographic process occurs in the column (http://www.waters.com/WatersDivision/ContentD.asp?watersit=JDRS-5LTGBH)

Types of HPLC

HPLC chromatography has been divided into four types; normal phase, reversed phase, size exclusion, and ion exchange chromatography.

Normal phase chromatography

Normal phase HPLC (NP-HPLC) was the first kind of HPLC setup used, and it retains analyte based on polarity. This method uses a polar stationary phase and a non-polar mobile phase, and it used when the analyte of interest has a polar nature. The polar analyte associates with and is retained by the polar stationary phase. NP-HPLC has fallen out of favour recently with the development of reversed phase HPLC. Figure 3 shows elution order in normal phase HPLC

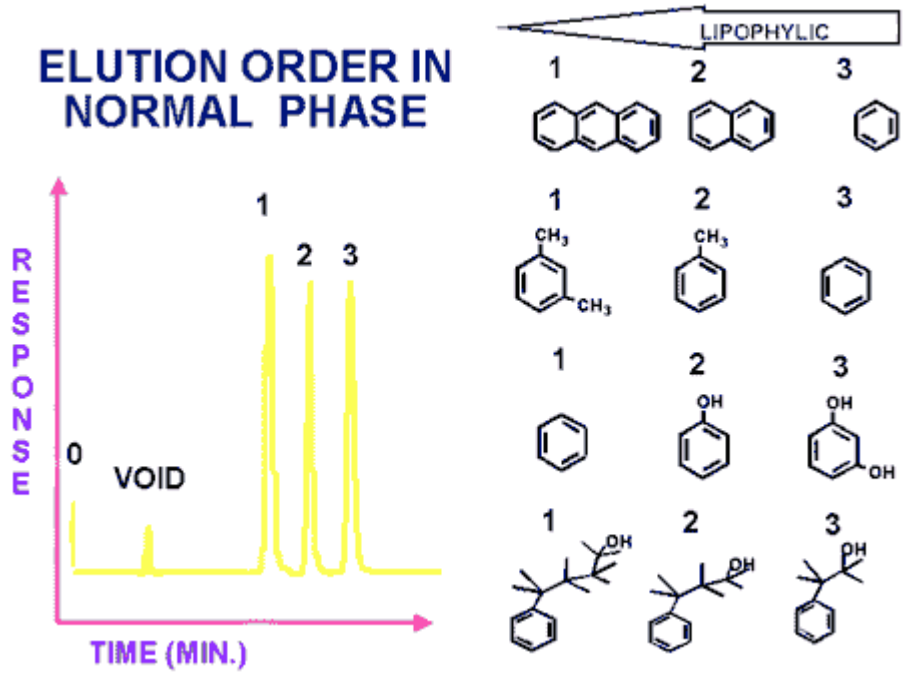

Figure A.3. The elution order in normal phase HPLC

Reversed phase chromatography

The reversed phase HPLC (RP-HPLC) consists of a non-polar stationary phase and a polar mobile phase. It was developed due to the increasing interest in large non-polar biomolecules. One common stationary phase is a silica which has been treated with RMe_2SiCl, where R is a straight chain alkyl group such as $C_{18}H_{37}$ or C_8H_{17}. The retention time is therefore longer for molecules which are non-polar in nature, allowing polar

molecules to elute more readily. Reversed phase columns are quite difficult to damage compared with normal silica columns. However, they should never be used with strong aqueous bases as these will destroy the silica. They can be used with aqueous acid but the column should not be exposed to the acid for too long, as it can corrode the metal parts of the HPLC equipment. The metal content of HPLC columns must be kept low if the best possible ability to separate substances is to be retained. A good test for the metal content of a column is to inject a sample which is a mixture of 2,2'- and 4,4- bipyridine. Because the 2,2'-bipyridine can chelate the metal. It is normal that when a metal ion is present on the surface of the silica the shape of the peak for 2,2-bipyridine will be distorted, tailing will be seen on this distorted peak. Figure 4 shows elution order in reversed phase HPLC

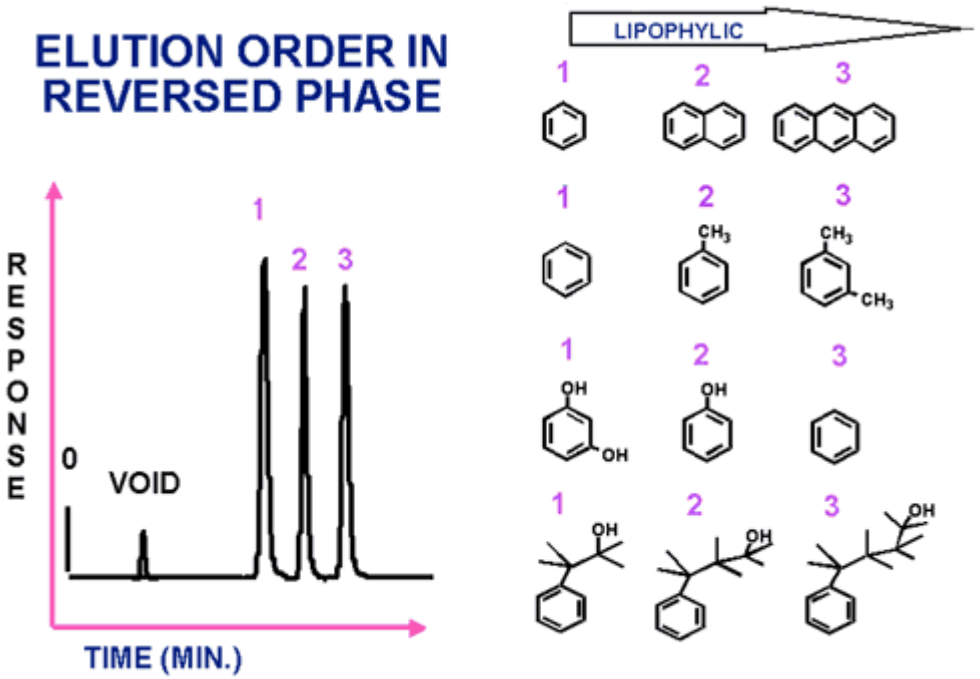

Figure A.4. The elution order in reversed phase HPLC.

Size exclusion chromatography

Size exclusion chromatography (SEC), also known as gel permeation chromatography or gel filtration chromatography. SEC separates particles on the basis of size. It is generally a low resolution chromatography and thus it is often reserved for the final, "polishing" step of purification. It is also useful for determining the tertiary structure and quaternary structure of purified proteins.

Ion exchange chromatography

Ion exchange chromatography allows the separation of ions and polar molecules based on the charge properties of the molecules. It can separate proteins based on their isoelectric points and is often used as a first step in protein purification. Both positively-charged and negatively-charged molecules can be separated based on their charge, meaning that this process is not just restricted to proteins. Figure 5 shows ion exchange inside a pore in the stationary phase.

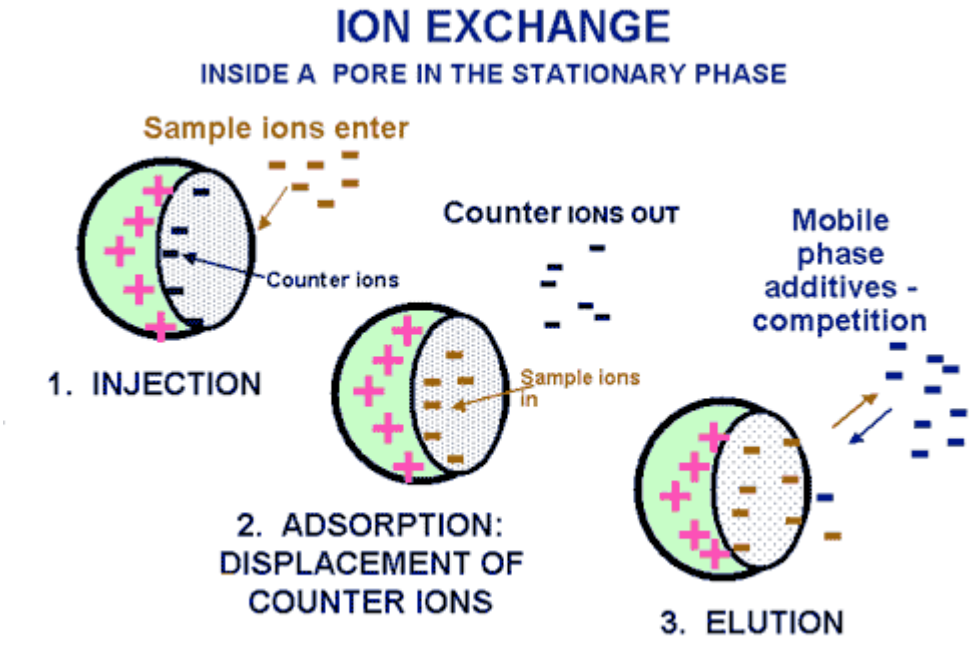

Figure 5. Ion exchange inside a pore in the stationary phase.

HPLC detectors

Detectors are instruments which sense the presence of a compound passing through, and provide an electronic signal to a recorder or computer data station. Output is usually peaking, that is, the chromatogram. As the analytes exit the column, they can be detected by various means such as refractive index (RID) monitors, electrochemical, ultraviolet-absorbance (UV), fluorescence and evaporative light scattering detection (ELSD). Changes in the mobile phase can indicate the presence of an analyte. The amount of analyte leaving the column will determine the intensity of the signal produced in the detector. The detector measures a signal peak as each analyte leaves the column. By comparing the time it takes for the peak to show up (retention time), with the retention times for a mixture of known compounds, the components of unknown sample mixtures

can be identified. By measuring the signal intensity (response) and comparing it to the response of a known amount of that particular analyte, the amount of analyte in the mixture can be known.

UV detectors can only identify compounds that contain a chromophore molecule, which is able to absorb UV radiation.

ELSD is a universal HPLC detection method which is able to detect a wide range of different compounds. This method involves transforming the eluent from the HPLC column into a fine spray, evaporating the spray droplets and then identifying the resultant aerosol particles by light scattering.

Aerosol charge detection is a more sensitive version of ELSD that can detect compounds of the same molecular weight. The aerosol particles are not detected by light scattering but are given an electrical charge by passing them close to a stream of charged nitrogen. The charged aerosol particles are then detected by an electrometer, which generates a signal in direct proportion to the quantity of each particle.

RID is one of universal analyte detector. Solvent used with RID must remain the same throughout separation. The detector is a very temperature and flow sensitive and difficult to stabilize baseline.

For fluorescence detector (FD), the excitation wavelength generates fluorescence emission at a higher wavelength. The analytes must have fluorophore group, can react analyte with fluorophore reagent but it is very sensitive and selective. There are more difficult methods transfer and the results are very dependent upon separation conditions.

HPLC 1100 series and RID HP 1047A for sugars determination

The HP 1047A has to keep away from open doors and windows, ventilation fans, direct sunlight, vibration sources and heating equipment. Temperature fluctuations and air flow affect performance and cause an unstable base line.

Optimizing RID HP 1047A

These are some practical hints to optimize the use of RID HP 1047A.

1. Solvent Delivery system

The solvent delivery system must produce a very stable and pulse free flow. Pressure pulses in the flow stream cause baseline noise and drift. If the solvent delivery system has a multichannel capability, the mobile phase should be premixed in a reservoir and pump from one channel only. The flow rate can affect baseline stability. Noise caused by eddy currents in the flow cell increases as flow rate increases. The rate of heat transfer changes as the flow rate changes; this can cause baseline instability until thermal equilibrium is reached.

2. Inlet Tubes

The HP 1047A inlet tube should be insulated using the pipe insulation(0890-1032), this ensures that the thermal stability in the flow system is easier to achieve.

3. Outlet Tubes

The HP 1047A outlet tube should have a wide internal diameter to avoid high back pressures which can cause baseline instability or even damage the flow cell. The tubing should not be coiled as this cause pressure pulses which produce reproducible spikes on the baseline.

4. Solvents

All solvents must be HPLC grade. Solvents must not contain any particulate matter and must be thoroughly degassed before use. Careful filtering removes suspended particulate matter which might contaminate the cell walls or reduce sensitivity by light scattering. Degassing prevents bubbles forming in the solvent as it passes through the flow cell. Filters should not exceed 2 μm in pore size. The filter material must not react with the solvent to cause solvent contamination. If the mobile phase is a combination of two or more solvents, these solvents must be thoroughly mixed. One method for solvent preparation is to first separately degas the pure solvents and then mix them to form the desired solvent composition, followed by a further 10 minutes degassing. This extra 10 minutes prevent any out gassing caused by mixing, but is not usually long enough to change the solvent composition. If the chromatogram contains a degasser, then mix the solvents and pass through the system directly. The effectiveness of continuously

degassing the mobile phase during the analysis depends on the solvents used and the length of the analysis. Continuing degassing will prevent a degassed mobile phase from re-absorbing air, but there are two side effects to consider:

Long-term retention-time changes with complex mobile phase. If the mobile phase comprises a mixture of solvents and one of these solvents is more volatile than the others, then continuous degassing can cause changes in retention times related to changing elution strength.

Long-term drift. The solvent trapped in the reference compartment may begin to degas at a fixed rate. This will cause a continuously increasing refractive index difference between the solvent in the reference compartment and the continuously degassed, flowing solvent in the sample compartment. This effect will cause long-term drift.

The overall performance of the HP 1047A will vary depending on the solvent used. Solvent properties such as viscosity and volatility are important factors to baseline stability.

Start up instructions for HPLC 1100 series and HP 1047A Before start up check if the HP 1047A connects to the HPLC HP 1100 series (Inst # 2709G), using Dual channel Interface (Inst # 2709H). When these two equipments connected, the green graph icon for Refractive Index Detector appears under the DAD Icon (labelled ADC) on System Diagram. Multi channel Interface shows blinking light on communication, light on active and ready.

Start up instructions;
1. Connect column (35101 Prevail Carbohydrate ES column, 250 x 4.6 mm, 5µm waters Fittings) into HPLC. Make sure the flow direction is corrected.
2. Turn on the Pump, Degasser, Autosampler injection system, Chromatograph and RID HP 1047A at lest 5 minutes before use.
3. Insure that the amount of solvent is adequate and that the waste collection container is in place. Check if the papers for result printing are sufficient for all runs.
4. On the computer screen; user name: hplc, password: hplchplc, Log on to: CAPE. CGA Bootp Server always run when using HPLC. Double click on Instrument 1 online to activate HP ChemStation Rev. A 06.01 (403) for LC and LC/MS system. After the

initializing the program is ready on Method & Run Control. Set method name and sequence name and save. Verify the column temperature is 40°C. RID HP 1047A runs appropriately at ambient temperature < 25 °C. Set the flow rate at 1 ml/minute, set solvent level on actual amount in the solvent bottle at the right channel (channel A or B or C or D).

5. Run the analysis method without injection by using HPLC grade water (DI water) for 24 hours to get thermal equilibrium for RID. Check for leaks, bubbles, and confirm the pump pressure to be with in limits. Fail in thermal equilibrium results in fluctuation on peaks and higher peak heights than real values.

6. Activate FLUSH valve then pump the degassed analytical mobile phase at the analysis flow rate through the sample and reference compartments of a flow cell for 90 minutes. (a mixture of 750 ml acetonitrile and 270 ml HPLC water provides good peaks and suitable times of appearances for sugar standards; fructose, glucose and sucrose). Set the range at 1 x 10^{-5} RIU in order to get integrator output at the highest value (32 mV). When FLUSH valve is activated the solvent will flow trough the sample and reference compartments. When FLUSH valve is deactivated the solvent will only flow through the sample compartment.

7. Deactivate FLUSH valve after 90 minutes then set front panel FINE ZERO to middle position by turn clockwise to full scale and turn anticlockwise for 5 rounds (or do it on the other way round). Then set INTEGRATOR fully clockwise.

8. Press BALANCE and wait for 15 minutes to stabilize baseline (when pressing BALANCE, the baseline will move up or down a little bit and go to a straight line). Check the baseline stability at test chromatogram conditions. If the baseline is unstable, activate the FLASH valve again and continue pumping degassed solvent through the flow cell until the drift and noise has stabilized, and then deactivate the FLUSH valve again.

9. Prepare sugar standards at different concentration to be references for the results from fruit juice samples. In order to make sure that the standard sample concentrations preparation are corrected, the YSI 2700 SELECT biochemical analyser can be easily used for glucose and sucrose concentration examination. Preparation of sugar standards can be done during stabilizing the equipment.

10. Start to run with one standard to see the system performance. System performance can be determined by calculating peak symmetry, base line noise, and the signal-to-noise ratio for a known amount of standard. Repeat at least three times for the same standard to get and average of retention time for all sugars. If the retention times appear at too long time

after injection, increase the flow rate but not more than the flow rate limit specification of the column. The carbohydrate column has the maximum flow rate at 1.5 mL/minute. Record the retention times and peak heights for all sugars in standard. If the analysis of standard demonstrates discrepancies, make corrections then rerun the standards. The peaks appear from three sugar standards will be fructose, follow by glucose and sucrose,
11. Load the samples from fruit and vegetable juices into an autosampler tray. (See detail for fruit and vegetable juice sample preparation for HPLC). Notify that fruit and vegetable juice samples can be used after preparation within one day only. After that the sugar contents will be decreased owing to respiration reactions or fermentation by micro organisms. Make sure that the equipments are ready to run the samples by resulted in a good performance from standards determination.
12. When the standard results are corrected, inject the samples. Samples that yield unacceptable results must be rerun or reanalyzed after corrective measures are taken. Automatic continuous running the samples can be done by setting the sequence table and sequence parameters under your method name and your sequence name. Click start when everything is ready. When HPLC run by automatic system the equipment will continue running until all sequences in sequence table finish. For RID, this system can be used for 5-10 samples, stabilizing is needed in between long run because of unstable baseline. Do not forget to change the number for the counter under sequence parameters whenever start to run new samples. The computer will over write new data on the same counter number. Separately short notes for detail on counter number would be a better way to make sure that the data will not mix up.

Quality control on HPLC runs

1. Record and compare the beginning pressure of each run. If the pressure varies by more than approximately 10% of the previous day's starting pressure then take the appropriate corrective action.
2. Record separately the daily number of runs for the guard column, inline filter and column. Record any adjustment repairs on the samples and equipment log.
3. If any sample produces a chromatogram with weak or off scale peaks, adjust possibility causes and rerun the sample.
4. If the peak does not elute within a mean retention time of approximately ±0.15 minute, determine cause of the drift, correct the problem, and rerun the sample.
5. Instrument operating conditions;

- Maintain records of all service, maintenance intervals and calibration done.
- Service the chromatograph and verify it meets the manufacturer's specifications at least every 18 months.
- Recalibrate the peak-naming table contained in the HPLC method file (if used) whenever the column is changed or when changes are made in the fluid path of the chromatograph.
- Verify injector carry over is with in manufacturer's tolerance, this may be done as part of the periodic maintenance procedure, or as part of the control procedure when performing analytes.
- Verify the instrument function; turn on the instrument 30 minutes before use. Check the solvent bottles, waste bottle, and the vacuum pump for degasser. Do not operate the chromatograph until any needed repairs or adjustments are performed.
- Visually verify that the pump shows no evidence of "pulsing" at a high flow rate.
- Verify the fluid path is free of any leaks
- Replace the inline filter and/or guard column if the day's starting pressure is • 150% of the initial pressure recorded when the component was installed, or if the total pressure exceeds the pressure limit recommended by the column manufacturer if available. The guard column should last approximately 250 injections.
- If the replacement of the inline filter and /or the guard column fails to bring the pressure into tolerance, replace the analytical column. Normally, the analytical column should last approximately 1000 injections. Check the column life from the column catalogue.
- Verify that the detector baseline is stable (no net baseline drift) while the chromatograph is operating under initial solvent conditions for the assay.

Shut down procedures

1. Click stop on the method and run control.
2. Click off for pump and other equipments appear on screen. Turn off the instrument 1 online program.
3. Turn off all equipment switches that was turned on at the beginning.
4. Take off all samples from the autosampler tray.

Sample HPLC Chromatograms

1. 2.5% fructose + 2.5% sucrose + 2.5% glucose

2. 5% fructose + 5% sucrose + 5% glucose

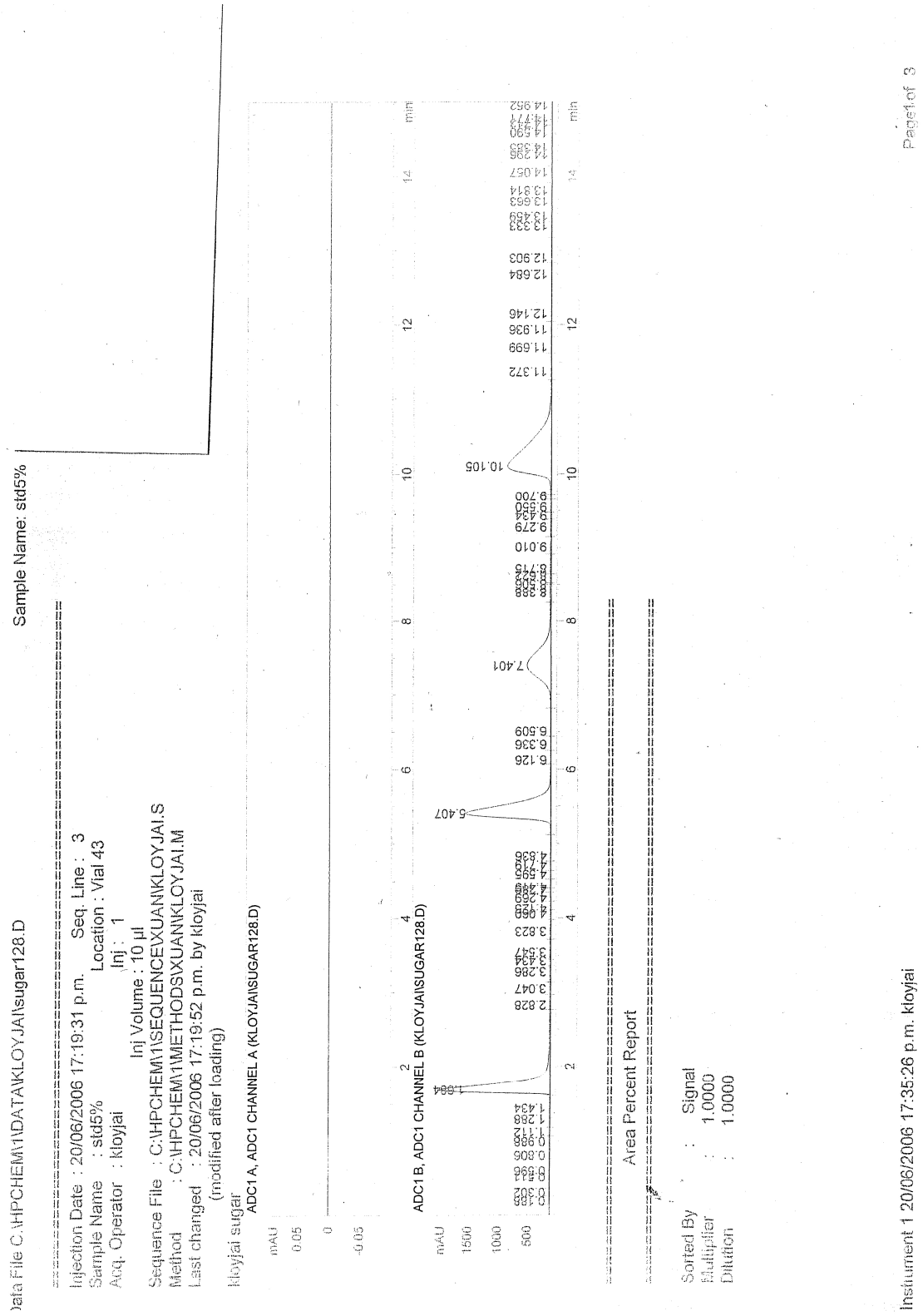

ata File C:\HPCHEM\1\DATA\KLOYJAI\sugar127.D Sample Name: std7.5%

Injection Date : 20/06/2006 17:02:36 p.m. Seq. Line : 2
Sample Name : std7.5% Location : Vial 42
Acq. Operator : kloyjai Inj : 1
Inj Volume : 10 µl
Sequence File : C:\HPCHEM\1\SEQUENCE\XUAN\KLOYJAI.S
Method : C:\HPCHEM\1\METHODS\XUAN\KLOYJAI.M
Last changed : 20/06/2006 17:02:57 p.m. by kloyjai
(modified after loading)
kloyjai sugar

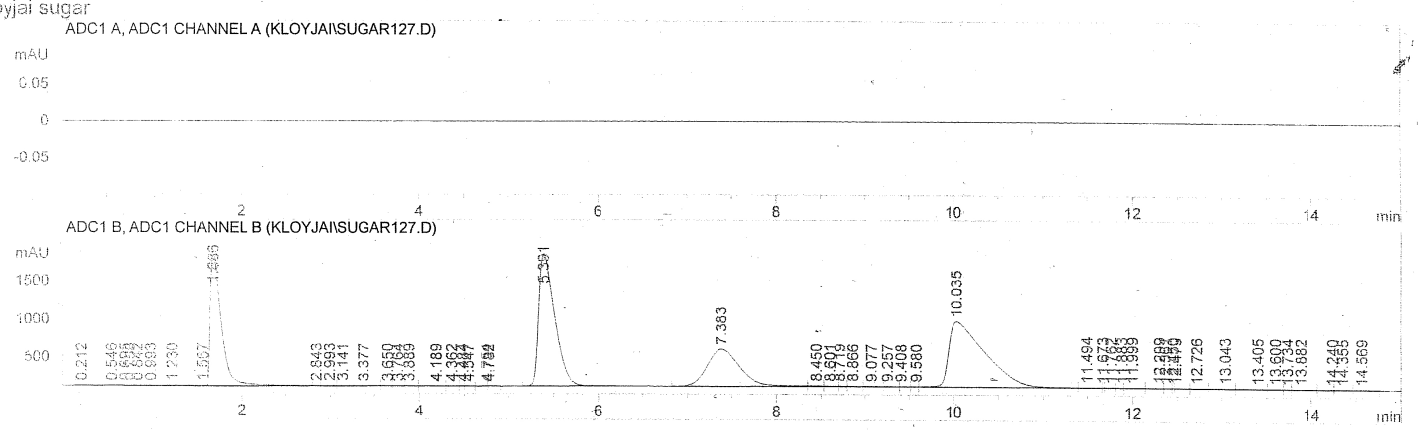

Area Percent Report

Sorted By : Signal
Multiplier : 1.0000
Dilution : 1.0000